Aus der
Klinik für Kardiologie, Pneumologie und Angiologie
(Direktor: Univ.-Prof. Dr. med. Malte Kelm)
der Medizinischen Fakultät
der Heinrich-Heine-Universität, Düsseldorf

Role of the circulating NO-synthase in the cardiovascular system

[Rolle der zirkulierenden Stickstoffmonoxid-Synthase im Herz-Kreislauf-System]

Habilitationsschrift
zur Erlangung der *Venia legendi*
für das Fach Experimentelle Medizin
an der Heinrich-Heine-Universität Düsseldorf

vorgelegt von
Miriam Margherita Cortese-Krott
aus Mailand, Italien

Düsseldorf, 2014

Für Daniel, der immer daran geglaubt hat.
E per mio Padre.

Erklärungen

Hiermit erkläre ich ehrenwörtlich, dass bei den wissenschaftlichen Untersuchungen, die Gegenstand der schriftlichen Habilitationsleistung sind, ethische Grundsätze und die jeweils gültigen Empfehlungen zur Sicherung guter wissenschaftlicher Praxis beachtet wurden.

Diese Habilitationsschrift wurde weder in gleicher noch in ähnlicher Form in einem anderen Prüfungsverfahren vorgelegt. Außerdem erkläre ich, dass ich bisher noch keine weiteren Habilitationsverfahren eingeleitet oder erfolglos beendet habe.

Düsseldorf, den 16.05.2014

Table of Contents

I - LIST OF PAPERS SELECTED FOR THIS HABILITATION

This work is based on following peer reviewed research papers (* denote equal contribution):

1. **Cortese-Krott, M. M.**, Fernandez, B. O., Santos, J. L., Mergia, E., Grman, M., Nagy, P., Kelm, M., Butler, A. and Feelisch, M. (2014). "Nitrosopersulfide ($SSNO^-$) accounts for sustained NO bioactivity of s-nitrosothiols following reaction with sulfide." *Redox Biol* 2: 234-244.
2. Merx MW*, Gorressen S*., van de Sandt A.M., **Cortese-Krott M.M**., Ohlig J., Stern M., Rassaf T., Gödecke A., Gladwin M.T., Kelm M. (2014). "Depletion of circulating blood NOS3 increases severity of myocardial infarction and left ventricular dysfunction." *Basic Res Cardiol* 109 (1):398-408
3. Wood, K. C.*, **Cortese-Krott, M. M.***, Kovacic, J. C., Noguchi, A., Liu, V. B., Wang, X., Raghavachari, N., Boehm, M., Kato, G. J., Kelm, M. and Gladwin, M. T. (2013). "Circulating blood endothelial nitric oxide synthase contributes to the regulation of systemic blood pressure and nitrite homeostasis." *Arterioscler Thromb Vasc Biol* 33(8): 1861-1871.
4. Horn, P.*, **Cortese-Krott, M. M.***, Amabile, N., Hundsdorfer, C., Kroncke, K. D., Kelm, M. and Heiss, C. (2012). "Circulating microparticles carry a functional endothelial nitric oxide synthase that is decreased in patients with endothelial dysfunction." *J Am Heart Assoc* 2(1) e003764.
5. **Cortese-Krott, M. M.**, Rodriguez-Mateos, A., Kuhnle, G. G., Brown, G., Feelisch, M. and Kelm, M. (2012). "A multilevel analytical approach for detection and visualization of intracellular no production and nitrosation events using diaminofluoresceins." *Free Radic Biol Med* 53(11): 2146-2158.
6. **Cortese-Krott, M. M.**, Rodriguez-Mateos, A., Sansone, R., Kuhnle, G. G., Thasian-Sivarajah, S., Krenz, T., Horn, P., Krisp, C., Wolters, D., Heiss, C., Kroncke, K. D., Hogg, N., Feelisch, M. and Kelm, M. (2012). "Human red blood cells at work: Identification and visualization of erythrocytic enos activity in health and disease." *Blood* 120(20): 4229-4237.
7. Heiss, C., Schanz, A., Amabile, N., Jahn, S., Chen, Q., Wong, M. L., Rassaf, T., Heinen, Y., **Cortese-Krott, M.M**., Grossman, W., Yeghiazarians, Y. and Springer, M. L. (2010). "Nitric oxide synthase expression and functional response to nitric oxide are both important modulators of circulating angiogenic cell response to angiogenic stimuli." *Arterioscler Thromb Vasc Biol* 30(11): 2212-2218.
8. Horn, P.*, **Cortese-Krott, M. M.***, Keymel, S., Kumara, I., Burghoff, S., Schrader, J., Kelm, M. and Kleinbongard, P. (2011). "Nitric oxide influences red blood cell velocity independently of changes in the vascular tone." *Free Radic.Res.* 45(6): 653-661.

II - ZUSAMMENFASSUNG

Rolle der zirkulierenden Stickstoffmonoxid-Synthase im Herz-Kreislauf-System.

Eine beeinträchtigte endotheliale Funktion und/oder eine verminderte Bioverfügbarkeit und/oder Bioaktivität von Stickstoffmonoxid (*nitric oxide*, NO) sind mit der Entstehung von koronärer Herzkrankheit stark verbunden. Im Herz-Kreislauf-System wird NO hauptsächlich im Endothel von einer endothelialen Stickstoffmonoxid-Synthase (eNOS) aus L-Arginin hergestellt. Auf diesem Grund wird das Endothel als Hauptquelle von NO und seiner zirkulierenden und vaskulären Metabolite, sowie als Hauptverantwortlicher für die pleiotropen Effekte von NO betrachtet. Andererseits werden Erythrozyten (*red blood cells*, RBC) als Fänger des endothelial-gebildeten NOs beschrieben. In der Literatur wird die Expression einer eNOS in den Subpopulationen der Hauptblutzellen beschrieben, jedoch ist die Funktion dieser zirkulierenden eNOS unklar. Die Haupthypothese der Arbeiten, welche in dieser Habilitationsschrift präsentiert werden, war, dass sowohl die endotheliale als auch die nicht-endotheliale eNOS den zirkulierenden Spiegel der NO-Metabolite regulieren und zur Regulation der vaskulären Homeöstase beitragen. Daher war das Ziel dieser Untersuchungen die Identifizierung des Beitrages der zirkulierenden eNOS zur Regulation der Gefäßfunktion, des Blutflusses und der Kardioprotektion in experimentellen und klinischen Modellen. Die Hauptergebnisse dieser Untersuchungen zeigen, dass: 1. die in Blutzellen exprimierte eNOS zur Regulation des zirkulierenden Pools von NO-Metaboliten, des Blutdrucks und zum Schutz des Myokard im I/R-Schaden beiträgt (§ 3.1-2); 2. rote Blutzellen und zirkulierende Mikropartikel eine aktive eNOS tragen, dessen Expression bei koronarer Herzkrankheit verringert ist (§ 3.3,5,7); 3. die erythrozytäre eNOS die Verformbarkeit und die Geschwindigkeit der RBC sowie den Blutfluss in der Mikrozirkulation beeinflusst (§ 3.4); 4. die Interaktion zwischen NO und Sulfid zu der Bildung weiterer bioaktiver NO/Sulfid-Metaboliten führt, die zur Regulation des vaskulären Tonus beitragen könnten. Zusammenfassend zeigen die Ergebnisse dieser Studien, dass nicht nur die endotheliale NO-Produktion, sondern auch die im Blut zirkulierende eNOS an der Regulation der kardiovaskulären Funktion beteiligt ist. Außerdem konnten Hinweise auf die Bildung weiterer bioaktiver NO-Metaboliten gefunden werden, welche über die Reaktion mit Sulfid entstehen und ebenfalls an der vaskulären Homöostase beteiligt sein könnten.

1. INTRODUCTION

The key event in the pathogenesis of arteriosclerosis is believed to be a dysfunction of the vessel endothelium. The endothelium has long been considered to be a "layer of nucleated cellophane," endowed with passive mechanic properties and act as a non-thrombogenic substrate for blood (Cines, Pollak *et al.* 1998). This view has changed radically. It is now evident that hemostasis and hematopoiesis, inflammatory reactions, antigen presentation, immunity, and lipoprotein metabolism involve close interactions between blood cells and vascular endothelium (Rotella, Giannini *et al.* 1996, Mantovani, Bussolino *et al.* 1997). The cross-talk between vascular and blood cells may occur *via* membrane bound signaling, but also by paracrine/exocrine signaling. Recently, it was suggested that even circulating membrane particles (microparticles, MP) shed by endothelial and blood cells may possess biological/pathological functions and mediate the communication between cells in the vasculature (Rautou, Vion *et al.* 2011). Endothelial dysfunction and/or damage predispose blood vessels to vasoconstriction, inflammation, leukocyte adhesion, thrombosis, proliferation of vascular smooth muscle cells, and have been proposed to contribute to accelerated atherogenesis (Vita 2011). Decreased production and/or bioactivity of nitric oxide (NO) are considered as hallmarks of endothelial dysfunction (Vita 2011)

1.1 NITRIC OXIDE: BIOCHEMISTRY, SIGNALING AND FUNCTIONS IN THE CARDIVASCULAR SYSTEM

NO is a short-lived signaling/regulatory product of the endothelium that is critically important for vascular health (Moncada, Palmer *et al.* 1991). The first biological activity attributed to NO was the ability to induce relaxation of preconstricted aortic vascular preparations, and for as long as its chemical nature remained unknown it was defined as 'endothelium-derived relaxing factor' (EDRF) (Furchgott and Zawadzki 1980, Palmer, Ferrige *et al.* 1987, Ignarro 1989). NO is now recognized to play a fundamental role in the control of vascular tone and blood flow and to represent a central signaling entity in the cardiovascular system (Vallance, Collier *et al.* 1989, Moncada 1997); moreover, it is also a critical player in neurotransmission, host defense and inflammatory processes (Bredt and Snyder 1994, Nathan 2002).

NO is enzymatically produced by NO synthases (NOS, EC 1.14.13.39), heme-containing proteins catalyzing the five-electron oxidation of the guanidino nitrogen of L-arginine to NO and citrulline. This process requires dioxygen and a number of cofactors including calcium ($Ca2^{+}$), calmodulin, NADPH, flavin mononucleotide (FMN), flavin adenine dinucleotide (FAD), and

tetrahydrobiopterin (Griffith and Stuehr 1995, Moncada 1997). The proposed reaction mechanism involves electron transfer from the flavin-bindings site *via* calmodulin to the heme group, where the oxidation of one of the guanidino nitrogens of L-arginine to the intermediate product, N-hydroxy-L-arginine takes place (Stuehr 2004). Tetrahydrobiopterin appears to be important in maintaining the enzyme in its active dimeric form (Griffith and Stuehr 1995, Stuehr 2004).

In mammals there are three distinct isoforms of NOS, encoded by three different genes. The human loci are defined as NOS1 (Gene ID 4842) coding for the neuronal nitric oxide synthase (nNOS), NOS2 (Gene ID 4843) for the inducible nitric oxide synthase (iNOS) and NOS3 (Gene ID: 4846) for the endothelial nitric oxide synthase (eNOS). Whereas iNOS typically produces high-output NO levels and participates in host defense, inflammatory stress and airway epithelial NO formation, the constitutively expressed isoforms, nNOS and eNOS, are lower NO output systems that are important for physiological processes such as neuronal signaling, inhibition of the hemostatic system, vasodilation and blood pressure control (Griffith and Stuehr 1995, Stuehr 2004).

The constitutively expressed enzymes eNOS and nNOS are activated after stimulation of specific receptors by various agonists (e.g., acetycholine, bradykinin, serotonin, adenosine, ADP:ATP, histamine, and thrombin), with consecutive increase of intracellular free Ca^{2+}. The binding of Ca^{2+} to the Ca^{2+}/calmodulin subunit of these proteins activates the enzyme to produce NO. In vascular tissue, the binding of NO to the Fe^{2+}-heme prostetic group of soluble guanylyl cyclase (sGC) activates this enzyme to produce cyclic guanosine-3-5-monophosphate (cGMP) from guanosine-5-triphosphate (GTP). The signal is then transduced to downstream elements of the signaling cascade, including cGMP-dependent protein kinases, cGMP-gated cation channels, and cGMP-regulated phosphodiesterase (Denninger and Marletta 1999).

Instead, iNOS is not expressed in endothelial cells under basal non-inflammatory conditions and its activity is mainly regulated at transcriptional level. The molecular mechanism of iNOS gene induction presents species-dependent variations (Kleinert, Schwarz *et al.* 2003). Interestigly, iNOS-derived output synthesis of NO leads to long term protection of endothelial cells against ROS-mediated cell death *via* activating the transcription factor nuclear factor, erythroid derived 2, like 2 (Nrf2) and regulation of glutathione (GSH) synthesis (Cortese-Krott, Suschek *et al.* 2009).

1.2 ENDOTHELIAL eNOS-DERIVED NO AND THE CIRCULATING POOL OF NO METABOLITES

In healthy blood vessels, eNOS-derived NO contributes to the regulation of blood flow and blood pressure, as well as to the inhibition of platelet activation and aggregation and leukocyte adhesion and migration (Sessa 2004). Furthermore, endothelial eNOS appears to

contribute to the formation of bioactive circulating and tissue NO metabolites, including nitrosothiols (RSNO), nitrosamine (RNNO), nitrite, nitrate (Kleinbongard, Dejam *et al.* 2003, Rassaf, Bryan *et al.* 2003, Heiss, Lauer *et al.* 2006, Rassaf, Heiss *et al.* 2006, Milsom, Fernandez *et al.* 2012). The NO metabolites, and in particular nitrosothiols and nitrite, can participate to important endocrine activities such as hypoxic vasodilation, blood pressure regulation, gene expression and cytoprotection following myocardial infarction (Gladwin, Shelhamer *et al.* 2000, Cosby, Partovi *et al.* 2003, Bryan, Fernandez *et al.* 2005, Ali, Ping *et al.* 2006, Crawford, Isbell *et al.* 2006, Hendgen-Cotta, Merx *et al.* 2008, Lundberg, Gladwin *et al.* 2009, Shiva and Gladwin 2009, van Faassen, Bahrami *et al.* 2009, Murillo, Kamga *et al.* 2011, Totzeck, Hendgen-Cotta *et al.* 2012). Mice genetically deficient in eNOS ($eNOS^{-/-}$) are hypertensive and have lower circulating nitrite levels, demonstrating the importance of constitutively produced NO to formation of NO metabolites, blood pressure regulation and vascular homeostasis (Huang, Huang *et al.* 1995, Shesely, Maeda *et al.* 1996, Godecke, Decking *et al.* 1998, Kleinbongard, Dejam *et al.* 2003).

1.3 CIRCULATING eNOS : WHAT IS eNOS DOING IN BLOOD CELLS?

Conventional wisdom holds that the pleiotropic effects of eNOS are primarily determined by the enzyme located in the endothelium. In addition to endothelial cells, most circulating blood cells - including all main leukocyte subpopulations, platelet-rich plasma, but not purified platelets - also carry eNOS transcript and/or protein (Radomski, Palmer *et al.* 1990, Sase and Michel 1995, Aubry, Dugas *et al.* 1997, Mühl and Pfeilschifter 2003, Ozüyaman, Gödecke *et al.* 2005, Gambaryan, Kobsar *et al.* 2008, Saluja, Jyoti *et al.* 2011). Interestingly, also red blood cells (RBCs) carry a NOS activity and eNOS epitopes, which considering the abundance of RBCs as compared to other blood cells (i.e. 1000:1) might play an important role (Chen and Mehta 1998, Kleinbongard, Schulz *et al.* 2006). However, production of NO by hemoglobin-containing RBCs under normoxic conditions by a NOS appears paradoxical in view of earlier reports suggesting a major role of these blood cells in NO inactivation.

1.4 RED BLOOD CELLS IN CONTROL OF SYSTEMIC NITRIC OXIDE BIOAVAILABILITY.

It is an accepted dogma that RBCs take up and inactivate endothelium-derived NO *via* rapid reaction with oxyhemoglobin to form methemoglobin and nitrate. Yet it has also been shown that RBCs not only act as “NO sinks”, but synthesize, store, and transport NO metabolic products. Under hypoxic conditions in particular, it has been demonstrated that RBCs induce NO-dependent vasodilation (Cosby, Partovi *et al.* 2003, Webb, Patel *et al.* 2008). Mechanisms of release and potential sources of NO in RBCs are still a matter of debate, but candidates include iron-nitrosylhemoglobin, S-nitrosohemoglobin, and nitrite (Jia, Bonaventura *et al.* 1996,

Gladwin, Lancaster jr *et al.* 2003, Rassaf, Bryan *et al.* 2003, Herold 2004). The latter may be reduced to NO either *via* deoxyhemoglobin or xanthine oxidoreductase (XOR)-mediated reduction, or *via* spontaneous and carbonic anhydrase-facilitated disproportionation (Zweier, Wang *et al.* 1995, Cosby, Partovi *et al.* 2003, Nagababu, Ramasamy *et al.* 2003, Webb, Milsom *et al.* 2008, Aamand, Dalsgaard *et al.* 2009). Most of these processes show a clear dioxygen-dependence, and several are favored by low dioxygen tensions. The relative contribution of either mechanism to NO formation varies with dioxygen partial pressure along the vascular tree. In addition, RBCs release ATP when subjected to hypoxia, providing an alternative vasodilatory pathway (Ellsworth, Forrester *et al.* 1995).

In contrast to hypoxia-induced NO release from RBCs, their generation of NO under normoxic conditions is less well characterized. There is some evidence of a NOS-dependent NO production from RBCs in normoxia, suggesting that RBCs may contribute to the circulating pool of NO metabolites, and to overall tissue protection (Sprague, Stephenson *et al.* 1995, Yang, Nichols *et al.* 1996, Chen and Mehta 1998, Kleinbongard, Schulz *et al.* 2006). Treatement of RBC suspensions with NOS inhibitors decreased accumulation of NO metabolites and citrulline in the supernatant (Deliconstantinos, Villiotou *et al.* 1995, Yang, Nichols *et al.* 1996, Chen and Mehta 1998, Kleinbongard, Schulz *et al.* 2006). However, Kang et al. failed to measure citrulline production in RBC lysates, maybe because of loss of cellular structures or cofactors important for activity (Kang, Ford *et al.* 2000, Metha, Metha *et al.* 2000).

Taken together there is compelling evidence demonstrating that RBCs play a central role in control of NO bioavailability and the circulating NO pool as: 1. NO scavengers; 2. transporters of NO metabolites; 3 producers of NO under hypoxic conditions; 4. producers of NO/NO metabolites under normoxic conditions. The overall chemical/biochemical and enzymatic equlibria governing these reactions are not fully understood.

1.5 NITRIC OXIDE, RED BLOOD CELLS RHEOLOGY AND BLOOD FLOW IN THE MICROCIRCULATION

To supply organs with oxygen and nutrients, RBCs must deform to enter and transit vessels of the microcirculatory system (capillaries), which are narrower than their own diameter. Blood flow within the microcirculation is regulated by both vascular tone changes and rheological properties of blood cells (Mellander 1989, Pries and Secomb 2003). Capillary blood flow and RBC velocity strongly depend on RBC deformability, which defined as the ability of RBCs to deform under a given force (Driessen, Haest *et al.* 1980, Simchon, Jan *et al.* 1987, Lipowsky, Cram *et al.* 1993, Cabrales 2007). A role of NO in the control of RBC deformability has been proposed. NO donors affect RBC deformability as measured *in vitro* and *ex vivo* (Starzyk, Korbut *et al.* 1999, Mesquita, Picarra *et al.* 2002, Bor-Kucukatay, Wenby *et al.* 2003). Treatment of freshly isolated human RBCs with a NOS inhibitor decreased RBC deformability as measured

in vitro (Bor-Kucukatay, Wenby *et al.* 2003, Kleinbongard, Schulz *et al.* 2006). It is not known in what extent NOS/NO-dependent changes in RBC deformability might affect blood flow and RBC velocity in the microcirculation, and therefore might affect gas/nutrient exchanges.

1.6 RED BLOOD CELLS IN CARDIOPROTECTION: A ROLE OF NOS?

Only recently indexes of number, morphology, and function of RBCs have emerged as an independent and powerful risk factor in cardiovascular disease. Even modest anemia is associated with an increased mortality in patients with acute coronary syndromes, including acute myocardial infarction, as well as chronic heart failure, coronary artery bypass procedures, and bleeding complications (Moncada, Palmer *et al.* 1991, Anand, Kuskowski *et al.* 2005, Sabatine, Morrow *et al.* 2005, Kulier, Levin *et al.* 2007). This is not apparently explained by decreased capacity of transport of gases and nutrients to the tissue and is not reversible by the mere application of erythropoesis stimulating agents (Anand, Kuskowski *et al.* 2005). However, the mechanism of RBC-mediated cardioprotection is still not clear.

There is also preliminary evidence for an involvement of NOS in RBC-dependent protection against myocardial ischemia/reperfusion (I/R) injury. Treatment of isolated ischemic hearts with whole blood or washed RBCs under normoxic conditions protect from I/R injury in a NOS and arginase-dependent fashion (Yang, Nichols *et al.* 1996, Yang, Gonon *et al.* 2013). Of interest, both the presence of eNOS in blood and the inhibition of arginase, which increase the availability of L-arginine for the NOS, are needed to reduce infarct size and left ventricular dysfunction (Yang, Gonon *et al.* 2013).

1.7 THE NITRIC OXIDE / SULFIDE CROSS-TALK: NEW BIOACTIVE NO METABOLITES IN PLAY?

Hydrogen sulfide (H_2S), known as a noxious malodorous gas of volcanic and biogenic origin for centuries, has recently been shown to exert a multitude of beneficial biological effects, some of which have therapeutic potential (Li, Rose *et al.* 2011, Olson 2012). In physiological systems, only a small part of H_2S actually exists in the form of dissolved gas. As a diprotic weak acid with a mean pKa_1=7.0 and pKa_2>12 at 25°C, H_2S rapidly deprotonates to form hydrosulfide anions (HS^-) with negligible amounts of S^{2-} existing at physiological pH (Morse, Millero *et al.* 2002). For simplicity the three species in solution will be defined as “sulfide”.

Some similarities between some of the effects of NO and sulfide, in particular with regard to their role in control of vascular tone and blood pressure regulation, together with interesting mutual regulatory effects, raised the possibility of a cross-talk between these species (Ali, Ping *et al.* 2006, Kajimura, Fukuda *et al.* 2010, Yong, Hu *et al.* 2010, Shatalin, Shatalina *et al.* 2011, Yoon, Parajuli *et al.* 2011, King 2013, Kolluru, Shen *et al.* 2013, Li and Lancaster 2013). Peculiarly, pharmacological application of sulfide was shown to induce both vasodilation and

vasoconstriction *ex vivo*, and both *hypo*tensive and *hyper*tensive effects have been described *in vivo* (Ali, Ping *et al.* 2006, Yang, Wu *et al.* 2008). Wang surmised that the effects of sulfide may depend on the specific vascular bed (conductance vs. resistance vessels), cell type (endothelial vs. smooth muscle cells), concentration of sulfide and presence or absence of NO/NOS in a particular experimental setting (Wang 2011). The group of Moore proposed that vasoconstriction and hypertensive effects of lower sulfide doses were due to a direct chemical interaction between vascular NO and sulfide leading the formation of an intermediate, which was susceptible to destruction by addition of transition metals (Ali, Ping *et al.* 2006, Whiteman, Li *et al.* 2006, Yong, Cheong *et al.* 2011). These authors hypothesized that this intermediate might be a "nitrosothiol", probably thionitrous acid (HSNO) (Whiteman, Li *et al.* 2006).

HSNO was described by Williams as the obvious product of sulfide nitrosation (Williams 2004); likewise, HSNO is the obvious product of the reaction between HS^- and nitrosothiols. Indeed, a recent report suggests that HSNO is formed by direct reaction of S-nitrosoglutathione (GSNO) with sulfide in phosphate buffer at pH 7, and is stable enough to transport NO intermediates across cell membranes (Filipovic, Miljkovic *et al.* 2012). In contrast, earlier reports found this compound to be unstable and reactive, necessitating characterization of its isomerization properties to be carried out in a low temperature argon matrix (Nonella, Huber *et al.* 1987).

The reaction between sulfide and S-nitrosothiols has been shown to promote NO release, potentiating their vasorelaxant activity in aortic rings and allowing for nitrosothiol quantification by gas phase chemiluminescence (Ondrias, Stasko *et al.* 2008, Teng, Scott Isbell *et al.* 2008). It is not clear at present whether these effects of sulfide are due to post-translational modification of vascular proteins, accelerated nitrosothiol decomposition, or rather formation of novel NO-releasing intermediates, with potential pathophysiological significance (King 2013, Li and Lancaster 2013).

1.8 SUMMARY AND OPEN QUESTIONS

Decrease in NO bioavailability and/or bioactivity is considered as a hallmark of endothelial dysfunction and cardiovascular disease. In the cardiovascular system NO is mainly produced within the endothelium by an eNOS. Conventionally, the endothelium is considered as the main source of NO and its circulating metabolites, responsible for all the pleiotropic effects attributed to NO. On the other hand, RBCs are considered as scavengers of endothelial NO.

Following open questions remained: 1. What is the role of non-endothelial/circulating eNOS in systemic NO bioavailability and bioactivity? 2. What isoform of NOS is carried by RBCs and what is it doing there? 3. Are there new potentially bioactive metabolites of NO derived from the interaction between sulfide and NO participating in the control of vascular tone?

2. AIM

This work was based on the hypothesis that both endothelial and non-endothelial eNOS participate to the control of the levels of circulating NO metabolites, which transport NO signals. The aim of these studies was to identify the contribution of circulating eNOS carried by blood cell components in the regulation of vascular function tone, blood flow and tissue protection in experimental and clinical models. Specifically, following sub-topics were investigated: 1.the role of circulating eNOS in the regulation of systemic NO bioavailability, blood flow and cardioprotection; 2. the NOS in RBCs: isoform identity, NO production and role in blood rheology in the microcirculation; 3. the formation of novel potentially bioactive NO metabolites by the reaction of NO with sulfide.

3. SELECTED RESEARCH PAPERS

3.1. Circulating Blood Endothelial Nitric Oxide Synthase Contributes to the Regulation of Systemic Blood Pressure and Nitrite Homeostasis.

Published in *Arterioscler Thromb Vasc Biol.* 2013 Aug;33(8):1861-1871.

by Wood KC*, **Cortese-Krott MM***, Kovacic JC, Noguchi A, Liu VB, Wang X, Raghavachari, N, Boehm M, Kato GJ, Kelm M, Gladwin MT.

*contributed equally

OBJECTIVE. eNOS$^{-/-}$ mice are hypertensive with lower circulating nitrite levels, indicating the importance of constitutively produced NO to blood pressure regulation and vascular homeostasis. Although the current paradigm holds that this bioactivity derives specifically from the expression of eNOS in endothelium, circulating blood cells also express eNOS protein. A functional red cell eNOS that modulates vascular NO signaling has been proposed.

APPROACH & RESULTS. To test the hypothesis that blood cells contribute to mammalian blood pressure regulation *via* eNOS-dependent NO generation, we cross-transplanted wild-type and eNOS$^{-/-}$ mice, producing chimeras competent or deficient for eNOS expression in circulating blood cells. Surprisingly, we observed a significant contribution of both endothelial and circulating blood cell eNOS to blood pressure and systemic nitrite levels, the latter being a major component of the circulating NO reservoir. These effects were abolished by the NOS inhibitor L-NG-nitroarginine methyl ester and repristinated by the NOS substrate l-arginine and were independent of platelet or leukocyte depletion. Mouse erythrocytes were also found to carry an eNOS protein and convert ^{14}C-arginine into ^{14}C-citrulline in a NOS-dependent fashion.

CONCLUSIONS & SIGNIFICANCE. These are the first studies to definitively establish a role for a blood-borne eNOS, using cross-transplant chimera models, that contributes to the regulation of blood pressure and nitrite homeostasis. This work provides evidence suggesting that erythrocyte eNOS may mediate this effect.

3.2. Depletion of Circulating Blood eNOS (NOS3) Increases the Severity of Myocardial Infarction and Left Ventricular Dysfunction.

Published in *Basic Res Cardiol*. 2014 Jan;109(1):398.

by Merx MW*, Gorressen S*, van de Sandt AM, **Cortese-Krott MM**, Ohlig J, Stern M, Rassaf T, Gödecke A, Gladwin MT, Kelm M.

*contributed equally.

OBJECTIVE. NO produced by eNOS plays a central role in protection against myocardial I/R-injury. Subsets of circulating blood cells, including RBCs, carry an eNOS and contribute to blood pressure regulation. We aimed to verify the hypothesis that the circulating blood born eNOS could modulate the severity of myocardial infarction in a I/R model.

APPROACH & RESULTS. We cross-transplanted the bone marrow from wild-type and eNOS$^{-/-}$ mice into irradiated wild-type mice, producing chimeras lacking eNOS in blood cells (BC-/EC+) or the respective control mice (BC+/EC+). After 60-min closed-chest coronary occlusion followed by 24 h of reperfusion, we assessed cardiac function, infarct size (IS), nitrite/nitrate levels, RBCs deformability, and vascular reactivity. At baseline, BC-/EC+ chimera had lower nitrite levels in blood plasma (BC-/EC+: 2.13 ± 0.27 μM vs. BC+/EC+ 3.17 ± 0.29 μM; *p < 0.05), reduced DAF-FM-associated fluorescence within RBCs (BC-/EC+: 538.4 ± 12.8 mean fluorescence intensity (MFI) vs. BC+/EC+: 619.6 ± 6.9 MFI; ***p < 0.001) and impaired erythrocyte deformability (BC-/EC+: 0.33 ± 0.01 elongation index (EI) vs. BC+/EC+: 0.36 ± 0.06 EI; *p < 0.05), while vascular reactivity remained unaffected. Area at risk did not differ, but infarct size was higher in BC-/EC+ (BC-/EC+: 26 ± 3 %; BC+/EC+: 14 ± 2 %; **p < 0.01), resulting in decreased ejection fraction (BC-/EC+ 46 ± 2 % vs. BC+/EC+: 52 ± 2 %; *p < 0.05) and increased end-systolic volume. Application of the NOS inhibitor S-ethylisothiourea hydrobromide was associated with larger infarct size in BC+/EC+, whereas infarct size in BC-/EC+ mice remained unaffected.

CONCLUSIONS & SIGNIFICANCE. Increased infarct size, decreased cardiac function, NO levels in RBCs and RBC deformability in mice lacking eNOS in blood cells suggest a protective role of circulating eNOS in an acute model of myocardial I/R.

3.3. Human Red Blood Cells at Work: Identification and Visualization of Erythrocytic eNOS Activity in Health and Disease.

Published in *Blood.* 2012 Nov 15;120(20):4229-37.

by **Cortese-Krott MM**, Rodriguez-Mateos A, Sansone R, Kuhnle GG, Thasian-Sivarajah S, Krenz T, Horn P, Krisp C, Wolters D, Heiß C, Kröncke KD, Hogg N, Feelisch M, Kelm M.

OBJECTIVE. A NOS-like activity has been demonstrated in human RBCs, but doubts about its functional significance, isoform identity and disease relevance remain. The aim of this study was to isolate and characterize NOS from RBCs.

APPROACH & RESULTS. Using flow cytometry in combination with the NO-imaging probe DAF-FM we find that all blood cells form NO intracellularly, with a rank order of monocytes > neutrophils > lymphocytes > RBCs > platelets. The observation of a NO-related fluorescence within RBCs was unexpected given the abundance of the NO-scavenger oxyhemoglobin. Constitutive normoxic NO formation was abolished by NOS inhibition and intracellular NO scavenging, confirmed by laser-scanning microscopy and unequivocally validated by detection of the DAF-FM reaction product with NO using HPLC and LC-MS/MS. Using immunoprecipitation, ESI-MS/MS-based peptide sequencing and enzymatic assay we further demonstrate that human RBCs contain an eNOS that converts L-^{3}H-arginine to L-^{3}H-citrulline in a Ca^{2+}/calmodulin-dependent fashion. Moreover, in patients with coronary artery disease, red cell eNOS expression and activity are both lower than in age-matched healthy individuals and correlate with the degree of endothelial dysfunction.

CONCLUSIONS & SIGNIFICANCE. Thus, human RBCs constitutively produce NO under normoxic conditions *via* an active eNOS isoform, the activity of which is compromised in patients with coronary artery disease.

3.4. Nitric Oxide Influences Red Blood Cell Velocity Independently of Changes in the Vascular Tone.

Published in *Free Radic Res.* 2011 Jun;45(6):653-61.

by Horn P*, **Cortese-Krott MM***, Keymel S, Kumara I, Burghoff S, Schrader J, Kelm M, Kleinbongard P.

*contributed equally

OBJECTIVE. NO plays a key role in regulation of vascular tone and blood flow. In the microcirculation blood flow is strongly dependent on RBC deformability. *In vitro* NO increases RBC deformability. This study was based on the hypothesis that NO increases RBC velocity *in vivo* not only by regulating vascular tone, but also by modifying RBC deformability.

APPROACH & RESULTS. The effects of NO on RBC velocity were analyzed by intravital microscopy in the microcirculation of the chorioallantoic membrane (CAM) of the avian embryo at day 7 post-fertilization, when all vessels lack smooth muscle cells and vascular tone is not affected by NO. It was found that inhibition of enzymatic NO synthesis and NO scavenging decreased intracellular NO levels and avian RBC deformability *in vitro*. Injection of a NOS-inhibitor or a NO scavenger into the microcirculation of the CAM decreased capillary RBC velocity and deformation, while the diameter of the vessels remained constant.

CONCLUSIONS & SIGNIFICANCE. The results indicate that scavenging of NO and inhibition of NO synthesis decrease RBC velocity not only by regulating vascular tone but also by decreasing RBC deformability.

3.5. Circulating Microparticles Carry a Functional Endothelial Nitric Oxide Synthase that is Decreased in Patients with Endothelial Dysfunction.

Published in *J Am Heart Assoc.* 2012 Dec 31;2(1): e003764.

by Horn P*, **Cortese-Krott MM***, Amabile N, Hundsdörfer C, Kröncke KD, Kelm M, Heiss C

*contributed equally.

OBJECTIVE. Microparticles (MPs) are circulating membrane particles of less than a micrometer in diameter shed from endothelial and blood cells. Recent literature suggests that MPs are not just functionally inert cell debris but may possess biological functions and mediate the communication between vascular cells. As a significant proportion of MPs originate from platelets and endothelial cells, we hypothesized that MPs may harbor functional enzymes including an eNOS.

APPROACH & RESULTS. Using immunoprecipitation and Western blot analysis, we found that human circulating MPs carry an eNOS. Ca^{2+} and l-arginine-dependent NOS activity of crude enzyme extract from MPs was determined by measuring the conversion of ^{3}H-L-arginine to ^{3}H-citrulline and NOS-dependent nitrite production. NOS-dependent NO production in intact MPs was assessed by the NO-specific fluorescent probe MNIP-Cu. In patients with cardiovascular disease, endothelial dysfunction was associated with an increase in the total number of circulating MPs as well as a significant decrease in the expression and activity of eNOS in MPs. No difference in reactive oxygen species was noted in MPs isolated from either group.

CONCLUSIONS & SIGNIFICANCE. Our data further support the concept that circulating MPs may not only retain phenotypic markers but also preserve the functionality of enzymes of the cells they originate from, including eNOS.

3.6. Nitric Oxide Synthase Expression and Functional Response to Nitric Oxide are both Important Modulators of Circulating Angiogenic Cell Response to Angiogenic Stimuli.

Published in *Arterioscler Thromb Vasc Biol.* 2010 Nov;30(11):2212-8.

by Heiss C, Schanz A, Amabile N, Jahn S, Chen Q, Wong ML, Rassaf T, Heinen Y, **Cortese-Krott M**, Grossman W, Yeghiazarians Y, Springer ML.

OBJECTIVE. Circulating angiogenic cells (CACs), also termed endothelial progenitor cells, play an integral role in vascular repair and are functionally impaired in coronary artery disease (CAD). The role of nitric oxide (NO) in CAC function is poorly understood. We hypothesized that CAC migration toward angiogenic signals is modulated by both NOS expression and functional response to NO.

APPROACH & RESULTS. Similar to endothelial cells, CAC chemotaxis to vascular endothelial growth factor (VEGF) was blocked by inhibition of NOS, phosphatidylinositol 3-kinase, or guanylyl cyclase or by treatment with an NO scavenger. Addition of an NO donor (S-nitroso-N-acetylpenicillamine) and the NOS substrate l-arginine increased random cell migration (chemokinesis) and enhanced VEGF-dependent chemotaxis. Healthy CACs expressed endothelial NOS, but endothelial NOS was not detected in CAD patient CACs. Both chemokinesis and chemotaxis to VEGF of patient CACs were decreased compared with healthy CACs but were restored to healthy values by S-nitroso-N-acetylpenicillamine. In parallel, CAD patients exhibited lower flow-mediated vasodilation and plasma NO source nitrite than young, healthy subjects, indicating endothelial dysfunction with reduced NO bioavailability.

CONCLUSIONS & SIGNIFICANCE. NOS activity is required for CAC chemotaxis. In CAD patients, impairment of NOS expression and NO bioavailability, rather than response to NO, may contribute to dysfunction of CACs and limit their regenerative capacity.

3.7. A Multilevel Analytical Approach for Detection and Visualization of Intracellular NO Production and Nitrosation Events Using Diaminofluoresceins.

Published in *Free Radic Biol Med.* 2012 Dec 1;53(11):2146-58.

by **Cortese-Krott MM**, Rodriguez-Mateos A, Kuhnle GG, Brown G, Feelisch M, Kelm M.

OBJECTIVE: Diaminofluoresceins are widely used probes for detection and intracellular localization of NO formation in cultured/isolated cells and intact tissues. The fluorinated derivative 4-amino-5-methylamino-2',7'-difluorofluorescein (DAF-FM) has gained increasing popularity in recent years because of its improved NO sensitivity, pH stability, and resistance to photobleaching compared to the first-generation compound, DAF-2. Detection of NO production by either reagent relies on conversion of the parent compound into a fluorescent triazole, DAF-FM-T and DAF-2-T, respectively. Although this reaction is specific for NO and/or reactive nitrosating species, it is also affected by the presence of oxidants/antioxidants. Moreover, the reaction with other molecules can lead to the formation of fluorescent products other than the expected triazole. Thus additional controls and structural confirmation of the reaction products are essential. The aim of this study was to establish a multilevel analytical approach for detection and visualization of intracellular NO production and nitrosation events using DAF-FM.
APPROACH & RESULTS. Using human red blood cells as an exemplary cellular system we here describe robust protocols for the analysis of intracellular DAF-FM-T formation using an array of fluorescence-based methods (laser-scanning fluorescence microscopy, flow cytometry, and fluorimetry) and analytical separation techniques (reversed-phase HPLC and LC-MS/MS).
CONCLUSIONS & SIGNIFICANCE. When used in combination, these assays afford unequivocal identification of the fluorescent signal as being derived from NO and are applicable to most other cellular systems without or with only minor modification.

3.8. Nitrosopersulfide ($SSNO^-$) Accounts for Sustained NO Bioactivity of S-Nitrosothiols Following Reaction with Sulfide.

Published in *Redox Biol*. 2014 Jan 11;2:234-44.

by **Cortese-Krott MM**, Fernandez BO, Santos JL, Mergia E, Grman M, Nagy P., Kelm M, Butler A, Feelisch M.

OBJECTIVE. Sulfide salts are known to promote the release of nitric oxide (NO) from S-nitrosothiols and potentiate their vasorelaxant activity, but much of the cross-talk between hydrogen sulfide and NO is believed to occur *via* functional interactions of cell regulatory elements such as phosphodiesterases. Using RFL-6 cells as an NO reporter system we sought to investigate whether sulfide can also modulate nitrosothiol-mediated soluble guanylyl cyclase (sGC) activation following direct chemical interaction.

APPROACH & RESULTS. We find a U-shaped dose response relationship where low sulfide concentrations attenuate sGC stimulation by S-nitrosopenicillamine (SNAP) and cyclic GMP levels are restored at equimolar ratios. Similar results are observed when intracellular sulfide levels are raised by pre-incubation with the sulfide donor, GYY4137. The outcome of direct sulfide/nitrosothiol interactions also critically depends on molar reactant ratios and is accompanied by oxygen consumption. With sulfide in excess, a 'yellow compound' accumulates that is indistinguishable from the product of solid-phase transnitrosation of either hydrosulfide or hydrodisulfide and assigned to be nitrosopersulfide (perthionitrite, $SSNO^-$; λ max 412 nm in aqueous buffers, pH 7.4; 448 nm in DMF). Time-resolved chemiluminescence and UV-visible spectroscopy analyses suggest that its generation is preceded by formation of the short-lived NO-donor, thionitrite (SNO^-). In contrast to the latter, $SSNO^-$ is rather stable at physiological pH and generates both NO and polysulfides on decomposition, resulting in sustained potentiation of SNAP-induced sGC stimulation.

CONCLUSIONS & SIGNIFICANCE. Sulfide reacts with nitrosothiols to form multiple bioactive products; $SSNO^-$ rather than SNO^- may account for some of the longer-lived effects of nitrosothiols and contribute to sulfide and NO signaling.

4 - SUMMARY AND CONCLUSIONS.

These studies investigated the role of circulating eNOS in the regulation of cardiovascular function. The main findings of these studies are: 1. Circulating blood cell eNOS contributes to regulation of the circulating pool of NO metabolites, blood pressure and cardioprotection against I/R injury (§ 3.1-2). 2. Red blood cells and circulating microparticles carry an active eNOS, which expression is decreased in coronary artery disease (§ 3.3,5,7). 3. Red cell eNOS contributes to control of RBC deformability, RBC velocity and blood flow in the microcirculation (§ 3.4). 4. NO bioactivity can be modulated by sulfide (HS^-), the smallest endogenously produced thiol (§ 3.8).

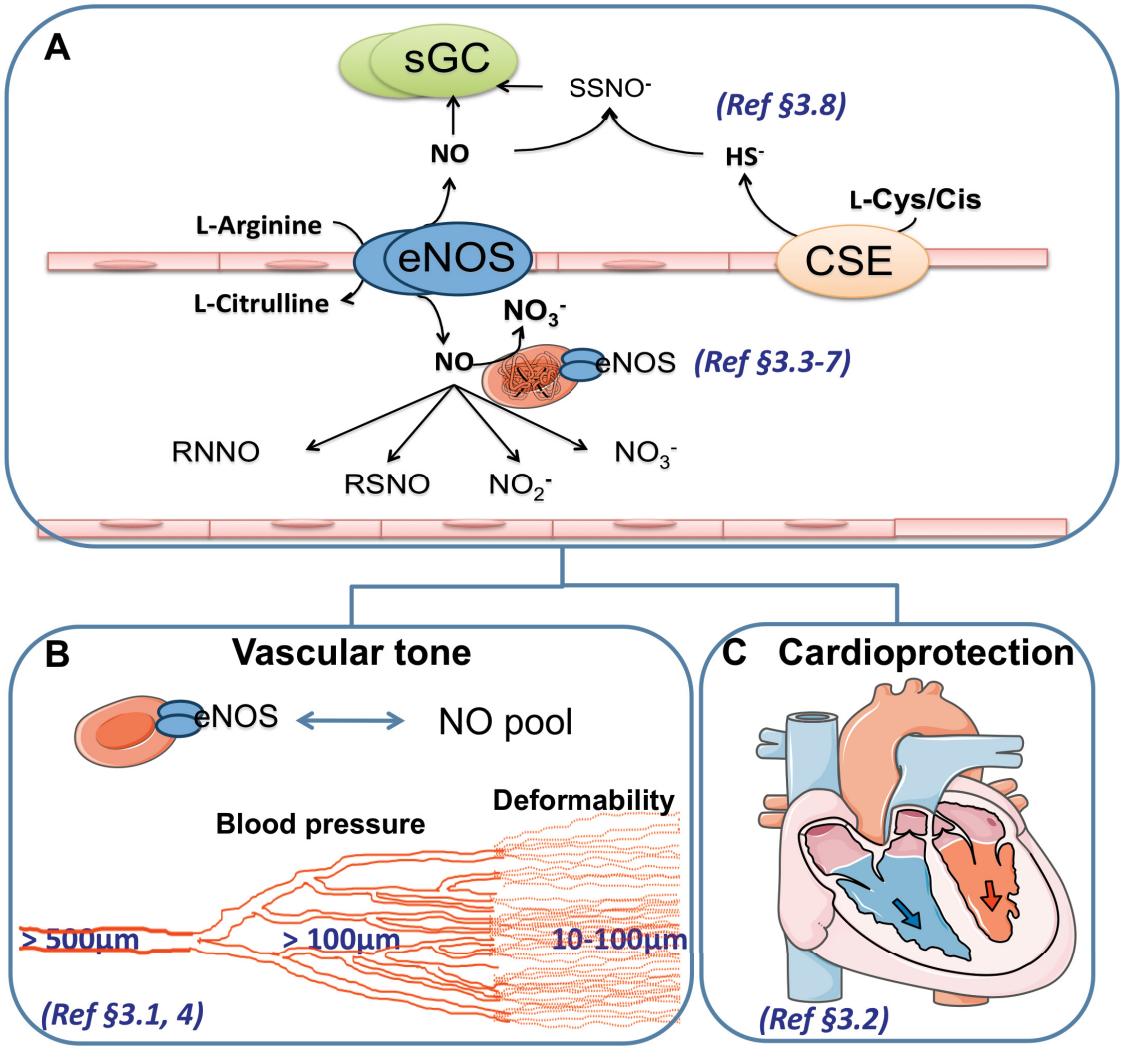

Figure 1 – Schematic representation of the main topics and findings of the studies presented in this thesis, with reference to the paragraph where the respective paper is described (§). A) Signaling in the blood and in the vessel endothelium. B) Vascular effects of circulating and red cell eNOS. C) Cardiac effects of circulating eNOS. Abbreviations: eNOS, endothelial nitric oxide synthase; RNNO, nitrosamine; RSNO, nitrosothiols, L-Cys, L-Cysteine; L-Cis, L-Cystine; CSE, cystathionine-γ-lyase; $SSNO^-$, nitrsopersulfide

4.1 SYSTEMIC EFFECTS OF CIRCULATING eNOS

The fundamental role of NO produced by circulating blood cells was demonstrated *in vivo* in chimera mice obtained by transplantation of bone marrow from eNOS$^{-/-}$ into lethally irradiated wild type mice, as described in § 3.1 (Wood, Cortese-Krott *et al.* 2013). These mice carry blood cells lacking eNOS, and are characterized by a significant decrease in circulating nitrite and nitrate levels in blood, as well as higher blood pressure, as compared to the controls. By depleting these mice from leukocytes or platelets, the differences between the chimeras lacking eNOS in blood and the wild type counterpart persisted. These results demonstrated for the first time that beside the enzyme that is expressed in the endothelium, also circulating blood cell eNOS plays a role in the control of vascular tone and blood pressure; furthermore, they suggest that RBCs, the most abundant cell population in blood, might be involved in mediating those effects.

If eNOS in blood indeed contributed to blood pressure regulation and nitrite production, then it is likely to also have effects under regenerative conditions, such as tissue repair following myocardial ischemia or stroke. In an acute model of myocardial I/R we found that chimeras lacking blood cell eNOS had increased infarct size, resulting in decreased ejection fraction and increased end systolic volume after 60 minutes ischemia and 24 hours of reperfusion, as described in § 3.2. (Merx, Gorressen *et al.* 2014). Application of the NOS inhibitor ethylenethiourea during ischemia and the first 5 minutes of reperfusion was associated with larger infarct size in mice carrying eNOS in blood, whereas infarct size in mice lacking blood cell eNOS was unaffected (Merx, Gorressen *et al.* 2014). RBCs from chimera lacking blood cell eNOS have decreased deformability, which may lead to decreased perfusion capacity of blood (Merx, Gorressen *et al.* 2014).

Taken together, these results show that circulating blood cell eNOS plays a role in the control of the circulating pool of NO metabolites, and further suggests a modulating role in I/R injury. Although compelling evidence indicates that RBC are involved in these effects, the blood cell populations responsible for cardioprotection have still to be identified.

4.2 eNOS IN RED BLOOD CELLS

The presence of a NOS-like activity in RBCs had been for a long time matter of controversy, and doubts about its functional significance, isoform identity and disease relevance remained. Using flow cytometry in combination with the NO-imaging probe DAF-FM we find that all blood cells form intracellular NO, with a rank order of monocytes > neutrophils > lymphocytes > RBCs > platelets, as described in § 3.3 (Cortese-Krott, Rodriguez-Mateos *et al.* 2012). The observation of a NO-related fluorescence within RBCs was unexpected given the abundance of the NO-scavenger oxyhemoglobin in these cells. Constitutive normoxic NO

formation was abolished by NOS inhibition and intracellular NO scavenging, confirmed by laser-scanning microscopy and unequivocally validated by detection of the DAF-FM reaction product with NO using HPLC and LC-MS/MS. Using immunoprecipitation, ESI-MS/MS-based peptide sequencing and enzymatic assay we further demonstrated that human RBCs contain an eNOS that converts L-^{3}H-arginine to L-^{3}H-citrulline in a Ca^{2+}/calmodulin-dependent fashion. Thus, these results show that human RBCs constitutively produce NO under normoxic conditions *via* an active eNOS isoform.

4.3. RED CELL ENOS, RBC DEFORMABILITY AND BLOOD FLOW

The ability of RBC to deform in response to physical forces (i.e. their deformability) is required for an efficient delivery of dioxygen and nutrients to the tissues. RBC deformability is known to reduce the viscosity of blood, and importantly allows the cells to participate in the flow and to enter and transit the capillaries that are even narrower than their own diameter (Wan, Forsyth *et al.* 2011). Thus, both capillary blood flow and RBC velocity strongly depend on RBC deformability (Chien 1987). Previous finding demonstrated that RBC deformability is increased by NO donors and decreased by inhibition of NOS activity (Bor-Kucukatay, Wenby *et al.* 2003, Kleinbongard, Schulz *et al.* 2006). We studied the effects of NO on RBC velocity by intravital microscopy in the microcirculation of the chorioallantoic membrane (CAM) of the avian embryo at day 7 post-fertilization, when all vessels lack smooth muscle cells and vascular tone is not affected by NO. We found that inhibition of enzymatic NO synthesis and NO scavenging decreased intracellular NO levels and avian RBC deformability *in vitro*. Injection of a NOS-inhibitor or a NO scavenger into the microcirculation of the CAM decreased capillary RBC velocity and deformation, while the diameter of the vessels remained constant (§ . The results indicate that scavenging of NO and inhibition of NO synthesis decrease RBC velocity not only by regulating vascular tone but also by decreasing RBC deformability.

4.4 ENOS IN MICROPARTICLES AND CIRCULATING ANGIOGENIC CELLS

MPs are circulating membrane particles of less than a micrometer in diameter shed from endothelial and blood cells. Using immunoprecipitation and Western blot analysis, we found that human circulating MPs carry an eNOS that converts L-^{3}H-arginine to L-^{3}H-citrulline in a Ca^{2+}/calmodulin-dependent fashion and produces NO, as described in § 3.5 (Horn, Cortese-Krott *et al.* 2012). Thus MPs are not just functionally inert cell debris, but may possess and carry biological functions from the originating cell and contribute to vascular homeostasis.

CACs, also termed endothelial progenitor cells, play an integral role in vascular repair. We found that similar to endothelial cells, CAC carry an eNOS and NOS activity is required for CAC chemotaxis in response to VEGF, as described in § 3.6 (Heiss, Schanz *et al.* 2010). In fact

CAC chemotaxis was blocked by inhibition of NOS, phosphatidylinositol 3-kinase, or sGC or by treatment with an NO scavenger. Addition of an the nitrosothiol S-nitroso-N-acetylpenicillamine and the NOS substrate l-arginine increased random cell migration (chemokinesis) and enhanced VEGF-dependent chemotaxis.

Taken together, these results show that different blood components carry an active eNOS. The relative contribution of these to the circulating pool of NO metabolites and cardiovascular hemodinamics has to be investigated in future.

4.5 DECLINE IN CIRCULATING ENOS ACTIVITY IN CORONARY ARTERY DISEASE.

Impaired endothelial function, decreased eNOS activity, and/or NO bioavailability are conditions strongly related to cardiovascular disease (Heiss, Lauer *et al.* 2006, Rassaf, Heiss *et al.* 2006). Perhaps one of the most surprising results from these studies (§ 3.3,5,6) is that expression and activity of circulating eNOS in red blood cells, CAC or MPs are decreased in patients with endothelial dysfunction as compared to healthy controls (Heiss, Schanz *et al.* 2010, Cortese-Krott, Rodriguez-Mateos *et al.* 2012, Horn, Cortese-Krott *et al.* 2013). We found that red eNOS expression and activity are decreased in patients with coronary artery disease as compared to age matched healthy controls and significantly correlate with flow-mediated dilation, a diagnostic marker of endothelial function and eNOS activity (Cortese-Krott, Rodriguez-Mateos *et al.* 2012). Similarly eNOS levels and activity are decreased in MPs from patients with peripheral artery occlusive disease as compared to young healthy controls. Moreover, eNOS could not be detected in CACs from CAD patients, and both chemokinesis and chemotaxis to VEGF were decreased compared with healthy CACs. Thus, a systemic eNOS deficiency and/or dysfunction appears to prevail in patients with cardiovascular disease the consequences of which are not limited to impaired vascular function, but may also affect function of blood cells and vascular homeostasis

4.7 MODULATION OF NO BIOAVAILABILITY BY SULFIDE

Nitrosothiols are an important storage form of NO (Rodriguez, Maloney *et al.* 2002, Broniowska and Hogg 2012). We found that the chemical reaction of nitrosothiols with sulfide leads to modulation of their NO-related bioactivity in a concentration-dependent fashion, giving rise to inhibition at low and potentiation at higher sulfide concentrations, as described in § 3.8(Cortese-Krott, Fernandez *et al.* 2014). Spectral analysis demonstrates that under conditions of excess sulfide $SSNO^-$ is formed, which release NO at higher rate and thus activates sGC more effectively than the starting nitrosothiol itself. While further detailed studies are warranted to identify the chemical nature and biological activity of other reaction products involved, the

chemical and biological properties of $SSNO^-$ suggest that nitrosopersulfide represents a new signaling entity at the cross-roads between sulfide and NO/polysulfide signaling.

The concentrations used in the present proof-of-principle studies are clearly well outside the physiologically relevant range. Nevertheless, the effects of sulfide on SNAP-induced cGMP accumulation in RFL-6 cells, suggest this interaction can occur also within cells; at present, this is mere speculation awaiting experimental confirmation by NMR and/or mass spectrometry based analytical techniques that allow unequivocal identification of $SSNO^-$ formation in cells and tissues.

The potential of sulfide to either attenuate or potentiate NO bioactivity may be of relevance to the regulation of vascular tone. From studies in rodent tissue we know that nitrosothiols are particularly abundant in the vasculature; the same seems to hold true for sulfide-related metabolites, at least in the aorta, and both, endothelial and smooth muscle cells have been shown to express the enzymatic machinery capable of generating H_2S (Rodriguez, Maloney *et al.* 2002, Levitt, Abdel-Rehim *et al.* 2011,Yang, Wu *et al.* 2008, Szabó and Papapetropoulos 2011, Kimura 2013). Sulfide may therefore contribute to the fine-tuning of NO bioactivity in the vasculature, either *via* modulation of intracellular cGMP concentrations following inhibition of PDE activity and/or, as demonstrated in the current study, by chemically reacting with nitrosothiols (Bucci, Papapetropoulos *et al.* 2010, Bucci, Papapetropoulos *et al.* 2012, Coletta, Papapetropoulos *et al.* 2012) .

4.8 SIGNIFICANCE

The studies presented here demonstrate that not only endothelial cells, but also blood cells contribute to the NO-dependent regulation of vascular homeostasis, and identify RBCs as active contributors to cardiovascular homeostasis and integrity.

RBCs are typically considered as shuttles of respiratory gases and nutrients for tissues, less so as compartments important to vascular integrity. However, RBC size distribution, number and integrity appear to profoundly affect cardiovascular morbidity and mortality as demonstrated in recent clinical studies with large patients cohorts (Sabatine, Morrow *et al.* 2005, Felker, Allen *et al.* 2007, Kulier, Levin *et al.* 2007, Anand 2008, Koch, Li *et al.* 2008, Tonelli, Sacks *et al.* 2008, Patel, Semba *et al.* 2010, Najjar, Rao *et al.* 2011). Patients with CAD and concomitant anemia have a poorer prognosis after myocardial infarction, percutaneous coronary intervention, and coronary artery bypass grafting, and are more prone to developing heart failure with fatal outcomes (Sabatine, Morrow *et al.* 2005, Kulier, Levin *et al.* 2007, Anand 2008). Surprisingly, erythropoietin treatment fails to improve diagnosis indicating that a compromised gas exchange/nutrient transport capacity of blood is insufficient to explain this outcome (Najjar, Rao *et al.* 2011). In a cohort of 40,000 patients baseline levels of hemoglobin

have been found to correlate with mortality after myocardial infarction according to a J-shaped relationship in that a mild decrease in baseline hemoglobin concentration (12-14 g/l) corresponds to a strong increase in mortality after acute cardiovascular events; these associations are difficult to explain by a decrease in the capacity of oxygen delivery to tissues (Bassand, Afzal *et al.* 2010).

Taken together, the results of these studies show that not only the endothelial NO production, but also the circulating eNOS contributes to the circulating pool of NO metabolites and play a role in the regulation of cardiovascular function. In addition, the cross-talk between NO and sulfide leads to formation of novel bioactive NO/sulfid metabolites, which may contribute to vascular homeostasis.

5 - AKWNOLEDGEMENTS

Writing the Acknowledgements part of a thesis is, I believe, for everybody quite a big challenge, and an emotional rolling coaster. All pictures describing every single moment of the path and the people met (and lost) on the way run in the head, and it is like watching a movie in the fast foreward mode, overwhelming somehow. I won't be able to name everybody, who helped me in this journey (sometimes only by saying the right word in the right moment), and I am going to forget to mention someone important for sure.

First, I would like to thank Univ-. Prof. Dr. Malte Kelm for carrying me to this important goal in my life (and different others), for believing in my qualities and giving me the chance to try, for teaching me the fine equilibrium between excellent science and scientific "business", and for challenging and pushing me a little, when needed. I will not be at this point writing the Aknowledgements without his help.

I have the rare fortune to have had people taking me on the hand, showing and teaching me how to do good science, how to write papers, how to think logically and how to believe in my creasy ideas and in me, without asking anything back. This kind of people are called Mentors sometimes. I need to thank Univ.-Prof. Dr. Victoria Kolb-Bachofen, Univ.-Prof. Klaus Dietrich-Kröncke and Univ.-Prof. Martin Feelisch for showing me the way.

I have to thank my friend Dr. Ulrike Hendgen-Cotta for a lot of things, so many that I cannot count, for being there for me everyday, and in particular for revising this thesis.

Without my people I would have never be able to do anything at all: I want to thank Sivatharsini Thasian-Sivarajah, Katerina Lysajah, Thomas Krenz and all my medical students past and present. I thank (already) Christina Panknin, Georg Wolf and Ralf Erkens, it is a real pleasure working with you guys. A though goes also to the people of the Cardiovascular research laboratory (actually to everybody), it is difficult to keep such a big lab and survive the "seasonal" depression and experimental issues without the help and collaboration of everybody. A special thank goes to Stefanie Becher, Simone Goressen, Anita Kossack, Thomas Krämer, Dominik Semmler, Christian Eickholt, Christos Ramos, Matthias Totzeck.

A big thank to the scientists who accepted to do creasy science with me and share with me their great expertise, knowledge, help and time: Thank you Christoph Suschek, Ana Rodriguez-

Mateos, Gunter GC Kuhnle, Evanthia Mergia, and from the Cardiology Department Patrick Horn, Roberto Sansone, Christian Heiss. A special thank goes to Christian Meyer and Tienush Rassaf for their help in different occasions.

The last words are for my family, my mother and my father, my brother, my aunt Maura and my uncle Francesco, my aunt Nice and my oncle Gianfrancesco "Dadú", my cousins Riccardo and Raffaella and for my fans during my whole life Gianna (Iaiu) and Enrico Veronesi, e a Cinzia Veronesi.

The very last words (and my heart) are for my husband Daniel, who always believed I will succeed and still believe I will continue to. Danke.

6 – REFERENCES

1 Aamand, R., Dalsgaard, T., Jensen, F. B., Simonsen, U., Roepstorff, A. and Fago, A. (2009). "Generation of nitric oxide from nitrite by carbonic anhydrase: a possible link between metabolic activity and vasodilation." *Am J Physiol Heart Circ Physiol* 297(6): H2068-H2074.

2 Ali, M. Y., Ping, C. Y., Mok, Y. Y., Ling, L., Whiteman, M., Bhatia, M. and Moore, P. K. (2006). "Regulation of vascular nitric oxide in vitroand in vivo; a new role for endogenous hydrogen sulphide?" *Br J Pharmacol* 149(6): 625-634.

3 Anand, I. S. (2008). "Anemia and chronic heart failure implications and treatment options." *J Am Coll Cardiol* 52(7): 501-511.

4 Anand, I. S., Kuskowski, M. A., Rector, T. S., Florea, V. G., Glazer, R. D., Hester, A., Chiang, Y. T., Aknay, N., Maggioni, A. P., Opasich, C., Latini, R. and Cohn, J. N. (2005). "Anemia and change in hemoglobin over time related to mortality and morbidity in patients with chronic heart failure: results from Val-HeFT." *Circulation* 112(8): 1121-1127.

5 Aubry, J. P., Dugas, N., Lecoanet-Henchoz, S., Ouaaz, F., Zhao, H., Delfraissy, J. F., Graber, P., Kolb, J. P., Dugas, B. and Bonnefoy, J. Y. (1997). "The 25-kDa soluble CD23 activates type III constitutive nitric oxide-synthase activity via CD11b and CD11c expressed by human monocytes." *J Immunol* 159(2): 614-622.

6 Bassand, J. P., Afzal, R., Eikelboom, J., Wallentin, L., Peters, R., Budaj, A., Fox, K. A., Joyner, C. D., Chrolavicius, S., Granger, C. B., Mehta, S. and Yusuf, S. (2010). "Relationship between baseline haemoglobin and major bleeding complications in acute coronary syndromes." *Eur Heart J* 31(1): 50-58.

7 Bor-Kucukatay, M., Wenby, R. B., Meiselman, H. J. and Baskurt, O. K. (2003). "Effects of nitric oxide on red blood cell deformability." *Am J Physiol Heart Circ Physiol* 284: H1577-H1584.

8 Bredt, D. S. and Snyder, S. H. (1994). "Nitric oxide: a physiologic messenger molecule." *Annu Rev Biochem* 63: 175-195.

9 Broniowska, K. A. and Hogg, N. (2012). "The chemical biology of S-nitrosothiols." *Antioxid Redox Signaling* 17(7): 969-980.

10 Bryan, N. S., Fernandez, B. O., Bauer, S. M., Garcia-Saura, M. F., Milsom, A. B., Rassaf, T., Maloney, R. E., Bharti, A., Rodriguez, J. and Feelisch, M. (2005). "Nitrite is a signaling molecule and regulator of gene expression in mammalian tissues." *Nat Chem Biol* 1(5): 290-297.

11 Bucci, M., Papapetropoulos, A., Vellecco, V., Zhou, Z., Pyriochou, A., Roussos, C., Roviezzo, F., Brancaleone, V. and Cirino, G. (2010). "Hydrogen sulfide is an endogenous inhibitor of phosphodiesterase activity." *Arterioscler Thromb Vasc Biol* 30(10): 1998-2004.

12 Bucci, M., Papapetropoulos, A., Vellecco, V., Zhou, Z., Zaid, A., Giannogonas, P., Cantalupo, A., Dhayade, S., Karalis, K. P., Wang, R., Feil, R. and Cirino, G. (2012). "cGMP-Dependent Protein Kinase Contributes to Hydrogen Sulfide-Stimulated Vasorelaxation." *PLoS One* 7(12): e53319.

13 Cabrales, P. (2007). "Effects of erythrocyte flexibility on microvascular perfusion and oxygenation during acute anemia." *Am J Physiol Heart Circ Physiol* 293: 1206-1215.

14 Chen, L. Y. and Mehta, J. L. (1998). "Evidence for the presence of L-arginine-nitric oxide pathway in human red blood cells: relevance in the effects of red blood cells on platelet function." *J Cardiovasc Pharmacol* 32(1): 57-61.

15 Chien, S. (1987). "Red cell deformability and its relevance to blood flow." *Annu Rev Physiol* 49: 177-192.

16 Cines, D. B., Pollak, E. S., Buck, C. A., Loscalzo, J., Zimmerman, G. A., McEver, R. P., Pober, J. S., Wick, T. M., Konkle, B. A., Schwartz, B. S., Barnathan, E. S., McCrae, K. R., Hug, B. A., Schmidt, A. M. and Stern, D. M. (1998). "Endothelial cells in physiology and in the pathophysiology of vascular disorders." *Blood* 91(10): 3527-3561.

17 Coletta, C., Papapetropoulos, A., Erdelyi, K., Olah, G., Módis, K., Panopoulos, P., Asimakopoulou, A., Gerö, D., Sharina, I. and Martin, E. (2012). "Hydrogen sulfide and nitric oxide are mutually dependent in the regulation of angiogenesis and endothelium-dependent vasorelaxation." *Proc. Natl. Acad. Sci. U.S.A.* 109(23): 9161-9166.

18 Cortese-Krott, M. M., Fernandez, B. O., Santos, J. L., Mergia, E., Grman, M., Nagy, P., Kelm, M., Butler, A. and Feelisch, M. (2014). "Nitrosopersulfide (SSNO(-)) accounts for sustained NO bioactivity of S-nitrosothiols following reaction with sulfide." *Redox Biol* 2: 234-244.

19 Cortese-Krott, M. M., Rodriguez-Mateos, A., Sansone, R., Kuhnle, G. G., Thasian-Sivarajah, S., Krenz, T., Horn, P., Krisp, C., Wolters, D., Heiss, C., Kroncke, K. D., Hogg, N., Feelisch, M. and Kelm, M. (2012). "Human red blood cells at work: identification and visualization of erythrocytic eNOS activity in health and disease." *Blood* 120(20): 4229-4237.

20 Cortese-Krott, M. M., Suschek, C. V., Wetzel, W., Kroncke, K. D. and Kolb-Bachofen, V. (2009). "Nitric oxide-mediated protection of endothelial cells from hydrogen peroxide is mediated by intracellular zinc and glutathione." *Am J Physiol Cell Physiol* 296(4): C811-820.

21 Cosby, K., Partovi, K. S., Crawford, J. H., Patel, R. P., Reiter, C. D., Martyr, S., Yang, B. K., Waclawiw, M. A., Zalos, G., Xu, X., Huang, K. T., Shields, H., Kim-Shapiro, D. B., Schechter, A. N., Cannon Iii, R. O. and Gladwin, M. T. (2003). "Nitrite reduction to nitric oxide by deoxyhemoglobin vasodilates the human circulation." *Nat Med* 9(12): 1498-1505.

22 Crawford, J. H., Isbell, T. S., Huang, Z., Shiva, S., Chacko, B. K., Schechter, A. N., rley-Usmar, V. M., Kerby, J. D., Lang, J. D., Jr., Kraus, D., Ho, C., Gladwin, M. T. and Patel, R. P. (2006). "Hypoxia, red blood cells, and nitrite regulate NO-dependent hypoxic vasodilation." *Blood* 107(2): 566-574.

23 Deliconstantinos, G., Villiotou, V., Stavrides, J. C., Salemes, N. and Gogas, J. (1995). "Nitric oxide and peroxynitrite production by human erythrocytes: a causative factor of toxic anemia in breast cancer patients." *Anticancer Res.* 15: 1435-1446.

24 Denninger, J. W. and Marletta, M. A. (1999). "Guanylate cyclase and the NO/cGMP signaling pathway." *Biochim Biophys Acta* 1411(2-3): 334-350.

25 Driessen, G. K., Haest, C. W., Heidtmann, H., Kamp, D. and Schmid-Schonbein, H. (1980). "Effect of reduced red cell "deformability" on flow velocity in capillaries of rat mesentery." *Pflugers Arch* 388(1): 75-78.

26 Ellsworth, M. L., Forrester, T., Ellis, C. G. and Dietrich, H. H. (1995). "The erythrocyte as a regulator of vascular tone." *Am J Physiol Heart Circ Physiol* 269(6): H2155-H2161.

27 Felker, G. M., Allen, L. A., Pocock, S. J., Shaw, L. K., McMurray, J. J., Pfeffer, M. A., Swedberg, K., Wang, D., Yusuf, S., Michelson, E. L. and Granger, C. B. (2007). "Red cell distribution width as a novel prognostic marker in heart failure: data from the CHARM Program and the Duke Databank." *J Am Coll Cardiol* 50(1): 40-47.

28 Filipovic, M. R., Miljkovic, J. L., Nauser, T., Royzen, M., Klos, K., Shubina, T., Koppenol, W. H., Lippard, S. J. and Ivanovic-Burmazovic, I. (2012). "Chemical Characterization of the Smallest S-Nitrosothiol, HSNO; Cellular Cross-talk of H2S and S-Nitrosothiols." *J Am Chem Soc* 134(29): 12016-12027.

29 Furchgott, R. F. and Zawadzki, J. V. (1980). "The obligatory role of endothelial cells in the relaxation of arterial smooth muscle by acetylcholine." *Nature* 288(5789): 373-376.

30 Gambaryan, S., Kobsar, A., Hartmann, S., Birschmann, I., Kuhlencordt, P. J., MÜLler Esterl, W., Lohmann, S. M. and Walter, U. (2008). "NO-synthase-/NO-independent regulation of human and murine platelet soluble guanylyl cyclase activity." *J Thromb Haemost* 6(8): 1376-1384.

31 Gladwin, M. T., Lancaster jr, J. R., Freeman, B. A. and Schechter, A. N. (2003). "Nitric oxide's reactions with hemoglobin: a view through the SNO-storm." *Nat Med* 9: 496-500.

32 Gladwin, M. T., Shelhamer, J. H., Schechter, A. N., Pease-Fye, M. E., Waclawiw, M. A., Panza, J. A., Ognibene, F. P. and Cannon III, R. O. (2000). "Role of circulating nitrite and S-nitrosohemoglobin in the regulation of regional blood flow in humans." *Proc Natl Acad Sci U.S.A.* 97: 11482-11487.

33 Godecke, A., Decking, U. K., Ding, Z., Hirchenhain, J., Bidmon, H. J., Godecke, S. and Schrader, J. (1998). "Coronary hemodynamics in endothelial NO synthase knockout mice." *Circ Res* 82(2): 186-194.

34 Griffith, O. W. and Stuehr, D. J. (1995). "Nitric oxide synthases: properties and catalytic mechanism." *Annu Rev Physiol* 57(1): 707-734.

35 Heiss, C., Lauer, T., Dejam, A., Kleinbongard, P., Hamada, S., Rassaf, T., Matern, S., Feelisch, M. and Kelm, M. (2006). "Plasma nitroso compounds are decreased in patients with endothelial dysfunction." *J Am Coll Cardiol* 47(3): 573-579.

36 Heiss, C., Schanz, A., Amabile, N., Jahn, S., Chen, Q., Wong, M. L., Rassaf, T., Heinen, Y., Cortese-Krott, M., Grossman, W., Yeghiazarians, Y. and Springer, M. L. (2010). "Nitric oxide synthase expression and functional response to nitric oxide are both important modulators of circulating angiogenic cell response to angiogenic stimuli." *Arterioscler Thromb Vasc Biol* 30: 2212-2218.

37 Hendgen-Cotta, U. B., Merx, M. W., Shiva, S., Schmitz, J., Becher, S., Klare, J. P., Steinhoff, H. J., Goedecke, A., Schrader, J., Gladwin, M. T., Kelm, M. and Rassaf, T. (2008). "Nitrite reductase activity of myoglobin regulates respiration and cellular viability in myocardial ischemia-reperfusion injury." *Proc Natl Acad Sci U.S.A.* 105(29): 10256-10261.

38 Herold, S. (2004). "The outer-sphere oxidation of nitrosyliron(II)hemoglobin by peroxynitrite leads to the release of nitrogen monoxide." *Inorg Chem Front* 43(13): 3783-3785.

39 Horn, P., Cortese-Krott, M. M., Amabile, N., Hundsdorfer, C., Kroncke, K. D., Kelm, M. and Heiss, C. (2013). "Circulating microparticles carry a functional endothelial nitric oxide synthase that is decreased in patients with endothelial dysfunction." *J Am Heart Assoc* 2(1): e003764.

40 Huang, P. L., Huang, Z., Mashimo, H., Bloch, K. D., Moskowitz, M. A., Bevan, J. A. and Fishman, M. C. (1995). "Hypertension in mice lacking the gene for endothelial nitric oxide synthase." *Nature* 377(6546): 239-242.

41 Ignarro, L. J. (1989). "Biological actions and properties of endothelium-derived nitric oxide formed and released from artery and vein." *Circ Res* 65(1): 1-21.

42 Jia, L., Bonaventura, C., Bonaventura, J. and Stamler, J. S. (1996). "S-nitrosohaemoglobin: a dynamic activity of blood involved in vascular control." *Nature* 380: 221-226.

43 Kajimura, M., Fukuda, R., Bateman, R. M., Yamamoto, T. and Suematsu, M. (2010). "Interactions of Multiple Gas-Transducing Systems: Hallmarks and Uncertainties of CO, NO, and H 2S Gas Biology." *Antioxid Redox Signal* 13(2): 157-192.

44 Kang, E. S., Ford, K., Grokulsky, G., Wang, Y. B., Chiang, T. M. and Acchiardo, S. R. (2000). "Normal circulating adult human red blood cells contain inactive NOS proteins." *J Lab Clin Med* 135: 444-451.

45 Kimura, H. (2014). "Production and physiological effects of hydrogen sulfide." *Antioxid Redox Signal,* 20(5):783-93.

46 King, S. B. (2013). "Potential biological chemistry of hydrogen sulfide (H2S) with the nitrogen oxides." *Free Radic Biol Med* 55: 1-7.

47 Kleinbongard, P., Dejam, A., Lauer, T., Rassaf, T., Schindler, A., Picker, O., Scheeren, T., Godecke, A., Schrader, J., Schulz, R., Heusch, G., Schaub, G. A., Bryan, N. S., Feelisch, M. and Kelm, M. (2003). "Plasma nitrite reflects constitutive nitric oxide synthase activity in mammals." *Free Radic Biol Med* 35(7): 790-796.

48 Kleinbongard, P., Schulz, R., Rassaf, T., Lauer, T., Dejam, A., Jax, T., Kumara, I., Gharini, P., Kabanova, S., Ozuyaman, B., Schnurch, H. G., Godecke, A., Weber, A. A., Robenek, M., Robenek, H., Bloch, W., Rosen, P. and Kelm, M. (2006). "Red blood cells express a functional endothelial nitric oxide synthase." *Blood* 107(7): 2943-2951.

49 Kleinert, H., Schwarz, P. M. and Forstermann, U. (2003). "Regulation of the expression of inducible nitric oxide synthase." *Biol Chem.* 384(10-11): 1343-1364.

50 Koch, C. G., Li, L., Sessler, D. I., Figueroa, P., Hoeltge, G. A., Mihaljevic, T. and Blackstone, E. H. (2008). "Duration of red-cell storage and complications after cardiac surgery." *N Engl J Med* 358(12): 1229-1239.

51 Kolluru, G. K., Shen, X., Bir, S. C. and Kevil, C. G. (2013). "Hydrogen sulfide chemical biology: Pathophysiological roles and detection." *Nitric Oxide* 35: 5-20.

52 Kulier, A., Levin, J., Moser, R., Rumpold-Seitlinger, G., Tudor, I. C., Snyder-Ramos, S. A., Moehnle, P. and Mangano, D. T. (2007). "Impact of preoperative anemia on outcome in patients undergoing coronary artery bypass graft surgery." *Circulation* 116(5): 471-479.

53 Kulier, A., Levin, J., Moser, R., Rumpold-Seitlinger, G., Tudor, I. C., Snyder-Ramos, S. A., Moehnle, P. and Mangano, D. T. (2007). "Impact of preoperative anemia on outcome in patients undergoing coronary artery bypass graft surgery." *Circulation* 116(5): 471-479.

54 Levitt, M. D., Abdel-Rehim, M. S. and Furne, J. (2011). "Free and Acid-Labile Hydrogen Sulfide Concentrations in Mouse Tissues: Anomalously High Free Hydrogen Sulfide in Aortic Tissue." *Antioxid Redox Signal* 15(2): 373-378.

55 Li, L., Rose, P. and Moore, P. K. (2011). Hydrogen Sulfide and Cell Signaling. Annu Rev Pharmacol Toxicol. **51:** 169-187.

56 Li, Q. and Lancaster, J. R., Jr. (2013). "Chemical foundations of hydrogen sulfide biology." *Nitric Oxide* 35C: 21-34.

57 Lipowsky, H. H., Cram, L. E., Justice, W. and Eppihimer, M. J. (1993). "Effect of erythrocyte deformability on in vivo red cell transit time and hematocrit and their correlation with in vitro filterability." *Microvasc Res* 46: 43-64.

58 Lundberg, J. O., Gladwin, M. T., Ahluwalia, A., Benjamin, N., Bryan, N. S., Butler, A., Cabrales, P., Fago, A., Feelisch, M., Ford, P. C., Freeman, B. A., Frenneaux, M., Friedman, J., Kelm, M., Kevil, C. G., Kim-Shapiro, D. B., Kozlov, A. V., Lancaster, J. R., Jr., Lefer, D. J., McColl, K., McCurry, K., Patel, R. P., Petersson, J., Rassaf, T., Reutov, V. P., Richter-Addo, G. B., Schechter, A., Shiva, S., Tsuchiya, K., van Faassen, E. E., Webb, A. J., Zuckerbraun, B. S.,

Zweier, J. L. and Weitzberg, E. (2009). "Nitrate and nitrite in biology, nutrition and therapeutics." *Nat Chem Biol* 5(12): 865-869.

59 Mantovani, A., Bussolino, F. and Introna, M. (1997). "Cytokine regulation of endothelial cell function: from molecular level to the bedside." *Immunol Today* 18: 231-240.

60 Mellander, S. (1989). "Functional aspects of myogenic vascular control." *J Hypertens Suppl* 7(4): S21-S30.

61 Merx, M. W., Gorressen, S., van de Sandt, A. M., Cortese-Krott, M. M., Ohlig, J., Stern, M., Rassaf, T., Godecke, A., Gladwin, M. T. and Kelm, M. (2014). "Depletion of circulating blood NOS3 increases severity of myocardial infarction and left ventricular dysfunction." *Basic Res Cardiol* 109(1): 398-408.

62 Mesquita, R., Picarra, B., Saldanha, C. and Martins e Silva, J. (2002). "Nitric oxide effects on human erythrocytes structural and functional properties - An in vitro study." *Clin Hemorheol Microcirc* 27: 137-147.

63 Metha, J. L., Metha, P. and Li, D. (2000). "Nitric oxide synthase in adult red blood cells: vestige of an earlier age or a biologically active enzyme?" *J Lab Clin Med* 135: 430-431.

64 Milsom, A. B., Fernandez, B. O., Garcia-Saura, M. F., Rodriguez, J. and Feelisch, M. (2012). "Contributions of nitric oxide synthases, dietary nitrite/nitrate, and other sources to the formation of NO signaling products." *Antioxid Redox Signal* 17(3): 422-432.

65 Moncada, S. (1997). "Nitric oxide in the vasculature: physiology and pathophysiology." *Ann NY Acad Sci* 811: 60-67; discussion 67-69.

66 Moncada, S., Palmer, R. M. and Higgs, E. A. (1991). "Nitric oxide: physiology, pathophysiology, and pharmacology." *Pharmacol Rev* 43(2): 109-142.

67 Morse, J. W., Millero, F. J., Cornwell, J. C. and Rickard, D. (2002). "The chemistry of the hydrogen sulfide and iron sulfide systems in natural waters." *Earth-Science Reviews* 24(1): 1-42.

68 Mühl, H. and Pfeilschifter, J. (2003). "Endothelial nitric oxide synthase: a determinant of TNFalpha production by human monocytes/macrophages." *Biochem Biophys Res Commun.* 310(3): 677-680.

69 Murillo, D., Kamga, C., Mo, L. and Shiva, S. (2011). "Nitrite as a mediator of ischemic preconditioning and cytoprotection." *Nitric Oxide* 25(2): 70-80.

70 Nagababu, E., Ramasamy, S., Albernethy, R. and Rifkind, M. (2003). "Active nitric oxide produced in the red cell under hypoxic conditions by deoxyhemoglobin-mediated nitrite reduction." *J Biol Chem.* 278: 46349-46356.

71 Najjar, S. S., Rao, S. V., Melloni, C., Raman, S. V., Povsic, T. J., Melton, L., Barsness, G. W., Prather, K., Heitner, J. F., Kilaru, R., Gruberg, L., Hasselblad, V., Greenbaum, A. B., Patel, M., Kim, R. J., Talan, M., Ferrucci, L., Longo, D. L., Lakatta, E. G. and Harrington, R. A. (2011). "Intravenous erythropoietin in patients with ST-segment elevation myocardial infarction: REVEAL: a randomized controlled trial." *JAMA* 305(18): 1863-1872.

72 Nathan, C. (2002). "Points of control in inflammation." *Nature* 420(6917): 846-852.

73 Nonella, M., Huber, R. and Ha, T.-K. (1987). "Photolytic Preparation and Isomerization of HNSO, HOSN, HSNO, and HONS in an Argon Matrix. An Experimental and Theoretical Study." *J Phys Chem* 91: 5203-5209.

74 Olson, K. R. (2012). "A Practical Look at the Chemistry and Biology of Hydrogen Sulfide." *Antioxid Redox Signal* 17(1): 32-44.

75 Ondrias, K., Stasko, A., Cacanyiova, S., Sulova, Z., Krizanova, O., Kristek, F., Malekova, L., Knezl, V. and Breier, A. (2008). "H(2)S and HS(-) donor NaHS releases nitric oxide from

nitrosothiols, metal nitrosyl complex, brain homogenate and murine L1210 leukaemia cells." *Pflugers Arch* 457(2): 271-279.

76 Ozüyaman, B., Gödecke, A., Küsters, S., Kirchhoff, E., Scharf, R. E. and Schrader, J. (2005). "Endothelial nitric oxide synthase plays a minor role in inhibition of arterial thrombus formation." *Thromb Haemost* 93(6):1161-7

77 Palmer, R. M., Ferrige, A. G. and Moncada, S. (1987). "Nitric oxide release accounts for the biological activity of endothelium-derived relaxing factor." *Nature* 327(6122): 524-526.

78 Patel, K. V., Semba, R. D., Ferrucci, L., Newman, A. B., Fried, L. P., Wallace, R. B., Bandinelli, S., Phillips, C. S., Yu, B., Connelly, S., Shlipak, M. G., Chaves, P. H., Launer, L. J., Ershler, W. B., Harris, T. B., Longo, D. L. and Guralnik, J. M. (2010). "Red cell distribution width and mortality in older adults: a meta-analysis." *J Gerontol A Biol Sci Med Sci* 65(3): 258-265.

79 Pries, A. R. and Secomb, T. W. (2003). "Rheology of the micorcirculation." *Clin Hemorheol Microcirc* 29: 143-148.

80 Radomski, M. W., Palmer, R. M. and Moncada, S. (1990). "An L-arginine/nitric oxide pathway present in human platelets regulates aggregation." *Proc Natl Acad Sci U.S.A.* 87(13): 5193-5197.

81 Rassaf, T., Bryan, N. S., Maloney, R. E., Specian, V., Kelm, M., Kalyanaraman, B., Rodriguez, J. and Feelisch, M. (2003). "NO adducts in mammalian red blood cells: too much or too little?" *Nat Med* 9: 481-482.

82 Rassaf, T., Heiss, C., Hendgen-Cotta, U., Balzer, J., Matern, S., Kleinbongard, P., Lee, A., Lauer, T. and Kelm, M. (2006). "Plasma nitrite reserve and endothelial function in the human forearm circulation." *Free Radic Biol Med* 41(2): 295-301.

83 Rautou, P. E., Vion, A. C., Amabile, N., Chironi, G., Simon, A., Tedgui, A. and Boulanger, C. M. (2011). "Microparticles, vascular function, and atherothrombosis." *Circ Res* 109(5): 593-606.

84 Rodriguez, J., Maloney, R. E., Rassaf, T., Bryan, N. S. and Feelisch, M. (2002). "Chemical nature of nitric oxide storage forms in rat vascular tissue." *Proc Natl Acad Sci U.S.A* 100(1): 336-341.

85 Rotella, C. M., Giannini, S., Galli, G., Cresci, B. and Tanini, A. (1996). "Role of endothelial cells in the pathogenesis of diabetic microangiopathy." *Diab Nutr Metab* 9: 273-289.

86 Sabatine, M. S., Morrow, D. A., Giugliano, R. P., Burton, P. B., Murphy, S. A., McCabe, C. H., Gibson, C. M. and Braunwald, E. (2005). "Association of hemoglobin levels with clinical outcomes in acute coronary syndromes." *Circulation* 111(16): 2042-2049.

87 Saluja, R., Jyoti, A., Chatterjee, M., Habib, S., Verma, A., Mitra, K., Barthwal, M. K., Bajpai, V. K. and Dikshit, M. (2011). "Molecular and biochemical characterization of nitric oxide synthase isoforms and their intracellular distribution in human peripheral blood mononuclear cells." *Biochim Biophys Acta* 1813(10): 1700-1707.

88 Sase, K. and Michel, T. (1995). "Expression of constitutive endothelial nitric oxide synthase in human blood platelets." *Life Sci* 57(22): 2049-2055.

89 Sessa, W. C. (2004). "eNOS at a glance." *J Cell Sci* 117(Pt 12): 2427-2429.

90 Shatalin, K., Shatalina, E., Mironov, A. and Nudler, E. (2011). "H2S: A Universal Defense Against Antibiotics in Bacteria." *Science (New York, N.Y.)* 334(6058): 986-990.

91 Shesely, E. G., Maeda, N., Kim, H. S., Desai, K. M., Krege, J. H., Laubach, V. E., Sherman, P. A., Sessa, W. C. and Smithies, O. (1996). "Elevated blood pressures in mice lacking endothelial nitric oxide synthase." *Proc Natl Acad Sci U.S.A.* 93(23): 13176-13181.

92 Shiva, S. and Gladwin, M. T. (2009). "Nitrite mediates cytoprotection after ischemia/reperfusion by modulating mitochondrial function." *Basic Res Cardiol* 104(2): 113-119.

93 Simchon, S., Jan, K. M. and Chien, S. (1987). "Influence of reduced red cell deformability on regional blood flow." *Am J Physiol* 253: H898-H903.

94 Sprague, R. S., Stephenson, A. H., Dimmitt, R. A., Weintraub, N. L., Branch, C. A., McMurdo, L. and Lonigro, A. J. (1995). "Effect of L-NAME on pressure-flow relationships in isolated rabbit lungs: role of red blood cells." *Am J Physiol* 269: H1941-H1948.

95 Starzyk, D., Korbut, R. and Gryglewski, R. J. (1999). "Effects of nitric oxide and prostacyclin on deformability and aggregability of red blood cells of rats ex vivo and in vitro." *J physiol Pharmacol* 50: 629-637.

96 Stuehr, D. J. (2004). "Enzymes of the L-arginine to nitric oxide pathway." *J Nutr* 134(10 Suppl): 2748S-2751S- discussion 2765S-2767S.

97 Szabó, C. and Papapetropoulos, A. (2011). "Hydrogen sulphide and angiogenesis: mechanisms and applications." *Br J Pharmacol* 164(3): 853-865.

98 Teng, X., Scott Isbell, T., Crawford, J. H., Bosworth, C. A., Giles, G. I., Koenitzer, J. R., Lancaster, J. R., Doeller, J. E., W Kraus, D. and P Patel, R. (2008). "Novel method for measuring S-nitrosothiols using hydrogen sulfide." *Methods Enzymol* 441: 161-172.

99 Tonelli, M., Sacks, F., Arnold, M., Moye, L., Davis, B., Pfeffer, M., Cholesterol, f. t. and Investigators, R. E. T. (2008). "Relation Between Red Blood Cell Distribution Width and Cardiovascular Event Rate in People With Coronary Disease." *Circulation* 117(2): 163-168.

100 Totzeck, M., Hendgen-Cotta, U. B., Luedike, P., Berenbrink, M., Klare, J. P., Steinhoff, H. J., Semmler, D., Shiva, S., Williams, D., Kipar, A., Gladwin, M. T., Schrader, J., Kelm, M., Cossins, A. R. and Rassaf, T. (2012). "Nitrite regulates hypoxic vasodilation via myoglobin-dependent nitric oxide generation." *Circulation* 126(3): 325-334.

101 Vallance, P., Collier, J. and Moncada, S. (1989). "Effects of endothelium-derived nitric oxide on peripheral arteriolar tone in man." *Lancet* 2(8670): 997-1000.

102 van Faassen, E. E., Bahrami, S., Feelisch, M., Hogg, N., Kelm, M., Kim-Shapiro, D. B., Kozlov, A. V., Li, H., Lundberg, J. O., Mason, R., Nohl, H., Rassaf, T., Samouilov, A., Slama-Schwok, A., Shiva, S., Vanin, A. F., Weitzberg, E., Zweier, J. and Gladwin, M. T. (2009). "Nitrite as regulator of hypoxic signaling in mammalian physiology." *Med Res Rev* 29(5): 683-741.

103 Vita, J. A. (2011). "Endothelial function." *Circulation* 124(25): e906-e912.

104 Wan, J., Forsyth, A. M. and Stone, H. A. (2011). "Red blood cell dynamics: from cell deformation to ATP release." *Integr Biol (Camb)* 3(10): 972-981.

105 Wang, R. (2011). "Signaling pathways for the vascular effects of hydrogen sulfide." *Curr Opin Nephrol Hypertens* 20(2): 107-112.

106 Webb, A., Milsom, A., Rathod, K., Chu, W., Qureshi, S., Lovell, M., Lecomte, F., Perrett, D., Raimondo, C., Khoshbin, E., Ahmed, Z., Uppal, R., Benjamin, N., Hobbs, A. and Ahluwalia, A. (2008). "Mechanisms underlying erythrocyte and endothelial nitrite reduction to nitric oxide in hypoxia: role for xanthine oxidoreductase and endothelial nitric oxide synthase." *Circ Res* 103(9): 957-964.

107 Webb, A. J., Patel, N., Loukogeorgakis, S., Okorie, M., Aboud, Z., Misra, S., Rashid, R., Miall, P., Deanfield, J., Benjamin, N., MacAllister, R., Hobbs, A. J. and Ahluwalia, A. (2008). "Acute blood pressure lowering, vasoprotective, and antiplatelet properties of dietary nitrate via bioconversion to nitrite." *Hypertension* 51(3): 784-790.

108 Whiteman, M., Li, L., Kostetski, I., Chu, S. H., Siau, J. L., Bhatia, M. and Moore, P. K. (2006). "Evidence for the formation of a novel nitrosothiol from the gaseous mediators nitric oxide and hydrogen sulphide." *Biochem Biophys Res Commun* 343(1): 303-310.

109 Williams, D. L. H. (2004). Nitrosation Reactions and the Chemistry of Nitric Oxide. Amsterdam, The Nederlands, Elsevier.

110 Wood, K. C., Cortese-Krott, M. M., Kovacic, J. C., Noguchi, A., Liu, V. B., Wang, X., Raghavachari, N., Boehm, M., Kato, G. J., Kelm, M. and Gladwin, M. T. (2013). "Circulating blood endothelial nitric oxide synthase contributes to the regulation of systemic blood pressure and nitrite homeostasis." *Arterioscler Thromb Vasc Biol* 33(8): 1861-1871.

111 Yang, B. C., Nichols, W. W. and Mehta, J. L. (1996). "Cardioprotective Effects of Red Blood Cells on Ischemia and Reperfusion Injury in Isolated Rat Heart: Release of Nitric Oxide as a Potential Mechanism." *J Cardiovasc Pharmacol Ther* 1(4): 297-306.

112 Yang, G., Wu, L., Jiang, B., Yang, W., Qi, J., Cao, K., Meng, Q., Mustafa, A. K., Mu, W., Zhang, S., Snyder, S. H. and Wang, R. (2008). "H(2)S as a physiologic vasorelaxant: Hypertension in mice with deletion of cystathionine gamma-lyase." *Science* 322(5901): 587-590.

113 Yang, J., Gonon, A. T., Sjoquist, P. O., Lundberg, J. O. and Pernow, J. (2013). "Arginase regulates red blood cell nitric oxide synthase and export of cardioprotective nitric oxide bioactivity." *Proc Natl Acad Sci U.S.A.* 110(37): 15049-15054.

114 Yong, Q.-C., Hu, L.-F., Wang, S., Huang, D. and Bian, J.-S. (2010). "Hydrogen sulfide interacts with nitric oxide in the heart: possible involvement of nitroxyl." *Cardiovasc Res* 88(3): 482-491.

115 Yong, Q. C., Cheong, J. L., Hua, F., Deng, L. W., Khoo, Y. M., Lee, H. S., Perry, A., Wood, M., Whiteman, M. and Bian, J. S. (2011). "Regulation of heart function by endogenous gaseous mediators-crosstalk between nitric oxide and hydrogen sulfide." *Antioxid Redox Signal* 14(11): 2081-2091.

116 Yoon, P. J., Parajuli, S. P., Zuo, D. C., Shahi, P. K., Oh, H. J., Shin, H. R., Lee, M. J., Yeum, C. H., Choi, S. and Jun, J. Y. (2011). "Interplay of hydrogen sulfide and nitric oxide on the pacemaker activity of interstitial cells of cajal from mouse small intestine." *Chonnam Medical Journal* 47(2): 72.

118 Zweier, J. L., Wang, P., Samouilov, A. and Kuppusamy, P. (1995). "Enzyme-independent formation of nitric oxide in biological tissues." *Nat Med* 1(8): 804-809.

7. – APPENDIX

7.1 LEBENSLAUF

7.1.1 Allgemeine Angaben

Name	**Cortese-Krott, Miriam Margherita**, Dr. rer. nat. Dr. (Geb. Cortese)
Geburtsdatum, -ort	04.09.1977, Mailand (Italien), weiblich
Eltern	Univ.-.Prof. Dr. Alessandro Cortese, Dr. Romana Cortese
Nationalität	italienisch
Familienstand	verheiratet mit Dipl.–Kfm. Daniel Krott
Kinder	/
Sprachen	Italienisch (Muttersprache), Englisch (fließend in Wort und Schrift), Deutsch (fließend in Wort, gut bis sehr gut in Schrift), Französisch (gut in Wort und Schrift),
Literarische Sprachen	Latein, Altgriechisch
Privatanschrift	Neustraße 38, 52066 Aachen
Institutsanschrift	CVRL - Cardiovascular Research Laboratory Klinik für Kardiologie, Pneumologie und Angiologie Universitätsklinikum der Heinrich-Heine-Universität Düsseldorf Universitätsstraße 1 40225 Düsseldorf Telefon: 0211 81 15893 miriam.cortese@uni-duesseldorf.de
derzeitige Position	Leiterin des CVRL - Cardiovascular Research Laboratory der Klinik für Kardiologie, Pneumologie und Angiologie

7.1.2 Schulausbildung und Schulabschluss

09/1983 - 06/1988	Grundschule. Scuola elementare „Piolti DeBianchi Gaspara Stampa“, Mailand
09/1988 - 06/1991	Mittelschule. Scuola Media Statale „O. Tabacchi“, Mailand
09/1991- 06/1996	Gymansium. Liceo Classico „A. Manzoni“, Mailand.
07/96 Maturitá (Abitur)	Maturitá Classica, Note 52/60. Liceo Classico „A. Manzoni“, Mailand.

7.1.3 Akademische Ausbildung mit Abschluss

Studium	03/2002, Laurea (italienische Promotion zum Dr. Biotechnologie), Fakultät für Pharmazie, Universität Mailand (110/110 cum laude, summa cum laude), Prof. Dr. C. Sirtori, Prof. Dr. G. Chiesa
	09/1996-12/2001, Biotechnologie, Fakultät für Pharmazie, Universität Mailand

7.1.4 Wissenschaftliche Abschlüsse

Promotion	2007, Pharmazie, Forschungsgruppe Immunologie, Institut für Molekulare Medizin Heinrich-Heine-Universität Düsseldorf, Promotion Dr. rer. nat. (summa cum laude), Prof. Dr. V. Kolb-

Bachofen, Prof. Dr. P. Proksch. Externer Gutachter: Prof. Dr. U. Förstermann, Johannes-Gutenberg-Universität Mainz

7.1.5 Beruflicher Werdegang ab Studienabschluss

seit 06/2009	Wissenschaftliche Mitarbeiterin/Postdoktorandin, Klinik für Kardiologie, Pneumologie und Angiologie, Universitätsklinikum Düsseldorf, Prof. Dr. M. Kelm
06/2008 – 05/2009	Wissenschaftliche Mitarbeiterin/Postdoktorandin, Klinik für Kardiologie, Pneumologie und Angiologie, Medizinische Klinik I, Universitätsklinikum Aachen, RWTH Aachen, Prof. Dr. M. Kelm
09/2006 – 06/2008	Wissenschaftliche Mitarbeiterin/Postdoktorandin, Klinik für Plastische Chirurgie, und Klinik für Gefäßchirurgie Universitätsklinikum Aachen, RWTH Aachen, Prof. Dr. N. Pallua, Prof. Dr. Ch. Suschek, Prof. Dr. M. Jacobs
12/2002 – 08/2006	Doktorandin, Heinrich-Heine-Universität Düsseldorf, Institut für Molekulare Medizin, Forschungsgruppe Immunbiologie, Prof. Dr. V. Kolb-Bachofen
03/2002 – 11/2002	Stipendiatin, DIBIT, S. Raffaele Hospital, Mailand
06/2000 – 03/2002	Promotionsstudentin, Atherosclerosis Labor, Fakultät für Pharmazie, Universität Mailand, Prof. Dr. C. Sirtori, Prof. Dr. G. Chiesa

7.1.6 Fortbildungen/Weiterbildungen

- Fachkunde gem. § 9 des geltendes Tierschutztgesetz
- Genhemigungbedürftiger Umgang mi fest eingebauten und umschlossenen radioaktiven Stoffen
- Fachkunde für Projekleiter und BBS (§ 15 Abs. 4 GenTSV)

7.1.7 Sonstiges/Preise

2013	**Eingeladene Referentin** (Invited speaker) „Gordon Research Conference on Nitric Oxide“, Ventura, CA, USA.
2012	**„Young Investigator award for excellence in science“**, Society for Free Radical Research international – Oxygen Club of California. „(-)-Epicatechin increases systemic Nrf2-dependent response and vascular function in mice“.
2011	„**Travel Award“**, Society of Free Radical Biology and Medicine (SFRBM) Meeting, Atlanta, GE, USA. Abstract: “Decreased expression and activity of red cell eNOS correlate with endothelial dysfunction in humans” (Vortrag)
2010	„**Young Investigator Award For Outstanding Translational Science“**, SFRBM/FRRI Meeting, Orlando, Florida. Abstract: “Isolation and characterization of an endothelial nitric oxide synthase in human red blood cells” (Vortrag)
2007 – 2008	**Mentee**, Mentoring Programm TANDEMplusMED für Frauenförderung in der Wissenschaft (Mentor: Prof. Salvador Moncada, The Wolfson Institute for Biomedical Research, University College London)
2006	**Young Investigator Awards** im Rahmen des “Second International Joint Meeting of the German and French Nitric Oxide Societies”, Hamburg

7.1.8 Mitgliedschaften

- Society of Free Radical Biology and Medicine
- The Biochemical society

7.1.9 Reviewertätigkeit

- Antioxidant and redox signaling (reviewer editor)

- Free Radical Biology and Medicine
- PLOSone
- Nitric Oxide-Biology and Medicine
- Toxicology Letters
- Biochemical pharmacology

7. 2 LEHRE

7.2.1 Praktika, Seminare, Vorlesungen

2002-2006	Praktikum – "Immunobiologische und Biochemische Verfahren für Medizinstudenten" (1 Woche/Semester), Forschungsgruppe Immunbiologie, Medizinische Fakultät, Heinrich-Heine-Universität Düsseldorf (Univ.-Prof. Dr. Victoria Kolb-Bachofen, and Univ.-Prof. Dr. Christoph Suschek)
Seit 2002	Seminar – Gute Wissenschaffliche Praxis, Einführung in praktische Labortätigkeiten (Bachelor/Masterstudenten, Doktoranden, Medizinstudenten, Technische Assistenten).
Seit 2010	Seminar - „Methods in cardiovascular research" Internes Seminar des Kardiologischen Labors, Klinik für Kardiologie, Angiologie und Pneumologie, Universitätsklinikum Düsseldorf (Univ.-Prof. Dr. M. Kelm)
Seit 2010	Seminar – "Integriertes Seminar Biochemie", Medizinische Fakultät, Heinrich-Heine-Universität Düsseldorf (Univ.-Prof. Dr. rer. nat W. Stahl)
Seit 2010	Seminar – "Laborsicherheit und Gentechnik". Internes Seminar des Kardiologischen Labors, Klinik für Kardiologie, Angiologie und Pneumologie, Universitätsklinikum Düsseldorf (Univ.-Prof. Dr. M. Kelm)
Seit 2012	Seminar – "Fortschritte translationaler Aspekte der Kardiologie", Medizinische Fakultät, Heinrich-Heine-Universität Düsseldorf
Seit 2012	Seminar – „Experimentelle Kardiologie" Medizinische Fakultät, Heinrich-Heine-Universität Düsseldorf
03/2014	Vorlesung – „Erythrocytes", IRTG, Medizinische Fakultät, Heinrich-Heine-Universität Düsseldorf

7.2.2 Betreute Dissertationen

Dr. med. Meike Munschow	Universitätsklinikum Aachen, RWTH, „Silver ions induce oxidative stress and intracellular zinc release in human skin fibroblasts MD, "magna cum laude" 2009 (First Supervisor. Prof. Dr. rer. nat. Christoph V. Suschek)
Dr. rer.nat. Thomas Krenz	Heinrich-Heine-Universität Düsseldorf, "The role of epicatechin in vascular control". 1. Gutachter: Univ.-Prof. Dr.med. Malte Kelm. 2. Gutachter: Univ.-Prof. Dr. rer. nat. Eckhart Lammert.
Tristan Römer	MedResSchool Düsseldorf. "New methods for studying the expression, activity and function of the NO synthase in human red blood cells" 1. Gutachter: Univ.-Prof. Dr.med. Malte Kelm. Prüfung am 22.5.2014
Franziska Strigl	MedResSchool Düsseldorf. The role of intracellular redox state and NO production in maus and human RBC from patients with CAD. 1. Gutachter: Univ.-Prof. Dr.med. Malte Kelm. Submitted.
Larissa Getinger	MedResSchool Düsseldorf. "Down-regulation of iNOS expression and activity via zinc: A new NO-mediated anti-inflammatory feedback mechanism?". 1. Gutachter: Univ.-Prof. Dr.med. Malte Kelm.
Friederike Oberle	MedResSchool Düsseldorf. "The role of (-)epicatechin in redox state and NO production in human endothelial cells". 1. Gutachter: Univ.-Prof. Dr.med. Malte Kelm.
Kim Weber	MedResSchool Düsseldorf. "The role of (-)epicatechin in control of redox state in vivo in mice". 1. Gutachter: PD Dr.med. Christian Heiss.

David Vujnovac	MedResSchool Düsseldorf. „Regulation of cGMP synthesis in RBC“. 1. Gutachter: Univ.-Prof. Dr.med. Malte Kelm.
Maximilian Ziegler	MedResSchool Düsseldorf. “Characterization of the eNOS/sGC/cGMP pathway in RBC”. 1. Gutachter: Univ.-Prof. Dr.med. Malte Kelm.
David Pullmann	MedResSchool Düsseldorf. “Role of gasotransmitters in the activation of Nrf2-mediated respense in the endothelium”. 1. Gutachter: Univ.-Prof. Dr.med. Malte Kelm.
Magalie Haeberlein	MedResSchool Düsseldorf. “Role of Nrf2 inducers in maintenance of redox state of endothelial cells”. 1. Gutachter: Univ.-Prof. Dr.med. Malte Kelm.
Mathias Weidenbach	MedResSchool Düsseldorf. “Role of Nrf2 in cardiovascular function in vivo” ”. 1. Gutachter: Prof. Dr.med. Malte Kelm.
Jens Brown	MedResSchool Düsseldorf. “Molecular mechanisms responsible for vasodilatatory activity of gasotransmitters ” 1. Gutachter: Univ.-Prof. Dr.med. Malte Kelm.
Guido Weipenhans	MedResSchool Düsseldorf. “Role of gasotransmitters in control of vascular function” 1. Gutachter: Univ.-Prof. Dr.med. Malte Kelm.
Annette Rauf	MedResSchool Düsseldorf. “Role of erythrocytes in production and control of gasotransmitters”. 1. Gutachter: Univ.-Prof. Dr.med. Malte Kelm.
Christina Panknin	Heinrich-Heine-Universität Düsseldorf, Promotion Pharmazie, „Role of red cell eNOS in regulation of the vascular tone“. 1. Gutachter: Univ.-Prof. Dr.med. Malte Kelm. 2.Gutachter: Univ.-Prof. Dr. Peter Proksch.

7.3. EINGEWORBENE DRITTMITTEL

2014-2016 **Funktion:** Projektleiter.

Projekttitel: “Role of red cell eNOS in cardioprotection against I/R Injury”.

Fördernde Organisation/Einrichtung: Forschungskommission, Medizinische Fakultät, Heinrich-Heine-Universität Düsseldorf.

Fördersumme: 100.000 €

2014-2015 **Funktion:** Projektleiter.

Projekttitel: "Red cell eNOS as a biomarker in endothelial dysfunction: significance to translational research."

Fördernde Organisation/Einrichtung: Grant4Target- Bayer Healtcare.

Fördersumme: 25.000 €

2012-2014 **Funktion:** Zweiter Projektleiter / Studenten-Betreuerin (Projektleiter: Univ.Prof.Dr. M. Kelm).

Projekttitel: “Role of dietary intervention for prevention of development of arterial hypertension in metabolic syndrome”.

Fördernde Organisation/Einrichtung: Research Training Group Vivid: "*In vivo* investigations in metabolic pathomechanisms and diseases in Düsseldorf", Heinrich-Heine-Universität, Düsseldorf.

Fördersumme: 105.000 €

2011-2013 **Funktion:** Projektleiter.

Projekttitel: "Role of non-endothelial eNOS in blood pressure regulation”.

Fördernde Organisation/Einrichtung: Forschungskommission, Medizinische Fakultät, Heinrich-Heine-Universität Düsseldorf.

Fördersumme: 150.000 €

7.4. VERZEICHNIS DER WISSENSCHAFLICHEN PUBLIKATIONEN

SUMME IF: 82.45
SUMME gewichtete IF: 58.40

7.4.1 Originalpublikationen

* geteilte Autorschaft

1. Rodriguez-Mateos A, Toro-Funes N, Cifuentes-Gomez T, **Cortese-Krott M**, Heiss C, Spencer JP. Uptake and metabolism of (-)-epicatechin in endothelial cells. *Arch Biochem Biophys***.** 2014 Apr 6. doi:10.1016/j.abb.2014.03.014. PubMed PMID: 24717599.

   IF 3.370; 5-Years-IF 3.097

2. **Cortese-Krott MM**, Fernandez BO, Santos JL, Mergia E, Grman M, Nagy P, Kelm M, Butler A, Feelisch M. Nitrosopersulfide (SSNO(-)) accounts for sustained NO bioactivity of S-nitrosothiols following reaction with sulfide. *Redox Biol.* 2014 Jan 11;2:234-44. doi: 10.1016/j.redox.2013.12.031. PubMed PMID: 24494198.

   IF not assigned (established in 2013)

3. Merx MW*, Gorressen S*, van de Sandt AM, **Cortese-Krott MM**, Ohlig J, Stern M, Rassaf T, Gödecke A, Gladwin MT, Kelm M. Depletion of circulating blood NOS3 increases severity of myocardial infarction and left ventricular dysfunction. *Basic Res Cardiol.* 2014 Jan;109(1):398. doi: 10.1007/s00395-013-0398-1. Epub 2013 Dec 18. PubMed PMID: 24346018.

   IF 5.904; 5-Years-IF 5.362

4. Stegbauer J, Friedrich S, Potthoff SA, Broekmans K, **Cortese-Krott MM**, Quack I, Rump LC, Koesling D, Mergia E. Phosphodiesterase 5 attenuates the vasodilatory response in renovascular hypertension. PLoS One. 2013 Nov 15;8(11):e80674. doi: 10.1371/journal.pone.0080674. PubMed PMID: 24260450.

   IF 3.730; 5-Years-IF 4.244

5. Wood KC*, **Cortese-Krott MM**,* Kovacic JC, Noguchi A, Liu VB, Wang X, Raghavachari N, Boehm M, Kato GJ, Kelm M, Gladwin MT. Circulating blood endothelial nitric oxide synthase contributes to the regulation of systemic blood pressure and nitrite homeostasis. *Arterioscler Thromb Vasc Biol*. 2013 Aug;33(8):1861-1871. Epub 2013 May 23. PubMed PMID: 23702660.

   IF 6.338; 5-Years-IF 6.986

6. Haendeler J, Mlynek A, Büchner N, Lukosz M, Graf M, Guettler C, Jakob S, Farrokh S, Kunze K, Goy C, Guardiola-Serrano F, Schaal H, **Cortese-Krott M**, Deenen R, Köhrer K, Winkler C, Altschmied J. Two isoforms of Sister-Of-Mammalian Grainyhead have opposing functions in endothelial cells and in vivo. *Arterioscler Thromb Vasc Biol.* 2013 Jul;33(7):1639-46. doi: 10.1161/ATVBAHA.113.301428. Epub 2013 May 16. PubMed PMID: 23685552.

   IF 6.338; 5-Years-IF 6.986

7. **Cortese-Krott MM,** Rodriguez-Mateos A, Kuhnle GG, Brown G, Feelisch M, Kelm M. A multilevel analytical approach for detection and visualization of intracellular NO production and nitrosation events using diaminofluoresceins. *Free Radic Biol Med.* 2012 Dec 1;53(11):2146-58. doi: 10.1016/j.freeradbiomed.2012.09.008. Epub2012 Sep 28. PubMed PMID: 23026413.

   IF 5.271; 5-Years-IF 5.969

8. **Cortese-Krott MM**, Rodriguez-Mateos A, Sansone R, Kuhnle GG, Thasian-Sivarajah S, Krenz T, Horn P, Krisp C, Wolters D, Heiß C, Kröncke KD, Hogg N, Feelisch M, Kelm M. Human red blood cells at

work: identification and visualization of erythrocytic eNOS activity in health and disease. *Blood.* 2012 Nov15;120(20):4229-37. doi: 10.1182/blood-2012-07-442277. Epub 2012 Sep 24. PubMed PMID: 23007404.

IF 9.060; 5-Years-IF 9.378

9. Horn P*, **Cortese-Krott MM***, Amabile N, Hundsdörfer C, Kröncke KD, Kelm M, Heiss C. Circulating microparticles carry a functional endothelial nitric oxide synthase that is decreased in patients with endothelial dysfunction. *J Am Heart Assoc.* 2012 Dec 31;2(1):e003764. doi: 10.1161/JAHA.112.003764. PubMed PMID: 23525410; PubMed Central PMCID: PMC3603231.

IF not assigned (established in 2012)

10. Horn P*, **Cortese-Krott MM***, Keymel S, Kumara I, Burghoff S, Schrader J, Kelm M, Kleinbongard P. Nitric oxide influences red blood cell velocity independently of changes in the vascular tone. *Free Radic Res.* 2011 Jun;45(6):653-61. doi:10.3109/10715762.2011.574288. Epub 2011 Apr 11. PubMed PMID: 21480762.

IF 2.878; 5-Years-IF 2.745

11. Heiss C, Schanz A, Amabile N, Jahn S, Chen Q, Wong ML, Rassaf T, Heinen Y,**Cortese-Krott** M, Grossman W, Yeghiazarians Y, Springer ML. Nitric oxide synthase expression and functional response to nitric oxide are both important modulators of circulating angiogenic cell response to angiogenic stimuli. *Arterioscler Thromb Vasc Biol.* 2010 Nov;30(11):2212-8. doi: 10.1161/ATVBAHA.110.211581. Epub 2010 Aug 12. PubMed PMID: 20705916; PubMed Central PMCID: PMC2959135.

IF 7.215; 5-Years-IF 7.544

12. **Cortese-Krott MM**, Münchow M, Pirev E, Hessner F, Bozkurt A, Uciechowski P,Pallua N, Kröncke KD, Suschek CV. Silver ions induce oxidative stress andintracellular zinc release in human skin fibroblasts. *Free Radic Biol Med.* 2009Dec 1;47(11):1570-7. doi: 10.1016/j.freeradbiomed.2009.08.023. Epub 2009 Sep 3.

IF 6.801; 5-Years-IF 5.791

13. **Cortese-Krott MM**, Suschek CV, Wetzel W, Kröncke KD, Kolb-Bachofen V. Nitric oxide-mediated protection of endothelial cells from hydrogen peroxide is mediated by intracellular zinc and glutathione. *Am J Physiol Cell Physiol.* 2009 Apr;296(4):C811-20. doi: 10.1152/ajpcell.00643.2008. Epub 2009 Feb 4. PubMed PMID: 19193864.

IF 4.013; 5-Years-IF 4.128

14. **Cortese MM**, Suschek CV, Wetzel W, Kröncke KD, Kolb-Bachofen V. Zinc protects endothelial cells from hydrogen peroxide via Nrf2-dependent stimulation of glutathione biosynthesis. *Free Radic Biol Med.* 2008 Jun 15;44(12):2002-12. doi: 10.1016/j.freeradbiomed.2008.02.013. Epub 2008 Mar 8. PubMed PMID: 18355458.

IF 5.399; 5-Years-IF 5.632

15. Opländer C, Wetzel W, **Cortese MM**, Pallua N, Suschek CV. Evidence for a physiological role of intracellularly occurring photolabile nitrogen oxides in human skin fibroblasts. *Free Radic Biol Med.* 2008 May 1;44(9):1752-61 doi: 10.1016/j.freeradbiomed.2008.01.030. Epub 2008 Feb 13. PubMed PMID: 18328270.

IF 5.399; 5-Years-IF 5.632

16. Bozkurt A, Tholl S, Wehner S, Tank J, **Cortese M**, O'Dey Dm, Deumens R, Lassner F, Schügner F, Gröger A, Smeets R, Brook G, Pallua N. Evaluation of functional nerve recovery with Visual-SSI--a novel computerized approach for the assessment of the static sciatic index (SSI). *J Neurosci Methods*. 2008 May 15;170(1):117-22.doi: 10.1016/j.jneumeth.2008.01.006. Epub 2008 Jan 18. PubMed PMID: 18325596.

    IF 2.114; 5-Years-IF 2.484

17. Opländer C, **Cortese MM**, Korth HG, Kirsch M, Mahotka C, Wetzel W, Pallua N, Suschek CV. The impact of nitrite and antioxidants on ultraviolet-A-induced cell death of human skin fibroblasts. *Free Radic Biol Med.* 2007 Sep 1;43(5):818-29.Epub 2007 May 31. PubMed PMID: 17664145.

IF 4.813; 5-Years-IF 5.512

18. Parolini C, Chiesa G, Gong E, Caligari S, **Cortese MM**, Koga T, Forte TM, Rubin EM. Apolipoprotein A-I and the molecular variant apoA-I(Milano): evaluation of the antiatherogenic effects in knock-in mouse model. *Atherosclerosis.* 2005 Dec;183(2):222-9. Epub 2005 Apr 21. PubMed PMID: 16285990.

IF 3.777

7.4.2 Übersichtsartikel

1. **Cortese-Krott MM**, Kelm M. Endothelial nitric oxide synthase in red blood cells: Key to a new erythrocrine function? *Redox Biol.* 2014 Jan 9;2:251-258. Review. PubMed PMID: 24494200.

    IF not assigned (established in 2013)

7.4.3 Andere Publikationen/Buchbeiträge

1. Kelm M., **Cortese-Krott MM**, Hendgen-Cotta, U., Horn,P. Stickstoffmonoxid und Nitrit als Mediatoren im kardiovaskulären System: Synthesewege, Speicherformen und Wirkmechanismen Jahrbuch der Heinrich-Heine-Universität Düsseldorf 2009/2010 Düsseldorf University Press, Duisburg (ss 49-62)
2. **Cortese, M. M.,** Kolb-Bachofen, V., Pallua, N., & Suschek, C. V. (2007). Deutsche Gesellschaft für Chirurgie. (H. U. Steinau, H. K. Schackert, & H. Bauer, Eds.) (Vol. 36, pp. 345–346). Berlin, Heidelberg: Springer Berlin Heidelberg. doi:10.1007/978-3-540-71123-0_116
3. **Cortese, M. M.,** HiPerferct transfection reagent (Qiagen) for transfecting synthetic siRNA in eukaryotic cells. Biocompare Product Review.Oct.13 2007; HP GenomeWide siRNA and HP Validated siRNA (Qiagen):pre-designed synthetic siRNA for knocking down the expression of genes in rat, mouse and human cells. Biocompare Product Review. Nov.2007 **www.biocompare.com**
4. Kolb-Bachofen V, **Cortese M**, Liebmann J, Koch S, Fitzner N. Regulation der Entzündungsreaktion-Eine wichtige Rolle für Stickstoffmonoxid. Jahrbuch der Heinrich-Heine-Universität Düsseldorf 2005/2006WAZ-Druck GmbH & Co.KG, Duisburg.
5. **Cortese MM** and Kolb-Bachofen V. Efficient siRNA transfection and low cytotoxicity allow study of nitric oxide-mediated effects in primary endothelial cells. QIAGEN News, 2005 Nov;3, e12

7.5. VERZEICHNIS DER WISSENSCHAFLICHEN VORTRÄGE UND POSTER

7.5.1 Eingeladene Vorträge

Cortese-Krott MM. Significance of red cell eNOS in health and disease. Invited presentation at the Gordon research conference on nitric oxide, February 2013, Ventura, CA

7.5.2 Wissenschaflichen Vorträge und Poster / indexed abstracts (ausgewält)

1. **M. M. Cortese-Krott**, T. Krenz, A. Rodriguez-Matheos, F. Oberle, K. Weber, D. Pullmann, M. Haeberlein, S. Thasian-Sivarajah, J. Spencer, M. Kelm and C. Heiss (2013). "Analysis of acute and chronic effects of (-)-

epicatechin on NO bioavailability and organ redox state in the cardiovascular system in vivo." *Nitric Oxide* 31: S43-S43**. Poster**. 5. International Meeting on the role of nitrite and nitrate in physiology, pathophysiology, and therapautics. May 4-5, 2013 Pittsburg, PA, USA.

2. **M. M. Cortese-Krott**, R. Sansone, S. Thasian-Sivarajah, M. Baaken, M. Ziegler, D. Vukjovic, C. Heiss and M. Kelm (2013). "Molecular and physiological aspects connecting red cell eNOS, red blood cell deformability and decreased microvascular function in patients with essential hypertension." *Nitric Oxide* 31: S43-S44.**Poster.** 5. International Meeting on the role of nitrite and nitrate in physiology pathophysiology and therapeutics. May 4-5, 2013 Pittsburg, PA, USA**.**

3. T. Krenz, **M. M. Cortese-Krott**, M. Totzeck, T. Rassaf, M. Kelm and C. Heiss (2013). "Laser Doppler perfusion imaging for non-invasive assessment of vascular responses in living mice." *Nitric Oxide* 31: S42-S43. **Poster.**5. International Meeting on the role of nitrite and nitrate in physiologym pathophysiology and therapautics. May 4-5, 2013 Pittsburg, PA, USA.

4. **M. M. Cortese-Krott,** T. Krenz, A. Rodriguez-Mateos, F. Oberle, K. Weber, S. Thasian-Sivarajah, M. Kelm and C. Heiss (2012). "(-)-Epicatechin Increases NO Bioavailability and Nrf2-Dependent Response in the Vessel Wall in Vivo." *Free Rad. Biol. Med* 53: S179-S179.**Vortrag. Young Investigator award.** 16th SFRRI Biennial Meeting 6-9 September 2012, London, UK.

5. **M. M. Cortese-Krott,** T. Krenz, A. Rodriguez-Mateos, F. Oberle, K. Weber, D. Pullmann, M. Haeberlein, S. Thasian-Sivarajah, J. Spencer, M. Kelm and C. Heiss (2013). "Analysis of acute and chronic effects of (-)-epicatechin on NO bioavailability and organ redox state in the cardiovascular system in vivo." *Nitric Oxide* 31: S43-S43. **Vortrag.** SFRBM's 19th Annual Meeting. November 14-18, 2012 San Diego, CA, USA**.**

6. T. Krenz, **M. M. Cortese-Krott**, M. Kelm and C. Heiss (2012). "Non-invasive assessment of vascular responses in living mice using laser doppler perfusion imaging." *Free Rad. Biol. Med* 53: S167-S167.**Poster.** SFRBM's 19th Annual Meeting. November 14-18, 2012 San Diego, CA, USA**.**

7. **M. M. Cortese-Krott**, R. Sansone, S. Sivarajah, A. Rodriguez-Mateos, G. G. Kuhnle, T. Krenz, C. Krisp, P. Horn, D. Wolters, C. Heiss and M. Kelm (2011). "Decreased expression and activity of red cell eNOS correlate with endothelial dysfunction in humans." *Free Rad. Biol. Med* 51: S157-S157. **Vortrag. Young Investigator award: Travel Award.** SFRBM's 18th Annual Meeting. November 14-18, 2012 Atlanta, GE, USA**.**

8. **Cortese-Krott MM**, Horn P, Krenz T, Krisp C, Sivarajah S, Lysaja K, Strigl F, Wolters D, Kröncke KDK, Heiß C, Kelm M. Isolation, characterization, and activity of an endothelilal nitric oxide sythase in human red blood cells. *Free Rad. Biol. Med.* 2010; **Vortrag. Young Investigator Award.** SFRBM's 17th Annual Meeting. Orlando FL, USA.

9. **Cortese-Krott, MM**, Getinger L., Opländer C, Kolb-Bachofen,V. Suschek CV. Down-regulation of iNOS expression and activity via zinc: A new NO-mediated anti-inflammatory feedback mechanism? *Nitric Oxide* .2008; 19 S35-S35. **Vortrag**. 6th International Meeting on Chemistry & Therapeutic Applications of Nitric Oxide, Bregenz, Austria.

10. **Cortese-Krott MM**, Suschek CV, Wetzel W, Kröncke KD, Kolb-Bachofen V. Nitric oxide induces the synthesis of glutathione and protects endothelial cells towards hydrogen peroxide via "free" zinc. *Free Rad. Biol. Med*. 2008; 45:S112-S112 **Poster.** SFRBM's 15th Annual Meeting. November 14-18, 2012 Atlanta, GE, USA**.**

11. **Cortese MM,** Suschek CV, Kolb-Bachofen V. Nitric oxide signaling leading to altered gene expression and oxidative stress resistance involves a zinc-dependent activation of transcription factors Nrf-2 and MTF-1. *Nitric Oxide* 2006; 14 (4): A12-A13. **Vortrag.** 5th International Meeting on Chemistry & Therapeutic Applications of Nitric Oxide. Monterey, CA,USA.

12. **Cortese MM**, Suschek CV, Kolb-Bachofen V. NO exerts anti-apoptotic effects in a zinc-dependent way: a new stress-signaling pathway. *Eur. J. Cell Biol.* 2005; 84: 115-115 Suppl. 55 **Poster.** EMBO Meeting. Heidelberg, Germany

7.6 AUSGEWÄHLTE ORIGINALARBEITEN

Redox Biology 2 (2014) 234–244

Contents lists available at ScienceDirect

Redox Biology

journal homepage: www.elsevier.com/locate/redox

Research Paper

Nitrosopersulfide ($SSNO^-$) accounts for sustained NO bioactivity of S-nitrosothiols following reaction with sulfide ☆

Miriam M. Cortese-Krott [a], Bernadette O. Fernandez [b], José L.T. Santos [b], Evanthia Mergia [c], Marian Grman [d], Péter Nagy [e], Malte Kelm [a], Anthony Butler [f], Martin Feelisch [b,*]

[a] Cardiovascular Research Laboratory, Department of Cardiology, Pneumology and Angiology, Medical Faculty, Heinrich Heine University of Düsseldorf, Düsseldorf, Germany
[b] Clinical and Experimental Sciences, Faculty of Medicine, University of Southampton, Southampton General Hospital, Tremona Road, Southampton, UK
[c] Institute for Pharmacology and Toxicology, Ruhr-University Bochum, Bochum, Germany
[d] Institute of Molecular Physiology and Genetics, Slovak Academy of Sciences, Bratislava, Slovak Republic
[e] Department of Molecular Immunology and Toxicology, National Institute of Oncology, Ráth György utca 7-9, Budapest, Hungary
[f] Medical School, University of St-Andrews, St-Andrews, Fife, Scotland

ARTICLE INFO

Article history:
Received 17 December 2013
Received in revised form
23 December 2013
Accepted 23 December 2013
Available online 11 January 2014

Keywords:
Hydrogen sulfide
Nitric oxide
Polysulfides
cGMP
HSNO
Nitroxyl

ABSTRACT

Sulfide salts are known to promote the release of nitric oxide (NO) from S-nitrosothiols and potentiate their vasorelaxant activity, but much of the cross-talk between hydrogen sulfide and NO is believed to occur via functional interactions of cell regulatory elements such as phosphodiesterases. Using RFL-6 cells as an NO reporter system we sought to investigate whether sulfide can also modulate nitrosothiol-mediated soluble guanylyl cyclase (sGC) activation following direct chemical interaction. We find a U-shaped dose response relationship where low sulfide concentrations attenuate sGC stimulation by S-nitrosopenicillamine (SNAP) and cyclic GMP levels are restored at equimolar ratios. Similar results are observed when intracellular sulfide levels are raised by pre-incubation with the sulfide donor, GYY4137. The outcome of direct sulfide/nitrosothiol interactions also critically depends on molar reactant ratios and is accompanied by oxygen consumption. With sulfide in excess, a 'yellow compound' accumulates that is indistinguishable from the product of solid-phase transnitrosation of either hydrosulfide or hydrodisulfide and assigned to be nitrosopersulfide (perthionitrite, $SSNO^-$; λ_{max} 412 nm in aqueous buffers, pH 7.4; 448 nm in DMF). Time-resolved chemiluminescence and UV–visible spectroscopy analyses suggest that its generation is preceded by formation of the short-lived NO-donor, thionitrite (SNO^-). In contrast to the latter, $SSNO^-$ is rather stable at physiological pH and generates both NO and polysulfides on decomposition, resulting in sustained potentiation of SNAP-induced sGC stimulation. Thus, sulfide reacts with nitrosothiols to form multiple bioactive products; $SSNO^-$ rather than SNO^- may account for some of the longer-lived effects of nitrosothiols and contribute to sulfide and NO signaling.

Introduction

Hydrogen sulfide (H_2S), known as a noxious malodorous gas of volcanic and biogenic origin for centuries, has recently been shown to exert a multitude of beneficial biological effects, some of which have therapeutic potential [1,2]. Pharmacological doses of simple sulfide salts have been demonstrated to protect tissues against ischemia-reperfusion injury [3,4]. Endogenous sulfide production appears to be involved in the physiological modulation of numerous cellular processes in almost every organ system, including control of vascular tone and blood pressure regulation [4]. It has been suggested that H_2S should be recognized as a third 'gasotransmitter', alongside nitric oxide (NO) and carbon monoxide [5,6], although this is not unanimously accepted [7].

In physiological systems, only a small part of H_2S actually exists in the form of dissolved gas. As a diprotic weak acid (mean $pKa_1 = 7.0$ and $pKa_2 > 12$ at 25 °C [8]), H_2S rapidly deprotonates to form hydrosulfide anions (HS^-) with negligible amounts of S^{2-} existing at physiological pH [8]. The relative amounts of the three species at equilibrium depend on temperature, pH, ionic strength, amount of H_2S gas leaving the solution, as well as "side" reactions including sulfide oxidation to form sulfite, sulfate, and thiosulfate, and polymerization reactions generating polysulfides

Abbreviations: DMF, dimetylformamide; DMSO, dimethylsulfoxide; CysNO, S-nitrosocysteine; GSNO, S-nitrosoglutathione; IPN, isopentyl nitrite; NO, nitric oxide; NO^+, nitrosonium; $SSNO^-$, nitrosopersulfide, perthionitrite, PDE, phosphodiesterase; RFL-6, rat fibroblastoid-like cell line; sGC, soluble guanylyl cyclase; SNO^-, thionitrite; SNAP, S-nitrosopenicillamine

* Correspondence to: Clinical and Experimental Sciences, Faculty of Medicine, University of Southampton, Southampton General Hospital, South Academic Block, Level F, Mailpoint 810, Tremona Road, Southampton, SO16 6YD, UK.
Tel.: +44 2 381 206891.
E-mail address: m.feelisch@soton.ac.uk (M. Feelisch).

2213-2317/$ - see front matter © 2014 The Authors. Published by Elsevier B.V. All rights reserved.
http://dx.doi.org/10.1016/j.redox.2013.12.031

and polythionates. These products themselves are characterized by complex ionization equilibria which may affect solution pH and thus concentrations of HS^- and dissolved H_2S [8,9]. For simplicity, all three forms co-existing in equilibrium (H_2S, HS^-, and S^{2-}) will hereinafter be referred to as 'sulfide'.

Striking similarities between some of the effects of NO and sulfide, in particular with regard to their role in control of vascular tone and blood pressure regulation, together with interesting mutual regulatory effects, raised the possibility of a cross-talk between these species [10–18]. Peculiarly, pharmacological application of sulfide was shown to induce both vasodilation [19] and vasoconstriction [10] *ex vivo*, and both *hypo*tensive and *hyper*tensive effects have been described in vivo [10,19]. Wang surmised that the effects of sulfide may depend on the specific vascular bed (conductance vs. resistance vessels), cell type (endothelial vs. smooth muscle cells), concentration of sulfide and presence or absence of NO/nitric oxide synthase in a particular experimental setting [20]. Moore et al. [10,21,22] proposed that vasoconstriction and hypertensive effects of lower sulfide doses were due to a direct chemical interaction between vascular NO and sulfide leading the formation of an intermediate, which was susceptible to destruction by addition of transition metals. These authors hypothesized that this intermediate might be a "nitrosothiol", probably thionitrous acid (HSNO) [21].

HSNO was described by Williams as the obvious product of sulfide nitrosation [23]; likewise, HSNO is the obvious product of the reaction between HS^- and nitrosothiols. Indeed, a recent report suggests that HSNO is formed by direct reaction of S-nitrosoglutathione (GSNO) with sulfide in phosphate buffer at pH 7, and is stable enough to transport NO intermediates across cell membranes [24]. In contrast, earlier reports found this compound to be unstable and reactive, necessitating characterization of its isomerization properties to be carried out in a low temperature argon matrix [25].

The reaction between sulfide and S-nitrosothiols has been shown to promote NO release, potentiating their vasorelaxant activity in aortic rings [26] and allowing for nitrosothiol quantification by gas phase chemiluminescence [27]. It is not clear at present whether these effects of sulfide are due to post-translational modification of vascular proteins, accelerated nitrosothiol decomposition, formation of NO-generating intermediates, or a combination of these putative mechanisms [17,18]. Independent of the above chemical studies, a recent report suggests that much of the H_2S/NO cross-talk might occur by modulation of cyclic nucleotide breakdown following inhibition of phosphodiesterase (PDE) activity [28].

The aim of the present study was to investigate whether sulfide can modulate S-nitrosothiol-mediated activation of the NO receptor soluble guanylyl cyclase (sGC) in a simple cellular system that lacks an endogenous NO production machinery and expresses low levels of PDE5 [29]. We found that sulfide modulates nitrosothiol bioactivity in a concentration-dependent manner. Under conditions of excess sulfide, a 'yellow compound' accumulates that has the potential to spontaneously release NO and activate sGC. We assign this species to be nitrosopersulfide ($SSNO^-$) and propose that this reaction product, rather than HSNO, is the main carrier of sustained NO bioactivity following interaction of sulfide with nitrosothiols.

Materials and methods

Materials

Ultrapure water (Milli-Q, Millipore), S-nitroso-N-acetyl-DL-penicillamine (SNAP), sodium persulfide (Na_2S_2, sodium disulfide; Sage Chemical Co., Ltd, Hangzhou, China), p-methoxyphenyl-morpholino-phosphinodithioic acid (GYY4137), 3-isobutyl-1-methylxanthine (IBMX) and 3′-methoxy-3-oxo-3H-spiro[isobenzofuran-1,9′-xanthen]-6′-yl 2-(pyridin-2-yldisulfanyl)benzoate (Washington State Probe-1, WSP-1) from Cayman Chemicals (Biomol, Hamburg, Germany) was used. Unless otherwise specified, all other chemicals were of the highest purity available and purchased from Sigma-Aldrich (Schnelldorf, Germany or Gillingham, Dorset, UK), cell culture plastics from Greiner (Frickenhausen, Germany), and other cell culture material from PAA (Pashing, Austria). Fetal bovine serum (FBS) was from Cambrex (Lonza, Cologne, Germany).

Cell culture

Rat fibroblastoid-like (RFL-6, ATCC CCL192™) cells were purchased from LGC Standards GmbH (Wesel, Germany) and cultured from passage 8–18 in T9 flasks using RPMI 1640, supplemented with 20% fetal bovine serum and antibiotics in a CO_2 incubator under standard cell culture conditions.

Preparation of stock solutions and RSNO/sulfide mixtures

Stock solutions of SNAP (100 mM, DMSO or DMF), IBMX (50 mM, DMSO), GYY4137 stocks (40 mM, DMSO), and WSP-1 (5 mM, DMSO) were kept aliquoted at −20 °C until use. Stock solutions of S-nitrosocysteine (CysNO) and S-nitrosoglutathione (GSNO) were freshly prepared via reaction of the reduced thiols with acidified nitrite [30] and used immediately. Na_2S stock solutions (200 mM) were prepared fresh before each experiment by dissolving anhydrous Na_2S in a strong buffer (TRIS or phosphate buffer 1 M at pH 7.4) and diluted further in 100 mM TRIS or phosphate buffer pH 7.4 immediately before use. Incubation mixtures of nitrosothiols with Na_2S were obtained by adding appropriate volumes of the stock solutions directly to the incubation buffer to achieve final concentrations of 1 mM for the nitrosothiol and 0.2–10 mM for sulfide, as indicated in text and figures.

Measurements of sGC activation by sulfide, SNAP, and its mixtures

sGC activity was estimated by measurement of intracellular cGMP levels of RFL-6 reporter cells as described [31], with minor modifications. Briefly, 1.5×10^5 cells/well were seeded into 6-well plates, grown for 48 h until confluence, washed twice with 1 ml phosphate buffered saline (PBS; pre-warmed to 37 °C), and pre-treated for 15 min with the PDE inhibitor IBMX (500 μM) in culture medium without serum (treatment medium). After washing with PBS, 1 ml fresh treatment medium was added and cells were then treated as indicated. In this system, SNAP and other NO-donors cause concentration-dependent increases in intracellular cGMP, which are fully inhibited by NO-scavengers (Fig. 1 and Fig. S1). To capture a wide-enough time window for NO bioactivity measurements, all SNAP/sulfide incubations were carried out for 30 min (during which time SNAP-induced cGMP elevations remained relatively constant; Fig. S1A). In a first set of experiments, SNAP and immediately thereafter Na_2S (or the vehicle controls) were added directly to the treatment medium at the concentrations indicated. In a second set of experiments, RFL-6 cells were pre-incubated with GYY4137 for 45 min, washed and then treated with SNAP. In a third set of experiments, stock solutions of nitrosopersulfide ($SSNO^-$) were prepared by reacting 1 mM SNAP with 10 mM Na_2S in 1 ml PBS or TRIS 100 mM pH 7.4. In a typical experiment, 10 μl of SNAP (100 mM/DMSO) and 100 μl Na_2S (100 mM/Tris 100 μM pH 7.4) were added to an amber centrifugation tube containing 890 μl Tris 100 μM pH 7.4. After 10 min of incubation at RT, excess sulfide was removed either by

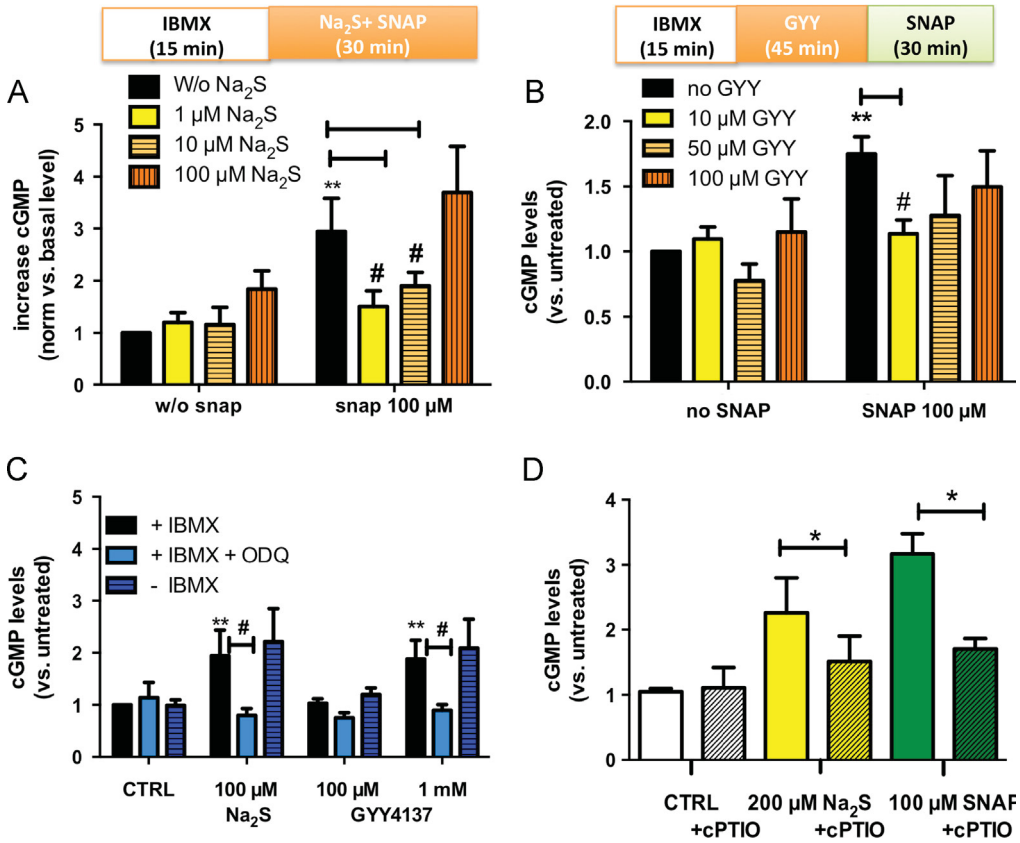

Fig. 1. Sulfide modulates s-nitrosothiol bioactivity in a concentration-dependent manner. (A) Changes in cGMP concentration after treatment of RFL-6 cells with Na_2S, SNAP, or their combination ($n=5$). (B) Effects of SNAP on cells pre-incubated with the sulfide donor GYY4137 ($n=4$). (C) Effects of sGC and PDE inhibition on Na_2S and GYY4137 induced activation of sGC ($n=4$). (D) Effects of cPTIO on sulfide and SNAP induced sGC activation ($n=3$) * $p<0.05$; ** $p<0.01$ vs. CTRL, # $p<0.05$, *T*-test.

precipitation with $ZnCl_2$ (20 µl of 500 mM $ZnCl_2$ to 1 ml yellow mixture; final concentration 10 mM), followed by a 1 min centrifugation at maximal speed, or by 10 min bubbling of the solution with nitrogen. Removal of sulfide was verified spectrophotometrically. The mix (2 µl, 20 µl, 200 µl) was then added to cell culture medium to reach a total volume of 1 ml (corresponding to a 1:500; 1:50; 1:5 dilution). In selected experiments, an sGC inhibitor (ODQ, 500 µM) or an NO scavenger (cPTIO, 500 µM) were added 5 min prior to the addition of sulfide and/or SNAP. The above dilution steps bring the theoretical maximal concentration of NO-containing bioactive material into the micromolar range. No signs of cell toxicity were observed following either of these treatments, as assessed by micro/macroscopic cell inspection and determination of protein content; the latter would have been reduced if a significant number of apoptotic/dead cells detached from the plates.

Cells were lysed in 0.1 M HCl at RT for 20 min, scraped, sonicated twice for 30 s at 4 °C, centrifuged at 30,000*g* for 10 min at 4 °C to remove cell debris, and the supernatant snap-frozen in liquid N_2 and kept at −80 °C until analysis. Protein concentrations in the supernatant were determined by a modified Bradford's protein assay (Roti®Nanoquant, Carl Roth GmbH+Co. KG, Karlsruhe, Germany) after pH equilibration with 200 mM TRIS pH 8. Intracellular cGMP levels were assessed by using DetectX-®High Sensitivity Direct Cyclic GMP kit by Arbor Assay (Biotrend, Cologne, Germany) as per manufacturer's instructions. Data were normalized for protein content and expressed as pmoles/ml/mg protein or as ratios compared to untreated cells. Changes in intracellular cGMP levels, normalized for protein content, were expressed as % of untreated control to further account for the variability in basal cGMP levels of untreated cells of different batches and passages (Fig. S1A, insert).

Determination of intracellular sulfide levels

Intracellular sulfide levels were determined by flow cytometry following loading of RFL-6 cells with 10 µM WSP-1 for 30 min. After washing with 1 ml pre-warmed PBS, cells were detached by addition of 2 ml Accutase® (PAA), and intracellular green fluorescence (λ_{ex} 488 nm, λ_{em} 519 nm) was assessed in a FACS-Verse flow cytometer (BD Bioscience, Heidelberg, Germany). Data were calculated as median fluorescence intensity (MFI) of loaded cells – background (ΔMFI) by plotting side-scatter (SSC) vs. fluorescence intensity in the FITC channel using FlowJo 10.0.6 (Tristar, Ashland, OR, USA).

Measurement of phopshodiesterase activity

RFL-6 cells cultured for 10 or 18 passages, were scraped, lyzed in homogenization buffer (triethanolamine (TEA)/HCl 50 mM, NaCl 50 mM, EDTA 1 mM, DTT 2 mM, benzamidine 0.2 mM, phenylmethylsulfonyl fluoride 0.5 mM and 1 µM pepstatin A, pH 7.4, 4 °C), and cleared by centrifugation (800 × g, 5 min, 4 °C). PDE activity in cell homogenates was measured by the conversion of [^{32}P]cGMP or [^{32}P]cAMP (synthesized from [α-^{32}P]GTP or [^{32}P]ATP using purified NO-sensitive guanylyl or adenylyl cyclase) to guanosine or adenosine and [^{32}P]phosphate in the presence of alkaline phosphatase at 37 °C for 7 min. Reaction mixtures (0.1 ml) contained 0.05–10 µl of the homogenates (~5 µg protein), [^{32}P]cGMP or [^{32}P]cAMP (~2 kBq), various cGMP concentrations (0.1, 1, or 5 µM), 12 mM $MgCl_2$, 3 mM dithiothreitol, 0.5 mg/ml bovine serum albumin, 2 or 4 U of alkaline phosphatase, and 50 mM TEA/HCl, pH 7.4. Reactions were stopped by adding 900 µl ice cold charcoal suspension (30% activated charcoal in 50 mM KH_2PO_4, pH 2.3). After pelleting the charcoal by centrifugation, [^{32}P]

phosphate in the supernatant was quantified by scintillation counting.

Reaction of sulfide with nitrosothiols

The spectroscopic and kinetic behavior of the reaction between sulfide and CysNO, GSNO and SNAP was followed by UV–visible spectroscopy in a FLUOstar Omega (BMG Labtech, Offenburg, Germany). Stock solutions (100 mM) were diluted 1:100 in 1 M TRIS pH 7.5, transferred to a UV-transparent 96-well plate (200 μl/well). The in-built automatic injector was filled with 50 mM Na_2S solution for in-well titration experiments. Spectra (200–800 nm) were acquired before and every 2 s for 100 cycles after injection of 1–20 μl aliquots of Na_2S. Spectra were analyzed using Omega data analysis software (BMG Labtech). All other studies were carried out in 3 ml-volume quartz cuvettes, kept at either 25.0 or 37.0 ± 0.02 °C with continuous stirring (t2 peltier-type cuvette holder with TC1 temperature controller, Quantum Northwest, Liberty Lake, WA, USA) using a Cary 60 UV/vis spectrophotometer and analyzed using WinUV software (Agilent Technologies, Wokingham, Berkshire, UK). No differences in spectral changes were observed whether SNAP was incubated with sulfide in the presence or absence of DTPA (100 μM), indicating that transition metal contamination of our buffers was negligible.

Sulfide/disulfide nitrosation on solid phase

A stationary nitrosothiol (RSNO) column was prepared using batch nitrosation of the thiol-containing resin, Ekathiol (Sigma-Aldrich; Lot 115H1121) in a small beaker. Briefly, 0.4 g dry resin was suspended in and washed extensively with ultrapure water before reduction of resin-bound sulfhydryl groups (0.71 mmol thiol/g resin) with a 10-fold molar excess of dithiothreitol (in 0.01 M NaOH) for 5 min at RT; thereafter, the reductant was removed by 5 successive washes with ultrapure water. Free sulfhydryl groups were nitrosated by addition of acidified nitrite ($NaNO_2$ in 1 M HCl; 2-fold molar excess), and allowed to react for 30 min at 4 °C in the dark. After a minimum of 5 washing steps with 10 ml ice-cold ultrapure water, the resin was equilibrated to pH 8.0 with 100 mM phosphate buffer and filled into two Pasteur pipettes with glass wool at the bottom. These mini-columns were washed 10 times with ice-cold phosphate buffer under dimmed lighting conditions. Sub-stoichiometric amounts of Na_2S or Na_2S_2 in phosphate buffer were loaded onto the columns and eluted with ice-cold phosphate buffer; fractions were collected directly into 1 ml quartz cuvettes and UV–vis spectra recorded using an Agilent 8453 diode array spectrophotometer and ChemStation software (Agilent Technologies).

Kinetics of NO release

In situ NO formation from SNAP (1 mM) with/without Na_2S (0.1–10 mM) in the presence or absence of the metal chelator DTPA (100 μM) in 1 M Tris or 100 mM phosphate buffer, pH 7.4, was monitored by gas phase chemiluminescence (CLD 77am sp; Ecophysics, Dürnten, Switzerland) using a custom-designed, water jacketed glass reaction chamber (15 ml total volume) kept at 25 ± 0.1 °C and continuously bubbled with nitrogen. 1 ml volumes of the respective SNAP/sulfide mixtures were premixed in Eppendorff vials, vortexed, and at the indicated time interval of incubation a 25 μl aliquot of the reaction mixture was transferred into the reaction chamber containing 15 ml buffer (dilution 1: 600) by means of a gas-tight syringe. NO concentration in the sample gas was recorded continuously and peak areas were integrated using an EPC-500/PowerChrom data processing system (eDAQ; Red Box Direct, Dublin, Ireland).

Oxygen consumption measurements

Changes in dissolved oxygen concentration in incubation mixtures of SNAP and sodium sulfide (in 100 mM phosphate buffer pH 7.4, as above) were monitored polarographically using a dual channel Clark-type electrode system (Digital Model 20; Rank Brothers Ltd, Cambridge) and LabChart (ADInstruments, Oxoford, UK); incubation volume was 3 ml; solutions were maintained at a constant temperature of 37 ± 0.5 °C using a circulating water bath. Reactions were typically started by the addition of SNAP to prewarmed sulfide-containing buffer solutions while continuously stirring, although the sequence of addition of sulfide or nitrosothiol did not have any effect on measured rates of oxygen consumption.

Statistical analysis

Data are reported as means ± SEM. ANOVA followed by an appropriate *post hoc* multiple comparison test (Tukey or Student's *T* test) was used to test for statistical significance.

Results

Sulfide modulates nitrosothiol bioactivity in a concentration-dependent manner

Nitrosothiols are known to activate and modulate sGC activity in vascular tissue and a wide variety of cellular preparations [32–34]. In this study, potential changes in nitrosothiol bioactivity by sulfide were investigated by analyzing SNAP-induced sGC activation in RFL-6 cells, a convenient NO reporter system lacking an active NO synthase and expressing low levels of PDE5 [31]. Total PDE activity in RFL-6 cells was found to be greater for cAMP than cGMP (295 ± 15 vs. 129 ± 14 pmol/mg/min, p10; $n=2$) and decreased on further passaging (111 ± 8 vs 81 ± 3 pmol/mg/min, p17; $n=2$). To minimize the effects of cell passage-dependent and sulfide-induced variations in PDE activity on intracellular cGMP levels, experiments were carried out in the presence of IBMX.

Using this system we found that sulfide modulates the NO bioactivity of SNAP to varying degrees, depending on the relative concentration ratio of sulfide over SNAP. Low sulfide concentrations (1–10 μM) inhibited sGC stimulation by 100 μM SNAP (Fig. 1A), whereas cGMP levels with equimolar concentrations of sulfide and SNAP were not different from those of SNAP alone (Fig. 1A). Similar results were obtained when intracellular sulfide levels were elevated by pre-incubating cells with the sulfide donor GYY4137. Pre-incubation with 10–100 μM GYY4137 increased intracellular fluorescence of the sulfide-specific probe WSP-1 (Fig. S1B) and inhibited SNAP-induced cGMP increases (Fig. 1B) in a concentration-dependent fashion. Unexpectedly, we found that high concentrations of sulfide (100 μM Na_2S or 1 mM GYY4137) increased cGMP even in the absence of SNAP (Fig. 1A and C). These sulfide-mediated cGMP increases were inhibited by either cPTIO or ODQ, but unaffected by the presence/absence of IBMX (Fig. 1C and D), indicating that the cGMP changes observed were NO/sGC-dependent but independent of PDE activity. Whether or not preformed NO-storage pools may account for this effect of sulfide warrants further investigation. SNAP-induced sGC activation was abolished by treating cells with the sGC inhibitor ODQ or the NO scavenger cPTIO (see Fig. 1D), indicating that effects were dependent on the release of NO with consecutive activation of sGC. Taken together, these results show that low concentrations of sulfide attenuate SNAP bioactivity whereas sGC stimulation by SNAP is fully restored at equimolar sulfide levels.

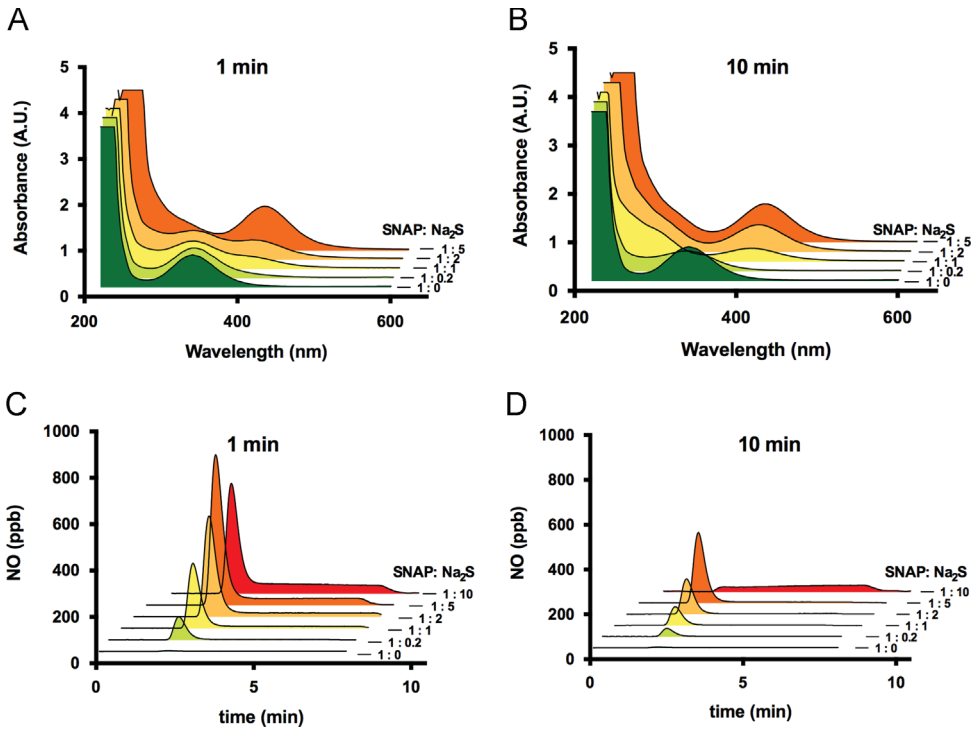

Fig. 2. The reaction between sulfide and nitrosothiols leads to formation of NO-releasing species. (A,B) UV–visible spectroscopic analyses of the reaction between SNAP and hydrosulfide at pH 7.4. Varying SNAP/Na_2S concentration ratios lead to formation of different products as assessed after 1 min (A) and 10 min of incubation (B); with excess sulfide accumulation of a 'yellow compound' (λ_{max} 412 nm) was observed. (C,D) Profiles of NO release from SNAP/Na_2S mixtures of different concentration ratios after 1 min (C) or 10 min of incubation (D). (For interpretation of the references to color in this figure legend, the reader is referred to the web version of this article.)

The reaction of sulfide with nitrosothiols leads to formation of more than one NO-releasing species

In order to characterize the chemical biology of interaction between SNAP and sulfide, we monitored the reaction using time-resolved UV/vis spectrometry and gas phase chemiluminescence (Fig. 2). SNAP decomposition (decrease in λ_{max} at 340 nm) was accompanied by absorbance increases in the region of 250–300 nm and 390–430 nm with a peak at λ_{max} 412 nm (Fig. 2A and B), and – under some conditions – transiently around 320 nm (Figs. 2 and 3A), indicative of the formation of multiple reaction products/intermediates. Nature, yield, rate of formation, and stability of these products were strictly dependent on the concentration ratio of the reactants (see Fig. 2A and B). Similar spectral changes, albeit with different kinetics, were observed when sulfide was allowed to react with two other nitrosothiols, CysNO and GSNO (Figs. S2A, S2B). To investigate the potential of reaction products to generate NO after complete decomposition of the starting material, aliquots of the reaction mixture of SNAP and sulfide were subjected to chemiluminescence analyses at different time points of co-incubation.

Transition metals in aqueous buffers can trigger nitrosothiol decomposition [35]; in our hands, SNAP alone produced a very small NO signal when experiments were carried out in the presence of the metal chelator DTPA (100 μM; Fig. 2C and D). However, peak NO release was markedly enhanced when SNAP was pre-incubated for 1 min with sulfide prior to injection into the reaction chamber (Fig. 2C). This enhancement of rate of NO formation was apparent at sub-stoichiometric concentrations of sulfide and became progressively more prominent as sulfide concentrations increased (1:1, 1:2, 1:5 and 1:10), seemingly matching the extent of formation of the 412 nm peak (Fig. 2A). A biphasic NO release profile was observed at higher sulfide concentrations, with a sharp initial peak followed by a more sustained lower level of NO production. Injection of aliquots of the reaction mixture that had been pre-incubated for 10 min revealed a decreased NO releasing capacity (Fig. 2D), indicative of ongoing decomposition of NO-generating entities. The long-lasting NO releasing component was observed only at higher sulfide concentration ratios. Since SNAP itself produces just traces of NO under these conditions (and the absorbance feature at 340 nm rapidly disappears on incubation with excess sulfide), the NO formation we detected could not have originated from SNAP itself; thus other products capable of releasing NO must have been formed in the course of the reaction.

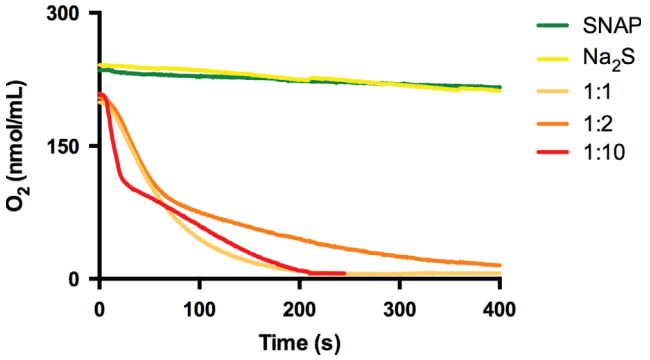

Fig. 3. Oxygen consumption by the reaction of SNAP with sulfide. Changes in dissolved oxygen (O_2) concentration in air-saturated phosphate buffer pH 7.4 by 1 mM SNAP (green tracing) or 2 mM Na_2S alone (yellow), as compared to mixtures of 1 mM SNAP and different concentration of sulfide (1, 2, 10 mM, final concentrations). Representative tracings of 3–4 separate runs at each condition yielding qualitatively identical results. (For interpretation of the references to color in this figure legend, the reader is referred to the web version of this article.)

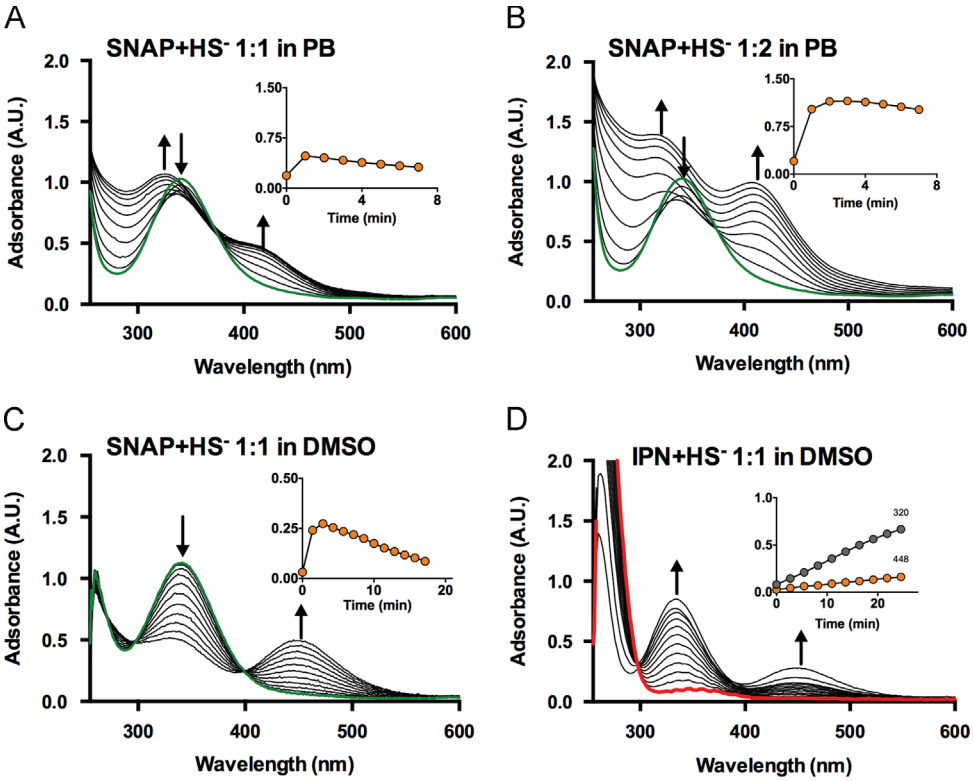

Fig. 4. Formation of SNO^- and $SSNO^-$ during the reaction of SNAP or isopentyl nitrite (IPN) with hydrosulfide (HS^-) under aqueous and non-aqueous conditions. (A,B) Reaction of Na_2S and SNAP in phosphate buffer (PB) at pH 7.4. Green line, starting spectrum of SNAP. Attributions: λ_{max} 320 nm=SNO^-; λ_{max} 412 nm=$SSNO^-$ (C) Reaction of Na_2S and SNAP in DMSO. Spectra taken in the first 60 s after the beginning of the reaction are shown. Attributions λ_{max} 448 nm=$SSNO^-$ (D) Reaction of isopentylnitrite (IPN) with Na_2S in DMSO. Red line, starting spectrum of IPN. Attributions: λ_{max} 325 nm=ONS^-; λ_{max} 448 nm=$SSNO^-$. Time interval for spectra: 0–60 s. Cycle time 0.1 s. Insets in (A–D) are depicting the time course of absorbance changes at 412 nm (A,B) or 448 nm (C,D).

Nitrosothiol/sulfide reactions are accompanied by the consumption of oxygen

Solutions of either NO or sulfide are known to slowly react with oxygen (autoxidation) [2,8]. In order to investigate whether the chemical interaction of sulfide with nitrosothiols affects the concentration of dissolved oxygen beyond that expected by the sum of either reactant alone we monitored oxygen consumption in SNAP/sulfide incubation mixtures. As depicted in Fig. 3, oxygen consumption rates accelerated dramatically on coincubation of SNAP and sulfide, exceeding that of either reaction partner by orders of magnitude. Although higher molar ratios of sulfide over SNAP tended to hasten oxygen consumption compared to equimolar levels no simple concentration dependence was apparent, with well-behaved second/pseudo first order rates adopting a biphasic kinetic profile whenever sulfide was in excess over SNAP. Such changes are difficult to rationalize by a simple enhancement of NO production alone but consistent with the formation of more reactive radical intermediates.

A 'yellow compound' is produced by reaction of nitrosothiols with excess sulfide and assigned to be nitrosopersulfide, $SSNO^-$

A major product of the reaction of SNAP (and other nitrosothiols, as demonstrated for CysNO and GSNO in Figs. S2A, S2B) with excess sulfide consists of a 'yellow compound' with a strong absorbance feature at 412 nm (Fig. 2A and B; Fig. 4A and B). Earlier work by Seel et al. [36] and Munro et al. [37] had described the formation of a similar absorbance feature with a maximum at 409–410 nm in the course of the reaction between sodium sulfide and NO or nitrosothiols, respectively; those experiments had been carried out in unbuffered strongly alkaline solutions, and both groups had attributed this peak to the formation of the stable yellow-colored nitrosodisulfide (perthionitrite) anion, $SSNO^-$. Our own experiments confirmed that the absorption maximum of the 'yellow compound' shows a small bathochromic shift on further alkalinization. When the reaction of SNAP and sulfide was carried out in polar organic solvents such as DMSO (Fig. 4C) or DMF (not shown) the absorbance maximum shifts to 448 nm, again consistent with observations by Seel et al. [38]. Under these conditions, another prominent absorbance feature with a maximum at 330 nm occurs (Fig. 4C). According to Seel et al. [38], this peak is indicative of the formation of thionitrite (SNO^-). The formation of either species was observed also when sulfide was reacted with the classical nitrosating agent, isopentyl nitrite (IPN), instead of SNAP; in this case, $SSNO^-$ formation was less pronounced and clearly preceded by the formation of SNO^- (Fig. 4D).

The reaction between sulfide and nitrosothiols was also carried out on solid phase by passing aqueous solutions of sulfide (0.1, 0.5, 2 μmoles in 100 μl of 100 mM phosphate buffer, pH 8) over a resin containing immobilized S-nitrosothiol moieties serving as a stationary nitrosonium (NO+) donor (Fig. 5). The higher concentration of sulfide produced a faint yellow band in the upper part of the packed resin that turned intensely yellow/orange on migrating down the column; this was accompanied by the formation of gas bubbles. The lower and medium concentrations of sulfide produced a step-like absorbance feature in the UV range, indicative of the formation of polysulfides. The absorption spectrum of the yellow eluate collected from the high sulfide fraction revealed a broad symmetrical peak between 320 and 500 nm (λ_{max} 412 nm). An identically colored solution with a peak absorbance at 412 nm was obtained when sodium disulfide (Na_2S_2) instead of Na_2S solutions were passed over the column.

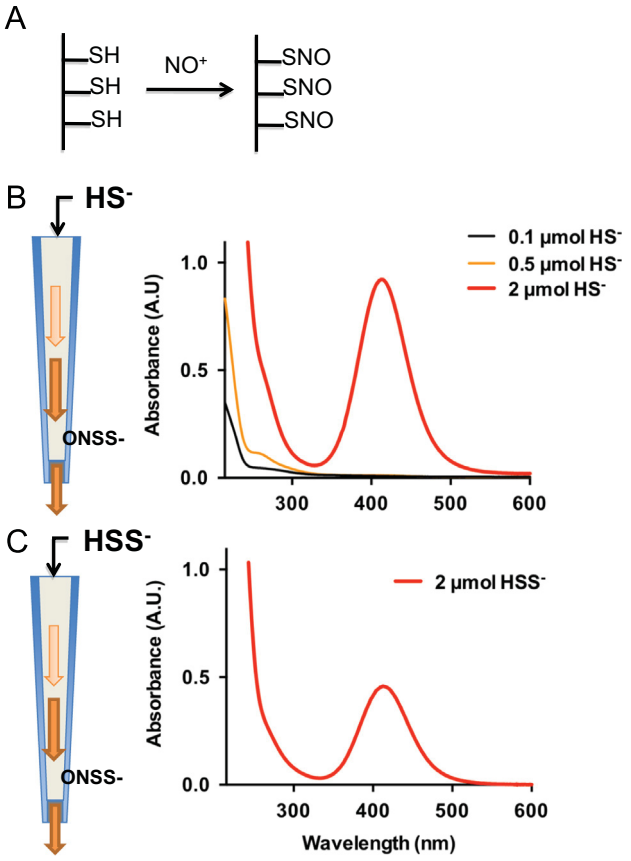

Fig. 5. Formation of $SSNO^-$ from the reaction between sulfide and immobilized S-nitroso moieties. (A) S-nitrosation by acidified nitrite of resin-bound sulfhydryl (–SH) groups (Ekathiol®) to form an immobilized nitrosothiol. (B,C) A solution of either Na_2S (B) or Na_2S_2 (C) is passed over the column and reacts with immobilized S-nitrosothiols to form $SSNO^-$ (λ_{max} 412 nm; high sulfide concentration) and polysulfides (< 280 nm; lower sulfide concentrations). Depicted results are representative of 4 independent experiments with different batches of nitrosated thiol-containing resin and various absolute amounts of sulfide (0.015–5 µmoles on column).

NO release from nitrosopersulfide accounts for sustained sGC activation by SNAP

The peak at λ_{max} 412 nm assigned to $SSNO^-$ was found to be rather stable at physiological pH ($t_{1/2} >> 30$ min at RT; Fig. 6A, inset). Given this anionic compound is formally a nitrosothiol we were surprised to see that its lifetime was seemingly unaffected by the presence of excess sulfide and/or addition of other reduced thiols (tested for glutathione and cysteine, both at 1 mM; Fig. S3). Addition of a strong base (NaOH) did not affect the stability of this substance either (Fig. S3), but acidification led to immediate disappearance of the yellow color with its absorbance feature at 412 nm, followed by formation of a colloidal suspension indicative of sulfur extrusion (not shown). By contrast, decomposition of the 'yellow compound' at physiological pH leads to formation of polysulfides (Fig. S4), which are susceptible to decomposition following reaction with dithiothreitol (DTT, 1 mM); no precipitation of sulfur was observed in the presence of excess sulfide.

Evidence for NO production during $SSNO^-$ decomposition was obtained using SNAP/Na_2S (1 mM/10 mM) mixtures that were pre-incubated for at least 10 min, and strongly diluted prior to testing by gas phase chemiluminescence (Fig. 6A and B; dilution 1:600) and sGC activation in RFL-6 cells (Fig. 6C and D; 1:5 to 1:500 dilution). Repeated injections of small 25 µl aliquots of the reaction mixture allowed the determination of an apparent 'half-life of the NO releasing activity' of the reaction products; as observed with the 412 nm peak (Fig. S3), the decomposition of the $SSNO^-$ specific portion of the NO peak occurred over a similar timescale (Fig. 6A and B). Parallel investigations of the SNAP/sulfide reaction mixture revealed a concentration-dependent increase in cellular cGMP levels in RFL-6 cells (Fig. 6C and D). Importantly, sGC activation by $SSNO^-$ was considerably more pronounced than that seen with SNAP (or sulfide) alone (Fig. 6C,D), blocked by addition of the NO scavenger cPTIO and the sGC inhibitor ODQ (Fig. 6D). Removing excess sulfide by zinc precipitation immediately before addition of the preincubated SNAP/sulfide mixture to the cells had either no effect on or slightly enhanced sGC activation by $SSNO^-$ (Fig. 6D).

Discussion

We here demonstrate that 1. sGC stimulation by nitrosothiols is modulated by variation in extracellular and intracellular sulfide levels; 2. chemical reaction of sulfide with nitrosothiols leads to distinct products, depending on the concentration ratio of the reactants; 3. with excess sulfide over nitrosothiols this reaction leads to formation of a stable 'yellow compound' which we assign to be nitrosopersulfide ($SSNO^-$); and 4. $SSNO^-$ decomposition generates enhanced NO bioactivity over that of SNAP alone. 5. Given that sulfide concentrations likely exceed those of nitrosothiols in most biological compartments, our data suggest that $SSNO^-$ is formed whenever NO and H_2S are co-generated and interact, thus contributing to the biological activity of both "hydrogen sulfide" and nitrosothiols. Considering the apparent stabilities of thionitrite (SNO^-) and nitrosopersulfide in the presence of reduced thiols (incl hydrosulfide), the latter rather than the former is likely to account for the sustained NO bioactivity of nitrosothiols. Taken together, our studies imply that $SSNO^-$ is a new signaling entity with the potential to generate both NO and polysulfides.

Chemistry of formation and decomposition of nitrosopersulfide

One of the most interesting aspects of our present studies relates to the observation that a 'yellow compound' is formed and accumulates whenever sulfide is in excess over nitrosothiols. On the basis of its spectral characteristics, and in agreement with work by Seel and Wagner [36,38] as well as Munro and Williams [37], we assign this product to be nitrosopersulfide ($SSNO^-$), a hybrid species containing a sulfane sulfur and a nitrosonium moiety attached to opposite ends of a sulfur atom. It formally belongs to the group of polysulfides (S_x^{2-}) and is its smallest NO-containing representative. Such a compound would seem to be of particular interest in the context of the cross-talk between the NO and the H_2S signaling pathways, an area of research that has attracted much interest lately, due to its propensity to generate both, NO and polysulfides/sulfane sulfur; the latter are becoming increasingly recognized as potent bioactive sulfide metabolites [39,40].

In the absence of transition metals or light, the homolytic decomposition of nitrosothiols (RSNO) to yield NO and a thiyl radical (Eq. 1) is a fairly slow process because the S–N bond is relatively strong [41].

$$RSNO \rightarrow RS^{\bullet} + {}^{\bullet}NO \quad (1)$$

However, nitrosothiols are unstable in the presence of reduced thiols. The expected reaction between a nitrosothiol and hydrosulfide, the smallest thiol and one of the strongest nucleophiles of physiological relevance, is transnitrosation to give thionitrous acid, a well-established if unstable species [42](Eq. 2).

$$RSNO + HS^- \rightarrow RS^- + HSNO \quad (2)$$

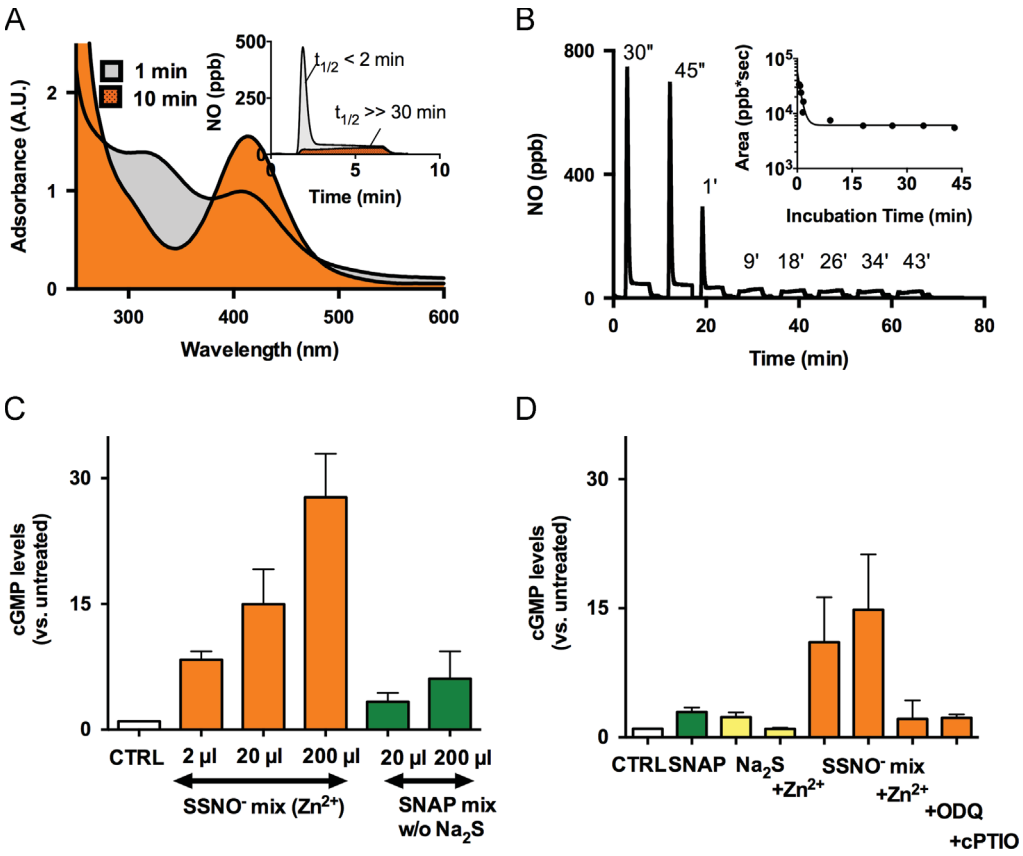

Fig. 6. Decomposition of $SSNO^-$ releases NO and activates of sGC. (A) UV–visible spectra (main panel) and chemiluminescent profile of NO release (inset) of a SNAP/Na_2S mixtures (1:10) at pH 7.4 following 1 min (gray) or 10 min (orange) of incubation at RT in 1 M TRIS buffer, pH 7.4. (B) Original chemiluminescence tracing of NO release over time of a SNAP/Na_2S mixture (1:10) incubated for the indicated time points. Inset: changes in total NO release (area under the curve) with increasing time of preincubation. (C) Dose-dependent sGC activation by the SNAP/Na_2S mixture (1:10) incubated for 10 min ($SSNO^-$ mix) compared to the same volumes of a control mix prepared with SNAP only (SNAP mix). (D) NO and sGC dependent cGMP increase in RFL-6 cells after incubation with 20 µl of the $SSNO^-$ mix compared to the effects of SNAP and sulfide (Na_2S) alone. "$+Zn^{2+}$" denotes removal of excess sulfide by zinc precipitation; indicated volumes were added directly to the cell culture medium to reach a total volume of 1 ml. (For interpretation of the references to color in this figure legend, the reader is referred to the web version of this article.)

Transnitrosation is a rapid reaction, and all of the HS^- should be converted into HSNO. Assuming a pKa for the latter similar to that of nitrous acid (HONO), at physiological pH this species is expected to exist largely in the form of the corresponding anion, thionitrite (SNO^-); in alkaline solution, thionitrite has an absorption maximum near 320 nm [43,44], which corresponds to one of the transient spectral features we observed in the present study (see Figs. 2 and 3).

Nitrosothiols act as vasodilators because of their ability to donate NO to sGC. HSNO might be expected do the same but, because of the mobile hydrogen in the molecule, it can undergo a number of other reactions, such as facile isomerization to three other species with the same formula (HNSO, HOSN, HSNO, HONS and their corresponding anions, respectively; (Eq. 3) [25]).

$$HNSO \rightleftharpoons HOSN \rightleftharpoons HSNO \rightleftharpoons HONS \quad (3)$$

Although the decomposition products of these species have not been investigated in great detail, they appear to be largely gaseous and/or form polymeric material [45]. Thus, HSNO will not deliver to sGC a stoichiometric amount of NO, as does RSNO. As a result, formation of HSNO/SNO^- results in reduced stimulation of sGC.

In the presence of higher concentrations of HS^- the situation is rather different as another reaction (nucleophilic attack of HS^-) becomes dominant.

$$HSNO + HS^- \rightarrow HSSH + NO^- \quad (4)$$

$$HSSH \rightleftharpoons H^+ + HSS^- \quad (5)$$

This is a second order reaction (rate$=k$[HSNO][HS^-]) and so, while negligible at low concentrations of HS^-, at higher hydrosulfide concentrations it dominates. The persulfide (hydrodisulfide anion; HSS^-) formed is also a strong nucleophile; it can undergo transnitrosation with RSNO in a fashion similar to HS^-.

$$RSNO + HSS^- \rightarrow RSH + SSNO^- \quad (6)$$

The resulting nitroso compound, nitrosopersulfide (perthionitrite; $SSNO^-$) appears, from our work and that of Seel et al. [36,43], to be considerably more stable than HSNO and, therefore, a better vasodilator. The formation of sulfur chains, admittedly a chain of only two in this instance, is so common in sulfur chemistry that to find evidence for the long-term presence of HSNO would be surprising. Longer sulfur chains are common at higher concentrations, and elemental sulfur exists, of course, as S_8. It is not unreasonable to postulate that, because of its enhanced stability, HSSNO/$SSNO^-$ is better able to provide sGC with NO. At the same time it is more mobile than RSNO and therefore a more versatile vasodilator. Some of the NO moiety is lost as nitroxyl anion, NO^- (Eq. 4), but vascular tissue can readily convert this to NO [46]. Thus, high concentrations of HS^- enhance the vasodilator activity of nitrosothiols.

Alternative routes to nitrosopersulfide formation may exists when thiol disulfides (RSSR') are present; in this case, alkyl persulfides (RSS^-) may be formed [47], which may serve as a source of HSS^- (Eqs. 6,7).

$$RSSR' + HS^- \rightarrow RSSH + R'S^- \quad (7)$$

$$RSSH + HS^- \rightarrow RS^- + HSSH \quad (8)$$

Nitrosopersulfide may also be formed via a radical pathway that starts with the homolytic cleavage of HSNO to generate sulfanyl (hydrosulfide radical, $HS^\bullet$), which is extremely reactive and immediately reacts with excess thiolate (in this case, HS^-) to form the hydrodisulfide radical ($HSS^{\bullet -}$).

$$HSNO \rightarrow HS^\bullet + {}^\bullet NO \quad (9)$$

$$HS^\bullet + SH^- \rightarrow HSS^{\cdot -} \quad (10)$$

This species then either reacts further with NO (to form nitrosopersulfide; Eq. 11) or oxygen (to form superoxide; Eq. 12).

$$HSS^{\bullet -} + {}^\bullet NO \rightarrow HSSNO \rightleftharpoons SSNO^- + H^+ \quad (11)$$

$$HSS^{\bullet -} + O_2 \rightarrow HSS^- + O_2^{\bullet -} \quad (12)$$

Thus, $SSNO^-$ might form via several different avenues [37]. Formation via HSNO seems a plausible route, since isopentyl nitrite (a prototypical nitrosating agent characterized by an alkyl nitrite (R-ONO) grouping) was demonstrated here to undergo a similar reaction in that it first leads to SNO^- generation, with $SSNO^-$ formation becoming apparent only much later (Fig. 4D). Those experiments were carried out in DMSO (as shown here) and DMF. The advantage of using these non-aqueous 'electron pair donor' solvents is that under these conditions, anions exist essentially in their "naked" form (unlike in water where solvation is via formation of hydrogen bonds), resulting in an enhancement of their nucleophilicity. In the case of $SSNO^-$, a large bathochromic shift from 412 nm (in aqueous solution) to 450 nm is observed; for SNO^- a lesser shift was apparent but a marked enhancement of molar UV-absorbance was seen. In DMSO/DMF one can also observe the vibrational fine structure of the R-ONO absorbance feature superimposed onto the broad nitrite peak while allowing for convenient monitoring of the formation of SNO^- and $SSNO^-$ at the same time. The same characteristic changes take place when the reaction of nitrosothiols with HS^- is carried out in those solvents, as we here demonstrate for SNAP and sulfide (compare Fig. 4A with 4C). Interestingly, the same final reaction product was formed when aqueous solutions of either Na_2S or Na_2S_2 were passed over a stationary nitrosothiol column (Fig. 5). Thus, the above routes are neither mutually exclusive, nor may they represent the only pathways through which $SSNO^-$ can be formed. Conceivably, multiple reaction pathways may occur in parallel, which would explain the complexity of spectral interconversions taking place (as becomes apparent when one analyzes sequential spectra of reaction mixtures and their absorbance-time records).

The products of $SSNO^-$ decomposition are NO and polysulfides as evidenced in the present study by the measurement of gas phase chemiluminescence and sGC activation (Fig. 6) and the spectral step-like absorbance features in the UV range characteristic of polysulfides (Figs. 2, 4 and 5 and S4). As expected, the potential of SNAP/HS^- mixtures to release NO correlated inversely with their peak absorbance at 412 nm, and as $SSNO^-$ decomposes, polysulfide absorbance at 290–300 nm increases (Fig. S4).

$$SSNO^- \rightarrow SS^{\bullet -} + NO^\bullet \quad (13)$$

$$SS^{\bullet -} \rightarrow S_4^{2-} \rightarrow \rightarrow (S_x^{2-}) \overset{H_2O}{\rightarrow} S_{(x-1)}^{2-} + H_2S \quad (14)$$

Assuming homolytic cleavage of $SSNO^-$, the most likely initial product formed in addition to NO is the disulfide radical, $SS^{\bullet -}$ (Eq. 13). Dimerization and reaction with excess thiolate may give rise to formation of higher polysulfides (S_x^{2-}/HS_x^-). In aqueous solutions at pH 7.4, this is followed by hydrolysis and disproportionation reactions, yielding polysulfides of varying chain lengths in addition to free H_2S [48] (Eq. 14).

What emerges from the above is that the reaction between nitrosothiols and sulfide is all but straightforward; this had already been observed by others before. Although carried out in unbuffered alkaline solutions rather than at physiological pH (and thus not directly comparable to the present observations at physiological pH), Munro et al. reported that the absorbance changes they observed at low sulfide concentrations were "not easily interpreted, and too complicated for a simple kinetic analysis," possibly due to "several rapid processes … occurring" [37]. Indeed, the complexity of the UV/vis spectral changes seen during the reaction of nitrosothiols with sulfide at different concentration ratios demonstrate that the stability and nature of the intermediates formed strongly depend on the relative concentration ratio of the reactants, with thionitrite, nitrosopersulfide and NO likely not the only products formed in this reaction.

What exactly accounts for the scavenging of NO – as indicated by the inhibition of SNAP-induced cGMP production in RFL-6 cells – is unclear at present. Similar functional results have been reported by Moore and coworkers using other NO-donors [10,21] but – to the best of our knowledge – this is the first time that an inhibition of NO bioactivity has been demonstrated for nitrosothiols. While the isomerization tendency of HSNO to form other products with lower NO generating potential likely plays a role, it is possible that additional NO-scavenging effects by reactive sulfur-oxy intermediates such as sulfite [49] or sulfur radical species are involved; the latter could either produce reactive oxygen species that scavenge NO by direct chemical reaction or act as temporary "NO sink" by forming S-nitroso species (with the potential to release NO further downstream, as demonstrated here for $SSNO^-$). Attempts to mechanistically investigate the possible involvement of radical intermediates by using spin traps i.e. DMPO would be of little help in this context as they will also trap NO and thus by definition lower NO bioavailability. Yet, if thiyl radical chemistry was indeed involved the nitrosothiol/HS^- interaction should also be accompanied by a reaction with "mother nature's spin trap", molecular oxygen. In fact, our own preliminary investigations (Fig. 3) confirm that dissolved oxygen is consumed upon reaction of SNAP with sulfide at rates exceeding those of either NO and sulfide autoxidation by far. This observation is interesting not only from a chemical perspective, but also because mitochondrial sulfide oxidation has been linked to physiological oxygen sensing [50]. The reaction of nitrosothiols with sulfide would seem to add an interesting "twist" to that story. Thus, both the oxygen dependence of the reaction and the mechanism accounting for the drop in NO bioavailability at lower sulfide concentrations would seem to merit further investigation.

Effects of sulfide on nitrosothiols bioactivity – is it all in the chemistry?

A series of recent investigations suggests that much of the H_2S/NO cross-talk in the vasculature occurs via modulation of cGMP breakdown following inhibition of PDE activity [28,51,52]. Consistent with this notion, the PDE5 inhibitor sildenafil has been shown to attenuate the vasorelaxant effects of NaHS in rat aorta [51]. In rat smooth muscle cells, treatment with IBMX led to an increase in cGMP whereas sulfide itself had little effect [28]. While sulfide was unable to directly activate isolated sGC or modify sGC stimlation by the NO donor DEA/NO [52], low concentrations of sulfide were found to inhibit cellular PDE preparations [28] and recombinant PDE5 [51]. However, these results are not without controversy as others, using the endothelial cell line RF/6A, failed to demonstrate a cGMP increase by sulfide [53].

We find that sulfide-mediated cGMP elevations in RFL-6 cells were inhibited by ODQ and unaffected by the presence of IBMX indicating that these effects are dependent on sGC activity, i.e. the

formation of cGMP rather than alterations in outward transport or enzymatic breakdown. Consistent with earlier reports [54], IBMX alone did not affect basal cGMP levels in RFL-6 cells, presumably as these cells do not have an active NO-synthase and express only low levels of PDE5 [29]. Accordingly, we did not observe any difference in SNAP-induced cGMP elevations from baseline in the presence or absence of IBMX; moreover, the cGMP-specific PDE activity of these cells was lower than the corresponding cAMP-related activity. Interestingly, the NO scavenger cPTIO significantly attenuated sGC activation by higher sulfide concentrations but had no effect on basal levels. This action profile is consistent with the notion that sulfide may contribute to sGC activation following direct chemical interaction with NO stores, although this possibility has not been experimentally verified. Taken together, the effects of sulfide on intracellular cGMP levels appear to be dependent on the interplay between cGMP production by sGC, cyclic nucleotide breakdown and possibly clearance pathways (e.g., alterations in cyclic nucleotide transport across membrane). If true, this might explain why responses to sulfide differ between cell type and vascular beds studied.

Physiological relevance of the sulfide/nitrosothiol interaction

The potential of hydrosulfide (and by inference, H_2S) to either attenuate or potentiate NO bioactivity may be of relevance to the regulation of vascular tone. From studies in rodent tissue we know that nitrosothiols, an important storage form of NO [55,56], are particularly abundant in the vasculature [56]; the same seems to hold true for sulfide-related metabolites (at least in the aorta [57]), and both, endothelial and smooth muscle cells have been shown to express the enzymatic machinery capable of generating H_2S [19,58,59]. Sulfide may therefore contribute to the fine-tuning of NO bioactivity in the vasculature, either via modulation of intracellular cGMP concentrations following inhibition of PDE activity [28,51,52] and/or, as demonstrated in the current study, by chemically reacting with nitrosothiols. Besides the transient formation of SNO^-, the two major bioactive intermediates produced in the course of the latter reaction appear to include nitrosopersulfide and polysulfides. The concentrations used in the present proof-of-principle studies are clearly well outside the physiologically relevant range. Nevertheless, the effects of sulfide on SNAP-induced cGMP accumulation in RFL-6 cells, as shown in Fig. 1, suggest this interaction can occur also within cells; at present, this is mere speculation awaiting experimental confirmation by NMR and/or mass spectrometry based analytical techniques that allow unequivocal identification of $SSNO^-$ formation in cells and tissues. However, since the outcome of this chemical cross-talk is strongly dependent on the relative concentration ratio of the reactants and linked to oxygen availability in several ways, in vivo experiments will ultimately be required to shed further light on the biological relevance of this interaction. The situation may be considerably more complex under pathophysiological circumstances as the kinetics of expression of the different enzymes required to sustain an enhanced production of both H_2S and NO likely diverges over the time-course of induction in different tissue compartments, giving rise to an interesting dynamic in what already looks like a complex interaction scenario under controlled conditions. The present observations may also help explain some of the conflicting results regarding the NO/sulfide interaction obtained by different investigators.

Conclusion

In summary, we have demonstrated that the chemical reaction of nitrosothiols with sulfide leads to modulation of their NO-related bioactivity in a concentration-dependent fashion, giving rise to inhibition at low and potentiation at higher sulfide concentrations. Spectral evidence demonstrates that under conditions of excess sulfide $SSNO^-$ is formed, which release NO at higher rate and thus activates sGC more effectively than the starting nitrosothiol itself. While further detailed study is warranted to identify the chemical nature and biological activity of other reaction products involved, the chemical and biological properties of $SSNO^-$ suggest that nitrosopersulfide represents a new signaling entity at the cross-roads between sulfide and NO/polysulfide signaling.

Acknowledgments

We would like to thank Alex Dyson and Mervyn Singer for letting us use their oxygen electrode setup, Sivatharsini Thasian-Sivarajah and David Pullmann for helping with EIA and UV–visible measurements, and Karol Ondrias for insightful comments. We are grateful to the Susanne-Bunnenberg-Stiftung of the Düsseldorf Heart Center (to MK), the COST action BM1005 (European Network on Gasotransmitters), the FP7 Marie Curie International Reintegration program (PIRG08-GA-2010-277006, to PN) and the Faculty of Medicine, University of Southampton (to MF) for financial support.

Appendix A. Supporting information

Supplementary data associated with this article can be found in the online version at http://dx.doi.org/10.1016/j.redox.2013.12.031.

Rererences

[1] L. Li, P. Rose, P.K. Moore, Hydrogen sulfide and cell signaling, Annu. Rev. Pharmacol. Toxicol. 51 (2011) (2011) 169–187.
[2] K.R.A. Olson, Practical look at the chemistry and biology of hydrogen Sulfide, Antioxid. Redox. Signal. 17 (2012) 32–44.
[3] J.W. Calvert, S. Jha, S. Gundewar, J.W. Elrod, A. Ramachandran, C.B. Pattillo, C. G. Kevil, D.J. Lefer, Hydrogen sulfide mediates cardioprotection through Nrf2 signaling, Circ. Res. 105 (2009) 365–374.
[4] R. Wang, Physiological implications of hydrogen sulfide: a whiff exploration that blossomed, Physiol. Rev. 92 (2012) 791–896.
[5] J.M. Fukuto, S.J. Carrington, D.J. Tantillo, J.G. Harrison, L.J. Ignarro, B.A. Freeman, A. Chen, D.A. Wink, Small molecule signaling agents: the integrated chemistry and biochemistry of nitrogen oxides, oxides of carbon, dioxygen, hydrogen sulfide, and their derived species, Chem. Res. Toxicol. 25 (2012) 769–793.
[6] R. Wang, Two's company, three's a crowd: can H_2S be the third endogenous gaseous transmitter? Faseb J. 16 (2002) 1792–1798.
[7] M. Feelisch, K.R. Olson, Embracing sulfide and CO to understand nitric oxide biology, Nitric Oxide: Biol. Chem./Off. J. Nitric Oxide Soc. 35 (2013) 2–4.
[8] J.W. Morse, F.J. Millero, J.C. Cornwell, D. Rickard, The chemistry of the hydrogen sulfide and iron sulfide systems in natural waters, Earth-Sci. Rev. 24 (2002) 1–42.
[9] P. Nagy, Z. Palinkas, A. Nagy, B. Budai, I. Toth, A. Vasas, Chemical aspects of hydrogen sulfide measurements in physiological samples, Biochim. Biophys. Acta 876-891 (1840) 2014.
[10] M.Y. Ali, C.Y. Ping, Y.Y. Mok, L. Ling, M. Whiteman, M. Bhatia, P.K. Moore, Regulation of vascular nitric oxide in vitro and in vivo; a new role for endogenous hydrogen sulphide? Br. J. Pharmacol. 149 (2006) 625–634.
[11] M. Kajimura, R. Fukuda, R.M. Bateman, T. Yamamoto, M. Suematsu, Interactions of multiple gas-transducing systems: hallmarks and uncertainties of CO, NO, and H_2S gas biology, Antioxid. Redox Signal. 13 (2010) 157–192.
[12] K. Shatalin, E. Shatalina, A. Mironov, E. Nudler, H2S: A universal defense against antibiotics in bacteria, Science (New York, N.Y.) 334 (2011) 986–990.
[13] P.J. Yoon, S.P. Parajuli, D.C. Zuo, P.K. Shahi, H.J. Oh, H.R. Shin, M.J. Lee, C.H. Yeum, S. Choi, J.Y. Jun, Interplay of hydrogen sulfide and nitric oxide on the pacemaker activity of interstitial cells of cajal from mouse small intestine, Chonnam Med. J. 47 (2011) 72.
[14] Q.-C. Yong, L.-F. Hu, S. Wang, D. Huang, J.-S. Bian, Hydrogen sulfide interacts with nitric oxide in the heart: possible involvement of nitroxyl, Cardiovasc. Res. 88 (2010) 482–491.
[15] G.K. Kolluru, X. Shen, S.C. Bir, C.G. Kevil, Hydrogen sulfide chemical biology: Pathophysiological roles and detection, Nitric Oxide: Biol. Chem./Off. J. Nitric Oxide Soc. 35 (2013) 5–20.

[16] G.K. Kolluru, X. Shen, C.G. Kevil, A tale of two gases: NO and H_2S, foes or friends for life? Redox Biol. 1 (2013) 313–318.
[17] S. Bruce King, Potential biological chemistry of hydrogen sulfide (H2S) with the nitrogen oxides, Free Radic. Biol. Med. 55 (2013) 1–7.
[18] Q. Li, J.R. Lancaster , Chemical foundations of hydrogen sulfide biology, Nitric Oxide: Biol. Chem./Off. J. Nitric Oxide Soc. 35C (2013) 21–34.
[19] G. Yang, L. Wu, B. Jiang, W. Yang, J. Qi, K. Cao, Q. Meng, A.K. Mustafa, W. Mu, S. Zhang, S.H. Snyder, R. Wang, H(2)S as a physiologic vasorelaxant: hypertension in mice with deletion of cystathionine gamma-lyase, Science 322 (2008) 587–590.
[20] R. Wang, Signaling pathways for the vascular effects of hydrogen sulfide, Curr. Opin. Nephrol. Hypertens. 20 (2011) 107–112.
[21] M. Whiteman, L. Li, I. Kostetski, S.H. Chu, J.L. Siau, M. Bhatia, P.K. Moore, Evidence for the formation of a novel nitrosothiol from the gaseous mediators nitric oxide and hydrogen sulphide, Biochem. Biophys. Res. Commun. 343 (2006) 303–310.
[22] Q.C. Yong, J.L. Cheong, F. Hua, L.W. Deng, Y.M. Khoo, H.S. Lee, A. Perry, M. Wood, M. Whiteman, J.S. Bian, Regulation of heart function by endogenous gaseous mediators-crosstalk between nitric oxide and hydrogen sulfide, Antioxid. Redox Signal. 14 (2011) 2081–2091.
[23] D.L.H. Williams, Nitrosation reactions and the chemistry of nitric oxide, Elsevier, Amsterdam, The Netherlands, 2004.
[24] M.R. Filipovic, J.L. Miljkovic, T. Nauser, M. Royzen, K. Klos, T. Shubina, W.H. Koppenol, S.J. Lippard, I. Ivanovic-Burmazovic, Chemical characterization of the smallest S-nitrosothiol, HSNO; cellular cross-talk of H_2S and S-nitrosothiols, J. Am. Chem. Soc. 134 (2012) 12016–12027.
[25] M. Nonella, R. Huber, T.-K. Ha, Photolytic preparation and isomerization of HNSO, HOSN, HSNO, and HONS in an argon matrix. An experimental and theoretical study, J. Phys. Chem. 91 (1987) 5203–5209.
[26] K. Ondrias, A. Stasko, S. Cacanyiova, Z. Sulova, O. Krizanova, F. Kristek, L. Malekova, V. Knezl, A. Breier, H(2)S and HS(-) donor NaHS releases nitric oxide from nitrosothiols, metal nitrosyl complex, brain homogenate and murine L1210 leukaemia cells, Pflügers Archiv. Eur. J. Physiol. 457 (2008) 271–279.
[27] X. Teng, T. Scott Isbell, J.H. Crawford, C.A. Bosworth, G.I. Giles, J.R. Koenitzer, J.R. Lancaster, J.E. Doeller, D. W Kraus, R. Patel, Novel method for measuring S-nitrosothiols using hydrogen sulfide, Methods Enzymol. 441 (2008) 161–172.
[28] M. Bucci, A. Papapetropoulos, V. Vellecco, Z. Zhou, A. Pyriochou, C. Roussos, F. Roviezzo, V. Brancaleone, G. Cirino, Hydrogen sulfide is an endogenous inhibitor of phosphodiesterase activity, Arterioscler. Thromb. Vasc. Biol. 30 (2010) 1998–2004.
[29] P.J. Kraft, D. Haynes-Johnson, S. Bhattacharjee, S.G. Lundeen, Y. Qiu, Altered activities of cyclic nucleotide phosphodiesterases and soluble guanylyl cyclase in cultured RFL-6 cells, Int. J. Biochem. Cell. Biol. 36 (2004) 2086–2095.
[30] J. Stamler, M. Feelisch, Preparation and detection of S-nitrosothiols, in: M. Feelisch, J. Stamler (Eds.), Methods in Nitric Oxide Research, John Wiley & Sons, Chichester, 1996, pp. 521–539.
[31] K. Ishii, H. Sheng, T.D. Warner, U. Förstermann, F. Murad, A simple and sensitive bioassay method for detection of EDRF with RFL-6 rat lung fibroblasts, Am. J. Physiol.- Heart Circulatory Physiol. 261 (1991) H598–H603.
[32] E. Noack, M. Feelisch, Molecular mechanisms of nitrovasodilator bioactivation, Basic. Res. Cardiol. 86 (2) (1991) 37–50.
[33] J.A. Riego, K.A. Broniowska, N.J. Kettenhofen, N. Hogg, Activation and inhibition of soluble guanylyl cyclase by S-nitrosocysteine: involvement of amino acid transport system L, Free Rad. Biol. Med. 47 (2009) 269–274.
[34] N.B. Fernhoff, E.R. Derbyshire, E.S. Underbakke, M.A. Marletta, Heme-assisted S-nitrosation desensitizes ferric soluble guanylate cyclase to nitric oxide, J. Biol. Chem. 287 (2012) 43053–43062.
[35] J. McAninly, D.L.H. Williams, S.C. Askew, A.R. Butler, C. Russell, Metal ion catalysis in nitrosothiol (RSNO) decomposition, J. Chem. Soc. Chem. Commun. (1993) 1758–1759.
[36] F. Seel, M. Wagner, Reaction of sulfides with nitrogen monoxide in aqueous solution, Z. Anorg. Allg. Chem. 558 (1988) 189–192.
[37] A.P. Munro, D.L.H. Williams, Reactivity of sulfur nucleophiles towards S-nitrosothiols, J. Chem. Soc., Perkin Trans. 2 (2000) 1794–1797.
[38] F. Seel, M. Wagner, The reaction of polysulfides with nitrogen monoxide in non-acqueous solvents- nitrosodisulfides, Z. Naturforsch 40 (1985) 762.
[39] Y. Kimura, Y. Mikami, K. Osumi, M. Tsugane, J. Oka, H. Kimura, Polysulfides are possible H_2S-derived signaling molecules in rat brain, Faseb J. 27 (2013) 2451–2457.
[40] R. Greiner, Z. Palinkas, K. Basell, D. Becher, H. Antelmann, P. Nagy, T.P. Dick, polysulfides link H_2S to protein thiol oxidation, Antioxid. Redox Signal. 19 (2013) 1749–1765.
[41] D.L.H. Williams, The chemistry of S-nitrosothiols, Acc. Chem. Res. 32 (1999) 869–876.
[42] Q.K. Timerghazin, G.H. Peslherbe, A.M. English, Structure and stability of HSNO, the simplest S-nitrosothiol, Phys. Chem. Chem. Phys. 10 (2008) 1532–1539.
[43] F. Seel, R. Kuhn, G. Simon, M. Wagner, B. Krebs, M. Dartmann, PNP-Perthionitrit und PNP-Monothionitrit. Zeitschrift für Naturforschung, Teil b, Anorg. Chemie, Org. Chem. 40 (1985) 1607–1617.
[44] M. Goehring, J. Messner, Zur Kenntnis der schwefligen Säure. III Das Sulfinimid und seine Isomeren, Z. Anorg. Allg. Chem. 268 (1952) 47–56.
[45] R.P. Müller, M. Nonella, J.R. Huber, Spectroscopic investigation of HSNO in a low temperature matrix. UV, vis, and IR-induced isomerisations, Chem. Phys. 87 (1984) 351–361.
[46] R.Z. Pino, M. Feelisch, Bioassay discrimination between nitric oxide (NO.) and nitroxyl (NO-) using L-cysteine, Biochem. Biophys. Res. Commun. 201 (1994) 54–62.
[47] N.E. Francoleon, S.J. Carrington, J.M. Fukuto, The reaction of H_2S with oxidized thiols: generation of persulfides and implications to H_2S biology, Arch. Biochem. Biophys. 516 (2011) 146–153.
[48] A. Kamyshny , J. Gun, D. Rizkov, T. Voitsekovski, O. Lev, Equilibrium distribution of polysulfide ions in aqueous solutions at different temperatures by rapid single phase derivatization, Environ. Sci. Technol. 41 (2007) 2395–2400.
[49] D. Littlejohn, K.Y. Hu, S.G. Chang, Kinetics of the reaction of nitric oxide with sulfite and bisulfite ions in aqueous solution, Inorg. Chem. 25 (1986) 3131–3135.
[50] K.R. Olson, N.L. Whitfield, Hydrogen sulfide and oxygen sensing in the cardiovascular system, Antioxid. Redox Signal. 12 (2010) 1219–1234.
[51] M. Bucci, A. Papapetropoulos, V. Vellecco, Z. Zhou, A. Zaid, P. Giannogonas, A. Cantalupo, S. Dhayade, K.P. Karalis, R. Wang, R. Feil, G. Cirino, cGMP-Dependent protein kinase contributes to hydrogen sulfide-stimulated vasorelaxation, PLoS ONE 7 (2012) e53319.
[52] C. Coletta, A. Papapetropoulos, K. Erdelyi, G. Olah, K. Módis, P. Panopoulos, A. Asimakopoulou, D. Gerö, I. Sharina, E. Martin, Hydrogen sulfide and nitric oxide are mutually dependent in the regulation of angiogenesis and endothelium-dependent vasorelaxation, Proc. Natl. Acad. Sci. U. S. A. 109 (2012) 9161–9166.
[53] W. Cai, M. Wang, P. Moore, H. Jin, T. Yao, Y. Zhu, The novel proangiogenic effect of hydrogen sulfide is dependent on Akt phosphorylation, Cardiovasc. Res. 76 (2007) 29–40.
[54] A. Honda, S.R. Adams, C.L. Sawyer, V. Lev-Ram, R.Y. Tsien, W.R.G. Dostmann, Spatiotemporal dynamics of guanosine 3',5'-cyclic monophosphate revealed by a genetically encoded, fluorescent indicator, Proc. Natl. Acad. Sci. 98 (2001) 2437–2442.
[55] K.A. Broniowska, N. Hogg, The chemical biology of S-nitrosothiols, Antioxid. Redox Signal. 17 (2012) 969–980.
[56] J. Rodriguez, R.E. Maloney, T. Rassaf, N.S. Bryan, M. Feelisch, Chemical nature of nitric oxide storage forms in rat vascular tissue, Proc. Natl. Acad. Sci. U. S. A. 100 (2002) 336–341.
[57] M.D. Levitt, M.S. Abdel-Rehim, J. Furne, Free and acid-labile hydrogen sulfide concentrations in mouse tissues: anomalously high free hydrogen sulfide in aortic tissue, Antioxid. Redox Signal. 15 (2011) 373–378.
[58] H. Kimura, Production and physiological effects of hydrogen sulfide, Antioxid. Redox Signal. (2013).
[59] C. Szabó, A. Papapetropoulos, Hydrogen sulphide and angiogenesis: mechanisms and applications, Br. J. Pharmacol. 164 (2011) 853–865.

Basic Res Cardiol (2014) 109:398
DOI 10.1007/s00395-013-0398-1

ORIGINAL CONTRIBUTION

Depletion of circulating blood NOS3 increases severity of myocardial infarction and left ventricular dysfunction

Marc W. Merx · Simone Gorressen · Annette M. van de Sandt · Miriam M. Cortese-Krott · Jan Ohlig · Manuel Stern · Tienush Rassaf · Axel Gödecke · Mark T. Gladwin · Malte Kelm

Received: 26 June 2013 / Revised: 25 November 2013 / Accepted: 6 December 2013 / Published online: 18 December 2013

Abstract Nitric oxide (NO) derived from endothelial NO synthase (NOS3) plays a central role in myocardial ischemia/reperfusion (I/R)-injury. Subsets of circulating blood cells, including red blood cells (RBCs), carry a NOS3 and contribute to blood pressure regulation and RBC nitrite/nitrate formation. We hypothesized that the circulating blood born NOS3 also modulates the severity of myocardial infarction in disease models. We cross-transplanted bone marrow in wild-type and $NOS3^{-/-}$ mice with wild-type mice, producing chimeras expressing NOS3 only in vascular endothelium (BC−/EC+) or in both blood cells and vascular endothelium (BC+/EC+). After 60-min closed-chest coronary occlusion followed by 24 h reperfusion, cardiac function, infarct size (IS), NO_x levels, RBCs NO formation, RBC deformability, and vascular reactivity were assessed. At baseline, BC−/EC+ chimera had lower nitrite levels in blood plasma (BC−/EC+: 2.13 ± 0.27 μM vs. BC+/EC+ 3.17 ± 0.29 μM; $*p < 0.05$), reduced DAF FM associated fluorescence within RBCs (BC−/EC+: 538.4 ± 12.8 mean fluorescence intensity (MFI) vs. BC+/EC+: 619.6 ± 6.9 MFI; $***p < 0.001$) and impaired erythrocyte deformability (BC−/EC+: 0.33 ± 0.01 elongation index (EI) vs. BC+/EC+: 0.36 ± 0.06 EI; $*p < 0.05$), while vascular reactivity remained unaffected. Area at risk did not differ, but infarct size was higher in BC−/EC+ (BC−/EC+: 26 ± 3 %; BC+/EC+: 14 ± 2 %; $**p < 0.01$), resulting in decreased ejection fraction (BC−/EC+ 46 ± 2 % vs. BC+/EC+: 52 ± 2 %; $*p < 0.05$) and increased end-systolic volume. Application of the NOS inhibitor *S*-ethylisothiourea hydrobromide was associated with larger infarct size in BC+/EC+, whereas infarct size in BC−/EC+ mice remained unaffected. Reduced infarct size, preserved cardiac function, NO levels in RBC and RBC deformability suggest a modulating role of circulating NOS3 in an acute model of myocardial I/R in chimeric mice.

Keywords Nitric oxide · Myocardial ischemia/reperfusion · Circulating NOS3

M.W. Merx and S. Gorressen equally contributed.

Electronic supplementary material The online version of this article (doi:10.1007/s00395-013-0398-1) contains supplementary material, which is available to authorized users.

M. W. Merx (✉) · S. Gorressen · A. M. van de Sandt · M. M. Cortese-Krott · J. Ohlig · M. Stern · T. Rassaf · M. Kelm
Division of Cardiology, Pneumology and Angiology, Department of Medicine, University Hospital Düsseldorf, Moorenstrasse 5, 40225 Düsseldorf, Germany
e-mail: marc.merx@med.uni-duesseldorf.de

A. Gödecke
Department of Cardiovascular Physiology, Heinrich-Heine-University, Düsseldorf, Germany

M. T. Gladwin
Vascular Medicine Institute, University of Pittsburgh, Pittsburgh, PA, USA

M. T. Gladwin
Division of Pulmonary, Allergy and Critical Care Medicine, Department of Medicine, University of Pittsburgh School of Medicine, Pittsburgh, PA, USA

Introduction

NO derived from the endothelial NO synthase (NOS3) regulates coronary blood flow, evokes positive inotropic and lusitropic effects, improves myocardial relaxation and optimizes cardiac performance [41]. NO participates in the regulation of myocardial metabolism [30]. It reduces the consumption of oxygen and the inotropic effect of

catecholamines by muscarinic, cholinergic, and beta-adrenergic receptor stimulation [1, 43].

During myocardial ischemia and reperfusion (I/R), NO exerts a cardioprotective role by a variety of mechanisms [15], e.g., it regulates mitochondrial respiration, thereby improving myocardial oxygenation [51]. Endogenous NO contributes to hibernation via reducing oxygen consumption and preserving calcium sensitivity and contractile function [15]. NO inactivates caspases by nitrosation and thus decreases myocyte apoptosis [15]. Whereas an increase in cardiac interstitial NO production could be observed during early I/R [29], which is in part derived from activated NOS isoforms [11], NO formation drops during ongoing I/R. In this acute phase, endothelium becomes dysfunctional, leukocyte adhesion increases and neutrophils migrate into the reperfused tissue. NOS3 knockout mice exhibit enlarged infarct sizes [20], while infarct size after I/R is reduced in animals with NOS3 overexpression [17, 44], suggesting a cardioprotective role for NOS3-derived NO in the setting of I/R.

NOS3 is not only expressed in the vascular endothelium but also in blood cells including B- and T-lymphocytes [42], eosinophils [50], and in red blood cells (RBCs) [5, 24]. RBCs are the most abundant blood cell population carrying a NOS3 and represent the major storage compartment of circulating NO metabolites [7, 39]. Red cell NOS3-dependent NO production alters the functional characteristics of the erythrocyte, including erythrocyte deformability, platelet activity and vascular tone [5, 24, 47]. Thus, in addition to the vascular endothelium, the RBCs are another source of vascular NOS-dependent NO production and contribute to the circulating NO pool [5, 24]. In addition, RBCs have "shuttle properties" and are able to accumulate and transport NO metabolites such as nitrite [9]. Application of RBCs with subsequent increase in NO release reduced the extent of irreversible myocardial tissue damage in isolated hearts [48].

We, therefore, hypothesized that circulating NOS3 decreases infarct size and subsequently preserves left ventricular function following myocardial I/R injury. To selectively assess infarct size in the absence or presence of circulating NOS3, we created chimera mice lacking or carrying blood cell NOS3 by transplanting bone marrow from NOS3$^{-/-}$ mice or wild type (WT) into WT mice, and analyzed infarct size after 60-min closed-chest coronary occlusion followed by 24 h of reperfusion.

Methods

Animals

Male C57BL/6 wild-type (WT) and NOS3$^{-/-}$ mice (endothelial nitric oxide synthase) (C57BL/6.129/Ola-eNOStm) [10] were kept according to federal regulations. All studies were approved by the state animal welfare commission. Mice ranged in body weight from 20 to 25 g and in age from 8 to 10 weeks for bone marrow transplantation.

Chimeras (irradiation and bone marrow transplantation)

To analyze the effects of the lack of NOS3 in blood cells in an acute model of myocardial I/R, we transplanted bone marrow from WT and NOS3$^{-/-}$ mice, producing chimeras which either do (BC+/EC+) or do not carry NOS3 in blood cells (BC−/EC+) as described previously [47] (See Online Resource 2 for detailed information).

Blood collection, RBC preparation and loading with DAF-FM

Blood was obtained from mice via heart puncture, anticoagulated with heparin and processed within 2 h. For loading with DAF-FM diacetate, whole blood was diluted 1:500 to a final concentration of $\sim 1.2 \times 10^4$ RBC/μl in cold phosphate buffered solution (PBS) as previously described [4, 5]. In brief, RBCs were loaded with 10 μM DAF-FM diacetate for 30 min at room temperature in the dark, or left untreated, washed in PBS and analyzed for DAF FM-associated fluorescence in a FACS Canto II (BD Biosciences) flow cytometer. For NOS inhibition, RBC suspensions were pre-incubated for 30 min with 3 mM L-NAME (L-N^G-nitroarginine methyl ester). The method was validated for detection of NO-related species in RBC by applying a multilevel analytical approach and separating the reaction products with RP-HPLC or LC/MS/MS, as described in [4, 5] (See Online Resource 2 for detailed information).

Measurement of nitrite/nitrate in plasma, heart tissue and aorta

Blood samples were collected by intra-cardiac puncture at baseline, after 5 min and 24 h of myocardial reperfusion. Blood and tissue samples were prepared for determination of nitrate and nitrite as previously described [12, 23, 38, 40] (See Online Resource 5 and 6 for detailed information).

Measurement of RBC deformability (ektacytometry)

Blood was drawn via heart puncture and collected in a heparinized tube for the measurement of RBC deformability. RBC deformability was measured by ektacytometry by the Laser-assisted optical rotational cell analyzer (LORCA, R&R Mechatronics) according to the manufacturer's instructions as previously described [16, 21]. RBC

deformability was expressed by the elongation index (EI), which was calculated from the elliptical RBC diffraction pattern as EI = $(L - W)/(L + W)$, where L and W are the length and width of the diffraction pattern, respectively (See Online Resource 9 for detailed information).

Langendorff setup

For isolated heart measurements, murine hearts were explanted at baseline (6 weeks after bone marrow transplantation), and mounted with retrograde perfusion at 100 mmHg constant pressure with modified Krebs–Henseleit buffer in an isolated heart apparatus (Hugo Sachs Elektronik), as previously described [31–33, 46] (See Online Resource 2 for detailed information).

Gel electrophoresis and western blot analysis

Mouse heart, mouse aorta and human endothelial cells were lysed with RIPA lysis buffer containing protease inhibitor cocktail (Roche Applied Science), as previously described [5, 47]. Total protein concentration was determined by the Lowry assay (DC Protein Assay, Bio-Rad). For gel electrophoresis, 80 µg heart lysates, 20 µg aortic lysates, or human umbilical endothelial cell lysate were loaded in 4–12 % Bis–Tris gel. For western blot analysis, proteins were transferred onto polyvinylidene fluoride membrane Hybond P (Amersham Biosciences, Munich, Germany). A pre-stained protein ladder (PageRuler Plus, Fermentas Life Science) was loaded into the gel to control for transfer efficiency. The membrane was blocked with 5 % nonfat dry milk (Bio-Rad) in TBS (10 mM Tris, 100 mM NaCl), incubated with a mouse anti-human anti-eNOS antiserum (overnight 4 °C 1:500) (BD Bioscience) diluted (1 h RT 1:1,000) in T-TBS (0.1 % Tween in TBS), washed for 30 min in T-TBS, and then incubated with HRP-conjugated goat anti-mouse antibody (1:5,000) from (BD Bio science).

Isometric force measurements in aortic rings

Thoracic aorta was removed as previously described at baseline (6 weeks after bone marrow transplantation) [45, 46]. Aortic rings were placed in an organ bath (Model Graz, Type 846, Hugo Sachs), under 1 g of tension, and bathed in 2 mL of Krebs buffer constantly gassed with 95 % O_2/5 % CO_2 at 37 °C. After equilibration phase (90 min), tissues were exposed to potassium chloride (80 nM) and subsequently phenylephrine (1 µM) to achieve maximal contraction. Afterwards relaxation response curves to increasing concentrations of acetylcholine (1 nM–10 µM) or to increasing concentrations of the NO donor sodium nitroprusside (SNP) (0.001–10 µM) were constructed. Contractility response to increasing concentrations of phenylephrine (1 nM–10 µM) was measured.

Myocardial ischemia and reperfusion protocol

A closed-chest model of myocardial I/R was utilized 6 week after bone marrow transplantation to reduce surgical trauma and consequent inflammatory reaction following I/R as compared to open-chest model [36]. At 3-day post-instrumentation myocardial ischemia was induced for 60 min of ischemia followed by 24 h of reperfusion (See Online Resource 2 for detailed information).

Assessment of infarct size (IS)

After 24 h of reperfusion, the animals were killed and heart was excised, rinsed in 0.9 % normal saline, left anterior descending artery (LAD) was re-occluded in the same location and 1 % Evans Blue dye was injected into the aortic root to delineate the area at risk (AAR) from not-at-risk myocardium, as published recently [14] (See Online Resource 2 for detailed information).

Echocardiography

Cardiac images were acquired using a Vevo 2100 high-resolution ultrasound scanner with 18–38 MHz linear transducer (VisualSonics Inc.). Echocardiography was performed as previously described [26]. Left ventricular (LV) end-systolic (ESV), end-diastolic volumes (EDV), LV ejection fraction (EF), cardiac output (CO) and stroke volume (SV) were calculated (See Online Resource 8 for detailed information).

ETU treatment

A subgroup of animals received *S*-ethylisothiourea hydrobromide (ETU) to achieve systemic NOS inhibition during ischemia and the first 5 min of reperfusion. During whole ischemia (60 min) and the first 5 min of reperfusion, ETU was administered at (0.245 µg/µl/min; i.p.) [46]. After 24 h of reperfusion, LV function was measured via echocardiography and infarct size was measured via triphenyltetrazoliumchlorid (TTC) staining in this subgroup.

Statistical analysis

The results are given as mean ± standard error of the mean (SEM). For repeated measurements, data were analyzed by two-way ANOVA followed by Bonferroni's post hoc test. Where indicated, an unpaired Student's t test was applied. $p = 0.05$ was set as the threshold of significance.

Results

Baseline characterization of chimeras after bone marrow transplantation

Inflammation

6 weeks after bone marrow transplantation, blood counts of both groups did not differ except for mean platelet volume (BC+/EC+: 5.75 ± 0.33 μm^3; $n = 21$ vs. BC−/EC+: 5.07 ± 0.18 μm^3; $n = 16$ ***$p < 0.001$) and lymphocytes (BC+/EC+: 0.93 ± 0.23 10^3/mm^3; $n = 21$ vs. BC−/EC+: 1.69 ± 1.18 10^3/mm^3; $n = 16$; *$p < 0.05$) (See Online Resource 3 for detailed information). To analyze for chronic persisting inflammation as a result of the transplantation, serum amyloid P (SAP) levels were determined in plasma via ELISA. No differences were seen between the groups (BC+/EC+: 68.1 ± 6.2 μg/ml; $n = 23$ and BC−/EC+ 64.7 ± 9.7 μg/ml, $n = 19$; n.s.) in blood plasma 6 weeks after bone marrow transplantation (See Online Resource 4).

NO_x levels

BC−/EC+ chimera showed a decreased DAF-FM associated fluorescence within RBCs (BC−/EC+: 538.4 ± 12.8 MFI) as compared to BC+/EC+ mice (619.6 ± 6.9 MFI, ***$p < 0.001$, $n = 5$ per group) 6 weeks after bone marrow transplantation (See Fig. 1a). The background signal observed in RBC from BC−/EC+ mice is not different from that obtained by loading human RBC treated with L-NAME (observed before [5]), and is due to the formation of fluorescent adducts of DAF-FM with molecules such as ascorbate, particularly abundant in RBC, and to the presence of fluorescent impurities in the stock solutions of DAF-FM DA, which are detectable only by analytical separative techniques as described previously [4]. Results provided evidence for a diminished NO formation in RBC under normoxic conditions in BC−/EC+.

Nitrite levels in BC−/EC+ chimera (2.13 ± 0.27 μM; $n = 11$) were lower in plasma compared to BC+/EC+ mice (3.17 ± 0.29 μM; $n = 10$; *$p < 0.05$) at baseline (See Fig. 1c). Nitrate levels were slightly but not significantly reduced in BC−/EC+ (121.60 ± 16.37 μM; $n = 11$) compared to BC+/EC+ mice (189.09 ± 22.77 μM; $n = 10$; n.s.) at baseline (See Fig. 1d). Nitrite (BC+/EC+:1.36 ± 0.15 μM, $n = 4$ vs. BC−/EC+: 1.53 ± 0.22 μM, $n = 3$; n.s.) and nitrate (BC+/EC+:18.31 ± 4.10 μM, $n = 4$ vs. BC−/EC+: 27.07 ± 7.14 μM, $n = 3$; n.s.) levels in heart tissue did not differ between both groups at baseline (i.e., 6-week post-

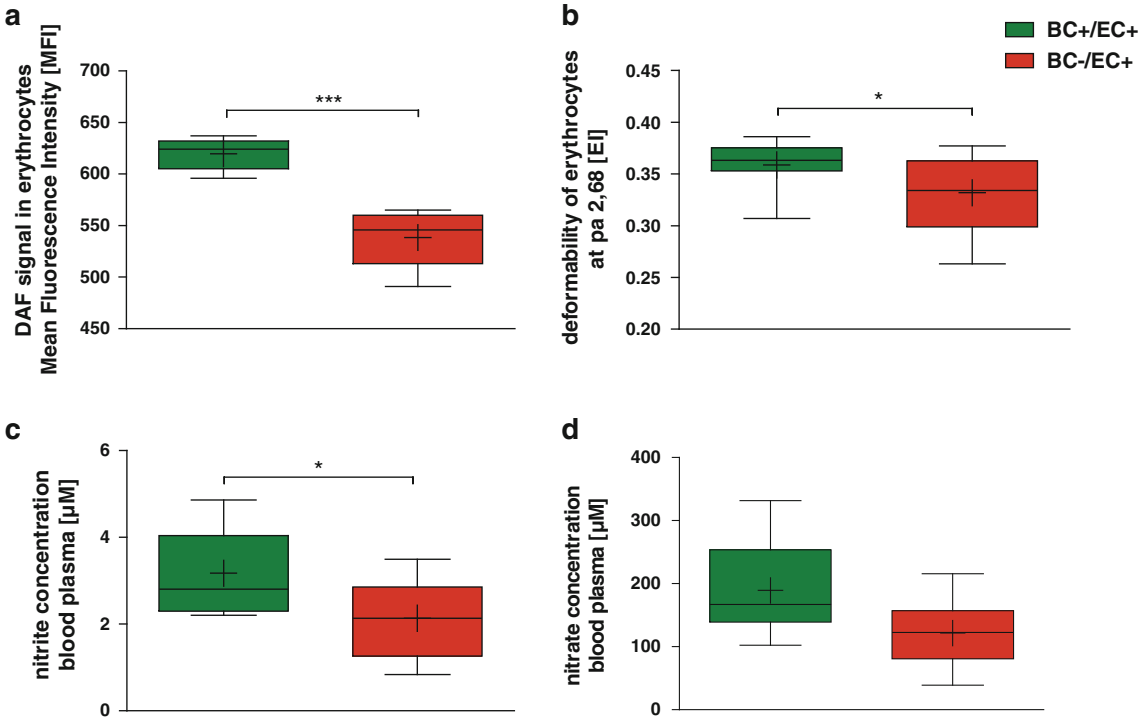

Fig. 1 Depletion of circulating NOS3 reduces NO bioavailability, RBC deformability, and plasma levels of nitrite and nitrate. Decreased DAF signal within erythrocytes (**a**, $n = 5$ per group, ***$p < 0.001$, unpaired Student's t test), reduced erythrocyte deformability (**b**, BC+/EC+ $n = 15$, BC−/EC+ $n = 16$, *$p < 0.05$, two-way ANOVA followed by Bonferroni's post hoc test) and diminished nitrite (**c**; BC+/EC+ $n = 10$, BC−/EC+ $n = 11$, *$p < 0.05$, two-way ANOVA followed by Bonferroni's post hoc test) and nitrate plasma levels (**d**; BC+/EC+ $n = 10$, BC−/EC+ $n = 11$; n.s.) were measured in BC−/EC+ compared to BC+/EC+ at baseline

bone marrow transplantation) (See Online Resource 5). Likewise, nitrite (BC+/EC+: 1.07 ± 0.10 µM, $n = 3$ vs. BC−/EC+: 1.01 ± 0.07 µM, $n = 3$; n.s.) and nitrate (BC+/EC+: 41.61 ± 12.56 µM, $n = 3$ vs. BC−/EC+: 31.51 ± 6.81 µM, $n = 3$; n.s.) levels in aorta did not differ between both groups at baseline (i.e., 6-week post-bone marrow transplantation) (See Online Resource 6).

RBC deformability

6 weeks after bone marrow transplantation, BC−/EC+ (0.33 ± 0.01 EI; $n = 16$ per group) exhibited decreased RBC deformability compared to BC+/EC+ (0.36 ± 0.01 EI; $n = 15$; $*p < 0.05$) (See Fig. 1b). Both groups demonstrated diminished RBC deformability compared to non-irradiated wild type 6 weeks after transplantation (0.39 ± 0.01 EI; $n = 15$; $***p < 0.001$).

Vascular reactivity

The effects of the transplantation procedure on vascular reactivity were assessed with three independent approaches. Ex vivo measurements of coronary flow (isolated hearts, Langendorff setup) of BC+/EC+ and BC−/EC+ revealed no differences in basal coronary flow (BC+/EC+: basal: 18.84 ± 1.91 ml/min/g vs. BC−/EC+: basal: 15.07 ± 1.08 ml/min/g, n.s.). After global brief ischemia, both groups responded with a uniform increase in coronary flow (BC+/EC+: basal: 18.84 ± 1.91 ml/min/g vs. reperfusion: 47.11 ± 1.67 ml/min/g, $***p < 0.001$, $n = 7$; BC−/EC+: basal: 15.07 ± 1.08 ml/min/g vs. reperfusion: 41.90 ± 2.94 ml/min/g, $***p < 0.001$, $n = 8$) (See Fig. 2a).

In vivo measurement of vascular reactivity was assessed by laser Doppler perfusion imaging, as changes in reactive

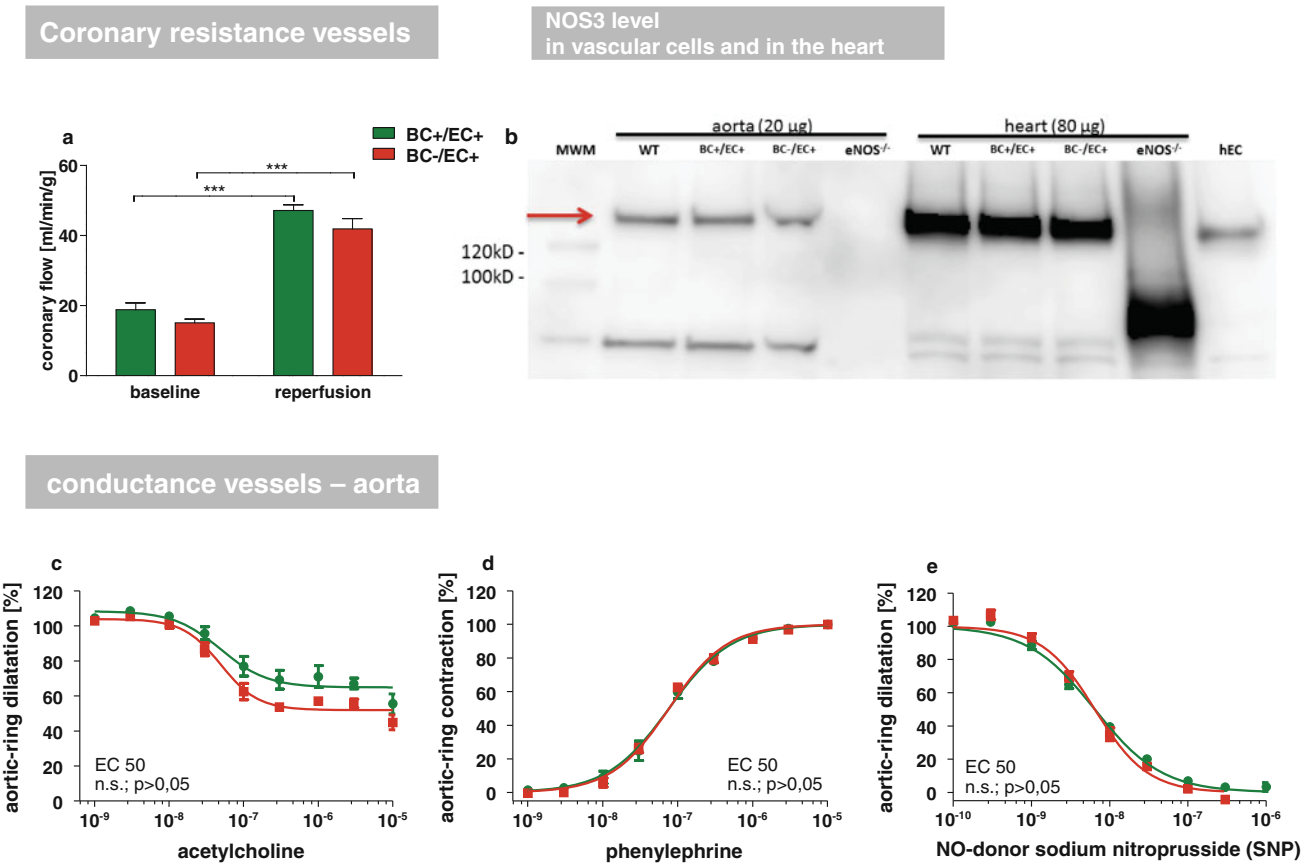

Fig. 2 Comparison of NOS3 expression and endothelial function in chimeric and WT mice. Ex vivo measurements of coronary flow from isolated hearts in Langendorff setup (**a**) of BC+/EC+ and BC−/EC+ revealed no significant differences at baseline and after global ischemia (flow corrected for heart weight; BC+/EC+ $n = 7$, BC−/EC+ $n = 8$, n.s.). NOS3 expression in hearts from BC+/EC+, BC−/EC+ and WT mice was assessed by Western blot analysis and compared with NOS3 expression in aortic tissue. No differences were detected between the displayed groups, while heart tissue exhibited overall higher NOS3 level than aortic tissue (**b**). Isometric force measurements in aortic rings (**c**–**e**). BC+/EC+ and BC−/EC+ revealed no significant difference in the mean effective concentration (EC 50) and, therefore, no different vessel characteristics at baseline ($n = 5$ per group, n.s., EC50 tested with unpaired Student's t test)

hyperemic response following short-term vascular occlusion in the hind limb of BC+/EC+ and BC−/EC+ mice. The measurements revealed no differences in all parameters investigated (See Online Resource 7). Basal mean perfusion before induction of hind limb ischemia (BC+/EC+: 99 ± 5 %; $n = 14$; BC−/EC+: 106 ± 6 %; $n = 12$; n.s.), the time till reperfusion peak (maximum mean perfusion) (BC+/EC+: 42 ± 3 s; $n = 14$; BC−/EC+: 43 ± 3 s; $n = 12$; n.s.) and the area under the curve of the reperfusion signal (BC+/EC+: 1.106 ± 56; $n = 14$ BC−/EC+: 1.186 ± 91; $n = 12$; n.s.) did not differ between both groups.

Vascular reactivity of aortic rings from BC+/EC+ and BC−/EC+ mice was compared by wire myography. After pre-contraction with KCl response curves to acetylcholine, phenylephrine and SNP were determined as the response of EC50 to the applied substances. For all three conditions, no difference in the mean effective concentration (EC 50) and, therefore, no differences in endothelium-dependent and endothelium-independent vascular function were observed (See Fig. 2c–e).

NOS3 levels in heart and aorta

NOS3 expression in the heart and aorta from BC+/EC+, BC−/EC+ and WT mice was assessed by Western blot analysis. No differences were detected between the analyzed groups (See Fig. 2b).

Left ventricular function

Depletion of blood cell NOS3 did not modify left ventricular function at baseline (6 weeks after bone marrow transplantation) as determined by M-mode and B-mode measurements, indicating equal left ventricular function in BC−/EC+ compared to BC+/EC+.

Left ventricular ejection fraction (BC+/EC+: 61 ± 1 %; BC−/EC+: 62 ± 1 %; n.s), end-systolic volume (BC+/EC+: 25 ± 1 µl; BC−/EC+: 25 ± 1 µl; n.s) and end-diastolic volume (BC+/EC+: 66 ± 2 µl, $n = 22$; BC−/EC+: 66 ± 2 µl, $n = 25$; n.s.) did not differ between both groups (See Fig. 4 and Online Resource 8).

Response of chimeras to myocardial ischemia/reperfusion

Blood cell NOS3 reduces infarct size following myocardial ischemia/reperfusion

Infarct size was increased in BC−/EC+ compared to BC+/EC+ (BC−/EC+: 26 ± 3 %; $n = 6$; BC+/EC+: 14 ± 2 %; $n = 9$ per group; $^{**}p < 0.01$), while AAR per LV did not differ between both groups (BC−/EC+: 50 ± 1 %; $n = 6$ BC+/EC+: 51 ± 2 %; $n = 9$ per group; n.s.) (See Fig. 3).

Left ventricular function after 24 h of reperfusion

After 24 h of reperfusion, systolic left ventricular function was impaired with reduced ejection fraction (BC−/EC+ 46 ± 2 %; $n = 19$ vs. BC+/EC+: 52 ± 2 %; $n = 21$; $^{*}p < 0.05$) (See Fig. 4 and Online Resource 8) and increased end-systolic volume (BC−/EC+: 41 ± 2 µl; $n = 19$ vs. BC+/EC+: 34 ± 3 µl; $n = 21$; $^{*}p < 0.05$) in BC−/EC+ compared to BC+/EC+ (See Online Resource 8).

ETU treatment

Application of the global NOS inhibitor ETU was associated with increased infarct size (ETU: 36 ± 3 %; $n = 6$ vs. without ETU: 14 ± 2 %; $n = 9$; $^{*}p < 0.05$) in BC+/EC+, whereas BC−/EC+ demonstrated no differences after

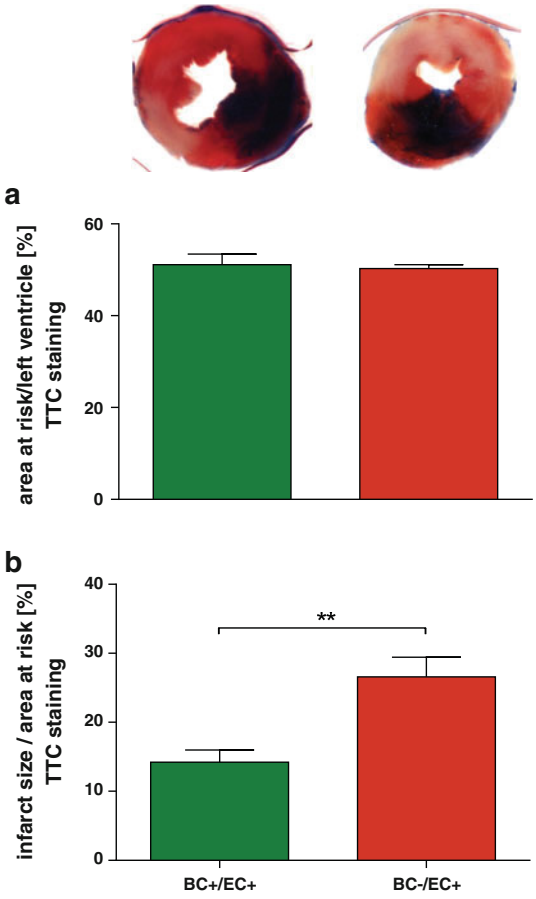

Fig. 3 Depletion of circulating NOS3 increases infarct size following acute myocardial ischemia/reperfusion. While AAR per LV did not differ between both groups, infarct sizes were significantly increased in BC−/EC+ ($n = 6$) compared to BC+/EC+ ($n = 9$, $^{**}p < 0.01$, unpaired Student's t test)

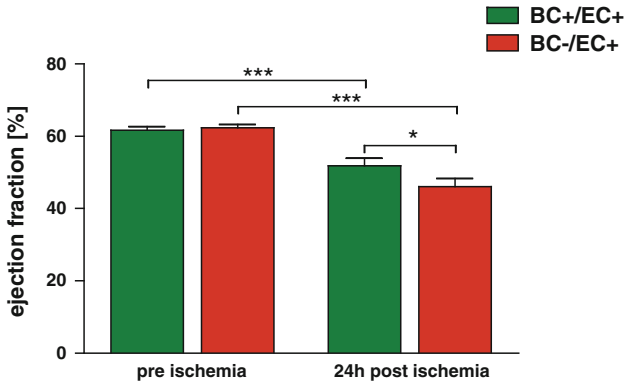

Fig. 4 Depletion of circulating NOS3 impairs cardiac function following myocardial ischemia/reperfusion. After 60 min of ischemia and 24 h of reperfusion, ejection fraction (via echocardiography) was significantly impaired in BC+/EC+ ($n = 21$) and BC−/EC+ ($n = 19$) compared to baseline (BC+/EC+: $n = 22$, BC−/EC+: $n = 25$, $^{***}p < 0.001$ baseline vs. 24 h post ischemia, two-way ANOVA followed by Bonferroni's post hoc test). Increased infarct size in BC−/EC+ was associated with significantly reduced ejection fraction compared to BC+/EC+ ($^{*}p < 0.05$, two-way ANOVA followed by Bonferroni's post hoc test)

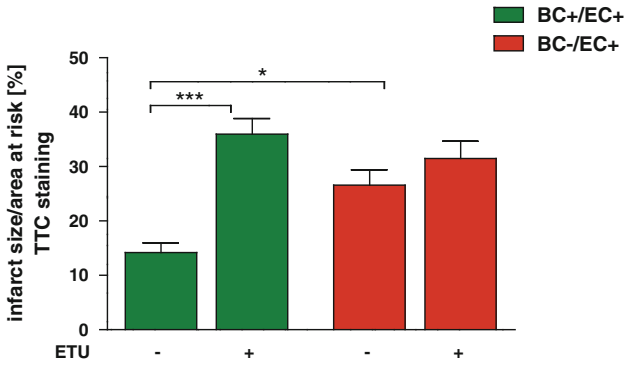

Fig. 5 Circulating NOS3 contributes to reduced infarct size. Application of the global NOS inhibitor S-ethylisothiourea hydrobromide (ETU) was associated with a further increase in infarct size in BC+/EC+ (without ETU $n = 9$; with ETU $n = 6$; $^{***}p < 0.001$; one-way ANOVA followed by Bonferroni's post hoc test), whereas BC−/EC+ (without and with ETU $n = 6$) demonstrated no significant differences after global NOS inhibition

global NOS inhibition (ETU: 32 ± 3 %; $n = 6$ without ETU: 27 ± 3 %; $n = 6$; n.s.) (See Fig. 5).

Nitrite in early and late reperfusion: blood cell NOS3 contributes to endogenous NO pool and improves NO bioavailability in the early reperfusion phase

Blood plasma nitrite levels were slightly reduced in BC−/EC+ plasma at 5 min (BC−/EC+: 0.90 ± 0.18 μM vs. BC+/EC+:1.95 ± 0.41 μM; $n = 4$ per group; n.s.) and 24 h of reperfusion (BC−/EC+: 1.21 ± 0.18 μM; $n = 7$ vs. BC+/EC+: 1.56 ± 0.26 μM; $n = 6$; n.s.) compared to BC+/EC+ (See Online Resource 9a). Nitrate concentration in plasma was significantly reduced in BC−/EC+ (5 min: 95.45 ± 21.40 μM; $n = 4$ and 24 h: 74.38 ± 7.42 μM; $n = 5$) compared to BC+/EC+ (5 min: 224.12 ± 57.12 μM; $n = 4$; $^{*}p < 0.05$ and 24 h: 178.84 ± 16.37 μM; $n = 6$; $^{*}p < 0.05$) at 5 min and 24 h of reperfusion (See Online Resource 9b). Nitrite and nitrate concentration in heart tissue did not differ between both groups at 5 min (nitrite: BC+/EC+: 1.42 ± 0.24 μM; BC−/EC+: 1.36 ± 0.23 μM, $n = 4$ per group, n.s.; nitrate: BC+/EC+: 21.92 ± 1.74 μM, $n = 3$ vs. BC−/EC+: 12.32 ± 2.17 μM, $n = 4$, n.s) and 24 h of reperfusion (nitrite: BC+/EC+: 0.41 ± 0.06 μM vs. BC−/EC+: 0.31 ± 0.12 μM, $n = 3$ per group, n.s.; nitrate: BC+/EC+: 12.78 ± 0.48 μM vs. BC−/EC+: 13.67 ± 4.09 μM, $n = 3$ per group; n.s.).

Blood cell NOS3 preserved erythrocyte deformability 24-h post-ischemia

RBC deformability was diminished in BC−/EC+ (0.27 ± 0.01 EI; $n = 16$) compared to BC+/EC+ (0.35 ± 0.01 EI; $n = 15$; $^{***}p < 0.001$) 24 h after reperfusion. Furthermore, BC−/EC+ showed a decrease in RBC deformability after 24 h of reperfusion compared to baseline (0.33 ± 0.01 EI; $n = 16$; $^{**}p < 0.05$). In contrast, RBC deformability was not affected by I/R in BC+/EC+ chimeras (0.36 ± 0.06 EI; $n = 15$; n.s.) (See Online Resource 9c).

Discussion

The main findings of the present study are: (1) circulating NOS3 reduces infarct size in a myocardial ischemia/reperfusion model of chimeric mice; (2) this translates into a sustained reduction of LV function; (3) depletion of circulating NOS3 reduces circulating NO pool by 1/3, as evidenced by reduced plasma levels of nitrite; (4) circulating NOS3 limits RBC deformability.

In the present study, depletion of circulating NOS3 is associated with increased infarct size and impaired left ventricular function. In accordance with these findings, global depletion of $NOS3^{-/-}$ increased infarct size and impaired LV function after I/R [20], and conventional wisdom holds that these effects are primarily determined by the lack of NOS3 in the vessel endothelium. Our data suggest that endothelial NOS3 is unable to compensate for the depletion of circulating NOS3 alone in terms of reduction of tissue damage and preservation of left ventricular function as a result of myocardial I/R in the current chimeric model. It is conceivable that endothelial dysfunction, which occurs during I/R and is associated with

endothelial NOS3 uncoupling, limits the functional capacity of endothelial NOS3 [8]. We did not find any differences in vascular function in the two mice groups, as assessed in both conductance and resistance vessels. Thus, we exclude that differences in endothelial functionality between groups might have caused differences in infarct size. In the context of myocardial ischemia, NOS inhibition exacerbates myocardial I/R injury [25]. In our study, application of the global NOS inhibitor ETU was associated with increased infarct size in BC+/EC+, whereas BC−/EC+ demonstrated no differences after global NOS inhibition. Therefore, circulating NOS3 limits infarct size and this translates into preserved LV function in a myocardial I/R model.

We examined nitrite and nitrate levels in plasma and heart tissue as a marker of systemic NO bioavailability at baseline, 5 min and 24 h after ischemia. Both groups showed a significant decrease in nitrite plasma levels 5 min after ischemia compared to baseline. Whereas mice with depleted circulating NOS3 show more reduced plasma nitrite levels compared to animals carrying circulating NOS at baseline and 5 min after ischemia. However, nitrite heart tissue levels remain stable and show no difference between both groups at all examined time points. Both groups are obviously able to maintain their nitrite/nitrate concentration to a certain degree in the analyzed tissues (heart and aorta) at baseline and at least in the first 5 min of reperfusion independently of surrounding plasma levels. Therefore, depletion of circulating NOS3 was associated with nitrite levels reduced by 1/3 at baseline compared to animals carrying circulating NOS3 only in plasma but not in heart tissue. These data confirm and expand recent findings in chimera obtained from the two further existing $NOS3^{-/-}$ strains [47] other than the one used in this study, and demonstrate that circulating NOS3 plays a central role in determining the circulating NO pool. These reduced levels of circulating nitrite likely contribute to the greater tissue damage in BC−/EC+ chimeras, as previously shown in WT mice [13, 14]. Nevertheless, the exact quantitative contribution of circulating NOS3 to the circulating nitric oxide metabolite (NO_x) pool cannot be assessed accurately without analyzing nitrite/nitrate content in whole blood and the differentially in the individual blood cell types as well as plasma. While this was not primarily the aim of the present study, it certainly represents a limitation and should be addressed in further studies.

The organism is able to reduce nitrite to NO, thus potentially compensating for an impaired NOS activity/NO bioavailability, [6]. Nitrite is, therefore, considered as an "ischemic NO buffer" [14]. Various nitrite reductases exist, which are effective at different oxygen partial pressures along the vascular tree: (1) hemoglobin, which reduces nitrite at 20–60 mmHg oxygen, (2) myoglobin, which is active below 4 mmHg oxygen, and (3) xanthine oxidase and the acidic reduction which reduce nitrite at 0 mmHg oxygen and low pH [28]. In mice feed with a controlled nitrite/nitrate low diet, both the circulating and the endothelial NOS3 contribute to 70–90 % of the total plasma nitrite levels [22, 24]. Chimeras exhibit elevated plasma nitrite levels compared to non-transplanted wild types. This might be related to a chronic inflammation within the bone marrow due to a subclinical rejection [27]. A strong persisting systemic inflammation was excluded in the chimeras of the present study by determining the concentration of SAP in the blood plasma, a well-established murine marker of inflammation [37], and by serial assessment of white blood cells counts. As discussed above, the lower nitrite levels in BC−/EC+ chimera indicate the contribution of circulating NOS3 to nitrite bioavailability. NO itself and nitrite, both emerging from constitutive endothelial and blood born NOS3 activity, may contribute to the cardioprotective effect in the reperfused myocardium.

During circulation, RBCs constantly change their shape as they are exposed to a range of dynamic shear stresses, and are able to respond to these forces by changing their shape [3]. This property of RBCs is defined as deformability and contributes to blood fluidity, blood flow and the passage of RBCs through capillaries with diameters smaller than their resting diameter [35, 49]. In the present study, we found that depletion of circulating NOS3 was associated with reduced RBC deformability, as previously shown in human RBC treated with NOS inhibitors [2] and a further reduction of RBC deformability was measured in BC−/EC+ mice following myocardial I/R and may contribute to myocardial damage. In fact, in patients with coronary artery disease (CAD) and diabetes mellitus, pathological alterations of hemostatic and hemorheological properties have been found to be associated with an increased incidence of coronary events [18, 19] and contribute to increased morbidity of these patients due to disturbances in blood flow [21]. Furthermore, it is known that oxidative stress and impaired NO bioavailability are able to reduce the deformability of RBCs [34]. A more extensive reduction of NO bioavailability and increase of ROS concentration within RBCs are probable reasons for the further decrease in deformability of RBCs in the BC−/EC+ group compared to group BC+/EC+ after myocardial I/R. The preserved deformability of RBCs as observed in BC+/EC+ mice might positively impact coronary blood flow particularly in the border zone of an ischemic area and thus might also contribute to reduce infarct size and limited left ventricular function in our model of myocardial I/R.

In conclusion, we here present evidence that circulating NOS3 reduced infarct size leading to sustained left ventricular dysfunction in an acute model of myocardial I/R in

chimeric mice. Depletion of circulating NOS3 reduces NO bioavailability and limits RBC deformability in this model. For future analyses of mechanisms underlying the protective effects of circulating NOS3 in I/R injury, it would certainly be beneficial to use a conditional erythrocyte-specific knockout model to exclude any confounding factors due to irradiation/bone marrow transplantation and to identify the specific role of blood cell subpopulations in these effects.

Acknowledgments This work was supported in part by ME1821/2-3 to MWM and ME1821/3-1 [FOR809] to MWM and MK, RA969/4-2 and RA969/7-1 to TR and KE405/5-1 to MK and the Susanne-Bunnenberg-Stiftung at Düsseldorf Heart Center. We thank S. Becher, R. Taskesen for excellent technical assistance and Sivatharsini Thasian-Sivarajah for performing the western blot analysis.

Conflict of interest On behalf of all authors, the corresponding author states that there is no conflict of interest.

References

1. Balligand JL, Feron O, Dessy C (2009) eNOS activation by physical forces: from short-term regulation of contraction to chronic remodeling of cardiovascular tissues. Physiol Rev 89:481–534. doi:10.1152/physrev.00042.2007
2. Bor-Kucukatay M, Wenby RB, Meiselman HJ, Baskurt OK (2003) Effects of nitric oxide on red blood cell deformability. Am J Physiol Heart Circ Physiol 284:H1577–H1584. doi:10.1152/ajpheart.00665.2002
3. Chien S (1987) Red cell deformability and its relevance to blood flow. Annu Rev Physiol 49:177–192. doi:10.1146/annurev.ph.49.030187.001141
4. Cortese-Krott MM, Rodriguez-Mateos A, Kuhnle GG, Brown G, Feelisch M, Kelm M (2012) A multilevel analytical approach for detection and visualization of intracellular NO production and nitrosation events using diaminofluoresceins. Free Radic Biol Med 53:2146–2158. doi:10.1016/j.freeradbiomed.2012.09.008
5. Cortese-Krott MM, Rodriguez-Mateos A, Sansone R, Kuhnle GG, Thasian-Sivarajah S, Krenz T, Horn P, Krisp C, Wolters D, Heiss C, Kroncke KD, Hogg N, Feelisch M, Kelm M (2012) Human red blood cells at work: identification and visualization of erythrocytic eNOS activity in health and disease. Blood 120:4229–4237. doi:10.1182/blood-2012-07-442277
6. Cosby K, Partovi KS, Crawford JH, Patel RP, Reiter CD, Martyr S, Yang BK, Waclawiw MA, Zalos G, Xu X, Huang KT, Shields H, Kim-Shapiro DB, Schechter AN, Cannon RO 3rd, Gladwin MT (2003) Nitrite reduction to nitric oxide by deoxyhemoglobin vasodilates the human circulation. Nat Med 9:1498–1505. doi:10.1038/nm954
7. Dejam A, Hunter CJ, Pelletier MM, Hsu LL, Machado RF, Shiva S, Power GG, Kelm M, Gladwin MT, Schechter AN (2005) Erythrocytes are the major intravascular storage sites of nitrite in human blood. Blood 106:734–739. doi:10.1182/blood-2005-02-0567
8. Dumitrescu C, Biondi R, Xia Y, Cardounel AJ, Druhan LJ, Ambrosio G, Zweier JL (2007) Myocardial ischemia results in tetrahydrobiopterin (BH4) oxidation with impaired endothelial function ameliorated by BH4. Proc Natl Acad Sci USA 104:15081–15086. doi:10.1073/pnas.0702986104
9. Gladwin MT, Shelhamer JH, Schechter AN, Pease-Fye ME, Waclawiw MA, Panza JA, Ognibene FP, Cannon RO 3rd (2000) Role of circulating nitrite and *S*-nitrosohemoglobin in the regulation of regional blood flow in humans. Proc Natl Acad Sci USA 97:11482–11487. doi:10.1073/pnas.97.21.11482
10. Gödecke A, Decking UK, Ding Z, Hirchenhain J, Bidmon HJ, Gödecke S, Schrader J (1998) Coronary hemodynamics in endothelial NO synthase knockout mice. Circ Res 82:186–194. doi:10.1161/01.RES.82.2.186
11. Heinzel FR, Gres P, Boengler K, Duschin A, Konietzka I, Rassaf T, Snedovskaya J, Meyer S, Skyschally A, Kelm M, Heusch G, Schulz R (2008) Inducible nitric oxide synthase expression and cardiomyocyte dysfunction during sustained moderate ischemia in pigs. Circ Res 103:1120–1127. doi:10.1161/CIRCRESAHA.108.186015
12. Hendgen-Cotta U, Grau M, Rassaf T, Gharini P, Kelm M, Kleinbongard P (2008) Reductive gas-phase chemiluminescence and flow injection analysis for measurement of the nitric oxide pool in biological matrices. Methods Enzymol 441:295–315. doi:10.1016/S0076-6879(08)01216-0
13. Hendgen-Cotta UB, Kelm M, Rassaf T (2010) A highlight of myoglobin diversity: the nitrite reductase activity during myocardial ischemia-reperfusion. Nitric Oxide 22:75–82. doi:10.1016/j.nox.2009.10.003
14. Hendgen-Cotta UB, Merx MW, Shiva S, Schmitz J, Becher S, Klare JP, Steinhoff HJ, Goedecke A, Schrader J, Gladwin MT, Kelm M, Rassaf T (2008) Nitrite reductase activity of myoglobin regulates respiration and cellular viability in myocardial ischemia-reperfusion injury. Proc Natl Acad Sci USA 105:10256–10261. doi:10.1073/pnas.0801336105
15. Heusch G, Post H, Michel MC, Kelm M, Schulz R (2000) Endogenous nitric oxide and myocardial adaptation to ischemia. Circ Res 87:146–152. doi:10.1161/01.RES.87.2.146
16. Horn P, Cortese-Krott MM, Keymel S, Kumara I, Burghoff S, Schrader J, Kelm M, Kleinbongard P (2011) Nitric oxide influences red blood cell velocity independently of changes in the vascular tone. Free Radic Res 45:653–661. doi:10.3109/10715762.2011.574288
17. Janssens S, Pokreisz P, Schoonjans L, Pellens M, Vermeersch P, Tjwa M, Jans P, Scherrer-Crosbie M, Picard MH, Szelid Z, Gillijns H, Van de Werf F, Collen D, Bloch KD (2004) Cardiomyocyte-specific overexpression of nitric oxide synthase 3 improves left ventricular performance and reduces compensatory hypertrophy after myocardial infarction. Circ Res 94:1256–1262. doi:10.1161/01.RES.0000126497.38281.23
18. Jax TW, Peters AJ, Plehn G, Schoebel FC (2009) Hemostatic risk factors in patients with coronary artery disease and type 2 diabetes—a two year follow-up of 243 patients. Cardiovasc Diabetol 8:48. doi:10.1186/1475-2840-8-48
19. Jax TW, Peters AJ, Plehn G, Schoebel FC (2009) Relevance of hemostatic risk factors on coronary morphology in patients with diabetes mellitus type 2. Cardiovasc Diabetol 8:24. doi:10.1186/1475-2840-8-24
20. Jones SP, Girod WG, Palazzo AJ, Granger DN, Grisham MB, Jourd'Heuil D, Huang PL, Lefer DJ (1999) Myocardial ischemia-reperfusion injury is exacerbated in absence of endothelial cell nitric oxide synthase. Am J Physiol 276:H1567–H1573
21. Keymel S, Heiss C, Kleinbongard P, Kelm M, Lauer T (2011) Impaired red blood cell deformability in patients with coronary artery disease and diabetes mellitus. Horm Metab Res 43:760–765. doi:10.1055/s-0031-1286325

22. Kleinbongard P, Dejam A, Lauer T, Jax T, Kerber S, Gharini P, Balzer J, Zotz RB, Scharf RE, Willers R, Schechter AN, Feelisch M, Kelm M (2006) Plasma nitrite concentrations reflect the degree of endothelial dysfunction in humans. Free Radic Biol Med 40:295–302. doi:10.1016/j.freeradbiomed.2005.08.025
23. Kleinbongard P, Dejam A, Lauer T, Rassaf T, Schindler A, Picker O, Scheeren T, Gödecke A, Schrader J, Schulz R, Heusch G, Schaub GA, Bryan NS, Feelisch M, Kelm M (2003) Plasma nitrite reflects constitutive nitric oxide synthase activity in mammals. Free Radic Biol Med 35:790–796. doi:10.1016/S0891-5849(03)00406-4
24. Kleinbongard P, Schulz R, Rassaf T, Lauer T, Dejam A, Jax T, Kumara I, Gharini P, Kabanova S, Ozüyaman B, Schnürch HG, Gödecke A, Weber AA, Robenek M, Robenek H, Bloch W, Rösen P, Kelm M (2006) Red blood cells express a functional endothelial nitric oxide synthase. Blood 107:2943–2951. doi:10.1182/blood-2005-10-3992
25. Kobara M, Tatsumi T, Takeda M, Mano A, Yamanaka S, Shiraishi J, Keira N, Matoba S, Asayama J, Nakagawa M (2003) The dual effects of nitric oxide synthase inhibitors on ischemia-reperfusion injury in rat hearts. Basic Res Cardiol 98:319–328. doi:10.1007/s00395-003-0423-x
26. Krusche CA, Holthöfer B, Hofe V, van de Sandt AM, Eshkind L, Bockamp E, Merx MW, Kant S, Windoffer R, Leube RE (2011) Desmoglein 2 mutant mice develop cardiac fibrosis and dilation. Basic Res Cardiol 106:617–633. doi:10.1007/s00395-011-0175-y
27. Langrehr JM, Murase N, Markus PM, Cai X, Neuhaus P, Schraut W, Simmons RL, Hoffman RA (1992) Nitric oxide production in host-versus-graft and graft-versus-host reactions in the rat. J Clin Invest 90:679–683. doi:10.1172/JCI115911
28. Li H, Samouilov A, Liu X, Zweier JL (2001) Characterization of the magnitude and kinetics of xanthine oxidase-catalyzed nitrite reduction. Evaluation of its role in nitric oxide generation in anoxic tissues. J Biol Chem 276:24482–24489. doi:10.1074/jbc.M011648200
29. Martin C, Schulz R, Post H, Boengler K, Kelm M, Kleinbongard P, Gres P, Skyschally A, Konietzka I, Heusch G (2007) Microdialysis-based analysis of interstitial NO in situ: NO synthase-independent NO formation during myocardial ischemia. Cardiovasc Res 74:46–55. doi:10.1016/j.cardiores.2006.12.020
30. Martin C, Schulz R, Post H, Gres P, Heusch G (2003) Effect of NO synthase inhibition on myocardial metabolism during moderate ischemia. Am J Physiol Heart Circ Physiol 284:H2320–H2324. doi:10.1152/ajpheart.01122.2002
31. Merx MW, Flögel U, Stumpe T, Gödecke A, Decking UK, Schrader J (2001) Myoglobin facilitates oxygen diffusion. FASEB J 15:1077–1079. doi:10.1096/fj.00-0497fje
32. Merx MW, Liehn EA, Graf J, van de Sandt A, Schaltenbrand M, Schrader J, Hanrath P, Weber C (2005) Statin treatment after onset of sepsis in a murine model improves survival. Circulation 112:117–124. doi:10.1161/CIRCULATIONAHA.104.502195
33. Merx MW, Liehn EA, Janssens U, Lütticken R, Schrader J, Hanrath P, Weber C (2004) HMG-CoA reductase inhibitor simvastatin profoundly improves survival in a murine model of sepsis. Circulation 109:2560–2565. doi:10.1161/01.CIR.0000129774.09737.5B
34. Minetti M, Agati L, Malorni W (2007) The microenvironment can shift erythrocytes from a friendly to a harmful behavior: pathogenetic implications for vascular diseases. Cardiovasc Res 75:21–28. doi:10.1016/j.cardiores.2007.03.007
35. Mohandas N, Chasis JA, Shohet SB (1983) The influence of membrane skeleton on red cell deformability, membrane material properties, and shape. Semin Hematol 20:225–242
36. Nossuli TO, Lakshminarayanan V, Baumgarten G, Taffet GE, Ballantyne CM, Michael LH, Entman ML (2000) A chronic mouse model of myocardial ischemia-reperfusion: essential in cytokine studies. Am J Physiol Heart Circ Physiol 278:H1049–H1055
37. Pepys MB, Baltz M, Gomer K, Davies AJ, Doenhoff M (1979) Serum amyloid P-component is an acute-phase reactant in the mouse. Nature 278:259–261. doi:10.1038/278259a0
38. Rassaf T, Bryan NS, Kelm M, Feelisch M (2002) Concomitant presence of N-nitroso and S-nitroso proteins in human plasma. Free Radic Biol Med 33:1590–1596. doi:10.1016/S0891-5849(02)01183-8
39. Rassaf T, Bryan NS, Maloney RE, Specian V, Kelm M, Kalyanaraman B, Rodriguez J, Feelisch M (2003) NO adducts in mammalian red blood cells: too much or too little? Nat Med 9:481–482. doi:10.1038/nm0503-481
40. Rassaf T, Feelisch M, Kelm M (2004) Circulating NO pool: assessment of nitrite and nitroso species in blood and tissues. Free Radic Biol Med 36:413–422. doi:10.1016/j.freeradbiomed.2003.11.011
41. Rassaf T, Poll LW, Brouzos P, Lauer T, Totzeck M, Kleinbongard P, Gharini P, Andersen K, Schulz R, Heusch G, Mödder U, Kelm M (2006) Positive effects of nitric oxide on left ventricular function in humans. Eur Heart J 27:1699–1705. doi:10.1093/eurheartj/ehl096
42. Reiling N, Kröncke R, Ulmer AJ, Gerdes J, Flad HD, Hauschildt S (1996) Nitric oxide synthase: expression of the endothelial, Ca2+/calmodulin-dependent isoform in human B and T lymphocytes. Eur J Immunol 26:511–516. doi:10.1002/eji.1830260302
43. Schulz R, Rassaf T, Massion PB, Kelm M, Balligand JL (2005) Recent advances in the understanding of the role of nitric oxide in cardiovascular homeostasis. Pharmacol Ther 108:225–256. doi:10.1016/j.pharmthera.2005.04.005
44. Szelid Z, Pokreisz P, Liu X, Vermeersch P, Marsboom G, Gillijns H, Pellens M, Verbeken E, Van de Werf F, Collen D, Janssens SP (2010) Cardioselective nitric oxide synthase 3 gene transfer protects against myocardial reperfusion injury. Basic Res Cardiol 105:169–179. doi:10.1007/s00395-009-0077-4
45. Totzeck M, Hendgen-Cotta UB, Luedike P, Berenbrink M, Klare JP, Steinhoff HJ, Semmler D, Shiva S, Williams D, Kipar A, Gladwin MT, Schrader J, Kelm M, Cossins AR, Rassaf T (2012) Nitrite regulates hypoxic vasodilation via myoglobin-dependent nitric oxide generation. Circulation 126:325–334. doi:10.1161/CIRCULATIONAHA.111.087155
46. van de Sandt AM, Windler R, Gödecke A, Ohlig J, Zander S, Reinartz M, Graf J, van Faassen EE, Rassaf T, Schrader J, Kelm M, Merx MW (2013) Endothelial NOS (NOS3) impairs myocardial function in developing sepsis. Basic Res Cardiol 108:330. doi:10.1007/s00395-013-0330-8
47. Wood KC, Cortese-Krott MM, Kovacic JC, Noguchi A, Liu VB, Wang X, Raghavachari N, Boehm M, Kato GJ, Kelm M, Gladwin MT (2013) Circulating blood endothelial nitric oxide synthase contributes to the regulation of systemic blood pressure and nitrite homeostasis. Arterioscler Thromb Vasc Biol 33:1861–1871. doi:10.1161/ATVBAHA.112.301068
48. Yang BC, Nichols WW, Mehta JL (1996) Cardioprotective effects of red blood cells on ischemia and reperfusion injury in isolated rat heart: release of nitric oxide as a potential mechanism. J Cardiovasc Pharmacol Ther 1:297–306. doi:10.1177/107424849600100405
49. Yedgar S, Koshkaryev A, Barshtein G (2002) The red blood cell in vascular occlusion. Pathophysiol Haemost Thromb 32:263–268. doi:10.1159/000073578
50. Zanardo RC, Costa E, Ferreira HH, Antunes E, Martins AR, Murad F, De Nucci G (1997) Pharmacological and immunohistochemical evidence for a functional nitric oxide synthase system in rat peritoneal eosinophils. Proc Natl Acad Sci USA 94:14111–14114
51. Zhao X, He G, Chen YR, Pandian RP, Kuppusamy P, Zweier JL (2005) Endothelium-derived nitric oxide regulates postischemic myocardial oxygenation and oxygen consumption by modulation of mitochondrial electron transport. Circulation 111:2966–2972. doi:10.1161/CIRCULATIONAHA.104.527226

Arteriosclerosis, Thrombosis, and Vascular Biology

JOURNAL OF THE AMERICAN HEART ASSOCIATION

Circulating Blood Endothelial Nitric Oxide Synthase Contributes to the Regulation of Systemic Blood Pressure and Nitrite Homeostasis

Katherine C. Wood, Miriam M. Cortese-Krott, Jason C. Kovacic, Audrey Noguchi, Virginia B. Liu, Xunde Wang, Nalini Raghavachari, Manfred Boehm, Gregory J. Kato, Malte Kelm and Mark T. Gladwin

Arterioscler Thromb Vasc Biol. published online May 23, 2013;
Arteriosclerosis, Thrombosis, and Vascular Biology is published by the American Heart Association, 7272 Greenville Avenue, Dallas, TX 75231

Print ISSN: 1079-5642. Online ISSN: 1524-4636

Original Article

Circulating Blood Endothelial Nitric Oxide Synthase Contributes to the Regulation of Systemic Blood Pressure and Nitrite Homeostasis

Katherine C. Wood,* Miriam M. Cortese-Krott,* Jason C. Kovacic, Audrey Noguchi, Virginia B. Liu, Xunde Wang, Nalini Raghavachari, Manfred Boehm, Gregory J. Kato, Malte Kelm,† Mark T. Gladwin†

Objective—Mice genetically deficient in endothelial nitric oxide synthase (eNOS$^{-/-}$) are hypertensive with lower circulating nitrite levels, indicating the importance of constitutively produced nitric oxide (NO•) to blood pressure regulation and vascular homeostasis. Although the current paradigm holds that this bioactivity derives specifically from the expression of eNOS in endothelium, circulating blood cells also express eNOS protein. A functional red cell eNOS that modulates vascular NO• signaling has been proposed.

Approach and Results—To test the hypothesis that blood cells contribute to mammalian blood pressure regulation via eNOS-dependent NO• generation, we cross-transplanted wild-type and eNOS$^{-/-}$ mice, producing chimeras competent or deficient for eNOS expression in circulating blood cells. Surprisingly, we observed a significant contribution of both endothelial and circulating blood cell eNOS to blood pressure and systemic nitrite levels, the latter being a major component of the circulating NO• reservoir. These effects were abolished by the NOS inhibitor L-NAME and repristinated by the NOS substrate L-arginine and were independent of platelet or leukocyte depletion. Mouse erythrocytes were also found to carry an eNOS protein and convert ^{14}C-arginine into ^{14}C-citrulline in an NOS-dependent fashion.

Conclusions—These are the first studies to definitively establish a role for a blood-borne eNOS, using cross-transplant chimera models, that contributes to the regulation of blood pressure and nitrite homeostasis. This work provides evidence suggesting that erythrocyte eNOS may mediate this effect. **(*Arterioscler Thromb Vasc Biol*. 2013;33:00-00.)**

Hypertension is a complex multifactorial condition associated with cardiovascular disease. Experimental data in mouse models and human subjects point to a correlation between the production of nitric oxide (NO•) and its oxidative metabolites and hemodynamic parameters, such as nitrite and blood pressure (BP), respectively.[1–7]

NO• is produced by an NO synthase (NOS) catalyzing the conversion of L-arginine to equimolar amounts of NO• and citrulline in the presence of oxygen and the cofactors calcium, calmodulin, NADPH, and tetrahydrobiopterin.[8] There are 3 NOS isoforms, endothelial NOS (eNOS), inducible NOS (iNOS), and neuronal NOS (nNOS), expressed in multiple cell types, such as endothelium, epithelium, leukocytes, platelets, and neurons.[8] Whereas iNOS participates in host defense, inflammatory stress, and airway epithelial NO (NO•) formation, the constitutively expressed isoforms, nNOS and eNOS, are important to physiological processes that include neuronal signaling, inhibition of the hemostatic system, vasodilation, and BP control.

In the cardiovascular system, eNOS contributes to the regulation of blood flow and BP and is an inhibitor of platelet activation and aggregation, as well as leukocyte adhesion and migration. Furthermore, endothelial eNOS seems to contribute to the formation of bioactive circulating NO• metabolites, such as the nitrite anion and S-nitrosothiols, that mediate important endocrine activities, such as hypoxic vasodilation,[9,10] BP regulation,[6] and cytoprotection after myocardial infarction.[11,12] Mice genetically deficient in eNOS (eNOS$^{-/-}$) are hypertensive with lower circulating nitrite levels, indicating the importance of constitutively produced NO (NO•) to BP regulation and vascular homeostasis.[1–4,13]

Conventional wisdom holds that the pleiotropic effects of eNOS are primarily determined by enzyme expressed in the endothelium. In addition to endothelial cells (ECs), most circulating blood cells (BCs), including leukocytes,[14–18] platelets,[14,19,20] and red blood cells (RBCs),[21,22] also carry eNOS transcript and protein. In RBC, an active red cell eNOS modulates intrinsic

Received on: January 9, 2013; final version accepted on: May 9, 2013.

From the Hematology Branch (K.C.W., V.B.L., X.W., N.R., G.J.K.), Translational Medicine Branch (J.C.K., M.B.), and Murine Phenotyping Core (A.N.), National Heart, Lung, and Blood Institute, National Institutes of Health, Bethesda, MD; Cardiovascular Research Laboratory, Department of Internal Medicine, Division of Cardiology, Pulmonology and Vascular Medicine, Medical Faculty of the Heinrich-Heine-University of Düsseldorf, Düsseldorf, Germany (M.M.C.-K., M.K.); Cardiovascular Institute, Mount Sinai Hospital, New York, NY (J.C.K.); and Vascular Medicine Institute (M.T.G.) and Pulmonary, Allergy and Critical Care Medicine (M.T.G.), University of Pittsburgh, Pittsburgh, PA.

*K.C. Wood and M.M. Cortese-Krott shared first authorship.

†M. Kelm and M.T. Gladwin shared senior authorship.

The online-only Data Supplement is available with this article at http://atvb.ahajournals.org/lookup/suppl/doi:10.1161/ATVBAHA.112.301068/-/DC1.

Correspondence to Mark T. Gladwin, MD, Vascular Medicine Institute, University of Pittsburgh, NW 628 Montefiore Hospital, 3459 Fifth Ave, Pittsburgh, PA 15213. E-mail gladwinmt@upmc.edu or Malte Kelm, MD, Department of Internal Medicine, Division of Cardiology, Pulmonology and Vascular Medicine, Moorenstr. 5, 40225 Düsseldorf, Germany. E-mail malte.kelm@med.uni-duesseldorf.de

Arterioscler Thromb Vasc Biol **is available at http://atvb.ahajournals.org** **DOI: 10.1161/ATVBAHA.112.301068**

erythrocyte deformability, platelet activation, and extraerythrocytic NO• metabolites, such as nitrite.[21–24] A physiological in vivo effect for circulating eNOS on BP regulation or the formation of the circulating NO• metabolite reservoir has never been evaluated.

The aim of this work was to test in vivo the hypothesis that a functional circulating cell eNOS regulates systemic BP and the formation of the NO• metabolite pool. To limit eNOS functionality to circulating BCs, we used cross-transplantation methodologies with wild-type (WT) and eNOS$^{-/-}$ mice. The resulting chimeric mice were characterized for circulating nitrite levels and BPs (while anesthetized and awake), as well as eNOS expression and activity by Western blotting, real-time reverse transcriptase polymerase chain reaction, flow cytometry, enzymatic NOS activity, chemiluminescence detection, and functional wire myography.

Materials and Methods

Materials and Methods are available in the online-only Supplement.

Results

eNOS$^{-/-}$ Mice Are Hypertensive With Low Circulating Nitrite Levels

To investigate the hypothesis that circulating BC eNOS contributes to the control of BP, systemic BP—systolic and diastolic—was assessed and compared (to 2 decimal places accuracy) in awake mice by radiotelemetry and in anesthetized mice via carotid artery cannulation. Mice with global knockout of functional eNOS (eNOS$^{-/-}$) are hypertensive compared with normal WT mice (mean arterial pressure [MAP]: 126±3.18 versus 105.4±2.66 mm Hg; P=0.0016), confirming an important physiological role for eNOS in basal BP regulation (Figure 1A), as previously reported for this[13] and all other eNOS$^{-/-}$ strains.[2,4] They also show lower whole blood (0.72±0.08 μmol/L; Figure 1B) and plasma (0.38±0.04 μmol/L; Figure 1C) nitrite levels than WT mice (whole blood: 1.08±0.11 μmol/L and plasma: 0.50±0.54 μmol/L).[1] These values indicate the importance of the eNOS enzyme in regulating BP and nitrite homeostasis.

eNOS$^{-/-}$ Mice Lack Expression and Activity of Red Cell eNOS

RBCs make up the largest cellular compartment in blood and are the circulating reservoir for nitrite.[25] To define the presence of an active eNOS protein in RBCs and its deletion in eNOS$^{-/-}$ mice, immunocytochemistry and immunoprecipitation experiments were performed. Using laser scanning confocal microscopy, eNOS staining was found to strongly localize in RBCs (Ter-119–positive cells) from WT mice (Figure 1D, left) but not in RBCs from eNOS$^{-/-}$ mice (Figure 1D, middle). Incubation with IgG was also used to verify that staining was specific for eNOS protein. In these control samples, IgG staining was weakly and homogenously distributed across both cellular and noncellular areas and thus not cell-specific (Figure 1D, right). Mouse red cell eNOS was further characterized by immunoprecipitation and Western blot analysis. As shown in Figure 1E, eNOS (≈135 KD) is detected in RBCs from WT mice, but not knockout mice, demonstrating electrophoretic characteristics similar to mouse endothelial eNOS from immunoprecipitation-enriched samples, crude aortic lysates, and human ECs (Figure 1E, right lane). The densitometry of bands corresponding to eNOS in RBC and aorta of 3 independent gels is shown in Figure 1F.

To assess eNOS activity in WT RBCs, we analyzed conversion of radioactive (^{14}C-labeled) arginine to citrulline. We found that membrane preparations of WT RBCs efficiently converted ^{14}C-arginine into ^{14}C-citrulline (0.306±0.107 fmol/min for WT versus 0.107±0.061 fmol/min for eNOS$^{-/-}$), as determined by significantly higher (6-fold) reactive counts in the reaction supernatant versus their eNOS$^{-/-}$ counterparts (Figure 1G).

Vascular eNOS Expression Is Not Conferred by Bone Marrow Transplantation

WT and eNOS$^{-/-}$ mice were cross-transplanted to elucidate the contribution of BC eNOS to intravascular nitrite formation and physiological BP regulation in vivo. Chimeric animals resulting from this cross-transplantation strategy either expressed eNOS only in BC or in the entire rest of the animal, specifically the vascular EC. These mice are hereafter, respectively, referred to as BC+/EC− and BC−/EC+ chimeras to simply summarize group identity. Control chimeras globally competent (BC+/EC+) and globally deficient (BC−/EC−) for eNOS (ie, obtained by transplantation of WT bone marrow (BM) into irradiated WT mice or eNOS$^{-/-}$ BM into irradiated eNOS$^{-/-}$ mice) were created for comparison purposes using the same BM transplant protocol, with WT marrow transplanted into WT mice and eNOS$^{-/-}$ marrow transplanted into eNOS$^{-/-}$ mice (Figure 2A). At 6 to 8 weeks after transplantation, flow cytometric analysis of relative CD45 expression (45.1 versus 45.2, mismatched for BM donors and recipients) by peripheral leukocytes confirmed that the BC compartments of cross-transplanted WT and eNOS$^{-/-}$ BM recipients converted >90% to the donor phenotype (Figure 2B). Leukocyte and platelet counts were within normal ranges for all chimeras and did not significantly differ between groups (Table I in the online-only Data Supplement). Western blot analysis (Figure 2C) demonstrated that eNOS expression was undetectable in aortas of BC+/EC− chimeras, similar to untransplanted eNOS$^{-/-}$ (knockout) mice. These data were confirmed by real-time reverse transcriptase polymerase chain reaction (Figure 2D and 2E), indicating that transfer of WT BM into eNOS$^{-/-}$ recipients does not give rise to vascular eNOS expression. This finding is consistent with a recent lineage tracing study that uses GFP to show no significant contribution of transplanted eNOS WT cells to the vascular endothelium of eNOS$^{-/-}$ mice.[26] Thus, vessel walls of the chimeras used in this study retained their pretransplantation phenotypes, whereas blood took on the phenotype of the BM donor. The possibility of a role for compensatory upregulation of vascular cyclooxygenase-1 or cyclooxygenase-2 in the transplanted chimeras was also ruled out; reverse transcriptase polymerase chain reaction confirmed similar cyclooxygenase-1 (Figure 2F) and cyclooxygenase-2 (Figure 2G) mRNA expression in all 4 chimeric groups.

Vascular Reactivity and cGMP Levels Are Not Impaired by BM Transplantation

To assess the effects of lethal irradiation and BM transplantation on vascular function, wire myography was used to compare

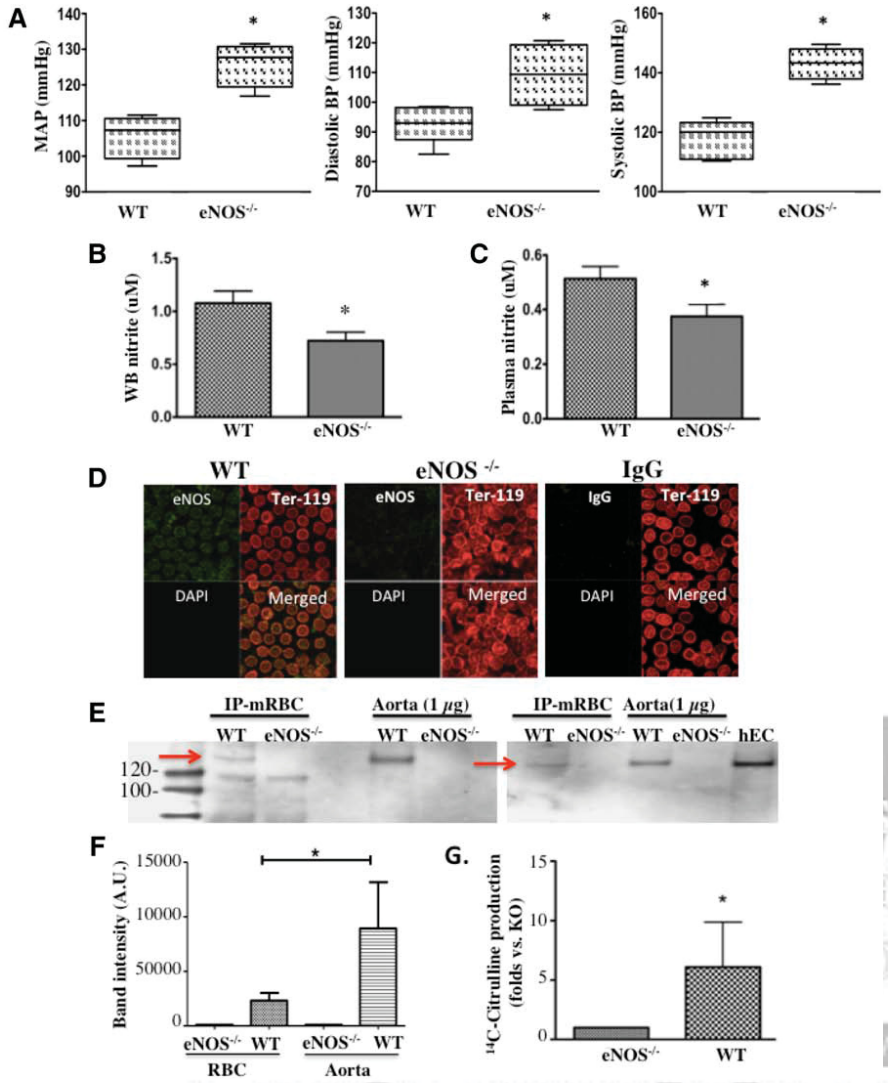

Figure 1. Mouse red blood cells (RBC) contain an active endothelial nitric oxide synthase (eNOS). In wild-type (WT) vs eNOS$^{-/-}$ mice: (**A**) mean arterial pressure (MAP), systolic blood pressure (BP), and diastolic BP (WT: n=5, KO: n=4); (**B**) whole blood (WB) nitrite (n=5 per group); and (**C**) plasma nitrite (n=5 per group). **D**, Laser scanning microscopic images representative of n=5 independent experiments showing positive staining for eNOS protein (green) in Ter-119^{pos} (red) RBCs freshly isolated from WT (**left**) and Harvard eNOS$^{-/-}$ (**center**) mice. Absence of nuclei in RBCs is shown by negative 4',6-diamidino-2-phenylindole (DAPI; blue) staining. IgG control showing negligible background staining. **E**, eNOS expression in RBCs from WT and Düsseldorf eNOS$^{-/-}$ mice was assessed by immunoprecipitation and Western blot analysis and compared with eNOS expression in aortic tissue (data from 2 of 6 independent gels are represented). **F**, Densitometric assessment of eNOS expression in mouse RBCs compared with aorta (n=3). **G**, Conversion of ^{14}C-arginine to ^{14}C-citrulline as a measurement of NOS activity in RBCs from WT and Harvard eNOS$^{-/-}$ mice (n=4 per group). Data are expressed as mean±SEM. *P<0.05.

vascular reactivity of aortic rings from mice competent for vascular eNOS (WT, BC+/EC+, BC−/EC+). Endothelial-independent (phenylephrine, sodium nitroprusside; Figure 3A and 3C) and endothelial-dependent (acetylcholine; Figure 3B) relaxation and contraction responses were similar between all 3 groups. Furthermore, cGMP levels were measured in the aortas of cross-transplanted Düsseldorf eNOS$^{-/-}$ chimeras (Figure 3D) as a parameter of eNOS-dependent vascular reactivity. Both BC−/EC+ and BC+/EC+ chimeras demonstrated cGMP levels similar to WT controls, indicating that any BP differences of chimeric mice lacking BC eNOS (BC−/EC+), compared with WT controls with global competency for eNOS (BC+/EC+), are not a consequence of altered vascular function from the irradiation and transplantation procedure.

Blood Cell eNOS Rescues eNOS$^{-/-}$ Mice From Hypertension and Low Nitrite Levels

To gain insight into relative contributions of BC versus vessel wall eNOS to circulating NO derivatives, we measured whole blood (Figure 4A) and plasma (Figure 4B) nitrite in anesthetized, cross-transplanted chimeras. Transplantation of WT recipients with marrow from eNOS$^{-/-}$ donors (BC−/EC+) decreased circulating nitrite levels by roughly one third compared with irradiated and transplanted WT controls (BC+/EC+; plasma: 0.53±0.10 μmol/L versus 0.79±0.07 μmol/L; P<0.05; whole blood: 0.81±0.14 versus 1.19±0.15; P<0.05). Conversely, transplantation of eNOS$^{-/-}$ recipients with marrow from WT donors (BC+/EC−) increased circulating nitrite levels compared with irradiated and transplanted eNOS$^{-/-}$ controls (BC−/EC−; plasma: 0.46±0.07 μmol/L versus 0.32±0.02 μmol/L; P=0.08; whole blood: 0.68±0.07 versus 0.49±0.02; P<0.05), indicating that both vascular and BC eNOS are important sources of circulating nitrite in vivo.

For concomitant measurement of both circulating nitrite levels and corresponding BPs, mice were analyzed under anesthetized conditions, and BP was measured by carotid artery cannulation (Figure 4C–4E). Transplantation of WT BM into eNOS$^{-/-}$ background (BC+/EC−) significantly decreased BPs relative to BC−/EC− chimeras (MAP: 87.33±2.88 versus 106.1±5.43 mm Hg; P=0.0014; Figure 4C). Similar results were obtained by radiotelemetry measurement of BP in awake BC+/EC− chimeras versus their BC−/EC− counterparts (Figure 5B; diastolic: P=0.0036; systolic: P=0.0112; MAP: P=0.0056). Although the BP-lowering effect afforded by BC eNOS in otherwise eNOS-deficient mice was low

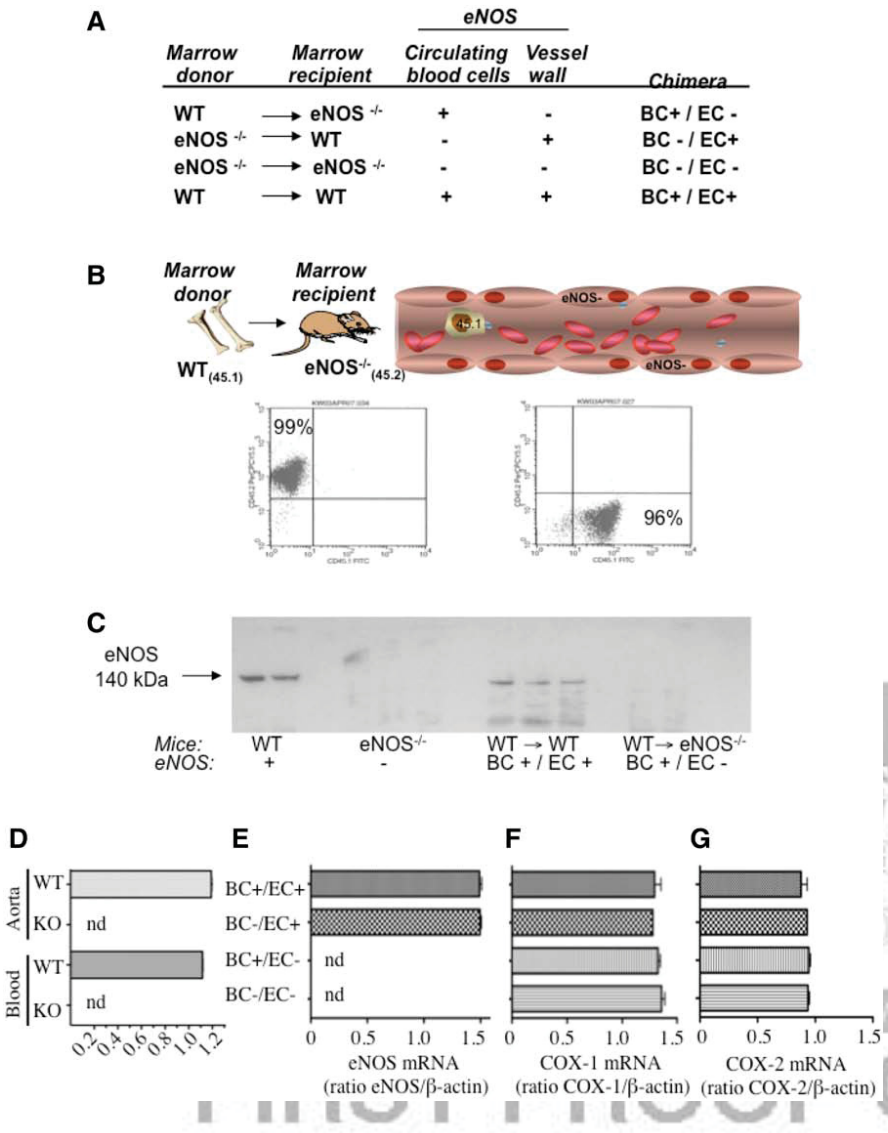

Figure 2. Transplantation of endothelial nitric oxide synthase (eNOS)–deficient recipients with bone marrow (BM) from wild-type (WT) donors does not confer eNOS expression on vascular endothelium. **A**, Table of BM-transplanted chimeras used in the present study, outlining mouse BM donors/recipients and sites of eNOS expression at 6 to 8 weeks after transplant. **B**, Representative flow cytometry data (histograms) evidencing ≥90% conversion of BM recipients' blood (peripheral leukocytes) to the donor phenotype (CD45.1 or CD45.2) before use in nitrite and blood pressure experiments (representative experiment of n=340+). **C**, Representative Western blot of aortic homogenates from WT mice (n=2, lanes 1–2), eNOS$^{-/-}$ mice (n=3, lanes 4–6), WT recipients of WT marrow (WT→WT; n=3, lanes 8–10), and eNOS-deficient recipients of WT marrow (WT→eNOS$^{-/-}$; n=2, lanes 12–13). **D**, eNOS mRNA in aortas and blood (all cellular components) of C57Bl/6J (WT) compared with eNOS-deficient (eNOS$^{-/-}$) mice. Ratios of eNOS/β-actin mRNA are given as mean±SEM for each group (n=2 per group). nd denotes nondetectable at 40 cycles. **E**, Cross-transplantation of eNOS$^{-/-}$ mice with WT marrow does not give rise to eNOS mRNA expression in aortas (BC+/EC+: n=2; BC-/EC+: n=3; BC+/EC–: n=5; BC–/EC–: n=3). Expression of (**F**) cyclooxygenase-1 (COX-1) and (**G**) cyclooxygenase-2 (COX-2) mRNA in aortas of cross-transplanted chimeras is similar between groups (BC+/EC+: n=3; BC–/EC+: n=2; BC+/EC–: n=4; BC–/EC–: n=3). BC+/EC+ (globally competent for eNOS), BC–/EC+ (deficient of blood eNOS), BC+/EC– (deficient of vascular eNOS), and BC–/EC– (globally deficient of eNOS). Ratios of β-actin mRNA are given as mean±SEM for each group. nd denotes nondetectable eNOS mRNA at 40 cycles. BC indicates blood cell; and EC, endothelial cell.

(5 mm Hg), radiotelemetry experiments demonstrated its reproducibility in 2 investigated eNOS$^{-/-}$ strains (Harvard and UNC; Figure 5C and 5D). In addition, transplantation of eNOS$^{-/-}$ BM into WT background significantly increased BPs relative to BC+/EC+ chimeras under awake conditions (Figure 5B; systolic: P=0.0171; diastolic: P<0.0001; MAP: P=0.0011), again supporting a role for BC eNOS in BP regulation. Differences in the baseline BPs obtained in the anesthetized versus awake BC–/EC+ chimeras suggest an effect for anesthesia (Figure 4C–4E and Figure 5B). The data also demonstrate an effect for eNOS in the vascular wall, apparent in anesthetized and awake BC+/EC– chimeras versus their BC+/EC+ counterparts (MAP [mm Hg] of 75.39±2.0 versus 106.1±5.43; P<0.05; Figure 4C and 36-hour MAP (area under the curve) of 4100 versus 3764; P=0.0003; Figure 5A and 5B). In sum, our findings support a role for blood eNOS, in addition to vascular eNOS, in BP regulation.

Given our previous observations of a contribution from both vascular and blood eNOS to intravascular nitrite and the proposed contribution of nitrite to BP regulation,[6,9,27] we also explored the relationship between mean plasma and whole blood nitrite levels versus MAP and found an inverse correlation between these parameters across all chimeric groups (plasma: r=–0.91; P<0.05; whole blood: r=–0.91; P=0.05; Figure 4F). Together, these data support an interrelated role for BC eNOS in nitrite formation and BP regulation. However, the cause and effect remain to be established.

Blood eNOS Lowers BP Independently of Blood iNOS, Platelets, and Leukocytes

Constitutive expression of eNOS in immune cells has been shown to serve overlapping physiological and pathophysiological roles, most notably in activating the proinflammatory profile (iNOS and nuclear factor-κB gene expression) of monocytes/macrophages (human and rodent) in a manner consistent with nanomolar-level NO• production that is Ca^{2+}/CAM- and cGMP-dependent.[28] The possibility that restoration of immune cell eNOS in an otherwise eNOS-deficient setting, such as the BC+/EC– chimera, could regulate BP was addressed in eNOS$^{-/-}$ mice cross-transplanted with BM from

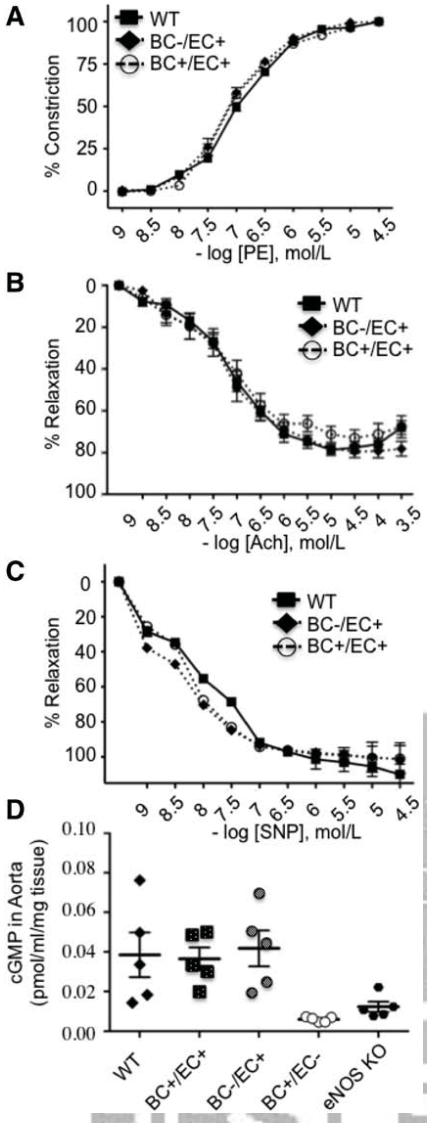

Figure 3. Lethal irradiation, bone marrow (BM) transplantation, and blood endothelial nitric oxide synthase (eNOS) deficiency do not impair endothelial and vascular smooth muscle cell function in aortic segments of BC–/EC+ and BC+/EC+ chimeras compared with wild-type (WT) controls. **A**, Contractions to cumulative concentrations of phenylephrine (PE: 10^{-9} to 10^{-4}) and relaxations to cumulative concentrations of (**B**) acetylcholine (Ach: 10^{-9} to $10^{-3.5}$) and (**C**) sodium nitroprusside (SNP: 10^{-9} to $10^{-4.5}$) were examined in segments preconstricted with PE (10^{-6}). We analyzed 2 rings/mouse (n=5 mice per group). No statistically significant differences in contraction or relaxation responses were noted between groups. **D**, cGMP concentration in aortic tissue of chimeras obtained from Düsseldorf eNOS$^{-/-}$ mice as assessed by enzymatic immunoassay. BC+/EC+ (globally competent for eNOS), BC–/EC+ (deficient of blood eNOS), and BC+/EC– (deficient of vascular eNOS), n=5 per group. Data are expressed as mean±SEM. BC indicates blood cell; and EC, endothelial cell.

iNOS$^{-/-}$ donors (BC $^{eNOS+}_{iNOS}$–/EC–). The resulting chimeric group, possessing blood eNOS but not blood iNOS, maintained a lower BP than the BC–/EC– group, indicating that blood iNOS was not participating in physiological BP control in these mice (Figure 4G).

We further investigated the BC type contributing to BP regulation by depleting BC+/BC– chimeras of their platelets or leukocytes. Platelet eNOS is a well-documented antagonist of platelet activation and aggregation.[29] Most leukocytes also express eNOS,[15–18] although its function in these cells is yet to be clearly defined. To determine whether platelets are the BC source of eNOS involved in physiological BP regulation, BC+/EC– chimeras and their hypertensive counterparts (BC–/EC–) were pharmacologically depleted of platelets (>90%) using an antithrombocyte serum (Table II in the online-only Data Supplement). Although platelet depletion lowered MAPs equally in both groups, the BP-lowering effect of red cell eNOS persisted between treated groups (18.45±2.54 mm Hg) to a similar extent between untreated (platelet-competent) groups (18.80±3.60 mm Hg; Figure 4H)

Leukocytes were also depleted using an anti-CD45 antibody that reacts with the pan-leukocyte antigen CD45 (Ly5), causing clearance of leukocytes from circulation. Treatment of BC+/EC– and BC–/EC– chimeras with this leukodepleting antibody substantially decreased their circulating leukocyte counts by ≥75% (Table II in the online-only Data Supplement). Similar to thrombocytopenia, leukopenia decreased BP in both treated groups but did not eradicate the significant BP-lowering effect of red cell eNOS (Figure 4H).

The persistence of lower arterial BPs in BC+/EC– chimeric mice, relative to eNOS$^{-/-}$ controls (BC–/EC–), after platelet- or leukocyte-depletion treatments indicates that platelet- and leukocyte-derived eNOS are not responsible for the BP-modulating effect of circulating blood eNOS and supports a role for a functional red cell eNOS in BP control.

Blood Cell eNOS Effects on BP Are abolished by NOS Inhibition in Conscious Mice

To further assess the role of blood eNOS availability and function in BP regulation, conscious BP responses to NOS inhibition with L-NAME or repristination with L-arginine were measured in BC+/EC– chimeras via radiotelemetry. Baseline BP (pretreatment) was allowed to stabilize for 10 days after BP sensor implantation. The average BP for the BC+/EC– group was significantly lower than that of its BC–/EC– counterpart (systolic: P=0.0112; diastolic: P=0.0036; MAP: P=0.0056), strongly supporting a role for blood eNOS in physiological BP regulation (Figure 5A). Mice were then treated with L-NAME in the drinking water for 4 days (days 11–14) followed by L-arginine in the drinking water for 3 days (days 15–17). BP averages were calculated for the hours 22:00 to 04:00 on day 10 (baseline), day 14 (L-NAME), and day 17 (L-arginine). Even in the absence of eNOS in the vascular wall and its exclusive presence in blood (BC+/EC–), BP responses to oral L-NAME and oral L-arginine followed a classical pattern (Figure 5C): L-NAME consumption increased MAP compared with baseline (3.16±4.77 mm Hg, NS), whereas L-arginine consumption decreased MAP compared with L-NAME (–7.43±4.43 mm Hg; P<0.05). These experiments, performed in chimeras generated from the Harvard eNOS$^{-/-}$ mouse (our usual eNOS-deficient mouse line used for all eNOS$^{-/-}$ experiments except where noted), were repeated in a second group of BC+/EC– chimeras generated from a different, commercially available eNOS$^{-/-}$ mouse (UNC).[4] The UNC BC+/EC– chimeras demonstrated similar significant MAP responses

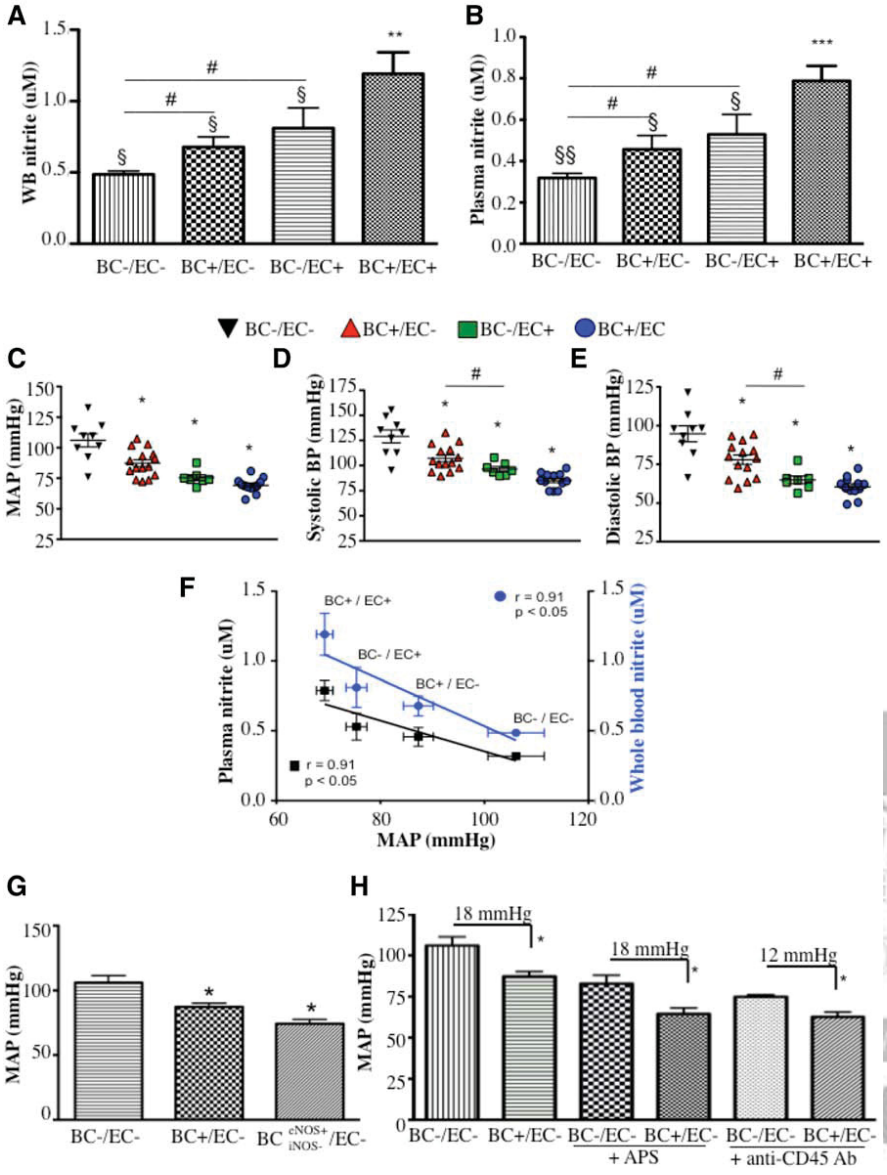

Figure 4. Blood cell endothelial nitric oxide synthase (eNOS) rescues eNOS$^{-/-}$ mice from low circulating nitrite levels and hypertension. Nitrite concentrations in (**A**) whole blood (BC+/EC+: n=10, BC−/EC+: n=8, BC+/EC−: n=8, BC−/EC−: n=7) and (**B**) plasma (BC+/EC+: n=10; BC−/EC+: n=5; BC+/EC−: n=8; BC−/EC−: n=7) of cross-transplanted chimeras. BC+/EC+ (globally competent for eNOS), BC−/EC+ (deficient of blood eNOS), BC+/EC− (deficient of vascular eNOS), and BC−/EC− (globally deficient of eNOS). Data are expressed as mean±SEM vs BC−/EC−: **P*<0.05 for plasma and whole blood; ***P*<0.005 for whole blood and *P*<0.0001 for plasma; §*P*<0.05 and §§*P*<0.005 vs BC+/EC+; #*P*<0.05 by 1-way *t* test; (**C**–**E**) blood pressures for eNOS$^{-/-}$ chimeras (BC−/EC+: n=8; BC+/EC+: n=12; BC+/EC−: n=14; BC−/EC−: n=9); (**C**) mean arterial pressure (MAP: *P*=0.0142 for BC−/EC+ vs BC+/EC+, *P*=0.0014 for BC+/EC− vs BC−/EC−); (**D**) systolic blood pressure (*P*=0.0008 for BC−/EC+ vs BC+/EC+, *P*=0.0018 for BC+/EC− vs BC−/EC−); and (**E**) diastolic blood pressure (*P*=0.0001 for BC−/EC+ vs BC+/EC+, *P*=0.0021 for BC+/EC− vs BC−/EC−) in anesthetized cross-transplanted chimeras. ***P*<0.005, ****P*<0.0005, and *****P*<0.0001 vs BC−/EC−. Blood pressure data analyzed by 1-way Student *t* test. **F**, Linear regression of MAP averages and nitrite concentrations in plasma (left *y* axis) and whole blood (right *y* axis) across all chimeric groups. Blood pressure data expressed as mean±SEM (SEM for BC−/EC− MAPs for whole blood and plasma are ±0.023 and 0.022 mm Hg, respectively). Correlations of blood pressure and plasma nitrite are expressed as *r* and *P* value for plasma (blue type) and whole blood (black type). Blood pressure–lowering effects of eNOS-competent blood occur independently of blood inducible NOS (iNOS), platelets, and leukocytes. **G**, MAP in anesthetized eNOS-deficient chimeras in the absence of blood eNOS (BC−/EC−: n=9), the presence of blood eNOS (BC+/EC−: n=15), and the presence of eNOS, but not iNOS (BC eNOS+iNOS^{-}/EC−, n=4) in blood. **P*<0.05 vs BC−/EC−; (**H**) MAPs in the absence or presence of platelet depletion (+APS; BC+/EC−: n=5 and BC−/EC−: n=7) or leukocyte depletion (+ anti-CD45 Ab; BC+/EC−: n=3 and BC−/EC−: n=4) in anesthetized BC+/EC− and BC−/EC− chimeras are shown. Blood pressure data are expressed as mean±SEM. BC indicates blood cell; and EC, endothelial cell.

to L-NAME (7.25±3.68 mm Hg; *P*<0.05) and L-arginine (−11.09±5.97 mm Hg, *P*<0.05; Figure 5D). These classical BP responses to the NO• synthase inhibitor and substrate, noted in separate BC+/EC− groups created from different eNOS$^{-/-}$ strains (Figure 5C and 5D) and absent in the UNC-eNOS$^{-/-}$ mice (as shown previously),[30] further support the existence of a BC eNOS that participates in physiological BP regulation. BC−/EC− obtained from the Harvard strain mounted a paradoxical (decreased BP) response to L-NAME (Figure I in the online-only Data Supplement), as previously shown for Harvard eNOS$^{-/-}$[13]; however, the differences were not statistically significant. Taken together, these results point to a role for NOS in the decreased BPs observed in the chimeras expressing eNOS only in blood. Until now, conventional wisdom has held that eNOS-mediated control of BP is primarily dependent on eNOS enzyme expressed in the endothelium. These data indicate that BC eNOS also contributes to the regulation of BP.

Discussion

The role of eNOS in vascular endothelium has been shown both in vitro and in vivo to participate in autocrine and paracrine NO• signaling and the control of basal BP.[8] Most circulating BCs, including leukocytes, platelets, and RBCs, have been shown to contain eNOS.[15–18,21,22,29,31] It has been suggested that red cell eNOS[21–24] is capable of producing NO• under normoxic conditions. Data from our laboratory and others have demonstrated NOS-derived effects exerted by RBCs, including inhibition of ADP-induced platelet aggregation,[22,32] protection of isolated, perfused hearts from ischemia/reperfusion injury,[33] as well as decreased RBC-released NO• metabolite (nitrite, nitrate, nitros(yl)ated species) levels in

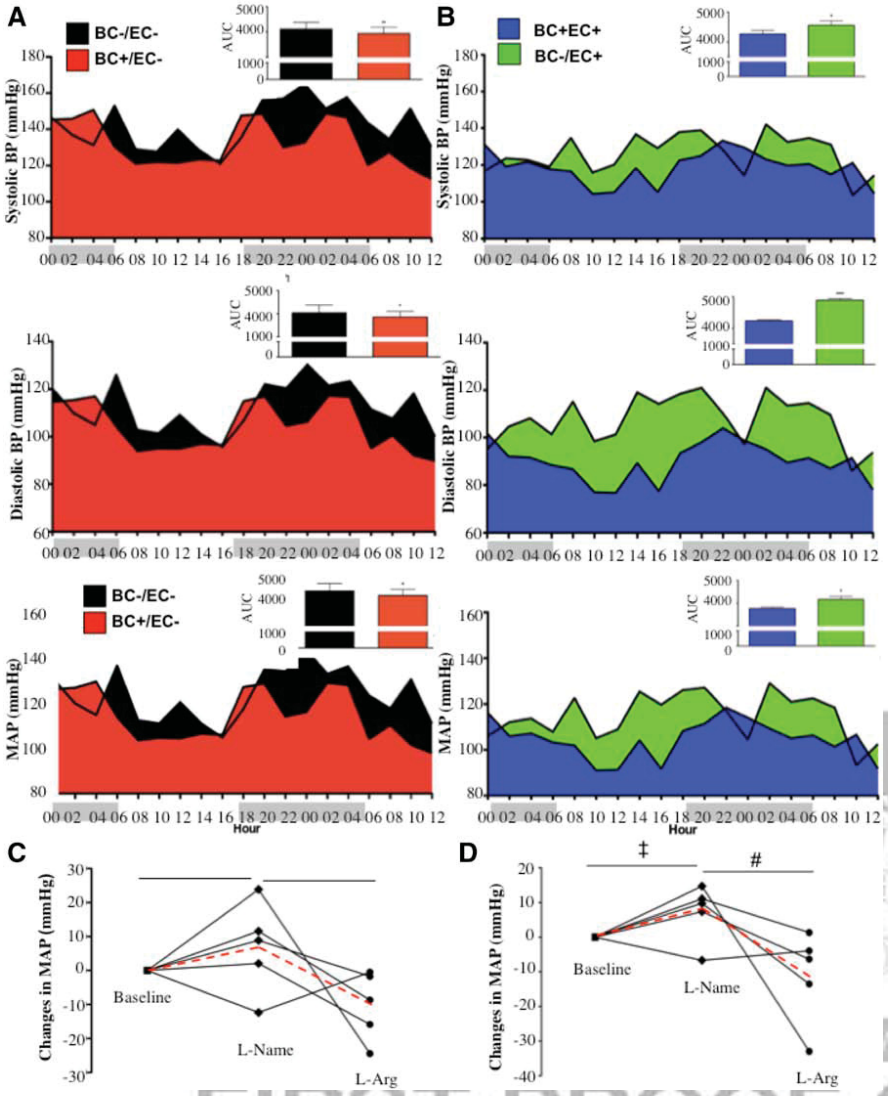

Figure 5. Blood pressure–lowering effects of endothelial nitric oxide synthase (eNOS)-competent blood are responsive to L-NAME and L-arginine (L-Arg) treatments. Thirty-six-hour radiotelemetry-detected baseline blood pressures (BPs) in (**A**) BC−/EC+ (n=3) vs BC+/EC+ (n=4) (systolic: P=0.0171; diastolic: P<0.0001; mean arterial pressure [MAP]: P=0.0011) and (**B**) BC+/EC− (n=3) vs BC−/EC− (n=4) (systolic: P=0.0112; diastolic: P=0.0036; MAP: P=0.0056), with group averages calculated for each 2-hour interval and area under the curve (AUC) by 2-way ANOVA. Comparisons of moving averages, assessed by 2-way ANOVA, were also statistically significant (P<0.0001). x axis depicts hours of darkness (gray shade) vs hours of light (white shade). Change in radiotelemetry-detected MAP (mm Hg) in (**C**) Harvard BC+/EC− chimeras (n=5) and (**D**) UNC BC+/EC− chimeras (n=5) after oral treatment with L-NAME or L-arginine. Blood pressure data for individual animals shown as solid lines; group averages shown as dashed red line. ‡P<0.05 for L-NAME vs baseline; #P<0.05 for L-arginine vs L-NAME; *P<0.05 using Student t test. BC indicates blood cell; and EC, endothelial cell.

response to NOS inhibition.[22,24] Circulating angiogenic cells also contain a functional eNOS, but their number in peripheral blood is <0.01% of peripheral blood mononuclear cell numbers (0.0067±0.0097 per 100).[34–36] However, RBCs are the most abundant cells in blood and transport hemoglobin and contain relatively high levels of nitrite.[25] Hence, it is reasonable to consider a role for RBCs as potential regulators of the circulating NO• pool and BP responses. However, a role for red cell eNOS in NO• signaling remains controversial, and a specific role for BC eNOS in BP regulation has not been investigated previously.

In the present study, cross-transplanted chimeric mice genetically competent or deficient for eNOS in circulating BCs are used to demonstrate a previously unrecognized role for BC eNOS in BP regulation and in vivo nitrite homeostasis. Our data support a persistent blood-derived eNOS effect on BP after in vivo platelet and leukocyte depletion, as well as RBC catalysis of arginine to citrulline and generation of intracellular NO• metabolites. Although these studies provide strong evidence for circulating BCs in NOS-dependent control of BP and nitrite production, definitive clarification of the role of the erythrocyte in this process will require the use of erythroid cell–specific knockout approaches in future studies.

We performed numerous control experiments to test the hypothesis that red cell eNOS regulates BP. We verified that endothelial function/integrity was not affected by our experimental setting, as demonstrated by an absence of change in endothelial-dependent and endothelial-independent vasodilation of aortic rings or aortic cGMP levels relative to the appropriate control group or WT mice. The BP-lowering effects of circulating BC eNOS were not a result of incorporation of BM cells into vascular endothelium, as demonstrated here by the absence of eNOS in Western blot–analyzed BC+/EC− aortas. Consistent with our observation, a recent study involving transplantation of GFP^{pos} (eNOS competent) BM into sublethally irradiated eNOS$^{-/-}$ mice confirmed that BM-derived endothelial progenitor cells do not incorporate into vascular endothelium.[26] Furthermore, we performed control experiments to rule out the contribution of other NOS isoforms to observed changes in BP. We did not detect a compensatory upregulation of other NOS isoforms or the cyclooxygenase 2 gene in the vasculature of the Harvard eNOS$^{-/-}$ mice, a finding that has been previously reported but remains controversial

because of reported disparities between different strains of eNOS$^{-/-}$ mice.[13,30,37–40] If other NOS isoforms are responsible for the BP effects we observed in the BC+/EC− chimeras, then a general NOS inhibitor, such as L-NAME, should have reversed those effects. We instead noted that the BC−/EC− chimera mounted a paradoxical hypotensive response to L-NAME treatment (shown in Figure I in the online-only Data Supplement), a result that has been previously described in the Harvard strain by different groups,[13,30] whereas the BC+/EC− chimera mounted the classical increased BP response. Paul Huang and others have reported an upregulation of nNOS in the Harvard eNOS knockout mouse[13,41,42] and have speculated on its possible role in the mutant's hypotensive BP response to L-NAME treatment.[13] In the presence of a nonspecific NOS inhibitor, such as L-NAME, a compensatory role for nNOS is unlikely to account for our observation. Furthermore, although Paul Kubes' group has shown that nNOS is upregulated in brain and skeletal muscle of the Harvard eNOS knockout mice, it was not sufficient to compensate for eNOS deficiency during H_2O_2-stimulated leukocyte infiltration in postcapillary venules.[43] H_2O_2 has been proposed by several groups as an important endothelium-derived hyperpolarizing factor, but in an NOS-dependent manner.[38,44] In addition, nonspecific effects of L-NAME treatment have been reported: antagonism of muscarinic acetylcholine receptors[45] and inhibition of cytochrome c reduction in vitro.[46] Indeed, we observed normal endothelial function in WT mice with elevated BP as a result of BC deficiency of eNOS (BC−/EC+ chimeras), an unexpected finding given the general association of elevated BP and endothelial dysfunction. A study by Suda et al[30] found that coronary vascular lesions develop in WT mice after long-term (8 week) treatment with L-NAME alone or with coadministration of L-NAME and the antihypertensive drug hydralazine, calling into question the nonspecific and BP-independent effects of L-NAME on vascular function.

With regard to a specific role for the RBC in these observations, we did not observe an effect of leukocytes or platelets on eNOS-dependent BP regulation. Reductions in BP in our BC+/EC− mice were not abrogated by platelet-, leukocyte-, or iNOS-depleting interventions, arguing against a significant role for any of these factors in physiological BP regulation. Although these interventions lowered BP in all groups, the difference in BP observed between the BC+/EC− and BC-/EC− chimeras remained significant and equivalent. The intervention-associated hypotensive responses could be attributable to deficiency of platelet- or neutrophil-derived thromboxane A(2),[47] reactive oxygen species, and augmented prostacyclin levels.[48] Our anti-leukocyte intervention targeted circulating lymphocytes and neutrophils alike (≥75% depletion). This may be important, given the antihypertensive effects previously shown to be elicited in rats and mice by thymocyte-[49] or neutrophil-depleting[50] interventions. It is unlikely that these hypotensive effects could have masked an augmentation in BP because of platelet or leukocyte eNOS deficiency, because the absolute decreases in BP in the BC+/EC− chimera remained constant with and without depletion of leukocytes and platelets.

A recent study evaluating similar chimera experiments reported results that differed from ours. That study observed no BP-reducing effect for GFP^{pos} WT BM when transplanted into eNOS$^{-/-}$ mice.[26] This discrepancy in BP results is likely attributable to differences in study design. Whole-body irradiation and BM transplantation are not without potentially confounding effects, thus the WT and eNOS$^{-/-}$ controls used in this study were also irradiated and BM transplanted, whereas the controls used in the other study were not.

Taken together, the findings from this study point consistently toward a functional circulating RBC eNOS that is active in physiological vasorelaxation and nitrite homeostasis and may make contributions to other as yet unidentified biological processes. If eNOS in blood can contribute to BP regulation and nitrite production, then it is likely to have effects under reparative conditions, such as after myocardial ischemia or stroke. Indeed, circulating BM-derived endothelial progenitor cells have been shown to participate in the neovascularization of jeopardized tissue.[51] A prior study by Ii et al[52] may have relevance to our observations. That study evaluated similar cross-transplantation experiments with BM-recipient mice subjected to experimental myocardial infarction. Cardioprotection was observed in the eNOS$^{-/-}$ mice receiving WT BM, which at the time was ascribed to NO• released by endothelial progenitor cells that had incorporated into ischemic myocardium. However, in that study only a small percentage of the incorporated endothelial progenitor cells and the cardiomyocytes in ischemic myocardium expressed eNOS, suggesting that the cardioprotection may have derived from circulating BC-derived eNOS activity or nitrite. As a final component of these NO•-related regenerative pathways, numerous groups have demonstrated that circulating nitrite can be reduced in the blood to form NO•, regulate hypoxic vasodilation, cytoprotection after ischemia/reperfusion events, and vascular angiogenesis.[9–11,53–55] It is likely that both direct NO• formation and signaling, as well as indirect NO• oxidation to nitrite, contribute to the therapeutic effects of red cell eNOS in angiogenesis, cytoprotection, and BP control.

In summary, the present study provides strong evidence that a circulating blood eNOS participates in nitrite homeostasis and BP regulation under physiological conditions (Figure 6). These findings provide novel insight into mechanisms of BP control that challenge our conventional perspectives on NO and nitrite signaling in blood, suggesting a more holistic regulation of vascular function, with both the circulating RBCs and the endothelium contributing to vascular homeostasis. The existence of a functional RBC eNOS opens the door to studies addressing the function and dysfunction of blood eNOS in health and disease, such as a role in RBC enzymopathies, hemoglobinopathies, and membranopathies, and in infectious diseases, such as malaria.

Clinical Perspective

Hypertension is a complex multifactorial condition associated with cardiovascular disease. Accumulating evidence points to a correlation between BP and circulating NO• metabolites, such as nitrite. The data presented here demonstrate a role for circulating BC eNOS in nitrite homeostasis and BP regulation under physiological conditions. A fruitful cycle of continuous NO• formation in blood might arise from BC eNOS under

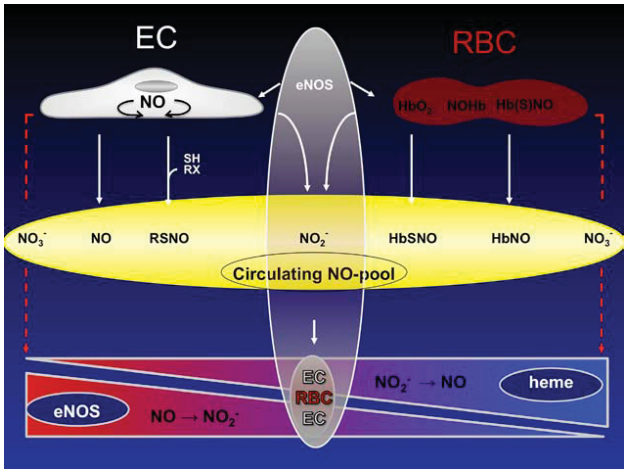

Figure 6. Contribution of blood cell endothelial nitric oxide synthase (eNOS) to regulation of the circulating nitric oxide (NO•) pool and blood pressure under normoxic and hypoxic conditions. The circulating NO• pool consists of various NO•-related species that transport bioactive NO• in the mammalian circulation. These oxygenated and nitros(yl)ated NO• species are interconvertible. NO• bioactivity within this pool is regulated by the surrounding redox conditions at the site of delivery. Under hypoxic conditions, NO• is formed in blood by the nitrite reductase activity of heme-containing proteins, including deoxyhemoglobin. Under normoxic conditions, NO• can be produced by eNOS in endothelial cells (EC) and scavenged by oxyhemoglobin in red blood cells (RBC). An eNOS-derived NO• production in blood cells may offset oxyhemoglobin-dependent NO• scavenging, thereby safeguarding vasodilatory activity in adjacent normoxic vessels. Furthermore, eNOS activity in RBCs might contribute to their intracellular storage pool of NO• equivalents, such as nitrite. Thus, a fruitful cycle of continuous NO• formation in blood might arise from blood cell eNOS under normoxic conditions and deoxyhemoglobin-mediated reduction of nitrite under hypoxic conditions. EC indicates endothelial cells; HbO_2, oxyhemoglobin; HbSNO, s-nitrosated hemoglobin; NO-Hb, nitrosylated hemoglobin; RBC, red blood cells; RSH, thiols; RSNO, nitrosated thiols; and RX, other reactive groups.

normoxic conditions and deoxyhemoglobin-mediated reduction of nitrite under hypoxic conditions. This cycle of NO• formation within blood and the vasculature may be impaired in cardiovascular disease, where a generalized eNOS dysfunction is often marked by eNOS uncoupling or protein deficiency. Indeed, recent years have seen anemia and RBC dysfunction identified as independent risk factors for cardiovascular disease. There is a growing recognition that intravascular hemolysis represents a fundamental mechanism for human disease through the release of cell-free plasma hemoglobin that inhibits NO• signaling in the subendothelial layer. It is common to hemoglobinopathies and hemolytic anemia, as well as to the RBC storage lesion of aged blood used in transfusion therapy, and may be driven by red cell eNOS-linked enzymopathies and membranopathies.[56–62] Thus, our findings may illuminate novel avenues for assaying the general status of eNOS activity and cardiovascular health in the human body.

Acknowledgments

We thank Paul Huang and Axel Gödecke for providing the Harvard and Düsseldorf mice genetically deficient in endothelial nitric oxide synthase (eNOS$^{-/-}$), respectively. We thank the staff of the Murine Phenotyping Core and the Laboratory of Animal Medicine and Surgery facility for assistance with the radiotelemetry-monitored blood pressure experiments, Sivatharsini Sivarajah for the Western blot analysis of mouse red blood cells, and Simone Zander for providing the Chimeras from Düsseldorf eNOS$^{-/-}$ mice. We acknowledge the professional skills and advice of Dr Christian Heiß, Dr Christian A. Combs, and Dr Daniela Malide (Light Microscopy Core Facility, National Heart, Lung, and Blood Institute, National Institutes of Health) and Prof Dr Dieter Häussinger for use of the FACS Canto II flow cytometer.

Sources of Funding

This work was supported, in part, by National Institutes of Health (NIH) grants R01HL098032, RO1HL096973, RC1DK085852, the Institute for Transfusion Medicine, Hemophilia Center of Western Pennsylvania (M.T. Gladwin), the Division of Intramural Research of the National Heart, Lung and Blood Institute, NIH (G.J. Kato), the Deutsche Forschungsgemeinschaft (405/5-1 and FOR809TP7 Me1821/3-1 to M. Kelm), and the Forschungskommission of the Medical Faculty of the Heinrich-Heine-University of Düsseldorf (to M. Cortese-Krott).

Disclosures

Dr Gladwin is a coinventor on a National Institutes of Health government patent application on the use of nitrite salts for cardiovascular diseases. The other authors report no conflicts.

References

1. Kleinbongard P, Dejam A, Lauer T, Rassaf T, Schindler A, Picker O, Scheeren T, Gödecke A, Schrader J, Schulz R, Heusch G, Schaub GA, Bryan NS, Feelisch M, Kelm M. Plasma nitrite reflects constitutive nitric oxide synthase activity in mammals. *Free Radic Biol Med*. 2003;35:790–796.
2. Gödecke A, Decking UK, Ding Z, Hirchenhain J, Bidmon HJ, Gödecke S, Schrader J. Coronary hemodynamics in endothelial NO synthase knockout mice. *Circ Res*. 1998;82:186–194.
3. Gregg AR, Schauer A, Shi O, Liu Z, Lee CG, O'Brien WE. Limb reduction defects in endothelial nitric oxide synthase-deficient mice. *Am J Physiol*. 1998;275:H2319–H2324.
4. Shesely EG, Maeda N, Kim HS, Desai KM, Krege JH, Laubach VE, Sherman PA, Sessa WC, Smithies O. Elevated blood pressures in mice lacking endothelial nitric oxide synthase. *Proc Natl Acad Sci U S A*. 1996;93:13176–13181.
5. Sobko T, Marcus C, Govoni M, Kamiya S. Dietary nitrate in Japanese traditional foods lowers diastolic blood pressure in healthy volunteers. *Nitric Oxide*. 2010;22:136–140.
6. Webb AJ, Patel N, Loukogeorgakis S, Okorie M, Aboud Z, Misra S, Rashid R, Miall P, Deanfield J, Benjamin N, MacAllister R, Hobbs AJ, Ahluwalia A. Acute blood pressure lowering, vasoprotective, and antiplatelet properties of dietary nitrate via bioconversion to nitrite. *Hypertension*. 2008;51:784–790.
7. Kapil V, Milsom AB, Okorie M, Maleki-Toyserkani S, Akram F, Rehman F, Arghandawi S, Pearl V, Benjamin N, Loukogeorgakis S, Macallister R, Hobbs AJ, Webb AJ, Ahluwalia A. Inorganic nitrate supplementation lowers blood pressure in humans: role for nitrite-derived NO. *Hypertension*. 2010;56:274–281.
8. Balligand JL, Feron O, Dessy C. eNOS activation by physical forces: from short-term regulation of contraction to chronic remodeling of cardiovascular tissues. *Physiol Rev*. 2009;89:481–534.
9. Cosby K, Partovi KS, Crawford JH, et al. Nitrite reduction to nitric oxide by deoxyhemoglobin vasodilates the human circulation. *Nat Med*. 2003;9:1498–1505.
10. Maher A, AB. M, Gunaruwan P, Abozgula K, Ahmed I, Weaver R, Thomas P, Ashrafian H, GV. B, James P, Frenneaux M. Hypoxic modulation of exogenous nitrite-induced vasodilation in humans. *Circulation*.2008:117:670–677
11. Duranski MR, Greer JJ, Dejam A, Jaganmohan S, Hogg N, Langston W, Patel RP, Yet SF, Wang X, Kevil CG, Gladwin MT, Lefer DJ. Cytoprotective effects of nitrite during *in vivo* ischemia-reperfusion of the heart and liver. *J Clin Invest*. 2005;115:1232–1240.
12. Gonzalez FM, Shiva S, Vincent PS, Ringwood LA, Hsu LY, Hon YY, Aletras AH, Cannon RO 3rd, Gladwin MT, Arai AE. Nitrite anion

provides potent cytoprotective and antiapoptotic effects as adjunctive therapy to reperfusion for acute myocardial infarction. *Circulation*. 2008;117:2986–2994.
13. Huang PL, Huang Z, Mashimo H, Bloch KD, Moskowitz MA, Bevan JA, Fishman MC. Hypertension in mice lacking the gene for endothelial nitric oxide synthase. *Nature*. 1995;377:239–242.
14. Chen LY, Mehta JL. Variable effects of L-arginine analogs on L-arginine-nitric oxide pathway in human neutrophils and platelets may relate to different nitric oxide synthase isoforms. *J Pharmacol Exp Ther*. 1996;276:253–257.
15. Saluja R, Jyoti A, Chatterjee M, Habib S, Verma A, Mitra K, Barthwal MK, Bajpai VK, Dikshit M. Molecular and biochemical characterization of nitric oxide synthase isoforms and their intracellular distribution in human peripheral blood mononuclear cells. *Biochim Biophys Acta*. 2011;1813:1700–1707.
16. Mühl H, Pfeilschifter J. Endothelial nitric oxide synthase: a determinant of TNFalpha production by human monocytes/macrophages. *Biochem Biophys Res Commun*. 2003;310:677–680.
17. Aubry JP, Dugas N, Lecoanet-Henchoz S, Ouaaz F, Zhao H, Delfraissy JF, Graber P, Kolb JP, Dugas B, Bonnefoy JY. The 25-kDa soluble CD23 activates type III constitutive nitric oxide-synthase activity via CD11b and CD11c expressed by human monocytes. *J Immunol*. 1997;159:614–622.
18. de F, Sanchez de Miguel L, Farre J, Gomez J, Romero J, Marcos-Alberca P, Nunez A, Rico L, Lopez-Farre A. Expression of an endothelial-type nitric oxide synthase isoform in human neutrophils: modification by tumor necrosis factor-alpha and during acute myocardial infarction. *J Am Coll Cardiol*.2001:37:800–807.
19. Sase K, Michel T. Expression of constitutive endothelial nitric oxide synthase in human blood platelets. *Life Sci*. 1995;57:2049–2055.
20. Radomski MW, Palmer RM, Moncada S. An L-arginine/nitric oxide pathway present in human platelets regulates aggregation. *Proc Natl Acad Sci U S A*. 1990;87:5193–5197.
21. Cortese-Krott MM, Rodriguez-Mateos A, Sansone R, Kuhnle GG, Thasian-Sivarajah S, Krenz T, Horn P, Krisp C, Wolters D, Heiß C, Kröncke KD, Hogg N, Feelisch M, Kelm M. Human red blood cells at work: identification and visualization of erythrocytic eNOS activity in health and disease. *Blood*. 2012;120:4229–4237.
22. Kleinbongard P, Schulz R, Rassaf T, et al. Red blood cells express a functional endothelial nitric oxide synthase. *Blood*. 2006;107:2943–2951.
23. Mihov D, Vogel J, Gassmann M, Bogdanova A. Erythropoietin activates nitric oxide synthase in murine erythrocytes. *Am J Physiol Cell Physiol*. 2009;297:C378–C388.
24. Ulker P, Sati L, Celik-Ozenci C, Meiselman HJ, Baskurt OK. Mechanical stimulation of nitric oxide synthesizing mechanisms in erythrocytes. *Biorheology*. 2009;46:121–132.
25. Dejam A, Hunter CJ, Pelletier MM, Hsu LL, Machado RF, Shiva S, Power GG, Kelm M, Gladwin MT, Schechter AN. Erythrocytes are the major intravascular storage sites of nitrite in human blood. *Blood*. 2005;106:734–739.
26. Perry TE, Song M, Despres DJ, Kim SM, San H, Yu ZX, Raghavachari N, Schnermann J, Cannon RO 3rd, Orlic D. Bone marrow-derived cells do not repair endothelium in a mouse model of chronic endothelial cell dysfunction. *Cardiovasc Res*. 2009;84:317–325.
27. Bailey SJ, Winyard P, Vanhatalo A, Blackwell JR, Dimenna FJ, Wilkerson DP, Tarr J, Benjamin N, Jones AM. Dietary nitrate supplementation reduces the O2 cost of low-intensity exercise and enhances tolerance to high-intensity exercise in humans. *J Appl Physiol*. 2009;107:1144–1155.
28. Connelly L, Jacobs AT, Palacios-Callender M, Moncada S, Hobbs AJ. Macrophage endothelial nitric-oxide synthase autoregulates cellular activation and pro-inflammatory protein expression. *J Biol Chem*. 2003;278:26480–26487.
29. Randriamboavonjy V, Fleming I. Endothelial nitric oxide synthase (eNOS) in platelets: how is it regulated and what is it doing there? *Pharmacol Rep*. 2005;57:59–65.
30. Suda O, Tsutsui M, Morishita T, Tanimoto A, Horiuchi M, Tasaki H, Huang PL, Sasaguri Y, Yanagihara N, Nakashima Y. Long-term treatment with N(omega)-nitro-L-arginine methyl ester causes arteriosclerotic coronary lesions in endothelial nitric oxide synthase-deficient mice. *Circulation*. 2002;106:1729–1735.
31. Dudzinski DM, Michel T. Life history of eNOS: partners and pathways. *Cardiovasc Res*. 2007;75:247–260.
32. Chen LY, Mehta JL. Evidence for the presence of L-arginine-nitric oxide pathway in human red blood cells: relevance in the effects of red blood cells on platelet function. *J Cardiovasc Pharmacol*. 1998;32:57–61.
33. Yang BC, Nichols WW, Mehta JL. Cardioprotective Effects of Red Blood Cells on Ischemia and Reperfusion Injury in Isolated Rat Heart: Release of Nitric Oxide as a Potential Mechanism. *J Cardiovasc Pharmacol Ther*. 1996;1:297–306.
34. Fürstenberger G, von Moos R, Senn HJ, Boneberg EM. Real-time PCR of CD146 mRNA in peripheral blood enables the relative quantification of circulating endothelial cells and is an indicator of angiogenesis. *Br J Cancer*. 2005;93:793–798.
35. Mariucci S, Rovati B, Bencardino K, Manzoni M, Danova M. Flow cytometric detection of circulating endothelial cells and endothelial progenitor cells in healthy subjects. *Int J Lab Hematol*. 2010;32:e40–e48.
36. Schmidt-Lucke C, Fichtlscherer S, Aicher A, Tschöpe C, Schultheiss HP, Zeiher AM, Dimmeler S. Quantification of circulating endothelial progenitor cells using the modified ISHAGE protocol. *PLoS One*. 2010;5:e13790.
37. Kojda G, Laursen JB, Ramasamy S, Kent JD, Kurz S, Burchfield J, Shesely EG, Harrison DG. Protein expression, vascular reactivity and soluble guanylate cyclase activity in mice lacking the endothelial cell nitric oxide synthase: contributions of NOS isoforms to blood pressure and heart rate control. *Cardiovasc Res*. 1999;42:206–213.
38. Takaki A, Morikawa K, Tsutsui M, Murayama Y, Tekes E, Yamagishi H, Ohashi J, Yada T, Yanagihara N, Shimokawa H. Crucial role of nitric oxide synthases system in endothelium-dependent hyperpolarization in mice. *J Exp Med*. 2008;205:2053–2063.
39. Zhao X, Chen YR, He G, Zhang A, Druhan LJ, Strauch AR, Zweier JL. Endothelial nitric oxide synthase (NOS3) knockout decreases NOS2 induction, limiting hyperoxygenation and conferring protection in the postischemic heart. *Am J Physiol Heart Circ Physiol*. 2007;292:H1541–H1550.
40. Sharp BR, Jones SP, Rimmer DM, Lefer DJ. Differential response to myocardial reperfusion injury in eNOS-deficient mice. *Am J Physiol Heart Circ Physiol*. 2002;282:H2422–H2426.
41. Meng W, Ayata C, Waeber C, Huang PL, Moskowitz MA. Neuronal NOS-cGMP-dependent ACh-induced relaxation in pial arterioles of endothelial NOS knockout mice. *Am J Physiol*. 1998;274:H411–H415.
42. Meng W, Ma J, Ayata C, Hara H, Huang PL, Fishman MC, Moskowitz MA. ACh dilates pial arterioles in endothelial and neuronal NOS knockout mice by NO-dependent mechanisms. *Am J Physiol*. 1996;271:H1145–H1150.
43. Sanz MJ, Hickey MJ, Johnston B, McCafferty DM, Raharjo E, Huang PL, Kubes P. Neuronal nitric oxide synthase (NOS) regulates leukocyte-endothelial cell interactions in endothelial NOS deficient mice. *Br J Pharmacol*. 2001;134:305–312.
44. Takaki A, Morikawa K, Murayama Y, Yamagishi H, Hosoya M, Ohashi J, Shimokawa H. Roles of endothelial oxidases in endothelium-derived hyperpolarizing factor responses in mice. *J Cardiovasc Pharmacol*. 2008;52:510–517.
45. Buxton IL, Cheek DJ, Eckman D, Westfall DP, Sanders KM, Keef KD. NG-nitro L-arginine methyl ester and other alkyl esters of arginine are muscarinic receptor antagonists. *Circ Res*. 1993;72:387–395.
46. Peterson DA, Peterson DC, Archer S, Weir EK. The non specificity of specific nitric oxide synthase inhibitors. *Biochem Biophys Res Commun*. 1992;187:797–801.
47. Vanhoutte PM. COX-1 and vascular disease. *Clin Pharmacol Ther*. 2009;86:212–215.
48. Vanhoutte PM, Tang EH. Endothelium-dependent contractions: when a good guy turns bad! *J Physiol*. 2008;586:5295–5304.
49. Khraibi AA. Association between disturbances in the immune system and hypertension. *Am J Hypertens*. 1991;4:635–641.
50. Morton J, Coles B, Wright K, Gallimore A, Morrow JD, Terry ES, Anning PB, Morgan BP, Dioszeghy V, Kühn H, Chaitidis P, Hobbs AJ, Jones SA, O'Donnell VB. Circulating neutrophils maintain physiological blood pressure by suppressing bacteria and IFNgamma-dependent iNOS expression in the vasculature of healthy mice. *Blood*. 2008;111:5187–5194.
51. Jujo K, Ii M, Losordo DW. Endothelial progenitor cells in neovascularization of infarcted myocardium. *J Mol Cell Cardiol*. 2008;45:530–544.
52. Ii M, Nishimura H, Iwakura A, Wecker A, Eaton E, Asahara T, Losordo DW. Endothelial progenitor cells are rapidly recruited to myocardium and mediate protective effect of ischemic preconditioning via "imported" nitric oxide synthase activity. *Circulation*. 2005;111:1114–1120.
53. Dezfulian C, Raat N, Shiva S, Gladwin MT. Role of the anion nitrite in ischemia-reperfusion cytoprotection and therapeutics. *Cardiovasc Res*. 2007;75:327–338.
54. Frérart F, Lobysheva I, Gallez B, Dessy C, Feron O. Vascular caveolin deficiency supports the angiogenic effects of nitrite, a major end product of nitric oxide metabolism in tumors. *Mol Cancer Res*. 2009;7:1056–1063.

55. Raat NJ, Noguchi AC, Liu VB, Raghavachari N, Liu D, Xu X, Shiva S, Munson PJ, Gladwin MT. Dietary nitrate and nitrite modulate blood and organ nitrite and the cellular ischemic stress response. *Free Radic Biol Med*. 2009;47:510–517.
56. Gladwin MT, Kanias T, Kim-Shapiro DB. Hemolysis and cell-free hemoglobin drive an intrinsic mechanism for human disease. *J Clin Invest*. 2012;122:1205–1208.
57. Kim-Shapiro DB, Lee J, Gladwin MT. Storage lesion: role of red blood cell breakdown. *Transfusion*. 2011;51:844–851.
58. Donadee C, Raat NJ, Kanias T, et al. Nitric oxide scavenging by red blood cell microparticles and cell-free hemoglobin as a mechanism for the red cell storage lesion. *Circulation*. 2011;124:465–476.
59. Lee JS, Gladwin MT. Bad blood: the risks of red cell storage. *Nat Med*. 2010;16:381–382.
60. Minneci PC, Deans KJ, Zhi H, Yuen PS, Star RA, Banks SM, Schechter AN, Natanson C, Gladwin MT, Solomon SB. Hemolysis-associated endothelial dysfunction mediated by accelerated NO inactivation by decompartmentalized oxyhemoglobin. *J Clin Invest*. 2005;115:3409–3417.
61. Hod EA, Zhang N, Sokol SA, Wojczyk BS, Francis RO, Ansaldi D, Francis KP, Della-Latta P, Whittier S, Sheth S, Hendrickson JE, Zimring JC, Brittenham GM, Spitalnik SL. Transfusion of red blood cells after prolonged storage produces harmful effects that are mediated by iron and inflammation. *Blood*. 2010;115:4284–4292.
62. Baek JH, D'Agnillo F, Vallelian F, Pereira CP, Williams MC, Jia Y, Schaer DJ, Buehler PW. Hemoglobin-driven pathophysiology is an *in vivo* consequence of the red blood cell storage lesion that can be attenuated in guinea pigs by haptoglobin therapy. *J Clin Invest*. 2012;122:1444–1458.

Significance

These are the first studies, using cross-transplant chimera models, to definitively identify a mouse circulating blood endothelial nitric oxide synthase that regulates intravascular nitrite homeostasis, cGMP signaling, and the control of systemic blood pressure under physiological conditions. Our findings extend the current paradigm for endothelial generation of NO• and nitrite in the regulation of blood pressure, suggesting a contribution from circulating red blood cells to NO• and nitrite synthesis and vascular homeostasis. Hypertension is a complex multifactorial condition associated with cardiovascular disease. Accumulating evidence points to a correlation between blood pressure and circulating NO• metabolites, such as nitrite. The existence of a functional red blood cell endothelial nitric oxide synthase invites studies addressing the function and dysfunction of blood endothelial nitric oxide synthase in cardiovascular health and disease. Our findings may illuminate novel avenues for assaying the general status of endothelial nitric oxide synthase activity and cardiovascular health in the human circulation.

Materials and Methods

Materials

Phenylephrine (PE, P6126), acetylcholine (Ach, A6625), sodium nitroprusside (SNP, S0501), N (G)-nitro-L- arginine methyl ester (L-NAME, N5751) and L-Arginine (L-Arg, A8094) and NADPH (N0411) were purchased from Sigma. Purified rat anti-CD45 antibody (clone 30-F11) and Ter-119 (550565) were from BD Pharmingen (San Jose, CA). Anti-platelet serum (AIAD31440) was from Accurate Chemical (Westbury, NY). Bovine recombinant eNOS (60880) and the NOS activity assay (781001) were obtained from Cayman Chemical. Purified mouse anti-human eNOS antibody (610296) and rabbit anti-human eNOS was from BD Biosciences (San Joes, CA). Rabbit polyclonal anti-eNOS antibody (Ab66127) was from Abcam Inc. (Cambridge, MA). L-[^{14}C] arginine (NEC267E050UC) was from Perkin Elmer (Waltham, MA).

Blood collection and sample preparation

Blood was taken from the carotid artery and anticoagulated with citrate (for immunoprecipitation) or with heparin (for loading with fluorescent probes). All experiments were initiated within 2 hours of blood withdrawal. Whole blood was obtained via the carotid artery or inferior vena cava of donor mice (C57Bl/6J and Harvard eNOS$^{-/-}$).

The following manipulations were used to separate platelet rich plasma and hemoglobin from whole blood. In brief, blood was collected in a polypropylene tube containing 0.1 mL acid citrate dextrose buffer (Sigma) and then centrifuged at 120g, 4°C for 8 min and then at 14000 rpm, 4°C for 2 min. Between centrifugations, platelet rich plasma and buffy coat were removed by pipette and discarded. Leukocyte and platelet contamination were quantified with the aid of a hemocytometer and light microscope and did not exceed 0.05%. Leukocytes (25 uL blood sample) were stained by addition of 465 µL 3% citric acid and 10 µL 1% crystal violet (Sigma). Platelets (20 uL blood sample) were stained with the Unopette System (Becton Dickinson).

For protein identification, whole blood was collected in a syringe and centrifuged at 800 g for 15 min at room temperature (RT) to sediment RBCs prior to elution from the bottom of the syringe. Purity of the RBC preparations was confirmed using flow cytometry (FACS CANTO II; BD Bioscience, San Jose, CA, USA) and antibodies (as per manufacturer guidelines) specific for CD235 (glycophorin) as a RBC marker, CD45 as a leukocyte marker, and CD42 as a platelet marker.

Cells

Human umbilical vein endothelial cells (Promocell GmbH; Heidelberg, Germany) were cultured in 10 cm-diameter Petri plates (passages 1-4) using a commercial endothelial cell basal medium (Promocell GmbH, Heidelberg, Germany) supplemented with penicillin and streptomycin (*PAA* Laboratories GmbH, Cölbe, Germany). Cell pellets were obtained after detachment with trypsin.

Animals

Wild type C57BL/6 and B6.SJL-PTPRCPEP/BOY, B6.129P2-Nos3tm1Unc/J (UNC eNOS$^{-/-}$) and B6.129P2-NOS2 TM1 LAU/J (iNOS$^{-/-}$) were from Jackson Laboratories (Bar Harbor, ME).

Breeder stocks of Harvard eNOS$^{-/-}$ mice, backcrossed 10 generations to C57BL/6 mice, were from Dr. Paul L. Huang (Harvard University).[1] Homozygous matings produced offspring for this study. All animals were housed under pathogen-free conditions and only male mice were used for experiments. eNOS immunoprecipitation experiments in mouse red blood cells, as well as aortic cGMP studies were conducted using Düsseldorf eNOS$^{-/-}$ mice from Dr. Axel Gödecke (Heinrich Heine University of Düsseldorf).[2] Genetic identity of animals was routinely confirmed by PCR analysis of tail clip DNA using gene-specific probes. All surgical procedures were reviewed, approved and performed according to the criteria outlined in the NHLBI Animal Care and Use Committee and the LANUV Nordrhein-Westfalen guidelines. Mice were fed standard laboratory chow ad libitum until use in experiments.

Chimeras

Two congenic strains of WT mice on C57Bl/6 background (C57BL/6 and B6.SJL-PTPRCPEP/BOY) were used to mismatch BM donors and recipients for leukocyte antigen expression (CD45.2 versus CD45.1) to permit flow cytometric analysis of recipients' blood cell reconstitution to donor phenotype. BM cells were isolated from the femurs and tibias of donor mice and resuspended in sterile PBS to a 1-2 x10^7/mL final cell count. Recipients were lethally irradiated (two 500 rad doses, 3 hours apart). Following the second irradiation, 2-4 x10^6 donor BM cells in 200 µL of PBS were injected into the retroorbital sinus of each recipient. Chimeras were housed in autoclaved cages with 0.2% neomycin drinking water for 2 weeks, followed by normal drinking water. At 6-8 weeks post-transplant, chimeric mice were assessed by flow cytometry for conversion to donor phenotype prior to use in experiments.

Flow cytometry

Flow cytometry was used to verify reconstitution of BM transplanted chimeric mice. In brief, leukocytes (from 50 uL lysed whole blood) from chimeric mice were stained in vitro with FITC-labeled anti-CD45.1 (PharMingen, Inc.) and PerCP-Cy5.5 anti-CD45.2 antibodies (PharMingen, Inc.) and immediately analyzed by flow cytometry (BD FACSCaliber) to determine relative expression of CD45.1 versus CD45.2. Leukocytes were gated based on their size (forward light scatter) and granularity (side light scatter) in a double logarithmic scatter dot plot. The median fluorescence intensity (MFI) of 10,000 events within the leukocyte population was determined by analyzing the distribution histogram obtained by plotting green fluorescence intensity (FITC channel) against far-red fluorescence intensity (PerCP-Cy5.5 channel).

Immunoprecipitation, gel electrophoresis and western blot analysis

Mouse RBCs, mouse aorta and human endothelial cells were lysed with RIPA lysis buffer containing protease inhibitor cocktail (Roche Applied Science), as previously described.[3] Total protein concentration was determined by the Lowry assay (DC Protein Assay, Bio-Rad). For direct immunoprecipitation (IP), antibodies were purified from preservatives and contaminants by using Protein G coupled dynabeads (Invitrogen) and concentrated using an ultrafiltration column (Millipore) according to the manufacturer's' instructions. The antibodies were then cross-linked to Epoxy-Dynabeads (Invitrogen). RBC or aortic lysate in RIPA Buffer [4] was incubated overnight with crosslinked Dynabeads at 4°C, followed by washing and elution with loading buffer (Invitrogen). For gel electrophoresis, samples were loaded in Bis-Tris gel, 4-12%

(aorta from chimeras) or 3-8% or 7% NuPAGE Novex Tris/Acetate pre-cast gels (Invitrogen). For western blot analysis, proteins were transferred onto polyvinylidene fluoride (PVDF) membrane Hybond P (Amersham Biosciences, Munich, Germany), using a pre-stained protein ladder (PageRuler Plus, Fermentas Life Science) to control for the transfer. The membrane was blocked with 5% nonfat dry milk (Bio-Rad) in TBS (10 mM Tris, 100 mM NaCl), incubated with a mouse anti-human (overnight 4°C 1:500) or rabbit anti-eNOS antiserum (BD Bioscience) diluted (1 h RT 1:1000) in T-TBS (0.1% Tween in TBS), washed for 30 min in T-TBS, and then incubated with HRP-conjugated goat anti-mouse (1:5000 from Jackson Immuno Research Laboratories (chimeras) or BD Bioscience), or anti-rabbit antibody (1:5000 Rockland, PA, USA). The bands were visualized by autoradiography on Hyperfilm ECL (Amersham Biosciences) using SuperSignal West Pico or Femto Chemiluminescent Substrates (Pierce, Thermo Fisher Scientific,Waltham, MA, USA).

Real-Time reverse transcription polymerase chain reaction (RT-PCR)

Quantitative real-time RT-PCR was used to analyze gene expression of eNOS (NOS3), COX-1 and COX-2 in aortic tissue from C57Bl6/J, eNOS$^{-/-}$, and BM transplanted chimeric mice (groups: BC+/EC+, BC-/EC+, BC+/EC- and BC-/EC-). First-strand cDNA was synthesized on RNA (previously isolated from aortas) using random primers (Applied Biosystems; Norwalk, CT) in a reverse transcriptase reaction mixture (Superscript cDNA synthesis kit; Invitrogen, Carlsbad, CA). Quantitative real-time PCR assays were carried out with the use of gene-specific double fluorescently labeled probes (Applied Biosystems) in a 7900 Sequence Detector (PE Applied Biosystems) according to the manufacturer's instructions. In brief, PCR amplification was performed in a 384 well plate with a reaction mixture containing primer, probe, dNTP in real time PCR buffer and passive reference (ROX) fluorochrome, and the appropriate thermal cycling conditions. Samples were analyzed in triplicate and normalized to the housekeeping gene ß actin.

Immune-fluorescence staining

Freshly obtained whole blood was smeared across glass slides and allowed to air-dry for 20 min. Paraformaldehyde (4% in PBS) was then applied to the slides for 25 min. After washing, blocking and permeabilization were achieved by applying 5% Donkey serum in PBS with 0.05% Tween 20 for 1 hour. The blocking solution was then discarded and immune-fluorescence staining performed using primary antibodies against eNOS (#ab66127, Abcam) and Ter-119 (#550565, BD Pharmingen), both applied at 1:100 dilution for 1 hour. Control slides were routinely stained in parallel by substituting IgG, or the specific IgG isotype, from the same species for the primary antibody at the same final concentration. After brief washing, secondary antibodies (Rhodamine Red-X conjugated Donkey anti-Rat #712-296-153 and FITC conjugated Donkey anti-Rabbit #711-095-152; Jackson ImmunoResearch Laboratories) were applied for 1 hour, both at 1:200 dilution. After final washing, mounting media containing 4',6-diamidino-2-phenylindole (DAPI) (#H-1200, Vector Laboratories) and a cover slip were applied. Images were acquired using a Zeiss LSM 510 UV laser scanning confocal microscope system (Carl Zeiss GmbH). For WT, eNOS$^{-/-}$ and IgG controls, immune-fluorescence staining was performed at least eight times per group and using blood from ≥ 5 different mice.

Wire myography

Mice were anesthetized with ketamine chloride and xylazine (120 mg/kg and 6 mg/kg body weight i.p., respectively). After placing the mouse in the supine position, the right carotid artery was cannulated for systemic blood pressure measurement (PowerLab). The thoracic and abdominal cavities were opened through a midline incision. After achieving hemostasis, the thoracoabdominal aorta was carefully dissected, removed and placed in ice-cold physiologic salt saline (Krebs buffer). The composition of Krebs buffer was (mM): NaCl (119), KCl (4.5), $NaHCO_3$ (25), KH_2PO_4 (1.2), $MgSO_4$ (1.2), L-glucose (11) and $CaCl_2$ (2.5). Using a dissecting microscope, the attached fat and adventitia were meticulously removed by sharp dissection and clotted blood was flushed from the vessel lumen. Each aortic ring was used to generate a dose-response curve to test for: 1) contraction to phenylephrine (PE: 10^{-9} M to 10^{-4} M), 2) dilation to sodium nitroprusside (SNP: 10^{-9} M to $10^{-4.5}$ M), and 3) dilation to acetylcholine (Ach: 10^{-9} M to $10^{-3.5}$ M). For the determination of SNP and Ach dose-response relationships, aortic rings (3 mm length) were pre-contracted with 10^{-6} M PE. Endothelium-independent contraction was calculated as % contraction relative to maximal vessel tension (at the third 120 mMol KCl rinse). Endothelium-independent (SNP) and -dependent dilation (Ach) were calculated as % dilation relative to the pre-contraction tension (10^{-6} M PE). All experimental protocols were applied to C57Bl/6 mice and BM transplanted chimeras BC+/EC+ and BC-/EC+. Five mice (2 aortic rings per mouse) were included in each group.

Blood pressure measurements

Baseline blood pressures (mean arterial, systolic and diastolic) were measured under anesthesia (120 mg/kg ketamine and 6 mg/kg xylazine) via a heparinized catheter (in-line with a blood pressure transducer and using Powerlab software) surgically implanted in the right carotid artery of each mouse. Blood pressure was determined after a 20 min post-surgery stabilization period. Core body temperature was maintained at 35 ± 0.5°C.

The contribution of platelets and leukocytes to blood pressure was assessed in BC+/EC- and BC-/EC- chimeras treated with either anti-platelet serum (APS) or a purified rat anti-CD45 antibody (anti-CD45 Ab) to induce thrombocytopenia or leukopenia, respectively. Treatment with APS (62.5 µl/kg in 200 µl sterile PBS i.p. for 2 days) depleted circulating platelets by ≥ 90% and treatment with anti-CD45 antibody (dose: 1 mg/kg/day in sterile PBS i.p. for 2 days) depleted circulating leukocytes by ≥ 75%. Thrombocytopenia and leukopenia were confirmed by manual platelet and leukocyte counts, respectively. Neither treatment significantly altered hematocrits. Blood pressure measurements were made on the 2^{nd} or 5^{th} day following initiation of treatment with APS or anti-CD45 antibody, respectively.

Hemodynamic responses

BC+/EC- chimeras (made with Harvard $eNOS^{-/-}$ or UNC $eNOS^{-/-}$ mice) were surgically implanted (under temporary anesthesia: ketamine/xylazine or isoflurane) with a microminiaturized electronic monitor (PA-C10; Data Sciences International; St. Paul, MN, USA) attached to an indwelling aortic catheter. Digitized hemodynamic data were continuously sensed, processed and transmitted via radio frequency signals to a nearby receiver (acquisition period: 10 min every 2 hours). Mice were allowed a 10-day post-surgery stabilization period on

standard diet and drinking water before hemodynamic responses to NOS inhibition (L-NAME, 1g/L in drinking water for 4 days) or stimulation (L-Arginine, 2% in drinking water for 3 days) were assessed. Blood pressures were determined by averaging night-time data (22:00 to 4:00) on day 10 (baseline), day 14 (L-NAME) and day 17 (L-Arginine). Change in MAP is reported as mmHg ([L-NAME - baseline BP] and [L-Arg BP - L-NAME BP]).

cGMP levels in mouse aorta

The levels of cGMP in mouse aorta were assayed by using a DetectX High Sensitivity Direct cyclic GMP Immunoassay kit (Arbor Assay, Ann Arbor, MI, USA), following the manufacturer's instructions. The cGMP concentrations were normalized for protein content using the Lowry assay (DC Protein Assay, Bio-Rad).

Reductive chemiluminescence

Reductive chemiluminescence measurements were performed as previously described with minor modifications.[5, 6] Briefly, whole blood and plasma nitrite were measured in blood samples collected via carotid cannulation of anesthetized (120 mg/kg ketamine hydrochloride and 6 mg/kg xylazine) mice into sterile, nitrite-free, heparinized (0.5-1 IU) syringes. Whole blood nitrite was preserved by diluting it 1:4 in preservation solution (800 mM $K_3Fe(CN)_6$, , 10%, v/v Nonidet-40 substitute, and 100 mM *N*-ethylmaleimide. Plasma was obtained by centrifugation at 4°C and 14000 rpm for 2 min. Nitrite concentrations were determined by the tri-iodide assay[7] in a chemiluminescence NO• analyzer (Sievers NOA; Boulder, CO) using nitrite as a standard.[7]

NOS activity

RBC membrane extracts were prepared from platelet- and leukocyte-poor blood by 3 to 4 washing steps in 1 mL homogenization buffer (Cayman Chemical) and centrifugations at 14000 rpm, 4°C for 20 min to produce relatively hemoglobin-free RBC membrane preparations. NOS activity of 10 µl RBC membrane preparations was assayed by measuring the conversion of L-[^{14}C] arginine into L-[^{14}C] citrulline using a commercial kit (Cayman Chemicals), following the manufacturer's protocol with minor modifications. Reaction buffer (45 µL) contained 5 µL L-[^{14}C] arginine (concentration: 0.1mCi/mL, specific activity: >300mCi (11.1GBq/mmol), Perkin Elmer), 1 mM NADPH, 100 nM calmodulin, 2 mM $CaCl_2$ (final volume 65 µL). All samples were prepared in duplicate: 1) incubation at 37°C for 24 hours and 2) incubation at -20°C for 24 hours. After addition of 400 µL of stop buffer followed by freeze fracture at -20C for 20 min, L-[^{14}C] citrulline was eluted in 100 uL ion exchange resin and centrifuged at 2000 rpm, RT for 4 min. Proteins were precipitated using ice-cold methanol (600 µL) for 20 min at 20°C, and centrifugation for 2 min at 14000 rpm, to avoid color quenching. The increase in production of L-[^{14}C] Citrulline equivalents was calculated as follows:

$[WT_{37\cdot C}$ cpm – $WT_{-20\cdot C}$ cpm] / $[eNOS^{-/-}{}_{37\cdot C}$ cpm – $eNOS^{-/-}{}_{-20\cdot C}$ cpm].

The eNOS activity (fmol/min) was calculated as the conversion of the added radioactive L-[^{14}C] Arginine (cpm/fmol) into L-[^{14}C] Citrulline (cpm) during the considered reaction time.

Statistical analysis

All values are reported as mean ± SEM. Comparisons between groups were made using either Student's *t*-test or ANOVA followed by Bonferroni posthoc test for more than two group comparisons. Differences were deemed significant when $p < 0.05$. Statistical analyzes were performed using GraphPad Prism.

References

1. Huang PL, Huang Z, Mashimo H, Bloch KD, Moskowitz MA, Bevan JA, Fishman MC. Hypertension in mice lacking the gene for endothelial nitric oxide synthase. Nature. 1995:377:239-242
2. Godecke A, Decking UK, Ding Z, Hirchenhain J, Bidmon HJ, Godecke S, Schrader J. Coronary hemodynamics in endothelial no synthase knockout mice. Circ Res. 1998:82:186-194
3. Cortese-Krott MM, Suschek CV, Wetzel W, Kroncke KD, Kolb-Bachofen V. Nitric oxide-mediated protection of endothelial cells from hydrogen peroxide is mediated by intracellular zinc and glutathione. Am J Physiol Cell Physiol. 2009:296:C811-820
4. Cortese MM, Suschek CV, Wetzel W, Kroncke KD, Kolb-Bachofen V. Zinc protects endothelial cells from hydrogen peroxide via nrf2-dependent stimulation of glutathione biosynthesis. Free Radic Biol Med. 2008:44:2002-2012
5. Pelletier MM, Kleinbongard P, Ringwood L, Hito R, Hunter CJ, Schechter AN, Gladwin MT, Dejam A. The measurement of blood and plasma nitrite by chemiluminescence: Pitfalls and solutions. Free Radic Biol Med. 2006:41:541-548
6. Dejam A, Hunter CJ, Pelletier MM, Hsu LL, Machado RF, Shiva S, Power GG, Kelm M, Gladwin MT, Schechter AN. Erythrocytes are the major intravascular storage sites of nitrite in human blood. Blood. 2005:106:734-739
7. MacArthur PH, Shiva S, Gladwin MT. Measurement of circulating nitrite and s-nitrosothiols by reductive chemiluminescence. J Chromatogr B Analyt Technol Biomed Life Sci. 2007:851:93-105

Supplemental Tables

Table SI. Hematocrit (Hct), platelet, white blood cell (WBCs) and polymorphonuclear leukocyte (PMNs) counts in untreated C57Bl/6J (WT), eNOS deficient (KO) and cross-transplanted chimeras.

Group	Hct (%)	Platelets (10^3)	WBCs (10^3)	PMNs (10^3)
Untreated				
WT	39.9 ± 0.8 n=9	1285 ± 91.9 n=8	38.0 ± 4.2 n=9	9.8 ± 0.9 n=9
KO	40.1 ± 0.8 n=7	1541 ± 88.0 n=7	39.9 ± 4.3 n=7	10.4 ± 1.0 n=7
BC+/EC+	43.9 ± 0.9 n=14	1665 ± 116.5 n=7	63.6 ± 7.2 n=10	16.1 ± 3.0 n=7
BC-/EC+	40.2 ± 2.1 n=5	1181 ± 413.0 n=2	85.5 ± 3.0 n=3	25.1 ± 1.3* n=3
BC+/EC-	41.7 ± 1.2 n=12	1511 ± 69.0 n=13	49.4 ± 12.0 n=10	17.2 ± 3.3 n=10
BC-/EC-	42.6 ± 0.8 n=11	1510 ± 102.1 n=9	56.0 ± 7.7 n=5	14.3 ± 1.9 n=5

Using One-way ANOVA and Bonferroni post-hoc test: * denotes P < .05 vs WT.

Table SII. Platelet, white blood cell (WBCs) and polymorphonuclear leukocyte (PMNs) counts in BC+/EC- and BC-/EC- chimeras before and after platelet- (APS) or leukocyte-depleting (anti-CD45 Ab) treatment.

* denotes P < 0.05 and ** denotes P<0.0001 using one-way ANOVA and Bonferroni post-hoc test.

Group	Platelets (10^3)		WBCs (10^3)		PMNs (10^3)	
	Pre	Post	Pre	Post	Pre	Post
APS						
BC+/EC- (n=5)	1557± 62.8	128.0 ± 17.8**		20.2 ± 5.4		9.8 ± 1.0
BC-/EC- (n=8)	1571± 92.4	120.0 ± 18.1**		21.2 ± 5.9		7.5 ± 0.6
Anti-CD45 Ab						
BC+/EC- (n=3)			61.7± 1.2	20.9 ± 8.1**	21.5± 3.4	10.5 ± 7.1*
BC-/EC- (n=4)			62.0± 6.3	10.9 ± 2.2**	16.1± 0.8	3.6 ± 0.4 *

Using One-way ANOVA and Bonferroni post-hoc test: * denotes P<.05 and ** denotes P < .0001 vs pre-treatment.

Table SIII. Baseline systolic and diastolic blood pressures of cross-transplanted eNOS$^{-/-}$ chimeras during hours of daylight and darkness.

	Systolic BP		**Diastolic BP**	
Group	Day	Night	Day	Night
	AUC (mmHg)		**AUC (mmHg)**	
BC+/EC+ (n=4)	1111	1263	825.3	974.4
BC-/EC+ (n=3)	1263	1317	1083	1130
BC+/EC- (n=3)	1230	1415	962.1	1121
BC-/EC- (n=4)	1325	1553	1051	1219
	p-value		**p-value**	
BC-/EC+ vs **BC+/EC+**	0.0053*	0.2729	0.0006**	0.0160*
BC+/EC- vs **BC-/EC-**	0.0494*	0.1488	0.0385*	0.1351
BC+/EC- vs **BC-/EC+**	0.6026	0.0010*	0.0445*	0.7572

Day: 0600 to 1800 hours, Night: 1800 to 0600 hours. Group averages calculated for each 2 hour interval and area under the curve (AUC) by Two-way ANOVA with Bonferroni post-hoc test. * denotes $p<0.05$ and ** denotes $p<0.005$.

Supplemental Figure I

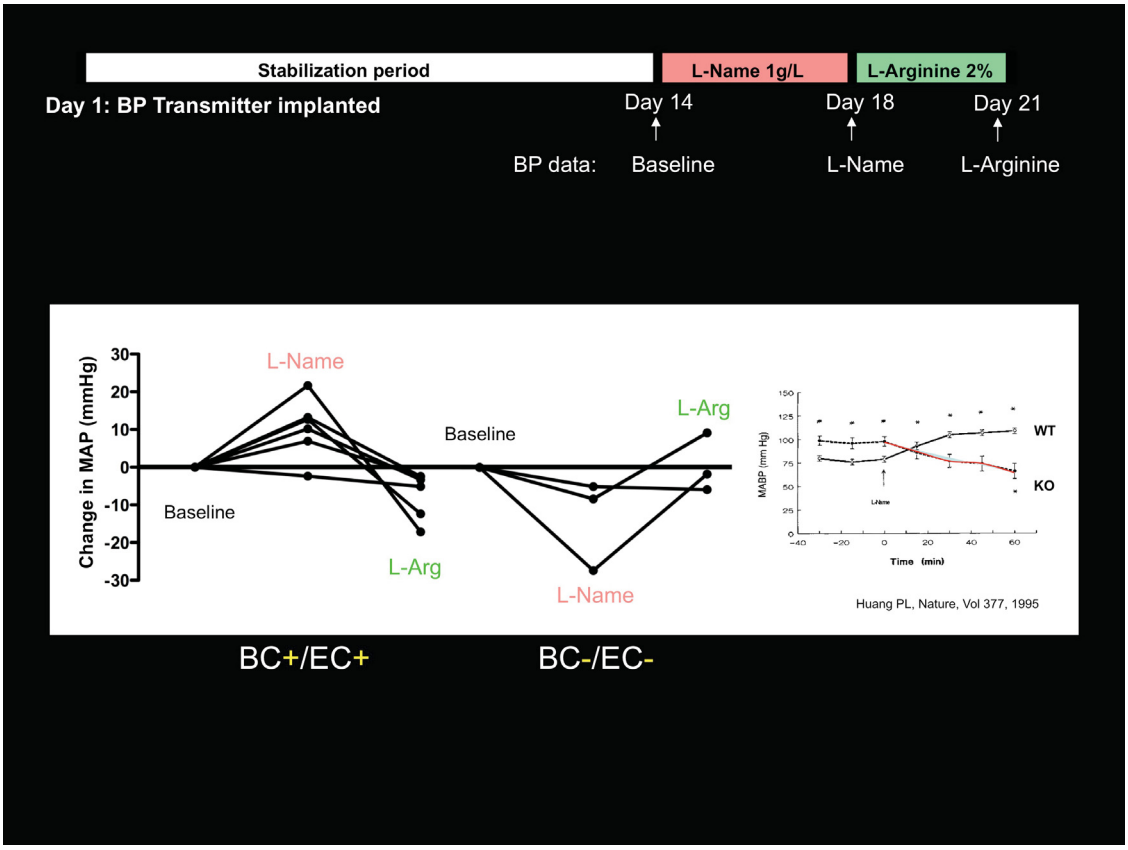

Figure SI. Paradoxical response to L-NAME of BC-/EC- mice, similar to Harvard eNOS$^{-/-}$ mice. Harvard BC+/EC+ chimeras (n = 5) and BC-/EC- chimeras (n = 3) after oral treatment with L-NAME or L-Arg. Blood pressure data for individual animals shown as solid lines. Comparison of MAP responses to L-NAME treatment by WT and Harvard eNOS KO mice, as reported by Huang et al. (inset graph).[13]

Circulating Microparticles Carry a Functional Endothelial Nitric Oxide Synthase That Is Decreased in Patients With Endothelial Dysfunction

Patrick Horn, Miriam Margherita Cortese-Krott, Nicolas Amabile, Claas Hundsdörfer, Klaus-Dietrich Kröncke, Malte Kelm and Christian Heiss

J Am Heart Assoc. 2013;2:e003764; originally published December 31, 2012;
doi: 10.1161/JAHA.112.003764
The *Journal of the American Heart Association* is published by the American Heart Association, 7272 Greenville Avenue, Dallas, TX 75231
Online ISSN: 2047-9980

ORIGINAL RESEARCH

Circulating Microparticles Carry a Functional Endothelial Nitric Oxide Synthase That Is Decreased in Patients With Endothelial Dysfunction

Patrick Horn, MD; Miriam Margherita Cortese-Krott, PhD; Nicolas Amabile, MD, PhD; Claas Hundsdörfer, PhD; Klaus-Dietrich Kröncke, PhD; Malte Kelm, MD; Christian Heiss, MD

***Background*—**Microparticles (MPs) are circulating membrane particles of less than a micrometer in diameter shed from endothelial and blood cells. Recent literature suggests that MPs are not just functionally inert cell debris but may possess biological functions and mediate the communication between vascular cells. As a significant proportion of MPs originate from platelets and endothelial cells, we hypothesized that MPs may harbor functional enzymes including an endothelial NO synthase (eNOS).

***Methods and Results*—**Using immunoprecipitation and Western blot analysis, we found that human circulating MPs carry an eNOS. Ca^{2+} and L-arginine-dependent NOS activity of crude enzyme extract from MPs was determined by measuring the conversion of [^{3}H]-L-arginine to [^{3}H]-citrulline and NOS-dependent nitrite production. NOS-dependent NO production in intact MPs was assessed by the NO-specific fluorescent probe MNIP-Cu. In patients with cardiovascular disease, endothelial dysfunction was associated with an increase in the total number of circulating MPs as well as a significant decrease in the expression and activity of eNOS in MPs. No difference in reactive oxygen species was noted in MPs isolated from either group.

***Conclusions*—**Our data further support the concept that circulating MPs may not only retain phenotypic markers but also preserve the functionality of enzymes of the cells they originate from, including eNOS. **(*J Am Heart Assoc.* 2012;1:e003764 doi: 10.1161/JAHA.112.003764)**

Key Words: endothelial dysfunction • endothelial function • endothelial nitric oxide synthase • microparticles

Microparticles (MPs) are shed membrane particles of less than a micrometer in diameter thought to be budded into the circulation from endothelial cells and various blood cells, including platelets, leukocytes, and erythrocytes.[1–3] Thus, circulating MPs constitute a heterogeneous population of different cellular origins, numbers, size, and antigenic composition. Proposed mechanisms of MP generation include apoptosis and cellular activation by cytokines.[1–3] MPs circulate in blood from healthy individuals, and their numbers are increased in several cardiovascular diseases and conditions that predispose to cardiovascular disease.[1–3] MPs have long been considered functionally inert cell debris, and the number of circulating MPs in blood was proposed to be a marker of endothelial damage and platelet activation.[1,3] More recently, it was appreciated that MPs harbor a number of membrane and cytoplasmatic proteins from the cells they originate from[4–6] and, therefore, may play a role as a disseminated storage pool of bioactive effectors in intercellular communication mediating effects in cardiovascular physiology and pathophysiology.[1–3,7,8]

The enzyme endothelial nitric oxide synthase (eNOS) and its product nitric oxide (NO) play a central role in the control of vascular homeostasis.[9,10] A significant proportion of circulating MPs originate from platelets and endothelial cells, which both express eNOS. We hypothesized that MPs may harbor a functional eNOS. Therefore, we analyzed eNOS expression and activity in MPs isolated from healthy individuals, as well as from patients with cardiovascular disease, a condition characterized by impaired eNOS activity and/or expression.

From the Division of Cardiology, Pulmonology, and Vascular Medicine (P.H., M.M.C.-K., M.K., C. Heiss), Institute for Biochemistry and Molecular Biology (K.-D.K.), and Institute for Organic and Macromolecular Chemistry (C. Hundsdörfer), University Duesseldorf, Duesseldorf, Germany; INSERM U970, Paris Cardiovascular Research Center, France (N.A.).

Dr Horn and Dr Cortese-Krott contributed equally to this study.

Correspondence to: PD Dr. med. Christian Heiss, MD, Division of Cardiology, Pulmonology, and Vascular Medicine, Medical Faculty, University Duesseldorf, Moorenstr. 5, 40225 Duesseldorf, Germany. E-mail: christian.heiss@med.uni-duesseldorf.de

Received September 5, 2012; accepted October 29, 2012.

Methods

Human Volunteers

Blood was taken from the cubital veins of healthy human volunteers and cardiovascular disease (CVD) patients with documented endothelial dysfunction (Table 1). All subjects gave written informed consent. Procedures were conducted in conformity with the principle embodied in the Declaration of Helsinki and approved by the ethics committee of the Heinrich Heine University. Inclusion was based on a diagnosis of coronary artery disease (CAD), defined as >70% stenosis of ≥1 coronary artery. Exclusion criteria consisted of the presence of heart rhythms other than sinus rhythm, clinical diagnosis of heart failure (NYHA III or IV), recent or current inflammatory condition, renal insufficiency (GFR <60 mL/min), active malignancies within the last year, pre- or perimenopausal state, documented noncompliance with medication, and active smoking (>1 cigarette/day).

Materials

Fluoresceine isothiocyanate (FITC)–conjugated monoclonal mouse anti-human CD235 (glycoforin) antibody was purchased from Miltenyi Biotech (Bergisch Gladbach, Germany), PE-conjugated mouse anti-human CD62E came from Beckton Dickinson Pharmingen (Heidelberg, Germany). FITC-conjugated monoclonal mouse anti-human CD45 antibody, PC5-conjugated mouse anti-human CD41, and PE-conjugated mouse anti-human CD144 antibodies and Flow-Count fluorospheres were from Beckman Coulter (Krefeld, Germany). Materials for immunoprecipitation, gel electrophoresis, and Western blots were purchased from Invitrogen (Darmstadt, Germany). Purified monoclonal mouse anti-human eNOS and purified rabbit anti-eNOS antiserum were from BD Bioscience (Erembodegem, Belgium). We also used a mouse monoclonal anti-eNOS (clone NOS-E1) from Sigma (Deisenhofen, Germany) and phenazine methosulfate (PMS) from Biomol (Enzo Lifescience). L-N^5-(1–iminoethyl)-ornithine (L-NIO) and N^G-nitro-L-arginine-methyl ester monohydrochloride (L-NAME) were from Alexis Biochemicals (Loerrach, Germany). Size-standard microbeads (1 μm) were purchased from Polyscience, Inc. (Eppelheim, Germany). DiD Vybrant Cell, MitoSOX red, and 2′,7′-dichlorodihydrodiclorofluorescein diacetate (DCF) were purchased from Invitrogen (Karlsruhe, Germany), and chloro [[2,2'-[1,2-ethanediylbis[(nitrilo-κN)methylidyne]]bis[6-methoxyphenolato-κO]]]-manganese (EUK-134) was purchased from Europe BV (Leiden, Netherlands). 4-Methoxy-2-(1H-naphtho [2,3-d]imidazol-2-yl)phenol (MNIP-Cu) was synthesized as described.[11] Unless specified otherwise, chemicals were purchased from Sigma Aldrich (Sigma, Germany).

Blood Collection and Preparation of Platelet-Rich Plasma and Platelet-Free Plasma

Citrated blood (6 mL) was drawn from the cubital vein and processed within 2 hours. Platelet-rich plasma (PRP) was

Table 1. Characteristics of Study Subjects

	Healthy Volunteers, Mean±SEM	Patients With CVD, Mean±SEM	*P* Value
Age (y)	27±4	65±5	<0.01
n (Male/female)	12 (8/4)	9 (5/4)	
Body mass index (kg/m^2)	23.1±0.3	27.3±0.6	<0.01
Protein (g/dL)	7.2±1.5	6.8±1.2	0.651
Glucose (mg/dL)	86±13	144±18	<0.01
Cholesterol (mg/dL)	175±14	211±18	0.0.35
Triglycerides (mg/dL)	108±22	162±24	0.012
High-density lipoprotein (mg/dL)	62±5	52±8	0.082
Low-density lipoprotein (mg/dL)	109±19	155±12	0.04
White blood cells (per μL)	6512±882	4264±742	0.052
Polymorph nucleated cells (per μL)	3376±534	3287±502	0.802
Hemoglobin (g/dL)	14±1	12±1	0.079
Lymphocytes (per μL)	1343±134	1593±639	0.532
Monocytes (per μL)	498±54	801±436	0.12
Platelets (×1000/μL)	257±14	302±41	0.310
Mean arterial pressure (mm Hg)	65±5	80±5	0.012
Heart rate (per minute)	62±6	70±8	0.230

CVD indicates cardiovascular disease.

obtained by centrifugation of whole blood at 300*g* over 15 minutes at room temperature (RT). Platelet-free plasma (PFP) was obtained by 2 successive centrifugations of PRP at 10 000*g* for 5 minutes at RT. MP pellets and MP-free plasma samples were obtained by ultracentrifugation of the PFP at 30 000*g* for 90 minutes at 4°C. The protein concentration in the plasma of all blood donors did not differ significantly (Table 1).

Control of PFP Purification by Laser-Scanning Microscopy

PRP and PFP were incubated for 30 minutes with DiD, which is a lipophilic carbocyanine dye binding to the phospholipid bilayer of membranes. PFP and PRP were pelleted (30 000*g*, 90 minutes, 4°C), and smears were analyzed 1 to 2 minutes after preparation under a Zeiss LSM 510 confocal laser-scanning microscope (Carl Zeiss Jena GmbH, Jena, Germany) using a Zeiss Plan Neofluar 63×/1.3 oil DIC objective. DiD was excited with a XeNe laser using a 633-nm an beam splitter, and fluorescence was recorded with a 670-nm long-pass filter. Micrographs were taken at 37°C using an LSM software package (Carl Zeiss Jena GmbH). For each experiment, unstained samples served as the autofluorescence control.

Characterization of MP Subpopulations by Flow Cytometry

MP subpopulations were discriminated by flow cytometry according to the expression of established surface antigens as described previously.[12] Briefly, samples were incubated for 30 minutes with fluorochrome-labeled antibodies or matching isotype controls and analyzed in a Canto II flow cytometer (Beckton Dickinson, Heidelberg, Germany). Microbead standards (1.0 μm) were used to define MPs as <1 μm in diameter. The MP subpopulations were defined as follow: $CD41^+$ MPs as platelet-derived MPs; $CD62E^+$, $CD144^+$, or $CD31^+/CD41^-$ events as endothelial-derived MPs; $CD235^+$ as erythrocyte-derived MPs; and $CD45^+$ as leukocyte-derived MPs. The total number of MPs was quantified with flow-count calibrator beads (20 μL).

Immunoprecipiatation and Western Blot Analysis

An MP pellet from each individual was lysed by sonication at 4°C and resuspended in 0.2 mL lysis buffer with protease inhibitors (25 mmol/L Tris-HCl, 150 mmol/L NaCl, 1 mmol/L phenylmethanesulfonyl fluoride, 1 mg/mL aprotinin, 10 mg/mL leupeptin, 1 mmol/L EDTA, 50 mmol/L NaF, 1 mmol/L sodium orthovanadate, 1% Triton-X [pH 7.6]). Protein concentration was measured using a Biorad DC protein assay kit (Biorad, Munich, Germany). For immunoprecipitation MP lysate (30 μg/μL protein) was incubated for 1 hour at RT with 40 μg of a mouse anti-human eNOS antibody (BD Bioscience). Immune complexes were isolated by magnetic separation using 50 μL of washed magnetic protein G Dynabeads prepared as recommended by the manufacturer (Invitrogen). Western blot was performed as previously described.[13] Briefly, 30 μg of MP lysate or the immunocomplexes eluted from the magnetic beads were loaded on 10% NuPAGE Novex Tris/Acetate precast gels (Invitrogen). To control for contamination of plasma proteins in MP preparations, 30 μg of MP-free plasma (see above) was also loaded into the gels. As reference and normalization of band intensity, we loaded equal amounts (30 μg) of the same human umbilical endothelial cells (HUVECs) lysate in all gels. HUVECs were cultured as described previously.[14] Proteins were transferred onto PVDF membrane Hybond P (Amersham Biosciences, Munich, Germany). The membrane was stained with a rabbit anti-eNOS antiserum (1:1000; BD Bioscience) or mouse monoclonal anti-human eNOS antibody (Sigma Aldrich, Munich, Germany) and with a secondary HRP-conjugated goat anti-rabbit or anti-mouse antibody, respectively (1:5000; Rockland, PA). Equal loading was further controlled by staining duplicate gels by Coomassie Brilliant Blue.

Conversion of [^{3}H]-L-Arginine Into [^{3}H]-Citrulline

eNOS activity was determined in 100 μg of MP lysate by measuring the rate of conversion (pmol/min) of [^{3}H]-L-arginine to [^{3}H]-citrulline as previously described.[15] The reaction was conducted in a buffer at pH 7.4 containing flavin adenine dinucleotide (2 μmol/L), flavin mononucleotide (2 μmol/L), nicotinamide adenine dinucleotide phosphate (1 mmol/L), tetrahydrobiopterin dihydrochloride (6 μmol/L), Ca^{2+} (75 mmol/L), and calmodulin (0.04 μg/μL), for 2 hours at 37°C and stopped by the addition of cold EDTA (5 mmol/L) in HEPES (50 mmol/L) at pH 5.5. After separation of unreacted [^{3}H]-L-arginine from [^{3}H]-L-citrulline with Dowex ion exchange resin, the radioactive signal was detected in a liquid scintillation counter (Wallac 1409, Perkin Elmer, Rodgau, Germany). The amount of sample applied (100 μg MP lysate) was optimized in preliminary experiments by analyzing the rate of [^{3}H]-L-citrulline formation by a range of 25 to 250 μg of MP lysates. NOS activity was measured in the presence or absence of the specific NOS inhibitor L-NAME (1 mmol/L) or in the presence of Ca^{2+} chelators EDTA (1 mmol/L) and EGTA (1 mmol/L). The kinetic of the reaction was assessed by measuring [^{3}H]-citrulline equivalents produced at different times (15 to 120 minutes) as indicated compared with the reaction inhibited with L-NAME. In all experiments, recombinant bovine eNOS was used as a positive control. eNOS activity is reported as picomoles of [^{3}H]-citrulline formed per minute per milligram of total protein.

NOS-Derived Nitrite Production

MP lysate was diluted in a 250-μL reaction buffer containing Tris-HCL (50 mmol/L), NADPH (1 mmol/L), THB (6 μmol/L), calmodulin (100 nmol/L), and $CaCl_2$ (2.5 mmol/L) and incubated for 2 hours at 37°C in the presence or absence of the NOS substrate L-arginine (3 mmol/L), D-arginine (3 mmol/L), or the specific NOS inhibitor L-NIO (3 mmol/L). In all experiments, recombinant bovine eNOS was used as a positive control. The concentration of nitrite as the product of NO oxidation was measured by chemiluminescence.[16]

Analysis of NO Levels by Laser-Scanning Microscopy and Flow Cytometry

Intracellular NO levels were detected by staining MPs with MNIP, which was coordinated with Cu(II) to form a stable coordination compound, MNIP-Cu.[17] MNIP-Cu is a cell-permeable fluorescent probe that reacts rapidly and specifically with NO to generate a blue fluorescence. MNIP was synthesized as previously described.[11] Stock solutions of MNIP-Cu were prepared by mixing 1 volume of MNIP (1 mmol/L in dimethyl sulfoxide) and 2 volumes of $CuSO_4$ (2.5 mmol/L) and incubated for 30 minutes in the dark.

First, intracellular NO levels were assessed by laser-scanning microscopy. Platelet-poor plasma (PPP) was obtained as described for PFP but omitting the second centrifugation step. This led to platelet contamination that we used as a positive control in these experiments. To verify whether NO levels within the circulating MPs contain eNOS activity, PPP was pelleted by centrifugation preincubated with PBS as a control or with the NOS inhibitor L-NAME for 30 minutes at 37°C and then loaded with MNIP-Cu (10 μmol/L) for 15 minutes at RT in the dark. PPP smears were analyzed 1 to 2 minutes after preparation under a confocal laser-scanning microscope. Samples were excited with a UV laser enterprise, and emission was analyzed using a UV/488/543/633-nm beam splitter and a 350-nm long-pass filter. The platelets in the PPP served as a positive control, and MNIP-Cu-unloaded samples served as an autofluorescence control.

Second, intracellular NO levels were measured in intact MPs by flow cytometry. PFP was preincubated with PBS as a control or with the NOS inhibitor L-NAME for 30 minutes at 37°C and then loaded with MNIP-Cu (10 μmol/L) for 15 minutes at RT in the dark. Samples were analyzed immediately in a Canto II flow cytometer (Beckman Coulter). MNIP-Cu-unloaded samples served as an autofluorescence control.

Detection of Reactive Oxygen Species in MPs by Flow Cytometry

Intraparticular levels of reactive oxygen species (ROS) were measured by the staining of MPs with MitoSox and DCF diacetate. As a control, MPs were treated for 30 minutes at 37°C with 1 mmol/L H_2O_2 or with O_2^- generated by mixing 1 mmol/L PMS and 100 μmol/L NADPH. To scavenge ROS, MPs were treated with 80 μmol/L EUK 134, a membrane-permeable superoxide dismutase/catalase mimetic, where indicated.[18] MP preparations were loaded for 30 minutes at 37°C with 1 μmol/L DCF or with 1 μmol/L MitoSOX. Probes were then diluted 1:3 in cold PBS and measured in a flow cytometer excited with a 488-nm argon laser, and fluorescence signals were collected within the PE channel (em 585±42 nm) or the FITC channel (em 530±30 nm), respectively.

Flow-Mediated Dilation

Endothelial function was assessed by measuring flow-mediated dilation of the brachial artery by ultrasound (Sonosite Micromax, Bothell, WA) in combination with an automated analysis system (Brachial Analyzer, Medical Imaging Applications, Iowa City, IO) in a 21°C temperature-controlled room as described previously.[12]

Statistical Analyses

Results are expressed as mean±standard error of the mean (SEM). Student *t* tests and repeated-measures analysis of variance (ANOVA) with the Bonferroni post hoc test were used to evaluate the significance of differences in the mean values between different samples when comparing 2 or >2 samples, respectively. Patient characteristics were analyzed using nonparametric the Mann–Whitney *U* test. $P<0.05$ was considered statistically significant when 2 groups were compared. To avoid inflation of the alpha level, significance levels were adjusted (Bonferroni) when multiple comparisons were computed by dividing the *P* value by the number of post hoc tests performed.

Results

Human Circulating MPs Carry an Endothelial Nitric Oxide Synthase

Removal of platelet contamination is crucial for proteomic analysis of circulating MPs in plasma. We purified MPs by sequential centrifugation of human plasma. Analysis of the different fractions by flow cytometry and laser-scanning microscopy revealed that PRP contained both platelets with a size >1 μm, ranging from 1.5 to 3 μm in diameter, and MPs with a size <1 μm (Figure 1A). PFP did not contain any platelets (Figure 1B). The major subpopulations of MPs (Figure 1C) were identified to be of platelet origin ($CD41^+$, 40%), closely followed by endothelial origin ($CD41^-/CD31^+$,

25%; CD144$^+$, 28%; CD62e$^+$, 5%). Other subpopulations were erythrocyte-derived (CD235$^+$, 10%) and leukocyte-derived (CD45$^+$, 8%) MPs.

We found that MPs express an eNOS (Figure 2A), as demonstrated by both immunoprecipitation of eNOS with a mouse monoclonal anti-eNOS antibody from PFP (Figure 2A, lane 1) or Western blot analysis of a crude MP lysate (Figure 2A, lane 2). The same band at an approximate molecular weight of 135 kDa was also present in lysate from platelets and from human endothelial cells (Figure 2A, lanes 3+4). The specificity of the band was further confirmed by staining with a rabbit anti-eNOS antibody or a mouse monoclonal anti-eNOS antibody directed against different epitopes. No eNOS was detected in MP-free plasma (Figure 2A, bottom gel).

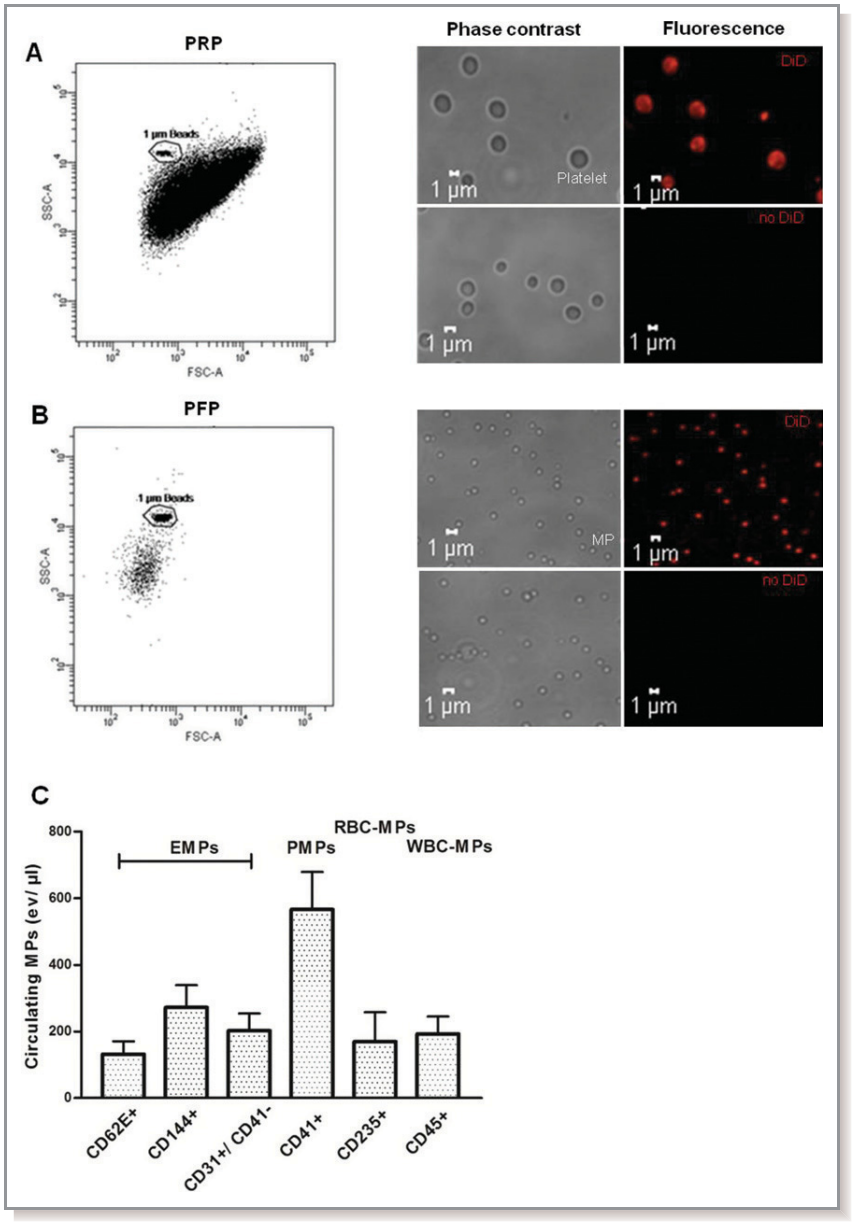

Figure 1. Analysis of composition and morphology of different fractions of human plasma obtained by sequential centrifugation. A, PRP contains a dense population comprising platelets with dimensions >1 μm and MPs with dimensions <1 μm, as shown by flow cytometry (left panel) and phase-contrast or fluorescence-based laser-scanning microscopy (middle and right panels). Membranes were stained with DiD. B, PFP contains MPs only. C, MP subpopulations in PFP were discriminated by flow-cytometric analysis according to the expression of membrane-specific antigens: EMPs, PMPs, RBC-MPs, and WBC-MPs. Values are mean±SEM. PRP indicates platelet-rich plasma; PFP, platelet-free plasma; MPs, microparticles; EMPs, endothelial-derived microparticles; PMPs, platelet-derived microparticles; RBC-MPs, erythrocyte-derived micoparticles; WBC-MPs, leukocyte-derived microparticles.

eNOS Protein in Circulating MPs Is Active and Produces NO

Enzymatic activity of eNOS was determined in MP lysate by analyzing the conversion of [^{3}H]-L-arginine to [^{3}H]-L-citrulline in the presence of NADPH, FAD, FMN, Ca^{2+}, and calmodulin. We measured a significant increase in [^{3}H]-citrulline production over time, which was inhibited by the addition of the specific NOS inhibitor L-NAME (Figure 2B). Ca^{2+}-chelation by EDTA and EGTA also strongly impaired [^{3}H]-L-citrulline production (Figure 2C).

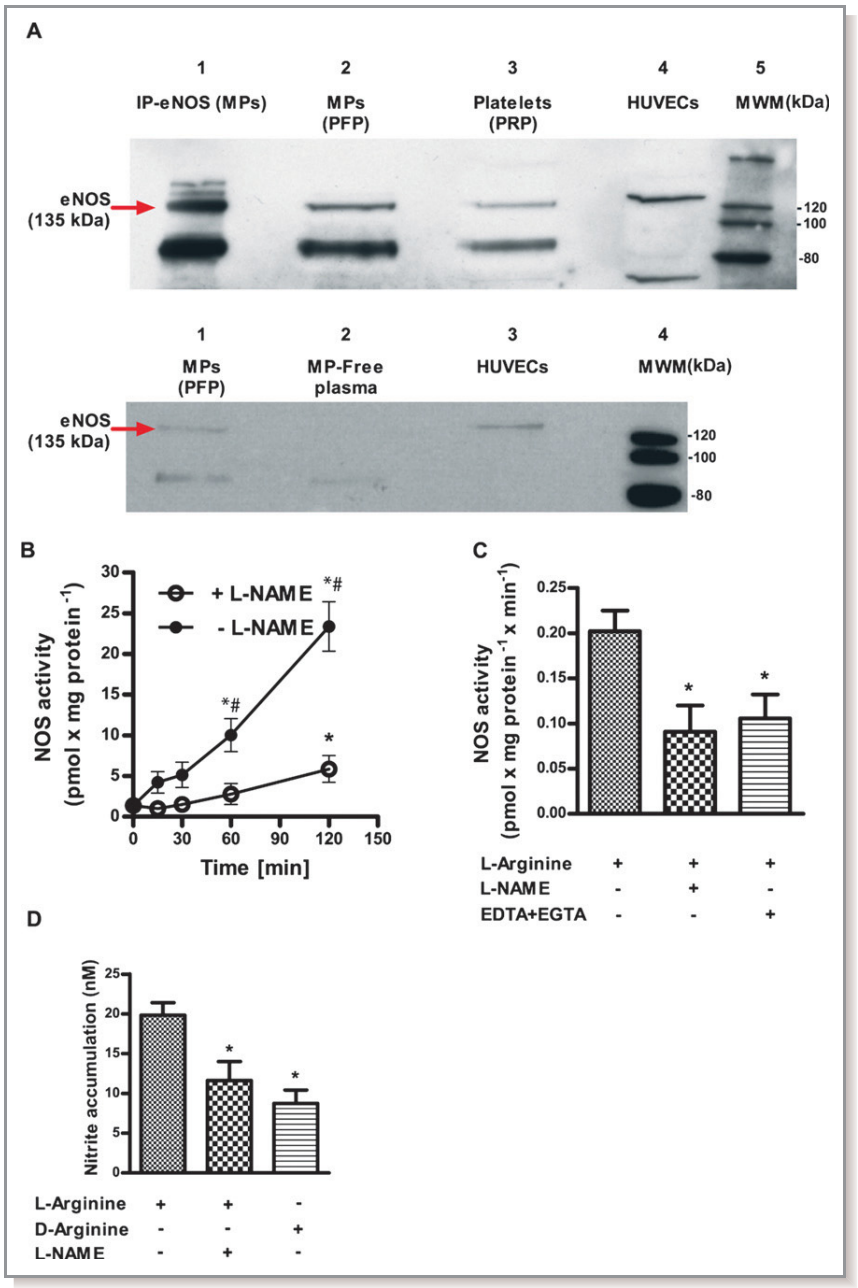

Figure 2. MPs express a functional eNOS. A, Western blot analysis of eNOS obtained by immunoprecipitation (IP) from human MPs, crude extracts of circulating MPs, and platelets, as well as HUVECs as a control (top) and MPs, MP-free plasma, and HUVECs (bottom). B, Crude MP lysate converted [^{3}H]-L-arginine to [^{3}H]-L-citrulline in a time-dependent fashion. *P<0.0125 compared with baseline, #P<0.0125 compared with L-NAME (2B). C, NOS activity is inhibited by the NOS inhibitor L-NAME and by the Ca^{2+} chelators EDTA and EGTA. D, NOS-dependent nitrite accumulation was substrate dependent (n=6). *P<0.025 compared with L-arginine only. P values represent Bonferroni-corrected significance levels. MPs indicates microparticles; eNOS, endothelial nitric oxide synthase; PRP, platelet-rich plasma; PFP, platelet-free plasma; HUVEC, human umbilical vein endothelial cell; MWM, molecular weight marker; L-NAME, N^G-nitro-L-arginine-methyl ester monohydrochloride.

NOS activity was also determined by measuring NOS-dependent nitrite accumulation in the presence of L-arginine and enzymatic cofactors. In the presence of L-arginine and Ca^{2+}/calmodulin, the measured nitrite accumulation was 19.8±1.8 nmol/L within 120 minutes of incubation. If the inactive substrate D-arginine was added instead of L-arginine or after the addition of the NOS inhibitor L-NAME, nitrite accumulation was significantly impaired (8.8±1.6 and 11.6±2.4 nmol/L, respectively; Figure 2D).

We also found that intact MPs produced NOS-derived NO. A significant increase in intraparticular fluorescence was achieved using a NO-specific membrane-permeable fluorescent probe (MNIP-Cu). The platelet contamination within PPP was used as a positive control in these experiments, as platelets are known to express an active eNOS producing NO. Laser-scanning microscopy revealed a blue fluorescence signal in MPs and platelets loaded with the NO probe MNIP-Cu (Figure 3A, upper panels). Pretreatment with the NOS inhibitor L-NAME significantly blunted fluorescent activity, comparable to the unloaded control MPs (Figure 3A, middle panels). The same observations were confirmed by flow cytometry (Figure 3B and 3C). Unloaded samples were analyzed to control for autofluorescence (Figure 3A, bottom panel, and Figure 3B, first peak).

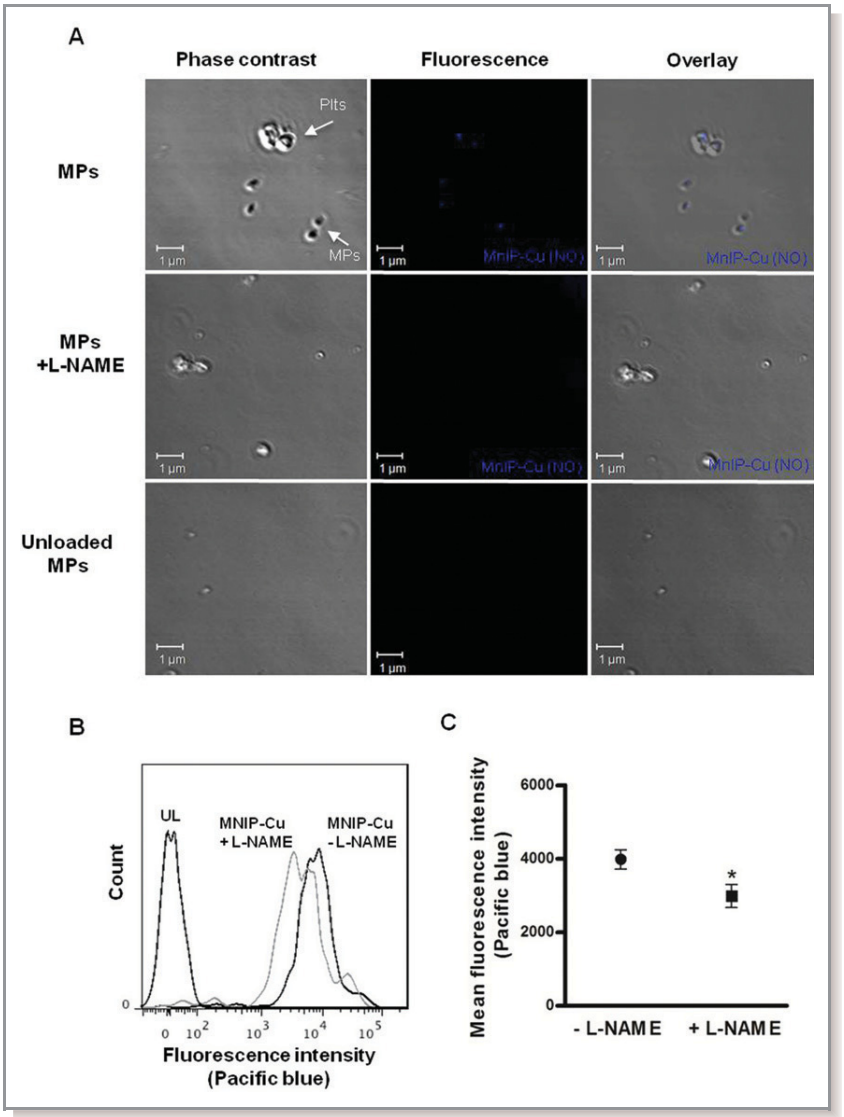

Figure 3. Direct detection of NO in human circulating MPs. MPs loaded with the NO fluorescent probe MNIP-Cu were highly fluorescent (CTRL), as measured by laser-scanning microscopy (A) and flow cytometry (n=10; B+C). The addition of the specific NOS inhibitor L-NAME decreased fluorescence. Unloaded MPs (UL) were used as a control for autofluorescence. *P<0.05 compared with samples without L-NAME. NO indicates nitric oxide; MPs, microparticles; NOS, nitric oxide synthase; L-NAME, N^G-nitro-L-arginine-methyl ester monohydrochloride; MNIP-Cu, 4-methoxy-2-(1H-naphtho[2,3-d]imidazol-2-yl)phenol.

Levels of MP eNOS Protein and Activity in Patients With Endothelial Dysfunction

Defective endothelial and platelet NO synthesis represents a major feature of endothelial dysfunction in cardiovascular disease (CVD). To verify whether their circulating "offspring" also show similar features, we investigated eNOS activity and NOS expression in MPs of patients with CVD and documented endothelial dysfunction as compared with healthy volunteers (see Table 1 for characteristics). Indicative of endothelial dysfunction, patients exhibited impaired flow-mediated vasodilation (7.5±0.4% versus 3.5±0.3%, *P*=0.001; Figure 4A).

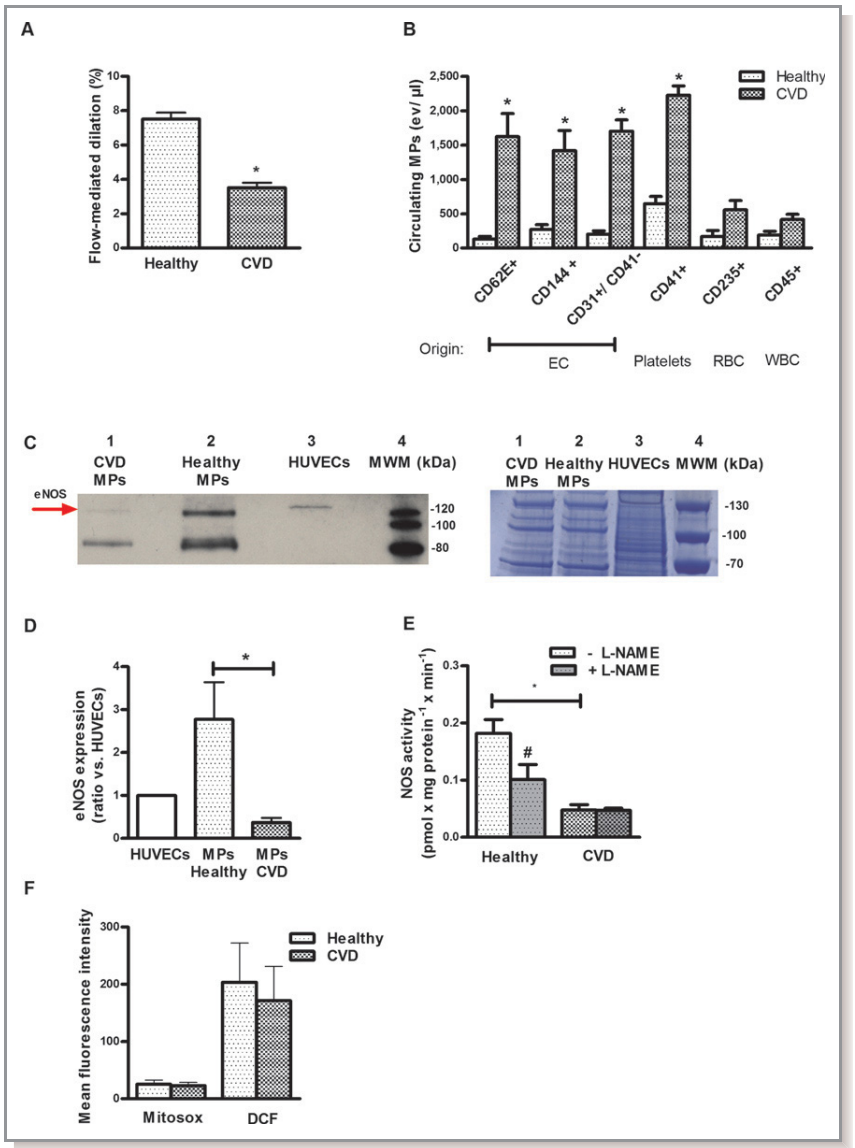

Figure 4. The MPs' eNOS activity is decreased in patients with endothelial dysfunction. Patients with cardiovascular disease (CVD) exhibited decreased endothelial function as assessed by flow-mediated vasodilation (A) and increased MPs levels (especially endothelial cell– and platelet-derived MPs) in plasma (B) compared with healthy subjects. C+D, MPs from these patients carry less eNOS protein compared with healthy controls. C, Western blot analysis, representative of n=5 independent gels (left); protein bands stained with colloidal Coomassie Brilliant Blue, confirming equal gel loading between samples (right). D, Densitometry band intensity was normalized vs a standard HUVEC lysate and was quantified using Image J software©. *P<0.017 compared with healthy subjects. E, NOS activity in MPs from CVD (L-citrulline synthesis) was decreased compared with healthy controls. F, Mean fluorescence intensity of MPs labeled with MitoSox, a probe for O_2^-, or DCF, a probe for ROS, did not significantly differ between groups (measured by flow cytometry). *P<0.05 compared with healthy subjects. Values are mean±SEM. MPs indicates microparticles; eNOS, endothelial nitric oxide synthase; EC, endothelial cell; RBC, red blood cell; WBC, white blood cell; HUVEC, human umbilical vein endothelial cell; L-NAME, N^G-nitro-L-arginine-methyl ester monohydrochloride; DCF, 2′,7′-dichlorodihydrodiclorofluorescein diacetate; ROS, reactive oxygen species.

The total number of circulating MPs was increased in the plasma of CVD patients compared with healthy controls (Figure 4B). This was mainly driven by an increase in endothelial cell– and platelet-derived MPs. In a subgroup of the study population, we analyzed eNOS expression and activity (n=11, healthy; n=7, CAD). In MPs circulating in the plasma of CVD patients, we detected significantly reduced levels of eNOS protein (Figure 4C) compared with in healthy volunteers. Figure 4D shows the densitometric analysis. Band intensity was normalized for the intensity of the eNOS band in HUVECs. Equal loading was confirmed by staining a duplicate gel with Coomassie Brilliant Blue.

Of interest, the NOS-dependent conversion of [^{3}H]-L-arginine to [^{3}H]-L-citrulline was largely abolished (Figure 4E), as also demonstrated by the lack of a measurable effect of the NOS inhibitor L-NAME.

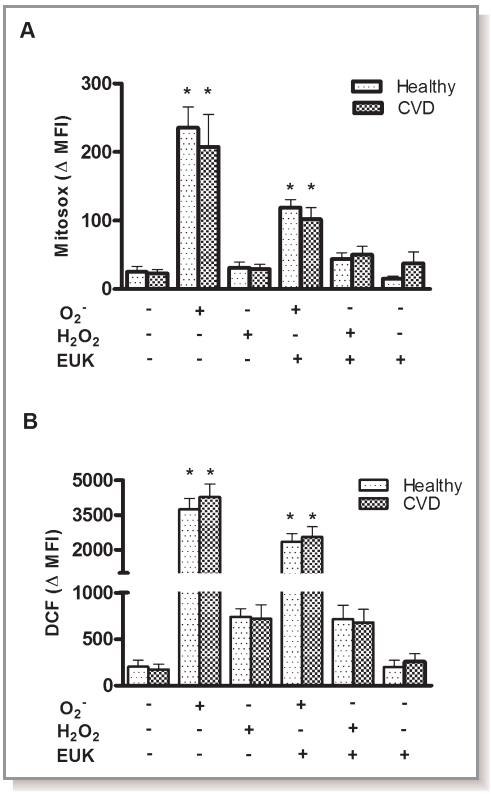

Figure 5. ROS levels in MPs from healthy subjects and patients with CVD. Mean fluorescence intensity of (A) MitoSox, a probe for O_2^-, and (B) DCF, a probe for ROS, did not significantly differ between groups. MPs were treated with PBS as a control, with an O_2^--generating system, with H_2O_2 or with the superoxide dismutase mimic EUK. MPs were stained with MitoSox (n=5) or with DCF diacetate (n=5) or were left unlabeled as an autofluorescence control. Probes were analyzed in a flow cytometer. *P<0.05 compared with the control. Values are mean±SEM. MPs indicates microparticles; ROS, reactive oxygen species; DCF, 2′,7′-dichlorodihydrodiclorofluorescein diacetate; CVD, cardiovascular disease. MFI, mean fluorescence intensity; EUK-134, chloro[[2,2'-[1,2-ethanediylbis[(nitrilo-κN)methylidyne]]bis[6-methoxy-phenolato-κO]]]-manganese.

We also compared superoxide generation in MPs from the patients with cardiovascular diseases and from healthy volunteers. Our data showed that the mean fluorescence intensity of MitoSox, a probe for O_2^-, as well as of DCF, a probe for ROS, measured by flow cytometry, did not significantly differ between the groups (Figure 4F). As a positive control, we treated MPs with O_2^- or with H_2O_2. This strongly increased intracellular fluorescence activity of MitoSox as well as of DCF. The addition of EUK 134, a cell membrane–permeable ROS scavenger, decreased the intracellular fluorescence activity of Mitosox and DCF (Figure 5). In summary, our data suggest that the decrease in NOS activity was mainly a result of decreased protein levels in MPs from CVD patients compared with healthy individuals, whereas ROS levels were unchanged.

Discussion

We have demonstrated that circulating MPs express an active eNOS and produce NO. In patients with cardiovascular diseases, impaired endothelium-dependent vasodilation was associated with decreased eNOS expression and activity in circulating MPs.

To the best of our knowledge, we have shown for the first time that human circulating MPs express a functionally active eNOS protein. Previously, Leroyer et al[19] identified an eNOS protein in MPs derived from cultured mouse endothelial cells. In addition, our data have shown that eNOS in circulating MPs is not just a nonfunctional residual protein of the original cell, but rather an enzyme retaining its catalytic function. Thus, we have shown that NOS is capable of converting L-arginine to L-citrulline and of producing NO in a substrate- and Ca^{2+}-dependent fashion. In intact MPs, we also demonstrated NOS-dependent NO production by detecting MNIP-Cu-derived fluorescence activity, which was inhibited by preincubating with a NOS inhibitor. Taken together, we have shown that MPs express an active eNOS that produces NO within the MPs.

We were not able to distinguish between the subpopulations of MPs by means of their contribution to overall eNOS. As shown in our present and in previous studies,[2] in healthy individuals, the major subpopulation of circulating MPs is derived from platelets and endothelial cells, both of which have eNOS localized to the membrane.[20–26] Nevertheless, leukocytes and erythrocytes also express an eNOS[27–30] and may also release MPs into circulation.

Here, we have shown for the first time that MPs isolated from patients with cardiovascular disease and endothelial dysfunction show less eNOS expression and activity than healthy volunteers' MPs. Moreover, in these patients an increase in the total amount of circulating MPs was measured, confirming previous research.[1–3]

Defective endothelial NO synthesis represents a major feature of endothelial dysfunction and vascular disease.[31,32] It was previously demonstrated in cardiovascular disease that endothelial cells[31,33] and platelets[34] exhibit decreased eNOS protein expression and NO release. Thus, our results show that under these pathological conditions, not only the parent cells of the predominant MP subpopulations are dysfunctional regarding eNOS expression and eNOS activity, but also their circulating "offspring." Therefore, eNOS activity of MPs may be a useful available readout of endothelial NOS activity in vivo. A global decrease in eNOS activity in endothelium and platelets as well as in the MPs originating from them may indicate global eNOS dysfunction in cardiovascular disease. Future studies in larger patient populations might address the questions of how eNOS expression is distributed among the MP subpopulations and whether MPs are able to transfer their "enzymatic legacy" to other cells in health and disease.

The consequences of decreased eNOS protein expression and NO release are not limited to the vessel wall,[31,33] but may also involve blood cells known to express this enzyme, including platelets,[34] endothelial progenitor cells,[14] or even circulating MPs, as shown in the present study. Considering the central role played by endothelial and blood cell eNOS in vascular homeostasis, it is also tempting to speculate that the eNOS activity of MPs may directly participate in this equilibrium, providing a further circulating source of NO. Future studies will aid further understanding of the (patho) physiological role of circulating eNOS in MPs.

Taken together, our data support the concept that MPs may not only retain phenotypic markers but also preserve the expression and functionality of enzymes of the cells they originate from, including eNOS, and may mediate and transport their physiological functions. In cardiovascular disease, an increase in endothelium-derived MP subpopulations accompanied by a decrease in MPs' eNOS activity may not merely be an index of a dysfunctional endothelium, but may also contribute to disturbed NO bioavailability and hence play a role in the pathophysiology of cardiovascular disease.

Sources of Funding

Christian Heiss and Miriam M. Cortese-Krott were supported by 2 independent research grants of the Forschungskommission, Medical Faculty, University Düsseldorf, and Malte Kelm was supported by grants from the Deutsche Forschungsgemeinschaft (DFG 405/5-1 and FOR809 TP7 Me1821/3-1), the Anton Betz Stiftung (26/2010), and the Susanne-Bunnenberg-Stiftung at Düsseldorf Heart Center.

Disclosures

None.

References

1. Amabile N, Rautou PE, Tedgui A, Boulanger CM. Microparticles: key protagonists in cardiovascular disorders. *Semin Thromb Hemost.* 2010;36:907–916.
2. Burnier L, Fontana P, Kwak BR, Angelillo-Scherrer A. Cell-derived microparticles in haemostasis and vascular medicine. *Thromb Haemost.* 2009;101:439–451.
3. George FD. Microparticles in vascular diseases. *Thromb Res.* 2008;122:55–59.
4. Garcia BA, Smalley DM, Cho H, Shabanowitz J, Ley K, Hunt DF. The platelet microparticle proteome. *J Proteome Res.* 2005;4:1516–1521.
5. Smalley DM, Root KE, Cho H, Ross MM, Ley K. Proteomic discovery of 21 proteins expressed in human plasma-derived but not platelet-derived microparticles. *Thromb Haemost.* 2007;97:67–80.
6. Banfi C, Brioschi M, Wait R, Begum S, Gianazza E, Pirillo A, Mussoni L, Tremoli E. Proteome of endothelial cell-derived procoagulant microparticles. *Proteomics.* 2005;5:4443–4455.
7. Hugel B, Martinez MC, Kunzelmann C, Freyssinet JM. Membrane microparticles: two sides of the coin. *Physiology (Bethesda).* 2005;20:22–27.
8. Morel O, Toti F, Hugel B, Freyssinet JM. Cellular microparticles: a disseminated storage pool of bioactive vascular effectors. *Curr Opin Hematol.* 2004;11:156–164.
9. Moncada S. Nitric oxide in the vasculature: physiology and pathophysiology. *Ann N Y Acad Sci.* 1997;811:60–67.
10. Ignarro LJ, Cirino G, Casini A, Napoli C. Nitric oxide as a signaling molecule in the vascular system: an overview. *J Cardiovasc Pharmacol.* 1999;34:879–886.
11. Brossette T, Hundsdorfer C, Kroncke KD, Sies H, Stahl W. Direct evidence that (-)-epicatechin increases nitric oxide levels in human endothelial cells. *Eur J Nutr.* 2011;50:595–599.
12. Heiss C, Amabile N, Lee AC, Real WM, Schick SF, Lao D, Wong ML, Jahn S, Angeli FS, Minasi P, Springer ML, Hammond SK, Glantz SA, Grossman W, Balmes JR, Yeghiazarians Y. Brief secondhand smoke exposure depresses endothelial progenitor cells activity and endothelial function: sustained vascular injury and blunted nitric oxide production. *J Am Coll Cardiol.* 2008;51:1760–1771.
13. Cortese-Krott MM, Munchow M, Pirev E, Hessner F, Bozkurt A, Uciechowski P, Pallua N, Kroncke KD, Suschek CV. Silver ions induce oxidative stress and intracellular zinc release in human skin fibroblasts. *Free Radic Biol Med.* 2009;47:1570–1577.
14. Heiss C, Schanz A, Amabile N, Jahn S, Chen Q, Wong ML, Jahn S, Angeli FS, Minasi P, Springer ML, Hammond SK, Glantz SA, Grossman W, Balmes JR, Yeghiazarians Y. Nitric oxide synthase expression and functional response to nitric oxide are both important modulators of circulating angiogenic cell response to angiogenic stimuli. *Arterioscler Thromb Vasc Biol.* 2010;30:2212–2218.
15. Bredt DS, Snyder SH. Isolation of nitric oxide synthetase, a calmodulin-requiring enzyme. *Proc Natl Acad Sci USA.* 1990;87:682–685.
16. Rassaf T, Preik M, Kleinbongard P, Lauer T, Heiss C, Strauer BE, Feelisch M, Kelm M. Evidence for in vivo transport of bioactive nitric oxide in human plasma. *J Clin Invest.* 2002;109:1241–1248.
17. Ouyang J, Hong H, Shen C, Zhao Y, Ouyang C, Dong L, Zhu J, Guo Z, Zeng K, Chen J, Zhang C, Zhang J. A novel fluorescent probe for the detection of nitric oxide in vitro and in vivo. *Free Radic Biol Med.* 2008;45:1426–1436.
18. Rong Y, Doctrow SR, Tocco G, Baudry M. Euk-134, a synthetic superoxide dismutase and catalase mimetic, prevents oxidative stress and attenuates kainate-induced neuropathology. *Proc Natl Acad Sci USA.* 1999;96:9897–9902.
19. Leroyer AS, Ebrahimian TG, Cochain C, Recalde A, Blanc-Brude O, Mees B, Vilar J, Tedgui A, Levy BI, Chimini G, Boulanger CM, Silvestre JS. Microparticles from ischemic muscle promotes postnatal vasculogenesis. *Circulation.* 2009;119:2808–2817.
20. Ohashi Y, Katayama M, Hirata K, Suematsu M, Kawashima S, Yokoyama M. Activation of nitric oxide synthase from cultured aortic endothelial cells by phospholipids. *Biochem Biophys Res Commun.* 1993;195:1314–1320.
21. Pollock JS, Forstermann U, Mitchell JA, Warner TD, Schmidt HH, Nakane M, Murad F. Purification and characterization of particulate endothelium-derived relaxing factor synthase from cultured and native bovine aortic endothelial cells. *Proc Natl Acad Sci USA.* 1991;88:10480–10484.
22. Sase K, Michel T. Expression of constitutive endothelial nitric oxide synthase in human blood platelets. *Life Sci.* 1995;57:2049–2055.
23. Wallerath T, Gath I, Aulitzky WE, Pollock JS, Kleinert H, Forstermann U. Identification of the no synthase isoforms expressed in human neutrophil granulocytes, megakaryocytes and platelets. *Thromb Haemost.* 1997;77:163–167.
24. Mehta JL, Chen LY, Kone BC, Mehta P, Turner P. Identification of constitutive and inducible forms of nitric oxide synthase in human platelets. *J Lab Clin Med.* 1995;125:370–377.

25. Radomski MW, Palmer RM, Moncada S. Characterization of the L-arginine: nitric oxide pathway in human platelets. *Br J Pharmacol.* 1990;101:325–328.
26. Muruganandam A, Mutus B. Isolation of nitric oxide synthase from human platelets. *Biochim Biophys Acta.* 1994;1200:1–6.
27. Kleinbongard P, Schulz R, Rassaf T, Lauer T, Dejam A, Jax TW, Kumara I, Gharini P, Kabanova S, Oezuyaman B, Schnuerch HG, Goedecke A, Weber AA, Robenek MJ, Robenek H, Bloch W, Roesen P, Kelm M. Red blood cells express a functional endothelial nitric oxide synthase. *Blood.* 2006;107:2943–2951.
28. Chen LY, Mehta JL. Evidence for the presence of L-arginine-nitric oxide pathway in human red blood cells: relevance in the effects of red blood cells on platelet function. *J Cardiovasc Pharmacol.* 1998;32:57–61.
29. Reiling N, Kroncke R, Ulmer AJ, Gerdes J, Flad HD, Hauschildt S. Nitric oxide synthase: expression of the endothelial, Ca2+/calmodulin-dependent isoform in human B and T lymphocytes. *Eur J Immunol.* 1996;26:511–516.
30. de Frutos, Sanchez de Miguel L, Farre J, Gomez J, Romero J, Marcos-Alberca P, Nunez A, Rico L, Lopez-Farre A. Expression of an endothelial-type nitric oxide synthase isoform in human neutrophils: modification by tumor necrosis factor-alpha and during acute myocardial infarction. *J Am Coll Cardiol.* 2001;37:800–807.
31. Li H, Forstermann U. Nitric oxide in the pathogenesis of vascular disease. *J Pathol.* 2000;190:244–254.
32. Widlansky ME, Gokce N, Keaney JF Jr, Vita JA. The clinical implications of endothelial dysfunction. *J Am Coll Cardiol.* 2003;42:1149–1160.
33. Cai H, Harrison DG. Endothelial dysfunction in cardiovascular diseases: the role of oxidant stress. *Circ Res.* 2000;87:840–844.
34. O'Kane PD, Reebye V, Ji Y, Stratton P, Jackson G, Ferro A. Aspirin and clopidogrel treatment impair nitric oxide biosynthesis by platelets. *J Mol Cell Cardiol.* 2008;45:223–229.

blood

2012 120: 4229-4237
Prepublished online September 24, 2012;
doi:10.1182/blood-2012-07-442277

Human red blood cells at work: identification and visualization of erythrocytic eNOS activity in health and disease

Miriam M. Cortese-Krott, Ana Rodriguez-Mateos, Roberto Sansone, Gunter G. C. Kuhnle, Sivatharsini Thasian-Sivarajah, Thomas Krenz, Patrick Horn, Christoph Krisp, Dirk Wolters, Christian Heiß, Klaus-Dietrich Kröncke, Neil Hogg, Martin Feelisch and Malte Kelm

Blood (print ISSN 0006-4971, online ISSN 1528-0020), is published weekly by the American Society of Hematology, 2021 L St, NW, Suite 900, Washington DC 20036.

Human red blood cells at work: identification and visualization of erythrocytic eNOS activity in health and disease

Miriam M. Cortese-Krott,[1] Ana Rodriguez-Mateos,[2] Roberto Sansone,[1] Gunter G. C. Kuhnle,[2] Sivatharsini Thasian-Sivarajah,[1] Thomas Krenz,[1] Patrick Horn,[1] Christoph Krisp,[3] Dirk Wolters,[3] Christian Heiß,[1] Klaus-Dietrich Kröncke,[4] Neil Hogg,[5] Martin Feelisch,[6] and Malte Kelm[1]

[1]Cardiovascular Research Laboratory, Department of Cardiology, Pulmonology and Angiology, Heinrich Heine University of Düsseldorf, Düsseldorf, Germany; [2]Department of Food and Nutritional Sciences, University of Reading, Reading, United Kingdom; [3]Biomolecular Mass Spectroscopy/Protein Center, Department of Analytical Chemistry, Ruhr University, Bochum, Germany; [4]Institute of Biochemistry and Molecular Biology I, Medical Faculty, Heinrich Heine University of Düsseldorf, Düsseldorf, Germany; [5]Department of Biophysics, Medical College of Wisconsin, Milwaukee, WI; and [6]University of Southampton, Clinical & Experimental Sciences, Faculty of Medicine, Southampton General Hospital, Southampton, United Kingdom

A nitric oxide synthase (NOS)–like activity has been demonstrated in human red blood cells (RBCs), but doubts about its functional significance, isoform identity and disease relevance remain. Using flow cytometry in combination with the nitric oxide (NO)–imaging probe DAF-FM we find that all blood cells form NO intracellularly, with a rank order of monocytes > neutrophils > lymphocytes > RBCs > platelets. The observation of a NO-related fluorescence within RBCs was unexpected given the abundance of the NO-scavenger oxyhemoglobin. Constitutive normoxic NO formation was abolished by NOS inhibition and intracellular NO scavenging, confirmed by laser-scanning microscopy and unequivocally validated by detection of the DAF-FM reaction product with NO using HPLC and LC-MS/MS. Using immunoprecipitation, ESI-MS/MS-based peptide sequencing and enzymatic assay we further demonstrate that human RBCs contain an endothelial NOS (eNOS) that converts L-^{3}H-arginine to L-^{3}H-citrulline in a Ca^{2+}/calmodulin-dependent fashion. Moreover, in patients with coronary artery disease, red cell eNOS expression and activity are both lower than in age-matched healthy individuals and correlate with the degree of endothelial dysfunction. Thus, human RBCs constitutively produce NO under normoxic conditions via an active eNOS isoform, the activity of which is compromised in patients with coronary artery disease. (*Blood*. 2012;120(20): 4229-4237)

Introduction

The key event in the pathogenesis of arteriosclerosis is believed to be a dysfunction of the endothelium with disruption of vascular homeostasis, predisposing blood vessels to vasoconstriction, inflammation, leukocyte adhesion, thrombosis, and proliferation of vascular smooth muscle cells. Red blood cells (RBCs) are typically considered as shuttles of respiratory gases and nutrients for tissues, less so compartments important to vascular integrity. Patients with coronary artery disease (CAD) and concomitant anemia have a poorer prognosis after myocardial infarction, percutaneous coronary intervention, and coronary artery bypass grafting, and are more prone to developing heart failure with fatal outcomes.[1-3] Surprisingly, erythropoietin treatment fails to improve diagnosis, indicating that a compromised gas exchange/nutrient transport capacity of blood is insufficient to explain this outcome.

Nitric oxide (NO) is an essential short-lived signaling/regulatory product of a healthy endothelium that is critically important for vascular health. Decreased production and/or bioactivity of NO are a hallmark of endothelial dysfunction and have been shown to contribute to accelerated atherogenesis. In the cardiovascular system, NO is continuously produced in endothelial cells (ECs) by the type III isoform of NO synthase (eNOS, NOS3; EC 1.14.13.39).[4] In addition to endothelial cells, some circulating blood cells also contain eNOS.

It is an accepted dogma that RBCs take up and inactivate endothelium-derived NO via rapid reaction with oxyhemoglobin to form methemoglobin and nitrate, thereby limiting NO available for vasodilatation. Yet it has also been shown that RBCs not only act as "NO sinks" but synthesize, store, and transport NO metabolic products. Under hypoxic conditions in particular, it has been demonstrated that RBCs induce NO-dependent vasorelaxation.[5,6] Mechanisms of release and potential sources of NO in RBCs are still a matter of debate, but candidates include iron-nitrosylhemoglobin,[7] S-nitrosohemoglobin,[8-10] and nitrite. The latter may form NO either via deoxyhemoglobin[5,11] or xanthine oxidoreductase (XOR)–mediated reduction,[6,12] or via spontaneous[12] and carbonic anhydrase-facilitated disproportionation.[13] Most of these processes show a clear oxygen-dependence, and several are favored by low oxygen tensions. The relative contribution of either mechanism to NO formation varies with oxygen partial pressure along the vascular tree. In addition, RBCs release ATP when subjected to hypoxia, providing an alternative vasodilatory pathway.[14]

Submitted July 11, 2012; accepted September 18, 2012. Prepublished online as *Blood* First Edition paper, September 24, 2012; DOI 10.1182/blood-2012-07-442277.

The online version of this article contains a data supplement.

Part of this work was presented in abstract form at the joint meeting of the Societies of Free Radical Biology and Medicine and the Free Radical Research International, Orlando, FL, November 2010, and Atlanta, GA, November 2011, respectively.

The publication costs of this article were defrayed in part by page charge payment. Therefore, and solely to indicate this fact, this article is hereby marked "advertisement" in accordance with 18 USC section 1734.

In contrast to hypoxia-induced NO release from RBCs, their generation of NO under normoxic conditions is less well characterized. Data from our and other laboratories have demonstrated a NOS-dependent NO production from RBCs in normoxia, suggesting that RBCs may contribute to the inhibition of platelet aggregation,[15,16] the circulating pool of NO metabolites,[15-18] and to overall tissue protection.[17,18] Treating RBCs with NOS inhibitors decreased accumulation of NO metabolites[16,19] and citrulline[15,18] in the supernatant. However, Kang et al failed to measure citrulline production in RBC lysates,[20] maybe because of loss of cellular structures or cofactors important for activity.[21] Another recent study failed to detect increases in ^{15}N-labeled nitrite/nitrate after the addition of ^{15}N-L-Arg to intact RBCs.[22] RBCs have been shown to express a protein containing epitopes of an eNOS.[6,15,16,20,23-25] However, positive staining with anti-iNOS antibodies has also been reported,[20,25] and others suggested that RBCs might express a novel NOS isoform.[23,25] Thus, doubts about the functional significance of the NOS-like activity in RBCs remain, and little is known about NOS isoform identity and disease relevance.

We therefore sought to definitively identify and characterize the activity of human red cell NOS using an advanced multilevel analytical approach. Using HPLC, LC-MS/MS, flow cytometry, laser scanning microscopy, and enzymatic assay together with functional studies we here demonstrate that human RBCs contain an active eNOS that gives rise to constitutive intracellular NO formation under normoxic conditions. We further show that this activity is compromised in CAD and correlates with the degree of endothelial dysfunction.

Methods

Study subjects

Blood drawn from human healthy subjects (25-33 years) was used for biochemical characterization of human red cell eNOS. To compare NOS expression with vascular function, 10 patients with endothelial dysfunction because of coronary artery disease (CAD), as diagnosed by coronary angiography, and 9 age-matched healthy subjects were recruited from the outpatient clinic of the Department of Cardiology, Pulmonology, and Angiology, Düsseldorf University Hospital. NOS activity was quantified in red cells from a randomized subset of the study population composed of 4 healthy individuals and 5 patients with CAD. All subjects provided written informed consent before enrollment. Procedures were conducted in accordance with the Declaration of Helsinki and approved by the local ethics committee of the Heinrich-Heine University of Düsseldorf. Endothelium-dependent dilation of the brachial artery was assessed noninvasively by measurement of flow-mediated dilatation (FMD) using high-resolution ultrasound (VIVID i, GE Healthcare).[26] FMD and endothelium-independent dilation were expressed as a percentage change from baseline. See supplemental Methods for further details (available on the *Blood* Web site; see the Supplemental Materials link at the top of the online article).

Comparative flow cytometric analysis of blood cells

Three aliquots of blood were processed for analysis of leukocytes, RBCs, and platelets, as described in supplemental Methods. Briefly, each aliquot was loaded with 10μM DAF-FM diacetate for 30 minutes at room temperature in the dark, or left untreated, washed in PBS and analyzed for DAF FM-associated fluorescence in a FACS Canto II flow cytometer. NO donors were applied to RBC preparations at the indicated concentrations after washing the DAF-FM-loaded cells. For NOS inhibition, RBC suspensions were preincubated for 30 minutes with 3mM L-NAME or 1mM L-NIO. Intracellular NO was scavenged by incubation of RBC suspensions for 30 minutes at 37°C with 250μM iron diethyldithiocarbamate (Fe[DETC]$_2$) prepared as described,[27] and then washed by centrifugation at 300*g* for 10 minutes at 4°C. Aliquots from these preparations were analyzed within 15 minutes in a FACS Canto II flow cytometer after further 1:3 dilution in PBS. Flow cytometric data were collected using the DIVA 5.0 software package and analyzed using FlowJo V7.5.5 (TreeStar). Median fluorescence intensity (MFI) was calculated from the histogram (distribution) plots of the green fluorescence signals (Ex 488 nm, Em 530 ± 30 nm) detected within the cell-specific gates (see Figure 1Ai, Bi, and Ci, gated cells are color-coded). MFIs of untreated samples served as autofluorescence controls. The acquisition voltage was adjusted before each measurement according to the position of the third fluorescence peak of standard latex beads (Rainbow beads, BD Bioscience).

Visualization of DAF-FM fluorescence in RBC by laser-scanning microscopy

Whole blood was diluted 1:10 in PBS and treated with 10 to 30μM DAF-FM diacetate for 30 minutes at room temperature or 37°C in the dark, washed and treated with 100μM spermine/NO (Sper/NO), or 100μM S-nitrosocysteine (SNOC) for 15 minutes. Unstained cells served as autofluorescence controls. Blood smears were analyzed 1 to 5 minutes after preparation under a Zeiss LSM 510 confocal laser-scanning microscope using a Zeiss Plan Neofluar 63/×1.3 oil DIC objective and excitation (Ex) 488 nm with UV/488/543/633 nm beam splitter. Fluorescence was recorded using a 540 to 30-nm bandpass filter and micrographs were taken at 37°C. Images were processed with Adobe Photoshop CS5 (Adobe Systems GmbH).

HPLC analysis of the nitrosation products of DAF-FM

Red cell pellets were diluted 1:500 in PBS, pretreated as described in the "Flow cytometry" section, washed, and loaded by 30 minutes incubation with 10μM DAF-FM diacetate at room temperature in the dark. After centrifugation at 300*g* for 10 minutes at 4°C, pellets were incubated with HPLC-grade DMSO for 30 minutes at room temperature in the dark and spun down at 13 000*g* for 10 minutes. The supernatants were analyzed by reversed-phase high performance liquid chromatography (HPLC) applying a method described for DAF-2[28] with some modifications, using an Agilent 1100 Series HPLC system (Agilent Technologies) with a diode array detector (set to 490 nm) and a fluorescence detector (Ex 490, Em 517) connected in series. The column used was a Phenomenex Luna C18 (2), (4.6 × 250 mm; 5 μm) fitted with a guard column, both kept at 25°C. The mobile phase consisted of 0.05% TFA in water (A) and 0.05% TFA in acetonitrile (B), using the following gradient settings (time/%A): 0 minutes–95%, 40 minutes–60%, 45 minutes–60% with a flow rate of 1 mL/min.

Identification of DAF-FM reaction products by LC-MS/MS

Mass spectra were run on an Agilent 6400 triple-quadrupole liquid chromatography mass spectrometry (LC-MS/MS) instrument operated in positive ion mode; samples were separated using a Kinetix C18 (2) column (2 × 50 mm; Phenomenex) with 0.1% aqueous formic acid (A) and methanol (B) as mobile phase (flow rate 200 μL/min, gradient [time, %A]: 0 minutes–80%, 1 minute–80%, 2.1 minute–30%. 3.1 minute–30%, 3.5 minutes 80%, 5 minutes–80%). DAF-FM (transition 413.2 → 369.12) and DAF-FM-T (transition 424.2 → 380.1) were detected using selective-reaction monitoring.

Immunoprecipitation, gel electrophoresis, and Western blot analysis

Crude protein extract was obtained by lysis of RBC pellets (1 mL) with toluene.[29] ECs were lysed as described.[30] Total protein concentration was determined by Lowry (DC Protein Assay, Bio-Rad). Probes (100 μg/μL protein) were incubated for 1 hour at room temperature with a mouse anti-human NOS3 antibody (40μg; BD Bioscience). Immunocomplexes were isolated by magnetic separation using protein G Dynabeads (Invitrogen) following the manufacturer's instruction. For gel electrophoresis, samples were loaded onto 7% NuPAGE Novex Tris/Acetate precast gels (Invitrogen), and protein bands were stained with colloidal Coomassie Brilliant Blue.[31] Western blot analysis was performed as previously

described[30] using rabbit anti-NOS3 antiserum (1:1000; BD Bioscience) and HRP-conjugated goat anti-rabbit antibody (1:5000; Rockland).

Peptide sequencing by ESI-MS/MS

In-gel digestion and peptide separation was performed as described in supplemental Methods. Eluting ions were transferred directly into a LTQ XL linear ion trap mass spectrometer (Thermo Fisher Scientific) equipped with an electrospray ionization device (spray voltage 1.8 kV, capillary temperature 180°C). Precursor ions were detected in a full MS scan from 400 to 2000 m/z. Full MS/MS spectra were acquired for the 10 most intense signals using a fill time of 100 ms for each MS/MS μscan. MS/MS spectra were interpreted with the SEQUEST algorithm implemented in the Proteome Discoverer software (Thermo Fisher Scientific) and searched against the human Swiss-Prot database (release 15.6/57.6). Peptide mass accuracy for precursor ions and tolerance for fragment ions were, respectively set to 2.5 and to 1 atomic mass units, allowing methionine oxidation as a possible chemical modification.

Peptide alignments

Peptide sequences were aligned with the sequences of all main NOS isoforms and eNOS splice variants using the constraint-based multiple alignment tool (COBALT) of the NCBI website (protein accession numbers NP_000611 = NOS1, nNOS; NP_000616 = NOS2, iNOS; NP_000594 = NOS3, isoform 1; with splicing variants of NOS3 as NP_001153581 = NOS3, isoform 2, NP_001153582 = NOS3, isoform 3, and NP_001153583 = NOS3, isoform 4). The position of the peptides in the conserved regions was visualized using Geneious Version 5.4 software (Biomatters).

Determination of NOS activity

The activity of the immunoprecipitated protein was determined by measuring the rate of conversion (fmol/min) of [^{3}H] L-arginine to [^{3}H] citrulline or [^{14}C] L-arginine to [^{14}C] citrulline as previously described,[32] in the presence or absence of the specific NOS inhibitors L-NAME (1mM each), or of Ca^{2+} (75μM) + calmodulin (0.04 μg/μL; see supplemental Methods for details).

Results

RBCs loaded with DAF-FM are fluorescent

To compare intracellular NO production between circulating blood cells, blood fractions enriched in leukocytes, platelets and erythrocytes were loaded with DAF-FM diacetate and analyzed by flow cytometry (Figure 1). Individual cell subpopulations were identified by staining with specific surface markers and by analysis of scatter dot plots (Figure 1A-C, subpanel i). Monocytes revealed the highest intracellular fluorescence intensity, followed by neutrophils, lymphocytes, RBCs, and platelets (Figure 1D). Whether these variations are because of differences in NO and/or reactive oxygen species (ROS) production, or dye uptake/processing remains to be investigated.

A DAF-FM–related fluorescence signal in RBCs was unexpected given the abundance of the NO scavenger oxyhemoglobin and the nitrosation scavengers glutathione and ascorbate in these cells. However, these original findings were confirmed by laser scanning microscopy (Figure 2A). DAF-FM-associated fluorescence was remarkably uniform with a typical doughnut-shaped fluorescence pattern, and strongly increased after addition of the NO donors Sper/NO (Figure 2A bottom panel) or S-nitrosocysteine. Fluorescence intensity varied up to 5-fold between cells of the same preparation (see histogram plot in Figure 1Bi and Figure 2B), was sensitive to changes in incubation temperature (37°C ≫ RT), and oxygen tension (21% O_2 > 5% O_2). Median fluorescence intensity (MFI) increases were markedly (20%-70%) inhibited by either preincubation of cells with the NOS-inhibitors, L-NAME (Figure 2C) and L-NIO (n = 6, P = .048 vs untreated control), or the lipophilic NO scavenger $Fe[DETC]_2$ (Figure 2D). This degree of inhibition is probably maximal considering the strong background fluorescence because of the formation of unspecific fluorescent adducts[33] and the presence of fluorescence impurities in the DAF-FM DA stock solution (see next section). Moreover, treating RBC with nitrite did not affect DAF-FM-dependent signal under neutral conditions, whereas at pH 5.5 only higher concentrations of nitrite (> 200μM) strongly increased intracellular fluorescence (data not shown).

Unexpectedly, MFI did not increase on addition of L-arginine (3mM) to intact cells. These findings are consistent with the lack of ^{15}N-nitrite/nitrate production after incubation of RBCs with exogenous ^{15}N-L-Arg[34] and indicate that constitutive red cell NOS activity does not rely on extracellular substrate supply. By contrast, treatment with the nitrosating NO donor SNOC markedly increased fluorescence intensity in a concentration-dependent manner (Figure 2B) and this was inhibited by addition of $Fe[DETC]_2$ as assessed by fluorimetry (not shown). Intermediate SNOC concentrations produced fluorescence intensity distributions distinct from those at other concentrations, suggesting cell-to-cell differences in SNOC uptake and/or metabolism (Figure 2B). Peak MFIs at maximal NO donor concentrations were similar and cell-to-cell variations small, indicative of comparable DAF-FM loading efficiencies. Thus fluorescence intensity variations at baseline likely reflect differences in constitutive NOS activity between cells. None of these treatments affected RBC morphology, as assessed in the transmitted light channel of the laser scanning microscope and by the lack of positional changes for the RBC population in the scatter dot plot using flow cytometry. Qualitatively identical results were obtained using fluorimetry (not shown). Although no changes in cell morphology or hemolysis were observed with these treatments at the concentrations used (which could have impeded flow cytometric analysis), a high NO/NOS-independent background signal was apparent using these techniques, even after correction for autofluorescence.

DAF-FM–related fluorescence in RBCs originates from reaction with NOS-derived NO

To confirm that the fluorescent signals detected by fluorimetry, laser scanning microscopy and flow cytometry were indeed because of intracellular nitrosation of DAF-FM to form DAF-FM-T, we analyzed the products of this reaction by HPLC and LC-MS/MS. A peak corresponding to DAF-FM-T (Figure 3C) was detected in loaded RBCs by reversed phase HPLC (Figure 3A). Combined use of selected reaction monitoring (ie, multiple reaction monitoring of the 413.1→369.1 and 424.1→380.1 transitions) by LC-MS/MS in parallel with HPLC allowed us to detect both DAF-FM-T and unreacted DAF-FM in RBCs pre-loaded with DAF-FM diacetate, thus providing unequivocal evidence for formation of DAF-FM-T and, therefore, constitutive NO production within RBCs (Figure 3B). Reassuringly, no peak corresponding to DAF-FM-T was detected in RBCs pre-treated with either the NOS inhibitor, L-NAME (Figure 3A middle panel and C, 10 of 12 samples; n = 5 independent experiments) or the lipophilic NO scavenger, $Fe[DETC]_2$ (Figure 3A bottom panel and D). Fluorescence quenching effects of the dark-colored $Fe[DETC]_2$ can be excluded because excess compound was removed by the washing steps before DAF-FM-T extraction.

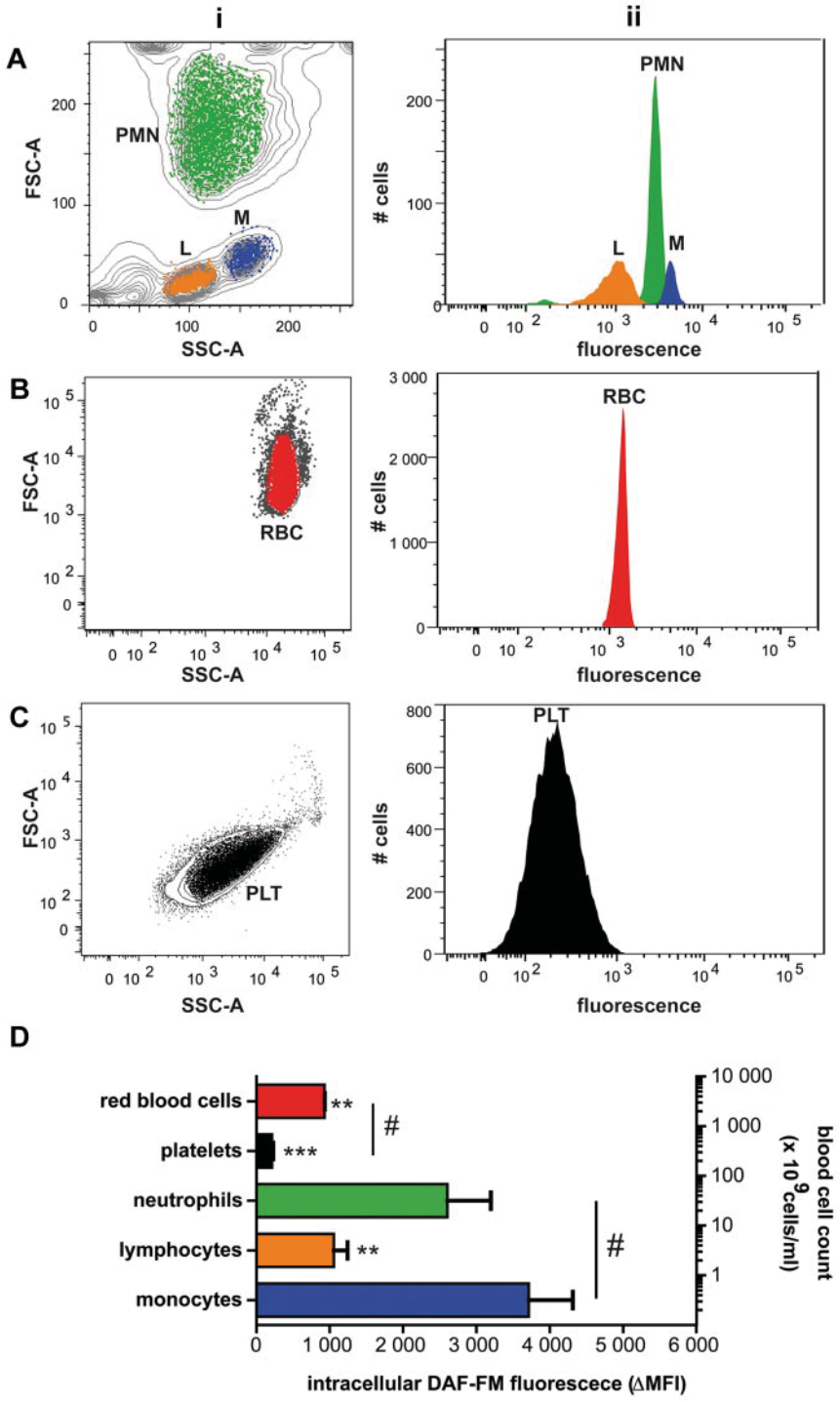

Figure 1. Hierarchy of DAF-FM–associated fluorescence intensity in human blood cells. (A-C) Blood was separated into platelet-rich plasma, leukocytes, and red blood cell fractions and loaded with DAF-FM diacetate. Blood cell subpopulations within each fraction were identified by flow cytometry on the basis of their FSC/SSC distribution (i) and by surface marker discrimination (not shown). The distribution of the green fluorescence signal measured in each gate is depicted in panel ii. L-lymphocytes, M-macrophages, PLT-platelets, PMN-polymorphonuclear granulocytes, RBC-red blood cells; SSC-side scatter, FSC-forward scatter. (D) Specific intracellular fluorescence of blood cell subpopulations (assessed as ΔMFI = median fluorescence intensity − background fluorescence) plotted in relation to blood composition (ie, relative levels of each cell in blood; right y-axis; n = 4; ANOVA $P = .0002$: Bonferroni versus monocytes $^{**}P < .01$; $^{***}P < .001$, #*t* test $P < .001$).

When plotting the area of the fluorescent peaks obtained by serial dilution of DAF-FM-T standards in RBC lysates against triazole concentrations (assuming 100% conversion efficiency of DAF-FM authentic standard into DAF-FM-T by reaction with SNOC) a linear relationship was apparent (Figure 3E; R = 0.9989; $P < .0001$). By interpolating the areas of the DAF-FM-T related peaks observed in 1.2×10^7 DAF-FM–loaded RBCs under basal conditions, we estimated that the average concentration of DAF-FM-T in these samples was 64 ± 12nM (n = 19). Assuming the reaction stoichiometry to be 1:1, the amounts of NO and/or nitrosating equivalents produced by a single RBC within 30 minutes at RT corresponds to at least 3.2×10^{-6} fmoles (Figure 3F).

RBCs contain the "classic" eNOS isoform

Having identified an intracellular constitutive NOS activity in RBCs, we next sought to isolate and identify the NOS isoform expressed in these cells. Crude hemolysates were prepared by osmotic lysis of RBC pellets with toluene/H_2O 1:1, which preserves protein structure and activity and avoids excessive dilution. We succeeded in immunoprecipitating an eNOS-like protein using a mouse monoclonal anti-eNOS antibody, either after enrichment of calmodulin-binding proteins by affinity chromatography (Figure 4A lanes 1 and 2) or directly from crude red cell lysates (Figure 4A lanes 3-4 and B). After separation of the proteins by SDS-PAGE

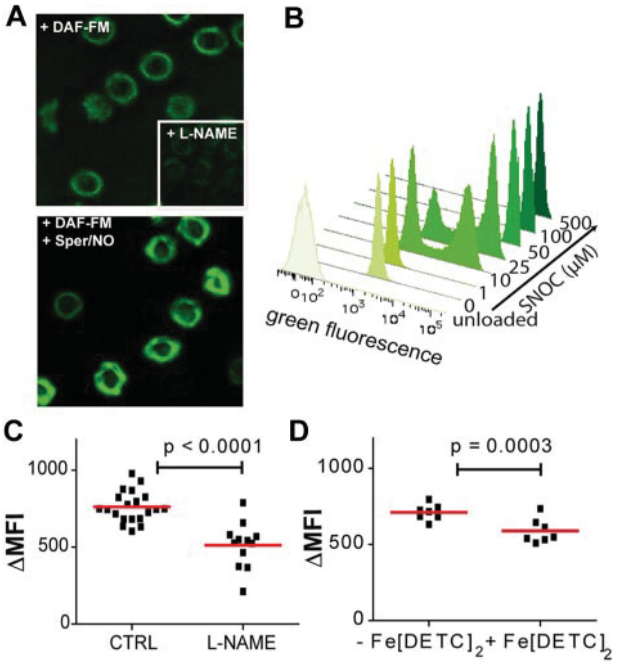

Figure 2. Visualization of intracellular NO production in RBCs. (A) Laser scanning micrographs of RBCs loaded with DAF-FM before (top) or after pretreatment with 3mM L-NAME (inset) and further incubation with 100μM Sper/NO (bottom). Please refer to "Methods" for details. (B) Fluorescence distribution plot of untreated cells (front lane), cells loaded with DAF-FM only (second lane), or further treated with 1 to 500μM SNOC (other lanes). Representative data from 6 experiments (C) Decrease in intracellular RBC fluorescence (ΔMFI) as assessed by flow cytometry after treatment with the NOS inhibitor L-NAME. (D) Intracellular RBC fluorescence (ΔMFI) after treatment with the NO scavenger $Fe[DETC]_2$. ΔMFI = median fluorescence intensity − background fluorescence.

under reducing conditions followed by coomassie staining, a band of ~135 kD was apparent in all samples (Figure 4A). The identity of this 135 kD band was confirmed by Western blotting using a polyclonal rabbit anti-human eNOS antibody (Figure 4B). Similar results were obtained using the rabbit antibody for immunoprecipitation and the mouse antibody for detection, as well as by staining the membrane with a mouse monoclonal anti-eNOS antibody directed against a different epitope of eNOS. No high-molecular-weight bands were detected if a mouse anti–human iNOS antibody was used for immunoprecipitation, or by adding antibodies and beads to a serum albumin solution.

To identify the immunoprecipitated protein(s), the 135 kD bands of 2 independent coomassie-stained gels were excised (one of them shown in Figure 4C) and subjected to analysis by liquid chromatography-mass spectrometry (LC-MS/MS). 4 different peptides all belonging to eNOS were identified. By alignment of the sequences of these peptides with those of the 3 NOS isoforms including all known splice variants of eNOS, we found that the identified peptides belong to 2 distinct, highly conserved regions of the reductase domain of the NOS protein (Figure 4D): the FMN reductase-like region (peptides 1 and 2) and the ferredoxin reductase (FNR)–like region (peptides 3 and 4) within the FAD-binding pocket (Figure 4D). All 4 peptide sequences showed 100% pairwise identity only with the full eNOS sequence, with peptides 3 and 4 aligning within a region in the C-terminal domain that is absent in the truncated splice variants. Thus, these results show that human RBCs carry a NOS3, the "classic" eNOS isoform constitutively expressed in endothelial cells.

Isolated red cell eNOS protein is catalytically active

To verify that the erythrocytic eNOS identified is indeed active we measured the ability of the immunoprecipitated protein to catalyze the in vitro conversion of ^{3}H-L-arginine to ^{3}H-citrulline in the presence of NADPH, FAD, FMN, Ca^{2+} and calmodulin. Figure 4E depicts the results from 5 independent experiments (ANOVA $P < .05$). We found that the protein is capable of producing 9.82 fmol/min citrulline under optimal substrate/cofactor supply conditions. Moreover, arginine to citrulline conversion was significantly inhibited by addition of the NOS inhibitor L-NAME (Figure 4E, IP versus IP+L-NAME $P < .05$) and markedly decreased in the absence of Ca^{2+}/calmodulin (Figure 4E, IP vs IP without Ca^{2+}/CaM; t test $P < .05$). Thus, the isolated eNOS is active and dependent on Ca^{2+}/calmodulin interaction.

Red cell eNOS expression and activity are compromised in patients with coronary artery disease

We explored endothelial function and erythrocytic eNOS expression levels and activity in patients with CAD, a condition associated with endothelial dysfunction, and age-matched healthy individuals. Clinical characteristics of the study population are summarized in supplemental Table 1. As expected, flow-mediated dilation of the brachial artery was significantly decreased in CAD patients, whereas maximal vasodilatation in response to GTN was not significantly different (supplemental Table 1). Patients with endothelial dysfunction showed a significantly lower expression of red cell eNOS compared with aged-matched healthy individuals (Figure 5A; mean red cell eNOS expression was 0.519 ± 0.083 vs 1.058 ± 0.55, unpaired t test $P < .0001$). Furthermore, univariate regression analysis revealed that erythrocytic eNOS expression correlated with endothelial function in humans ($R^2 = 0.318$, $F = 12.144$, $P = .002$; Figure 5A). Red cell eNOS activity was measured in a randomized subgroup of the study population by analyzing the conversion of ^{14}C-Arginine into ^{14}C-Citrulline catalyzed by the isolated protein (Figure 5B). We found that red cell eNOS activity was also significantly decreased in patients with endothelial dysfunction compared with the healthy control group ($P = .0337$, unpaired t test; Figure 5B). Taken together, these results indicate that human red cell eNOS activity mirrors vascular endothelial function.

Discussion

The key findings of our study are: (1) formation of NO and related nitrosative species occurs constitutively in all subtypes of human blood cells, with cell-specific intensity differences; (2) intracellular NO formation can be visualized in RBCs using diaminofluoresceins despite the abundance of the NO scavenger oxyhemoglobin and the nitrosation scavengers glutathione and ascorbate; (3) human RBCs contain a catalytically active version of the classic endothelial NOS isoform (eNOS, NOS3) that converts L-arginine to L-citrulline in a Ca^{2+}/calmodulin-dependent manner; (4) both expression and activity of red cell eNOS are compromised in CAD patients; and (5) the extent of eNOS impairment in RBCs correlates with the degree of endothelial dysfunction, demonstrating disease relevance of this blood cell derived NO activity.

Visualization of NO formation in blood cells and fluorescent probe chemistry

By comparing intracellular fluorescence intensities of different cell subpopulations from the same blood sample loaded with DAF-FM diacetate, almost the same fluorescence intensity was apparent in

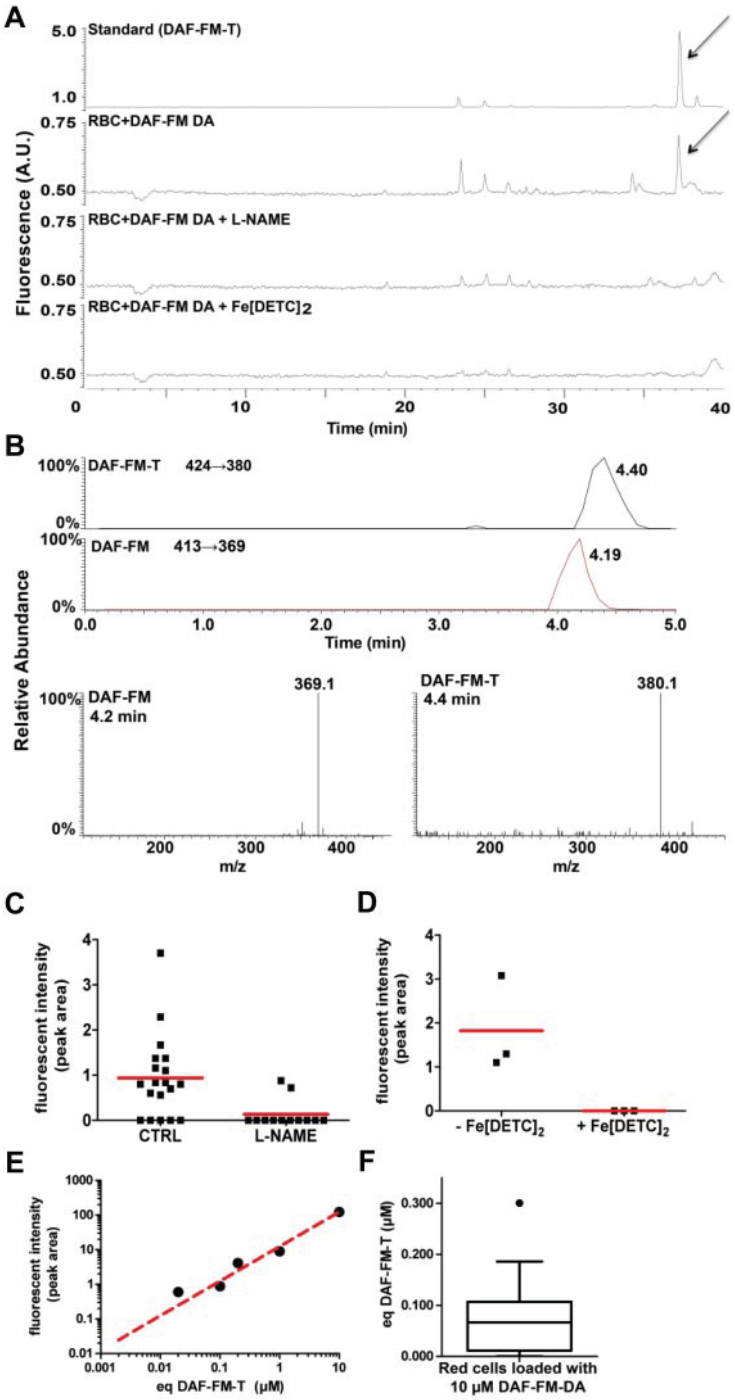

Figure 3. Suppression of NOS-mediated constitutive DAF-FM-T formation within RBCs after inhibition of NO synthesis or NO scavenging. (A) RBCs were left either untreated or pretreated with the specific NOS inhibitor L-NAME or the NO scavenger $Fe[DETC]_2$, washed, loaded with DAF-FM diacetate and analyzed by HPLC with fluorescence detection. (B) RBCs were treated as described in panel A and analyzed by LC-MS. The top panel shows the mass spectrum of the respective peaks at 4.2 minutes for DAF-FM and 4.4 minutes for DAF-FM-T. The bottom panels show the SRM chromatograms for DAF-FM-T, monitoring the fragmentation from 424 to 380 because of the loss of a CO_2 from the parent molecule, and DAF-FM monitoring the transition from 413 to 369. (C-D) DAF-FM-T related peak areas from 3 to 5 independent experiments with different blood donors; samples treated as in panel A. (E-F) Estimation of the DAF-FM-T quantities formed by constitutive NOS activity in RBCs. (E) Regression curve obtained by diluting DAF-FM-T standards in RBC lysates. Measured peak areas were plotted against DAF-FM-T concentrations, assuming 100% conversion of DAF-FM into DAF-FM-T. (F) Calculated DAF-FM-T equivalents (eq) formed in ~10^7 red cells loaded with DAF-FM diacetate and incubated for 30 minutes at room temperature. After removing the outlier (according to Tuckey, see box plot) the mean DAF-FM-T concentration in RBC was 64 ± 12nM (n = 19).

RBCs as in lymphocytes, and only ~ 2- to 3-fold lower values than in neutrophils (granulocytes) or monocytes. In blood of healthy individuals, the number of RBCs is approximately 3 orders of magnitude higher than the number of white cells. Our findings thus indicate that in the human circulation, RBCs not only transport the bulk of nitrite, the major intravascular NO storage form that becomes bioactivated under hypoxic conditions,[34] but also represent the largest cellular compartment in which NO is produced under normoxic conditions.

Although diaminofluoresceins are the most frequently used and best investigated NO imaging probes,[35,36] they do not react with NO directly. Initially, it was proposed that DAF-derivatives might interact with reactive nitrosating species derived from the reaction of NO with O_2 such as N_2O_3[37] or nitrous acid,[38] to form intermediary N-nitrosamines that are subsequently converted to the highly fluorescent triazole derivatives, DAF-2T or DAF-FM-T.[36] However, N_2O_3 is not likely to be formed efficiently in aqueous biologic environments, except in lipid membranes.[39] Therefore, Wardman[39] argued that DAFs may undergo one-electron oxidation to an anilinyl radical that subsequently reacts with NO in a radical-radical reaction. Both mechanisms are probably operating in concert inside cells. Although the former may explain the abundance of DAF-FM related fluorescence in membrane-rich compartments, the latter complicates the interpretation of results solely based on DAF-FM related fluorescence because of dependence of the latter on ROS formation. Because RBCs are particularly rich in the NO-scavenger hemoglobin

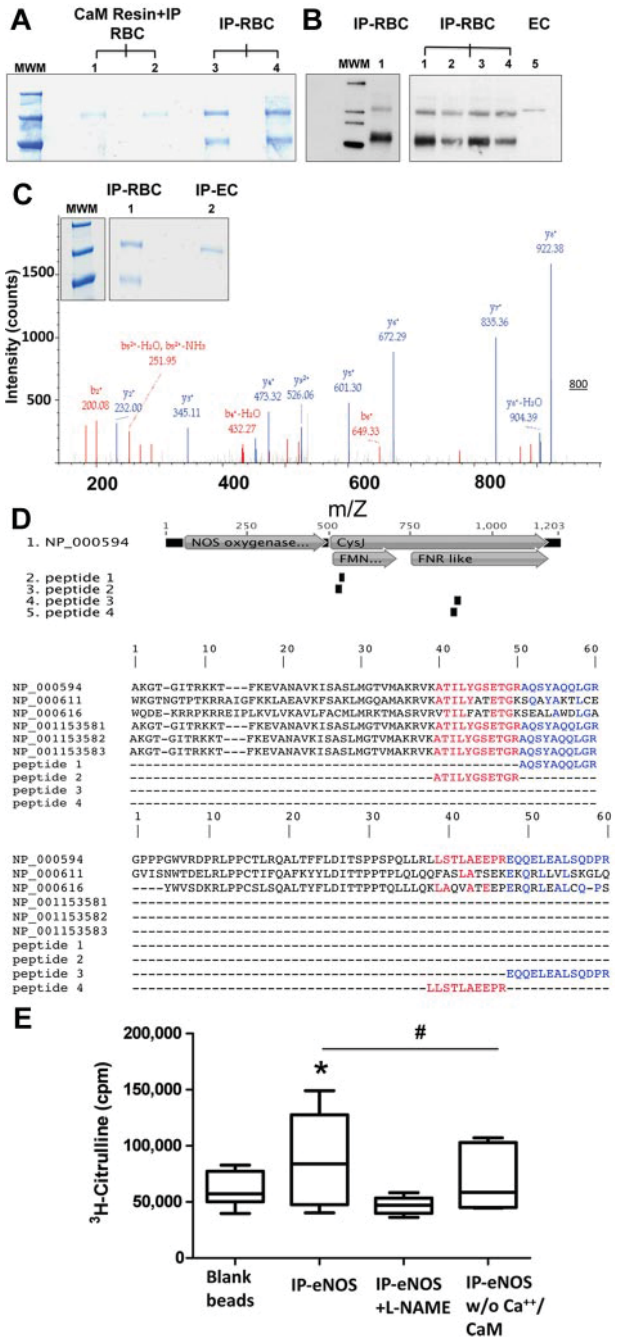

Figure 4. Human RBCs contain an active NOS3. (A) Constitutive NOS (135 kDa) was isolated from human RBCs by affinity chromatography with a calmodulin (CaM)–binding column followed by immunoprecipitation (IP) with a mouse anti–human NOS3 or directly by immunoprecipitation from crude RBC lysates (lanes 1 and 2, as well as 3 and 4 are independent samples). (B) The NOS enzyme was isolated directly from crude red cell lysates by immunoprecipitation with a mouse anti–human eNOS antibody and analyzed by Western blotting. As a control a crude EC lysate was loaded in lane 5 (MWM indicates molecular weight marker). (C) Coomassie gel used for identification purposes and representative example of peptide identification by LC-MS/MS sequencing; depicted is the fragmentation spectrum of the peptide AQSYAQQLGR. (D) Alignment of peptides identified by LC-MS/MS with sequences of nNOS, iNOS and all known eNOS splice variants. Top panel: Peptides 1 and 2 aligned within the FMN reductase-like region (FMN binding region), whereas peptides 3 and 4 aligned with the ferredoxin reductase (FNR)–like region (FAD and NADPH binding region). CysJ indicates sulfite reductase, α subunit (flavoprotein) region. NOS oxygenase indicates nitric oxide synthase eukaryotic oxygenase domain. Bottom panels: The sequences shown in detail and compared with the other NOS isoforms. The sequences of the peptides are identical with NOS3, isoform 1 only. NP_000611 = NOS1, nNOS, NP000616 = NOS2, iNOS, NP_000594 = NOS3, isoform 1. Splice variants of NOS3 are NP_001153581 = NOS3, isoform 2, NP_001153582 = NOS3, isoform 3, NP_001153583 = NOS3, isoform 4. (E) Activity

while also containing high concentrations of antioxidants, capable of scavenging nitrosating intermediates and/or reducing the oxidized probe, effective intracellular dye accumulation[28] probably accounts for the ability of diaminofluoresceins to detect NO intracellularly. Nevertheless, its detection in the vicinity of millimolar Hb in RBCs would seem to be reason enough to question the universal validity of the classic "hemoglobin NO-scavening paradigm" (see "Is red cell eNOS of relevance for cardiovascular disease?").

Origin of constitutive NO synthesis within RBCs

Using an advanced multilevel analytical approach we here provided unequivocal evidence for the conversion of DAF-FM into DAF-FM-T by NO formed by RBCs under normoxic conditions. RBCs contain both a constitutive Ca^{2+}-dependent NOS containing epitopes of an eNOS[6,15,16,25] and an active XOR.[6] Thus, enzymatic NO synthesis in RBCs might occur either via NOS-catalyzed L-arginine to citrulline conversion[15,16,18] or by XOR-mediated nitrite reduction.[6,12,40] We found that no DAF-FM-T was formed in the presence of the specific NOS inhibitors L-NAME and L-NIO, or by treating RBCs with $Fe[DETC]_2$, which is commonly used as NO spin-trap in ESR studies.[27] Similar results were obtained using flow cytometry. RBC preincubation with nitrite under normoxic conditions did not affect intracellular fluorescence either, ruling out a major role for nitrite in normoxic NO production detectable by DAF-FM. At pH 5.5 higher concentrations of nitrite ($> 200\mu M$) strongly increased intracellular fluorescence. Collectively, these results demonstrate that under normoxic conditions constitutive NO production in RBCs is largely NOS-dependent, whereas under hypoxic conditions it may involve nitrite reduction by deoxyhemoglobin,[5,11] XOR, carbonic anydrase,[13] and/or eNOS itself.[6,12]

Activity of a red cell NOS may be involved in the regulation of RBC lifespan,[41] deformability,[16,42,43] and potentially red cell velocity and blood flow.[43] This notion is in line with previous findings showing that NOS inhibitors abolish the antiplatelet effects of RBCs in vitro[15,16] and decrease the level of NO products released by isolated RBCs,[16,24] however do not affect intracellular nitrite concentrations.[44] Thus RBCs may also contribute to vascular homeostasis, independent of their "classic role" as transporters of oxygen, energy substrates and nutrients. Given the contribution RBCs make to the circulating NO pool and their role in hypoxic vasodilation[45] further studies are warranted to address its functional significance for the regulation of RBC function and beyond.

Isolation, isoform identification, and activity of red cell eNOS

Previous studies used antibodies directed against eNOS and iNOS epitopes for Western blotting or immunocytochemistry to probe for the presence of a NOS in RBCs and activity assays to measure either the RBC-dependent conversion of radiolabeled arginine into citrulline or the formation of NO oxidation products. Deliconstantinos et al isolated the protein by affinity chromatography using NADPH-binding protein affinity columns and measured L-NAME sensitive nitrite production by RBCs using a modified Griess reaction.[19] Using immunohistochemistry, Jubelin and Gierman found a protein that cross-reacted with antibodies directed against calmodulin, eNOS and iNOS,[25] whereas Western blot analysis of RBC lysates[15,20] and membranes[6,16] confirmed the presence of a

Figure 4. (continued) of immunoprecipitated red cell eNOS. The activity of NOS3 immunoprecipitated from RBCs was assessed by measuring the conversion of L-^{3}H-arginine to L-^{3}H-citrulline. Total radioactivity is expressed as counts per minute (cpm). (ANOVA $P = .0447$; Tukey IP versus IP+L-NAME $^*P < .05$; #IP versus Ca^{2+}/CaM t test $P = .0394$).

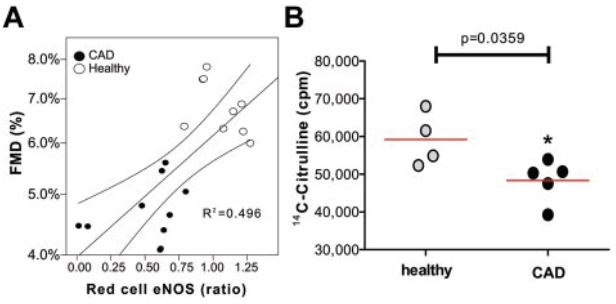

Figure 5. Changes in the red cell eNOS expression and activity in patients with endothelial dysfunction. (A) Monovariate linear correlation analysis between red cell eNOS expression as evaluated by Western blot analysis and endothelium-dependent flow mediated dilation (FMD) in patients affected with endothelial dysfunction and healthy individuals (healthy). (B) The activity of red cell eNOS was evaluated in a randomized subset of the groups by evaluating the conversion of ^{14}C-L-arg into ^{14}C-L-citrulline. Total radioactivity is expressed as counts per minute (cpm); *t* test **P* = .0359.

protein with eNOS epitopes. Two groups hypothesized that RBCs express a novel NOS isoform,[23,25] but no sequence confirmation analysis was provided.

The main technical hurdle in the biochemical characterization of proteins in RBCs is the presence of overwhelmingly high level of hemoglobin, which represents a formidable obstacle to purification, activity determination, immunostaining, and colorimetric/fluorimetric assay. In this study, we chose to isolate NOS from hemolysates under native conditions to permit combined structural and functional analysis. After purification of calmodulin-binding enzyme by affinity chromatography and immunoprecipitation using anti-eNOS antibodies, we identified a 135 kD-band by SDS-PAGE, indicating that red cell NOS contains both a calmodulin binding site and eNOS-like epitopes. Similar results were obtained when immunoprecipitation was performed directly from crude RBC lysates using different antibodies. Although these results strongly suggested that the 135 kD band isolated from RBCs was indeed an eNOS protein, further analyses were performed to obtain peptide sequences of tryptic digests by LC-MS/MS. Obtaining the sequence of 4 different peptides from 2 independent analyses permitted unequivocal identification of the protein as the classic eNOS (NOS3) isoform. Two of the 4 sequenced peptides aligned with 100% homology to the C-terminal region of eNOS, which is absent in the NOS3A-C splice variants. Less homology was observed with the sequences related to nNOS (NOS1) and iNOS (NOS2). We thus conclude that RBCs contain eNOS, the same protein that is constitutively expressed in endothelial cells. Two earlier studies suggested that RBCs also contain iNOS.[20,25] We are unable to confirm these reports as we failed to isolate any iNOS from crude human RBC lysates of healthy donors using specific anti-NOS2 antibodies for immunoprecipitation.

Although a L-NNA/L-NAME-inhibitable NOS activity was demonstrated by measuring NO metabolites or citrulline in the supernatant of intact erythrocytes[2,15,16,19] and RBC membranes,[16,23] 2 reports suggested RBCs harbor an inactive NOS.[20,22] It was important to confirm, therefore, that the protein identified as eNOS in our study was catalytically active, L-arginine:citrulline conversion was dependent on the presence of Ca^{2+}/calmodulin, and activity was inhibited by L-NAME. Although we cannot exclude the additional presence of minor amounts of other NOS isoforms in RBCs it appears that the majority of NO produced in these cells was generated by an active eNOS.

Is red cell eNOS of relevance to cardiovascular disease?

Perhaps one of the most surprising results from our studies is that red cell eNOS expression and activity significantly correlate with flow-mediated dilation, a diagnostic marker of endothelial function and eNOS activity. Similarly to endothelial eNOS dysfunction, red cell eNOS dysfunction may dependent on both decreased protein levels, and changes in regulation/catalytic activity. Impaired endothelial function, decreased eNOS activity, and/or NO bioavailability are conditions strongly related to cardiovascular disease.[26,46] Thus, a systemic eNOS deficiency and/or dysfunction appears to prevail in patients with cardiovascular disease the consequences of which are not limited to impaired vascular function, but may also affect function of platelets[47] and red blood cells.

A central challenge of any hypothesis proposing a role of RBC-derived NO in human (patho)physiology is to understand how NO formed by these cells can escape irreversible dioxygenation reaction with oxyhemoglobin, a rapid reaction known to convert NO to nitrate. A "metabolon complex" of deoxyhemoglobin, AE/band 3, carbonic anhydrase, aquaporin, and Rh-protein channels was proposed to explain nitrite protonation and may serve to facilitate the export of NO or its metabolites.[48] The localization of eNOS-immunoreactivity on the cytoplasmic side of the RBC membrane, as detected by immunogold-labeling and electron microscopy imaging,[16] supports the notion that the RBC membrane plays a central role in this process, possibly by effectively "compartmentalizing" NO production, signaling and scavenging machinery. Our results invite a rethink about the role of hemoglobin in NO biology, because its oxygenated form is considered an NO scavenger under any condition. Several factors have been identified that explain why endothelial NO escapes scavenging by hemoglobin,[8,11,45,48,49] but those discussions did not consider the possibility that NO might be produced in RBCs themselves. The observation that NO formation can be detected in the vicinity of abundant oxyhemoglobin would seem to warrant a careful reassessment of this universally accepted paradigm.

Summary and outlook

Only recently indices of RBC number, size, and function have emerged as independent risk factors of cardiovascular disease.[1-3] Not only endothelial cells, but also RBCs may contribute to NO-dependent regulation of vascular homeostasis. Our present findings suggest that red cell eNOS activity might serve the purpose of compensating for NO trapping by providing an efficient "NO shield" that maintains effective intracellular signaling. Moreover, red cell eNOS expression/activity might be a complementary diagnostic tool to assess vascular homeostasis and provide new therapeutic strategies for fighting cardiovascular disease.

Acknowledgments

The authors thank Katharina Lysaja for indispensable technical assistance; Profs Victoria Kolb-Bachofen, Dieter Häussinger, and Jeremy Spencer for allowing them to use the FluostarOPTIMA, the FACS Canto II flow cytometer, and the HPLC, respectively; and Prof Axel Gödecke for offering the use of his radioisotope facility.

This work was supported by the Deutsche Forschungsgemeinschaft (DFG 405/5-1 and FOR809 TP7 Me1821/3-1), the Anton Betz Stiftung, (26/2010), the Susanne Bunnenberg Stiftung at Düsseldorf Heart Center to M.K., and the Forschungskommission of the Medical Faculty of the Heinrich Heine University of Düsseldorf to M.M.C.-K. LC-MS analyses were conducted at the Chemical Analytical Facility, University of Reading.

Authorship

Contribution: M.M.C.-K. planned and executed experiments, analyzed data, and drafted the paper; A.R.-M. performed HPLC; R.S. recruited patients and measured FMD; G.G.C.K. ran LC-MS/MS for DAF-FM; S.T.-S., T.K., and P.H. performed experiments; C.K. carried out peptide sequencing; D.W. and C.H. assisted with the proteomics experiments and the study plan, respectively. K.-D.K. provided essential materials and intellectual input; N.H. provided essential intellectual input; M.F. provided conceptual and intellectual input and wrote the paper; and M.K. planned the study and wrote the paper.

Conflict-of-interest disclosure: The authors declare no competing financial interests.

Correspondence: Malte Kelm, Department of Cardiology, Pulmonology, and Vascular Medicine, Medical Faculty, Heinrich Heine University of Düsseldorf, Moorenstr 5, 40225 Düsseldorf, Germany; e-mail: malte.kelm@med-uni.duesseldorf.de.

References

1. Anand IS, Kuskowski MA, Rector TS, et al. Anemia and change in hemoglobin over time related to mortality and morbidity in patients with chronic heart failure: results from Val-HeFT. *Circulation*. 2005;112(8):1121-1127.
2. Kulier A, Levin J, Moser R, et al. Impact of preoperative anemia on outcome in patients undergoing coronary artery bypass graft surgery. *Circulation*. 2007;116(5):471-479.
3. Sabatine MS, Morrow DA, Giugliano RP, et al. Association of hemoglobin levels with clinical outcomes in acute coronary syndromes. *Circulation*. 2005;111(16):2042-2049.
4. Moncada S, Palmer RMJ, Higgs EA. Nitric oxide, biology pathophysiology and pharmacology. *Pharmacol Rev*. 1991;43:109-142.
5. Cosby K, Partovi KS, Crawford JH, et al. Nitrite reduction to nitric oxide by deoxyhemoglobin vasodilates the human circulation. *Nat Med*. 2003; 9(12):1498-1505.
6. Webb A, Milsom A, Rathod K, et al. Mechanisms underlying erythrocyte and endothelial nitrite reduction to nitric oxide in hypoxia: role for xanthine oxidoreductase and endothelial nitric oxide synthase. *Circ Res*. 2008;103(9):957-964.
7. Herold S. The outer-sphere oxidation of nitrosyliron(II)hemoglobin by peroxynitrite leads to the release of nitrogen monoxide. *Inorg Chem*. 2004; 43(13):3783-3785.
8. Jia L, Bonaventura C, Bonaventura J, et al. S-nitrosohaemoglobin: a dynamic activity of blood involved in vascular control. *Nature*. 1996;380: 221-226.
9. Gladwin MT, Lancaster Jr JR, Freeman BA, et al. Nitric oxide's reactions with hemoglobin: a view through the SNO-storm. *Nat Med*. 2003;9:496-500.
10. Rassaf T, Bryan NS, Maloney RE, et al. NO adducts in mammalian red blood cells: too much or too little? *Nat Med*. 2003;9:481-482.
11. Nagababu E, Ramasamy S, Albernethy R, et al. Active nitric oxide produced in the red cell under hypoxic conditions by deoxyhemoglobin-mediated nitrite reduction. *J Biol Chem*. 2003; 278:46349-46356.
12. Zweier JL, Wang P, Samouilov A, et al. Enzyme-independent formation of nitric oxide in biological tissues. *Nat Med*. 1995;1(8):804-809.
13. Aamand R, Dalsgaard T, Jensen FB, et al. Generation of nitric oxide from nitrite by carbonic anhydrase: a possible link between metabolic activity and vasodilation. *Am J Physiol Heart Circ Physiol*. 2009;297(6):H2068-H2074.
14. Ellsworth ML, Forrester T, Ellis CG, et al. The erythrocyte as a regulator of vascular tone. *Am J Physiol Heart Circ Physiol*. 1995;269(6): H2155-H2161.
15. Chen LY, Mehta JL. Evidence for the presence of L-arginine-nitric oxide pathway in human red blood cells: relevance in the effects of red blood cells on platelet function. *J Cardiovasc Pharmacol*. 1998;32:57-61.
16. Kleinbongard P, Schulz R, Rassaf T, et al. Red blood cells express a functional endothelial nitric oxide synthase. *Blood*. 2006;107(7):2943-2951.
17. Sprague RS, Stephenson AH, Dimmitt RA, et al. Effect of L-NAME on pressure-flow relationships in isolated rabbit lungs: role of red blood cells. *Am J Physiol*. 1995;269:H1941-H1948.
18. Yang BC, Nichols WW, Mehta JL. Cardioprotective effects of red blood cells on ischemia and reperfusion injury in isolated rat heart: release of nitric oxide as a potential mechanism. *J Cardiovasc Pharmacol Therapeut*. 1996;1:297-305.
19. Deliconstantinos G, Villiotou V, Stavrides JC, et al. Nitric oxide and peroxynitrite production by human erythrocytes: a causative factor of toxic anemia in breast cancer patients. *Anticancer Res*. 1995;15:1435-1446.
20. Kang ES, Ford K, Grokulsky G, et al. Normal circulating adult human red blood cells contain inactive NOS proteins. *J Lab Clin Med*. 2000;135: 444-451.
21. Mehta JL, Metha P, Li D. Nitric oxide synthase in adult red blood cells: vestige of an earlier age or a biologically active enzyme? *J Lab Clin Med*. 2000;135:430-431.
22. Böhmer A, Beckmann B, Sandmann J, et al. Doubts concerning functional endothelial nitric oxide synthase in human erythrocytes. *Blood*. 2012;119(5):1322-1323.
23. Bhattacharya S, Chakraborty PS, Basu RS, et al. Purification and properties of insulin-activated nitric oxide synthase from human erythrocyte membranes. *Arch Physiol Biochem*. 2001;109(5): 441-449.
24. Mihov D, Vogel J, Gassmann M, et al. Erythropoietin activates nitric oxide synthase in murine erythrocytes. *Am J Physiol Cell Physiol*. 2009; 297(2):C378-C388.
25. Jubelin BC, Gierman JL. Erythrocytes may synthesize their own nitric oxide. *Am J Hypertens*. 1996;9: 1214-1219.
26. Heiss C, Lauer T, Dejam A, et al. Plasma nitroso compounds are decreased in patients with endothelial dysfunction. *J Am Coll Cardiol*. 2006;47: 573-579.
27. Kleschyov AL, Mollnau H, Oelze M, et al. Spin trapping of vascular nitric oxide using colloid Fe(II)-diethyldithiocarbamate. *Biochem Biophys Res Commun*. 2000;275(2):672-677.
28. Rodriguez J, Specian V, Maloney R, et al. Performance of diamino fluorophores for the localization of sources and targets of nitric oxide. *Free Radic Biol Med*. 2005;38(3):356-368.
29. Giblett E, Anderson J. Electrophoretic analysis of polymorphic red cell enzymes. In: *Red Cell Metabolism*. Beutler E. Edinburgh, United Kingdom: Churchill Livingstone; 1986;108-123.
30. Cortese MM, Suschek CV, Wetzel W, et al. Zinc protects endothelial cells from hydrogen peroxide via Nrf2-dependent stimulation of glutathione biosynthesis. *Free Radic Biol Med*. 2008;44(12): 2002-2012.
31. Kang D, Gho YS, Suh M, et al. Highly sensitive and fast protein detection with coomassie brilliant blue in sodium dodecyl sulfate-polyacrylamide gel electrophoresis. *I Bull Korean Chem Soc*. 2002;23(11):1511-1512.
32. Bredt DS, Schmidt HHHW. The citrullin assay. In: *Methods in Nitric Oxide Research*. Feelisch M, Stamler JS, eds. Chichester, United Kingdom: John Wiley and Son; 1996;249-255.
33. Jourd'heuil D. Increased nitric oxide-dependent nitrosylation of 4,5-diaminofluorescein by oxidants: implications for the measurement of intracellular nitric oxide. *Free Radic Biol Med*. 2002; 33(5):676-684.
34. Dejam A, Hunter CJ, Pelletier MM, et al. Erythrocytes are the major intravascular storage sites of nitrite in human blood. *Blood*. 2005;106(2):734-739.
35. Hong H, Sun J, Cai W. Multimodality imaging of nitric oxide and nitric oxide synthases. *Free Radic Biol Med*. 2009;47(6):684-698.
36. Nagano T, Yoshimura T. Bioimaging of nitric oxide. *Chem Rev*. 2002;102(4):1235-1270.
37. Nakatsubo N, Kojima H, Kikuchi K, et al. Direct evidence of nitric oxide production from bovine aortic endothelial cells using new fluorescence indicators: diaminofluoresceins. *FEBS Lett*. 1998; 427(2):263-266.
38. Williams DL. *Nitrosation reactions and the chemistry of nitric oxide*. Elsevier; 2004.
39. Wardman P. Fluorescent and luminescent probes for measurement of oxidative and nitrosative species in cells and tissues: progress, pitfalls, and prospects. *Free Radic Biol Med*. 2007;43(7):995-1022.
40. Godber BLJ, Doel JJ, Sapkota GP, et al. Reduction of nitrite to nitric oxide catalyzed by xanthine oxidoreductase. *J Biol Chem*. 2000;275(11): 7757-7763.
41. Lang KS, Lang PA, Bauer C, et al. Mechanisms of suicidal erythrocyte death. *Cell Physiol Biochem*. 2005;15(5):195-202.
42. Bor-Kucukatay M, Wenby RB, Meiselman HJ, et al. Effects of nitric oxide on red blood cell deformability. *Am J Physiol Heart Circ Physiol*. 2003;284:H1577-H1584.
43. Horn P, Cortese-Krott MM, Keymel S, et al. Nitric oxide influences red blood cell velocity independently of changes in the vascular tone. *Free Radic Res*. 2011;45(6):653-661.
44. Vitturi DA, Teng X, Toledo JC, et al. Regulation of nitrite transport in red blood cells by hemoglobin oxygen fractional saturation. *Am J Physiol Heart Circ Physiol*. 2009;296(5):H1398-H1407.
45. Crawford JH, Isbell TS, Huang Z, et al. Hypoxia, red blood cells, and nitrite regulate NO-dependent hypoxic vasodilation. *Blood*. 2006;107(2):566-574.
46. Rassaf T, Heiss C, Hendgen-Cotta U, et al. Plasma nitrite reserve and endothelial function in the human forearm circulation. *Free Radic Biol Med*. 2006;41(2):295-301.
47. Gkaliagkousi E, Ritter J, Ferro A. Platelet-derived nitric oxide signaling and regulation. *Circ Res*. 2007;101(7):654-662.
48. Gladwin MT, Schechter A, Kim-Shapiro DB, et al. The emerging biology of the nitrite anion in signaling, blood flow and hypoxic nitric oxide homeostasis. *Nat Chem Biol*. 2005;1:308-314.
49. Kim-Shapiro DB, Schechter AN, Gladwin MT. Unraveling the reactions of nitric oxide, nitrite, and hemoglobin in physiology and therapeutics. *Arterioscler Thromb Vasc Biol*. 2006;26(4):697-705.

Free Radical Biology and Medicine 53 (2012) 2146–2158

Contents lists available at SciVerse ScienceDirect

Free Radical Biology and Medicine

journal homepage: www.elsevier.com/locate/freeradbiomed

Methods in Free Radical Biology and Medicine

A multilevel analytical approach for detection and visualization of intracellular NO production and nitrosation events using diaminofluoresceins

Miriam M. Cortese-Krott [a,*], Ana Rodriguez-Mateos [b], Gunter G. C. Kuhnle [b], Geoff Brown [c], Martin Feelisch [d], Malte Kelm [a]

[a] Cardiovascular Research Laboratory, Department of Cardiology, Pneumology, and Angiology, Medical Faculty, Heinrich Heine University, Düsseldorf 40225, Germany
[b] Department of Food and Nutritional Sciences, Reading, UK
[c] Department of Chemistry, University of Reading, Reading, UK
[d] Clinical & Experimental Sciences, Faculty of Medicine, University of Southampton, Southampton General Hospital, Southampton, UK

ARTICLE INFO

Article history:
Received 4 July 2012
Received in revised form
5 September 2012
Accepted 12 September 2012
Available online 28 September 2012

Keywords:
Nitric oxide
Fluorescence imaging
DAF-FM
DAF-2
Nitrosation
Red blood cells
Free radicals

ABSTRACT

Diaminofluoresceins are widely used probes for detection and intracellular localization of NO formation in cultured/isolated cells and intact tissues. The fluorinated derivative 4-amino-5-methylamino-2′,7′-difluorofluorescein (DAF-FM) has gained increasing popularity in recent years because of its improved NO sensitivity, pH stability, and resistance to photobleaching compared to the first-generation compound, DAF-2. Detection of NO production by either reagent relies on conversion of the parent compound into a fluorescent triazole, DAF-FM-T and DAF-2-T, respectively. Although this reaction is specific for NO and/or reactive nitrosating species, it is also affected by the presence of oxidants/antioxidants. Moreover, the reaction with other molecules can lead to the formation of fluorescent products other than the expected triazole. Thus additional controls and structural confirmation of the reaction products are essential. Using human red blood cells as an exemplary cellular system we here describe robust protocols for the analysis of intracellular DAF-FM-T formation using an array of fluorescence-based methods (laser-scanning fluorescence microscopy, flow cytometry, and fluorimetry) and analytical separation techniques (reversed-phase HPLC and LC-MS/MS). When used in combination, these assays afford unequivocal identification of the fluorescent signal as being derived from NO and are applicable to most other cellular systems without or with only minor modifications.

Introduction

Nitric oxide (NO; nitrogen monoxide) is a key signaling molecule that fulfills crucial regulatory functions in physiology and pathophysiology [1]. It is produced by virtually every cell throughout all organ systems via various enzymatic and nonenzymatic routes, and its chemistry and biochemistry are tightly linked to its biological function [2,3]. The reactivity of NO in biological systems depends on the rate of formation, the resultant local concentration, the localization of the NO source, the biological targets and reactants in its vicinity, as well as the rate of diffusion within the cell or tissue [2]. In addition to the direct actions of locally formed NO, its tonic production gives rise to the formation of even longer-lived adducts and metabolites, which can act as transport and storage forms of NO.

The measurement of NO and its metabolites in complex biological matrices is notoriously difficult and technically demanding because of the relatively low concentrations of NO and its complex interaction with various other biological constituents [4–9]. Methods for the detection of intracellular NO production include (1) chemiluminescence techniques using the reaction of NO with ozone (gas phase) [4–9] or with molecules such as lucigenin and luminol/H_2O_2 (liquid phase) [10]; (2) fluorimetry using fluorescent NO-specific probes [11–15]; (3) spectrophotometry monitoring either the formation of NO–hemoglobin or the co-oxidation reaction with oxyhemoglobin to form methemoglobin and nitrate [16]; (4) EPR spectrometry using hemoglobin, nitronyl nitroxides, and iron–dithiocarbamate complexes as spin traps [17,18]; (5) electrochemical methods using (micro)electrodes specific to NO [19]; and, theoretically, (6) gas chromatography and mass spectrometry (although detection limits achieved may prevent its direct detection in most cases). Other indirect assays include spectrophotometric, fluorimetric, or radiometric assays measuring the rather more stable NO metabolites nitrite and nitrate or the by-product of L-arginine oxidation by nitric oxide synthases, L-citrulline [4]. All these methods have a distinct specificity, sensitivity, reproducibility, and technical demand/feasibility.

* Corresponding author. Fax: +0211 8115493.
E-mail address: miriam.cortese@uni-duesseldorf.de (M.M. Cortese-Krott).

0891-5849/$ - see front matter © 2012 Elsevier Inc. All rights reserved.
http://dx.doi.org/10.1016/j.freeradbiomed.2012.09.008

Despite all the limitations and pitfalls [20,21] the use of fluorescent probes to detect the formation of reactive oxygen and nitrogen species in cells and tissues has strongly contributed to the development of research in the field of free radical biology and medicine. In addition to the qualitative confirmation of free radical production in various experimental models, in some cases these reagents have allowed useful insights into their subcellular compartmentalization. Moreover, fluorescent probes are relatively cheap and signals can be detected by standard bench equipment such as fluorimeters, flow cytometers, and fluorescence microscopes. The experimental setup (including the appropriate controls) and the analytical methods chosen to detect the formation of fluorescent products ought to be carefully evaluated, because these molecules are seemingly easy *to use*, yet not necessarily easy *to apply* [20,21]. This is particularly true for 4,5-diaminofluorescein (DAF-2) and its derivatives (DAFs), originally synthesized by Nagano and colleagues [11,12]. These compounds have become the most popular and widely used fluorescent probes for the measurement of NO production in mammalian cells [15] and tissues [12,22], as well as in invertebrates and plants [12,23]. NO-dependent fluorescent product formation in cells and tissues has been mainly evaluated using fluorescence microscopy, flow cytometry, and fluorimetry [12,15,22], but the specificity of this approach has been questioned repeatedly [20,24,25]. In fact, these techniques are not able to distinguish the NO-specific fluorescent signal produced by the triazole derivates from nonspecific fluorescent products formed by reaction with other biological cell constituents within cells [12,22,26–28]. Although additional controls have been included by some investigators to exclude that changes in, e.g., ascorbate may have contributed to the measured changes in DAF-related fluorescence, not all possibilities for false positives may be known to date. Other uncertainties relate to the cellular redox status, which may also affect the intensity of the fluorescent signal that is observed, together with a high background due to preferential accumulation of DAFs within certain compartments and autofluorescence of cells and tissues [22]. This may make it difficult to detect basal NO production and, in some cases, prevent investigators from picking up a signal altogether. Most of these problems can be tackled by appropriate combination of techniques, in particular those that provide independent structural confirmation of the identity of reaction products. To this end, we here provide a multilevel analytical approach that combines fluorescence-based techniques (confocal laser scanning "live" cell microscopy, flow cytometry, and fluorimetry) with analytical separation techniques (high-performance liquid chromatography (HPLC) and LC coupled with tandem mass spectrometry (LC-MS/MS)) applicable to the detection of NO formation in cells. Combining single-cell analysis techniques such as flow cytometry and microscopy with liquid chromatography and mass spectrometry allows 4-amino-5-methylamino-2′,7′-difluorofluorescein (DAF-FM) (and related probes) to be used for unequivocal identification of NO formation and visualization of its production in cells and tissues.

Principles

DAF-FM is a fluorinated DAF-2 derivative with improved NO sensitivity, pH stability, and resistance to photobleaching [13].

For NO imaging with DAFs, cells are typically loaded with the respective diacetate derivative (e.g., DAF-FM-DA), which is cleaved by intracellular esterases to form the negatively charged parent compound, e.g., DAF-FM (Fig. 1). The latter cannot cross the cell membrane and thus accumulates inside the cells. In the presence of NO and oxygen a highly fluorescent triazole (DAF-FM-T) is formed. An increased fluorescence activity compared to the background can be detected by using an appropriate fluorescence detector.

DAFs are the most frequently used and best investigated NO imaging probes [25,29]. However, it is important to point out that these probes do not directly react with NO. The precise reaction chemistry and the mechanisms leading to triazole formation inside cells are still unknown. Two different mechanisms have been proposed, which are summarized in Fig. 1. Initially, Nagano and colleagues proposed that one of the vicinal amino groups of the DAFs interacts with reactive nitrosating species derived from the reaction of NO with O_2, such as N_2O_3 [15] or nitrous acid [14], to form an intermediary *N*-nitrosamine that—after intramolecular reaction with the adjacent amino group—is subsequently converted to the highly fluorescent triazole derivative, DAF-2-T or DAF-FM-T [25]. Later, Wardman pointed out that N_2O_3 is not likely to be formed efficiently in aqueous biological environments, except in lipid membranes [20]. He argued that in the cytosol, formation of N_2O_3 may not be necessary, as the formation of the

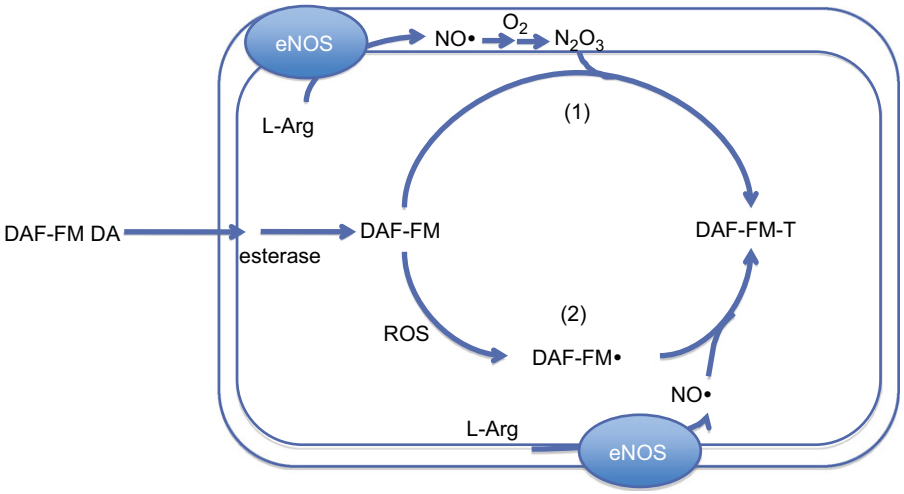

Fig. 1. Possible mechanisms of intracellular DAF-FM nitrosation within a cell having a source of NO. Endothelial NO synthase (eNOS) was chosen here simply as an example of an intracellular NO source; alternative sources of NO may originate from nitrite reduction and preformed storage forms of NO (not shown here for sake of simplicity). DAF-FM diacetate (DAF-FM-DA) diffuses into cells, where esterases hydrolyze the diacetate residues thereby trapping DAF-FM within the intracellular space. Here, DAF-FM reacts with NO (or derived molecules) to form the highly fluorescent corresponding triazole (DAF-FM-T). Two mechanisms have been proposed: (1) nitrosating species (such as dinitrogen trioxide, N_2O_3) formed by reaction of NO with oxygen, which are preferentially formed within the membrane, nitrosate DAF-FM to yield DAF-FM-T. (2) Alternatively, DAF-FM may be oxidized by reactive oxygen species (ROS) produced within the cells to a radical intermediate (DAF-FM$^{\bullet}$) that reacts directly with NO.

fluorescent triazole may occur—in analogy with lucigenin and luminol—in two stages, comprising a one-electron oxidation step to an anilinyl radical that subsequently reacts with NO in a radical–radical reaction [20]. This implies that DAF-2 derivatives after activation may detect both NO and N_2O_3, but also that these probes are susceptible to interference toward any reagent that serves to modify the steady-state concentration of the intermediate radical, including (1) oxidants, increasing its formation, and (2) antioxidants, potentially decreasing its formation (or reducing the oxidized probe) [20]. Indeed, Jourd'heuil observed an increase in the NO-dependent fluorescence signal of DAF-2 in the presence of oxidants [28]. Because high concentrations of antioxidants present in cells are able to scavenge nitrosating intermediates and/or reduce the oxidized probe, some of us argued that DAF-2 derivatives must be present at high, millimolar concentrations to allow detection of nitrosative chemistry inside cells [22].

An important aspect of consideration is the choice of method for measuring the formation of the fluorescent triazole. Methods that merely detect changes in fluorescence intensity, including fluorimetry, microscopy, and flow cytometry, cannot distinguish between specific (both NO- and DAF-dependent) and nonspecific (DAF-dependent but NO-independent) fluorescence signals. The latter could also be derived by formation of fluorescent adducts of DAFs with ascorbate and dehydroascorbate [27] or reaction with $HgCl_2$, as reported [22]. Although principally producing comparable results, these assays differ somewhat in selectivity; a side-by-side comparison of fluorescence-based techniques, as presented here later on, offers valuable insight into technique-specific assay characteristics. On the other hand, chromatographic separation techniques with fluorescence detection allow positive identification of the reaction products formed from DAFs inside cells.

All protocols presented in this paper have been optimized for one of the most challenging of biological targets, the human red blood cell (RBC). This contains not only high levels of low-molecular-weight antioxidants, such as glutathione and ascorbate, but also an abundance of hemoglobin, which have the ability to interfere with DAF-based detection by trapping NO, reacting with reactive nitrogen oxide species; affect DAF radical formation; and affect fluorescence quenching. In most cases, these assays can be applied without further change to other cellular systems.

Materials

(1) 4-Amino-5-methylamino-2′,7′-difluorofluorescein diacetate, Invitrogen (Karlsruhe, Germany), Cat. No. D-23844;
(2) 4-Amino-5-methylamino-2′,7′-difluorofluorescein, authentic standard, HPLC-grade, Sigma–Aldrich (Poole, UK), Cat. No. D1821-1 MG;
(3) BD-Falcon centrifuge and test tube, 50 ml, BD Bioscience (Heidelberg, Germany), Cat. No. 352098;
(4) BD-Falcon centrifuge and test tube, 5 ml, BD Bioscience, Cat. No. 352003;
(5) Cysteine hydrochloride (Cys–HCl), Sigma–Aldrich, Cat. No. C1276-10G;
(6) Eppendorf tubes, 1.5 ml, Axygen, Fisher Scientific, Cat. No. MTC-150-C;
(7) Eppendorf Safe-Lock microcentrifuge tubes, VWR International GmbH (Darmstadt, Germany), Cat. No. CA21008-960;
(8) Formic acid, HPLC grade, Fisher Scientific (Loughborough, UK), Cat. No. F/1900/PB17; acetonitrile, HPLC grade, Fisher Scientific, Cat. No. A/0626/17;
(9) HPLC vials from Chromacol, Fisher Scientific, Cat. No. VGA-100–145F;
(10) Hydrochloric acid (HCl), 5 M, Fisher Scientific, Cat. No. M/4056/17; sodium hydroxide (NaOH), Fisher Scientific, Cat. No. S/4920/53;
(11) Luna 3C18(2) 100 A guard cartridges, Phenomenex (Torrance, CA, USA), Cat. No. AJ0-4287;
(12) Luna C18(2) column (4.6 μm × 250 mm; 5 μm particle size), Phenomenex, Cat. No. 00F-4251-E0;
(13) C18(2) column (50 mm × 2.1 mm), Phenomenex, Cat. No. 00F-4251-E0;
(14) Methanol, HPLC grade, Fisher Scientific, Cat. No. M/4056/17;
(15) Sodium nitrite, pro analysis, ACS grade, Sigma–Aldrich, 31443-100 G;
(16) Phosphate-buffered solution (PBS), PAA Laboratories GmbH (Cölbe, Germany), Cat. No. H15-002;
(17) Sphero Rainbow calibration particles (six peaks), 6.0–6.4 μm, BD Bioscience, Cat. No. 556288;
(18) Trifluoroacetic acid, HPLC grade, Fisher Scientific, Cat. No. T/3258/PB05;
(19) Water, HPLC grade, Fisher Scientific, Cat. No. W/0106/17.

Instrumentation

(1) Analytical balance (sensitive to 0.1 mg);
(2) Pipettes;
(3) Water bath with shaking function or incubator/shaker for Eppendorf tubes;
(4) Centrifuge for 15- to 50-ml tubes and benchtop centrifuge, Rotina 38 R and Mikro 200 R, Hettich Lab Technology (Tuttlingen, Germany);
(5) Fluorimeter, FLUOstar Optima, equipped with fluorescence filters for excitation 485 nm and emission 520 nm, BMG Labtech (Offenburg, Germany);
(6) Flow cytometer, FACS Canto II; flow cytometric data were collected using the DIVA 5.0 software package and analyzed using FlowJo version 7.5.5 (TreeStar, Ashland, OR, USA);
(7) Laser-scanning microscope, Zeiss LSM 510 confocal, Carl Zeiss Jena GmbH (Jena, Germany), equipped with a Zeiss Plan Neofluar 63 × /1.3 oil DIC objective, 488 nm argon laser, and UV/488/543/633 nm beam splitter; fluorescence was recorded using a 540–30 nm bandpass filter, and micrographs were taken at 37 °C in a thermostated observation chamber;
(8) Agilent 1100 Series HPLC system, Agilent Technologies (Palo Alto, CA, USA), equipped with a quaternary pump (G1211A), an online vacuum degasser (G1379A), a thermostated autosampler (G1329A, G1330B), a thermostated column compartment (G1316A), a diode array detector (G1315B), and a fluorescence detector (G1321A);
(9) Mass spectrometer, Agilent 6400 triple–quadrupole LC-MS/MS instrument, Agilent Technologies, operated in positive-ion mode;
(10) Mass spectrometer, LTQ OrbiTrap, Thermo Fisher Scientific (Bremen, Germany);
(11) NMR spectrometer, 700 MHz on a Bruker Avance III spectrometer, Bruker Biospin (Fällanden, Switzerland).

Protocol

Visualization of NO-related nitrosation of DAF-FM within RBCs by laser-scanning microscopy, flow cytometry, and fluorimetry

Loading cells with DAF-FM-DA allows for visualization of NO-related nitrosation of DAF-FM within the intracellular space

using either live cell laser-scanning microscopy or flow cytometry. The former allows gaining insight into and documenting intracellular compartmentalization (e.g., to study NO formation in specific cell organelles), whereas the latter has the advantage of being able to look at larger cell numbers and the distribution of NO production across cell populations. Alternatively, changes in cell fluorescence can also be quantified by fluorimetry, although this does not allow morphological analysis or localization of the signal. Related protocols consist of loading cells with the probe by incubating them at room temperature or 37 °C for 15–60 min in the dark, washing to remove excess probe, and measuring the fluorescence activity with the technique of choice (Fig. 2). The nitrosating agent and NO donor *S*-nitrosocysteine (SNOC) may be applied as a positive control using the protocol described below [30]; for the preparation of stock solutions of other NO donors see [31]. In addition, an unloaded aliquot of cells should be kept to control for autofluorescence (Fig. 2). We recommend refraining from fixing cells to avoid interference or false positives due to the fixation process. Adherent cells might be cultured directly on coverslips [32], or in 96-well plates, and are detached by controlled proteolysis just before flow cytometric analysis.

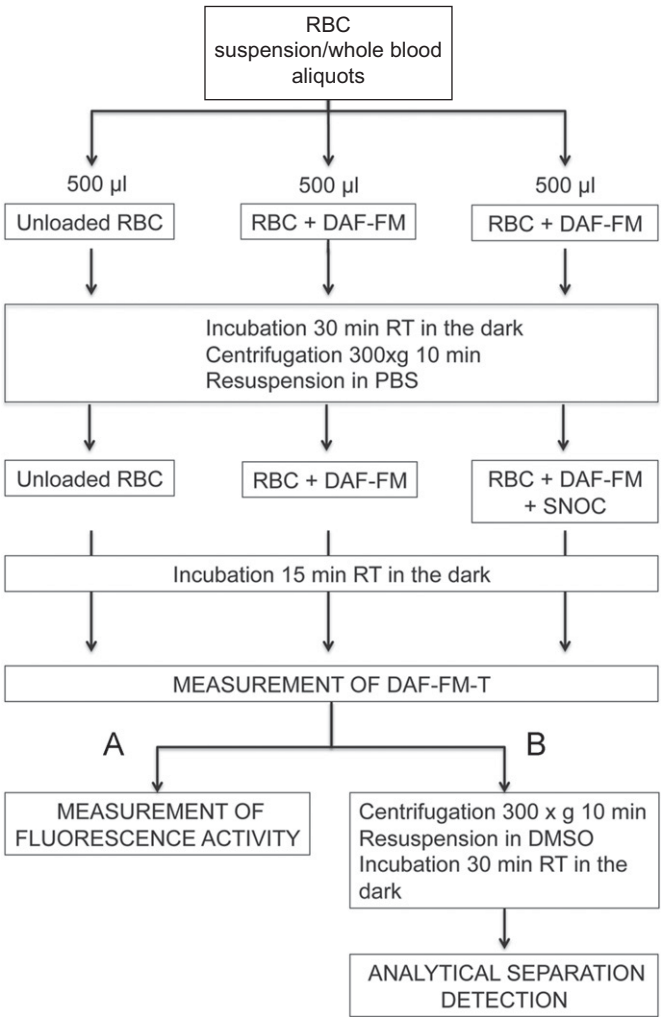

Fig. 2. Schematic representation of the DAF-FM loading protocol using red blood cells (RBCs) as an exemplary cellular system. Formation of the fluorescent product DAF-FM-T may be detected (A) by measurement of fluorescence activity using fluorescence microscopy, fluorimetry, or flow cytometry or (B) using analytical separative techniques.

Synthesis of SNOC (100 mM) [30]

(1) Dissolve 7.04 mg Cys–HCl in 192 µl double-distilled H_2O and keep on ice until use.
(2) Dissolve 2.76 mg $NaNO_2$ in 192 µl double-distilled water and keep on ice until use.
(3) Mix 192 µl Cys–HCl + 192 µl $NaNO_2$ + 8 µl 1 M HCl.
(4) Incubate 1 min at room temperature (RT); color of the solution will change to red.
(5) Equilibrate pH by adding 7–8 µl 1 M NaOH and use immediately.

Live cell laser-scanning microscopy

(1) Collect blood (1–2 ml) from the antecubital vein of healthy volunteers and add heparin (5000 U/ml).
(2) Dilute whole blood 1:10 in cold PBS and prepare 500-µl aliquots in amber Eppendorf tubes to protect DAF-FM from light.
(3) Add 1–3 µl 5 mM DAF-FM-DA (prepare by dissolving 5 µg in 20 µl dimethyl sulfoxide (DMSO) and use immediately; *do not place on ice, to avoid freezing of DMSO*). The final concentration will be 10–30 µM DAF-FM. Incubate for 30 min at RT in the dark. Keep an untreated blood aliquot as an autofluorescence control.
(4) Wash by centrifugation at 300 *g* for 10 min at 4 °C and resuspend in PBS.
(5) Add 25–100 µM SNOC and incubate for 15 min (as positive control) or leave untreated.
(6) Prepare blood smears on a glass slide with 10 µl sample.
(7) Analyze 1–2 min after preparation under a Zeiss LSM 510 confocal laser-scanning microscope (Carl Zeiss Jena GmbH) using a Zeiss Plan Neofluar 63 × /1.3 oil DIC objective and excitation

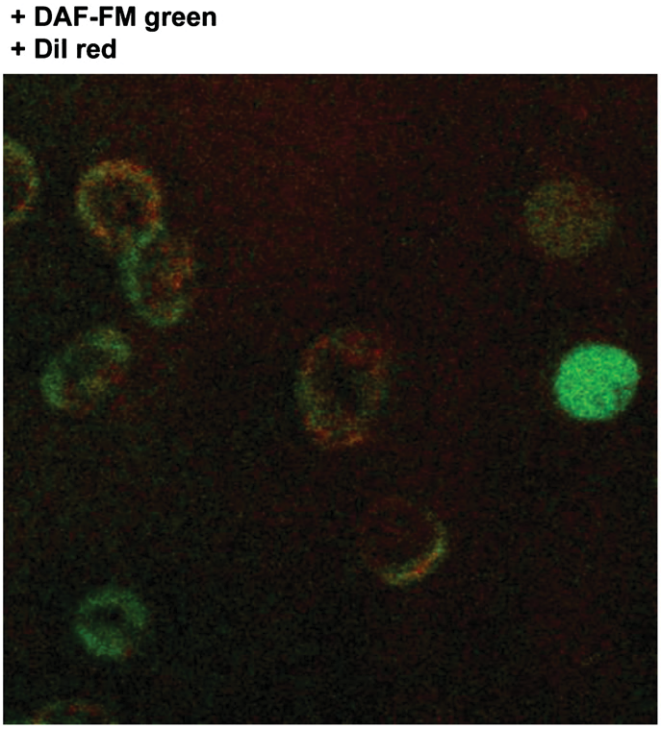

Fig. 3. Visualization of NO-related nitrosation of DAF-FM within RBCs. Micrograph of RBCs loaded with DAF-FM and the membrane stain Dil shows colocalization of the DAF-FM green fluorescence within the membrane. Representative data from 2–10 individual experiments.

488 nm with UV/488/543/633 nm beam splitter. Fluorescence should be recorded using a 540–30 nm bandpass filter.
Representative results are shown in Fig. 3.
Caveat: Exposure time should be adjusted on the SNOC-treated samples and kept constant during all measurements.

Flow cytometry

(1) Collect blood (10–12 ml) from the antecubital vein of healthy volunteers and add heparin (5000 U/ml).
(2) Dilute 1:500 in cold PBS by adding 30 µl to 15 ml PBS.
(3) Divide into 500-µl aliquots in amber Eppendorf tubes.
(4) Add 1 µl 5 mM DAF-FM-DA (dissolve 5 µg in 20 µl DMSO, and use immediately); final concentration will be 10 µM.
(5) Incubate for 30 min at RT.
(6) Wash by centrifugation at 300 g for 10 min at 4 °C.
(7) Resuspend in PBS; as a positive control add NO donors (Fig. 2).
(8) Dilute 1:3 in PBS and read fluorescence in a flow cytometer within 15 min.

The RBC population can be visualized in a double-logarithmic scatter-dot plot (foreword scatter vs side scatter). DAF-FM was excited with the 488-nm spectral line of the flow cytometer 488 nm argon laser and the signal was collected within the FITC channel (em 530 ± 30 nm). Data were collected using the flow cytometer software package (here we used DIVA 5.0; BD Bioscience).

Representative results are shown in Fig. 4.
Caveat: To standardize and ensure reliability of fluorescence acquisition, fluorescence acquisition voltage should be adjusted before each measurement according to the position of the fluorescence histogram of both the unstained control and the third fluorescence peak of standard latex beads (Rainbow beads; BD Bioscience).

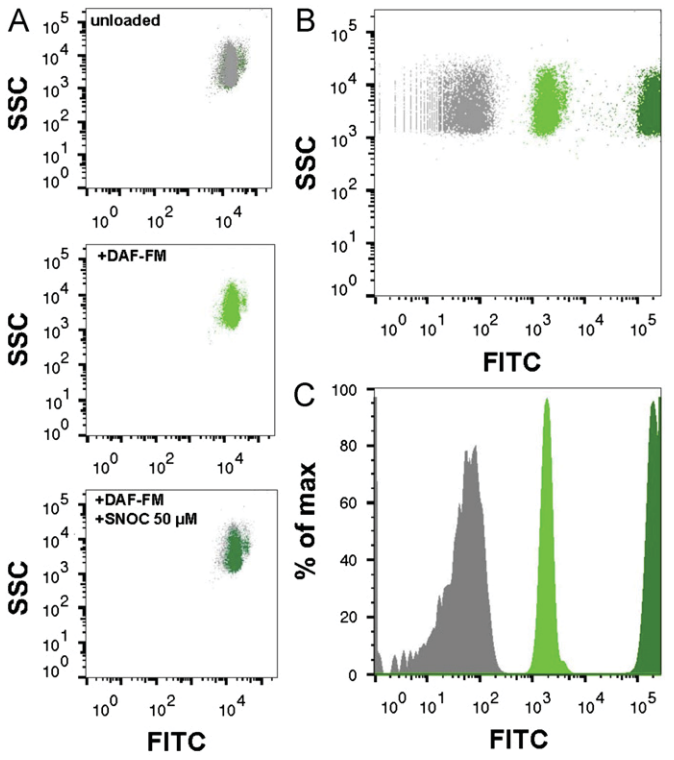

Fig. 4. Flow cytometric analysis of RBCs loaded with DAF-FM-DA. (A) Morphology of the RBC populations in a double-logarithmic scatter-dot plot. (B) Side scatter-fluorescence dot plot of unloaded cells, cells loaded with DAF-FM, and cells loaded with DAF-FM and treated with the NO donor, SNOC. (C) Fluorescence intensity distribution histogram. Representative data of $n=6$ experiments.

Fluorimetry

(1) For fluorimetric measurements follow steps 1–7 as described for flow cytometry, and refer to Table 1.
(2) Load 200 µl of samples/well in a dark 96-well plate and measure green fluorescence (ex 485, em 520).
Representative results are shown in Fig. 5.
Caveats: To ensure reproducibility of the measurements samples should be kept on ice and analyzed within 15 min. The gain should be adjusted in well mode by choosing the sample treated with SNOC (i.e., well within expected maximal intensity). Excitation time should be kept at a minimum as the fluorescence signal of fluorescein-based molecules increases on repeated exposure to light.

Analysis of DAF-FM and DAF-FM-T standards by reversed-phase HPLC and LC-MS/MS

To the best of our knowledge, no validated DAF-FM-T standard is available commercially. We prepared DAF-FM-T by reaction of DAF-FM authentic standard with SNOC (prepared as described above) and verified the purity of either stock solution by HPLC. Furthermore, we fully characterized the structure of DAF-FM by NMR and established the fragmentation patterns of both DAF-FM and DAF-FM-T by high-resolution MS (Figs. 6, 7, and 8). DAF-FM-T can be detected by HPLC with fluorescence detection, as well as by LC-MS/MS using selective-reaction monitoring (SRM) using the transition of 413.2→369.12 for DAF-FM and 424.2→380.1 for DAF-FM-T detection. Further details of the fragmentation reactions were investigated using ion trap experiments and D_2O exchange.

Preparation of DAF-FM-T

(1) Dissolve DAF-FM authentic standard (1 g) at a final concentration of 5 mM in HPLC-grade DMSO, divide into working aliquots, and keep frozen at −80 °C until use.
(2) Prepare DAF-FM-T standards by reaction of 50 µM DAF-FM with 1 mM SNOC in PBS for 30 min in the dark.

The reactants are shown in Fig. 6A.

Reversed-phase HPLC

This protocol is a modification of the method described by Rodriguez et al. for DAF-2 [22]. The method was run on an Agilent 1100 Series HPLC system (Agilent Technologies) equipped with a diode array detector and a fluorescence detector.

The column used was a Phenomenex Luna C18(2) column (4.6 µm × 250 mm; 5 µm particle size) fitted with a guard column (Phenomenex) kept constant at 25 °C.

The mobile phases were prepared as follows:

(1) Solvent A, 0.05% trifluoroacetic acid (TFA) in water;
(2) Solvent B, 0.05% TFA in acetonitrile.

The following gradient system was used with a flow rate of 1 ml/min (time, % solvent A): 0 min, 95%; 40 min, 60%; 45 min, 60%.

UV detection was set to 490 nm; fluorescence detection was conducted with an excitation wavelength of 490 nm and emission at 517 nm.

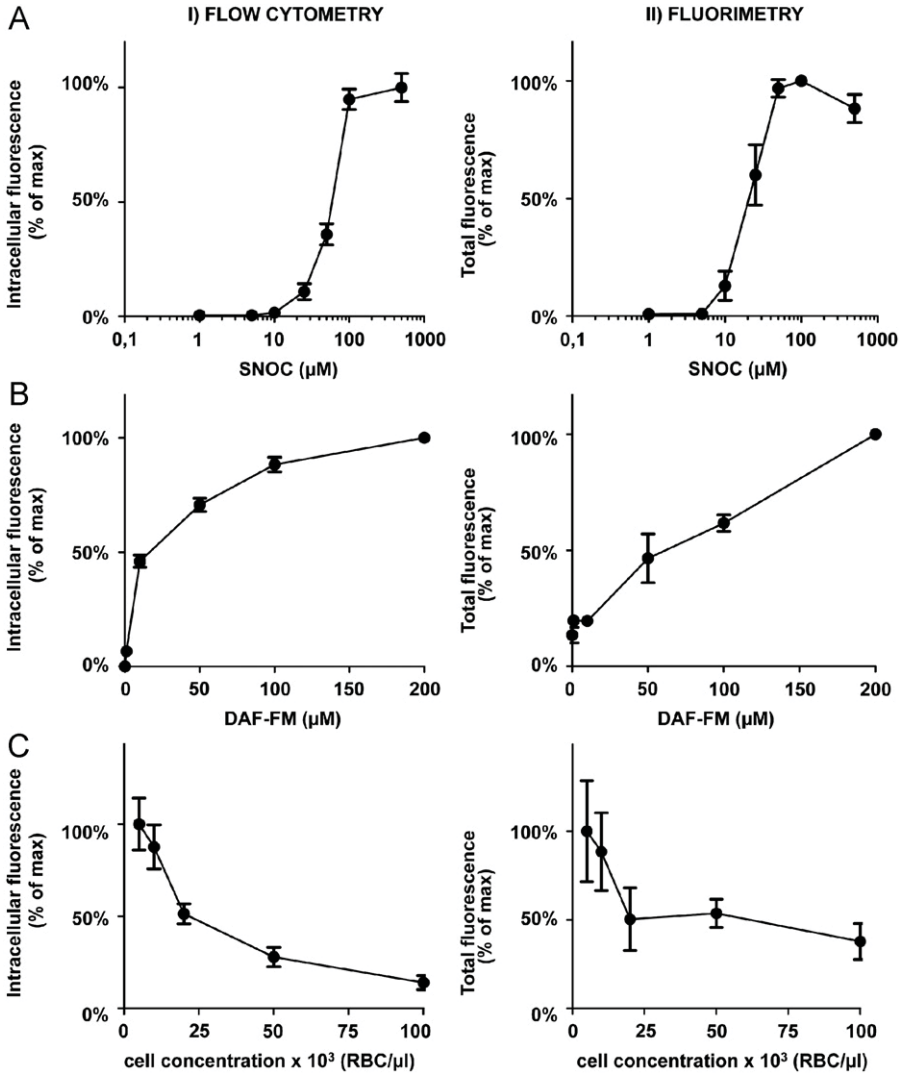

Fig. 5. Dependence of DAF-FM-associated fluorescence on NO donor and fluorescent probe concentration and on RBC number. Red cells were loaded with DAF-FM diacetate at the indicated concentrations or left untreated. Intracellular fluorescence was analyzed by flow cytometry (left) and fluorimetry (right). (A, B) Increase in fluorescence signal upon increasing concentrations of (A) SNOC and (B) DAF-FM diacetate. (C) Decrease in fluorescence signal upon increasing RBC density. Results are expressed as percentage of maximal fluorescence signal after correction for autofluorescence (means ± SEM, $n=6$).

Fig. 6B depicts representative chromatograms of DAF-FM (top) and DAF-FM-T (bottom). The peak corresponding to DAF-FM-T is marked by an arrow. Several minor fluorescent contaminants were present in the standards.

LC-MS/MS analysis

Mass spectrometric analyses were conducted using an LC-MS/MS instrument operating in positive-ionization mode. Samples were separated on a C18(2) column (50 mm × 2.1 mm). The mobile phases were prepared as follows:

(1) Solvent A, 0.1% aqueous formic acid;
(2) Solvent B, 100% methanol.

The following gradient system was used with a flow rate of 200 μl/min (time, % solvent A): 0 min, 80%; 1 min, 80%; 2.1 min, 30%; 3.1 min, 30%; 3.5 min, 80%; 5 min, 80%.

DAF-FM and DAF-FM-T were detected using SRM. The main fragmentation reaction of DAF-FM and DAF-FM-T in positive-ionization mode is the loss of CO_2.

Fig. 6C shows the pseudo-molecular ion of DAF-FM and DAF-FM-T (top row, protonated compound) and the main fragments (after loss of CO_2).

The fragmentation reactions of DAF-FM and DAF-FM-T were further investigated using high-resolution MS with an LTQ Orbitrap. Fig. 7 shows the proposed fragmentation pathway of DAF-FM and DAF-FM-T. After tautomeric rearrangement (Fig. 7, left), the primary fragmentation reaction is the loss of CO_2.

Structural analysis of DAF-FM by NMR

(1) Dissolve 1 mg DAF-FM authentic standard in 0.5 ml d_6-DMSO.
(2) Run ^{1}H NMR and ^{13}C NMR spectra of DAF-FM.

The structure and complete NMR assignments of DAF-FM (Fig. 8A) were established on the basis of various NMR spectra (^{1}H, ^{13}C, HSQC, HMBC, ^{1}H–^{1}H COSY, and NOESY), which were acquired from a solution (1 mg/0.5 ml) in d_6-DMSO at 700 MHz. The molecular formula for DAF-FM is $C_{21}H_{14}F_2N_2O_5$. However, the ^{1}H NMR spectrum shows only 8 distinct resonances (see the

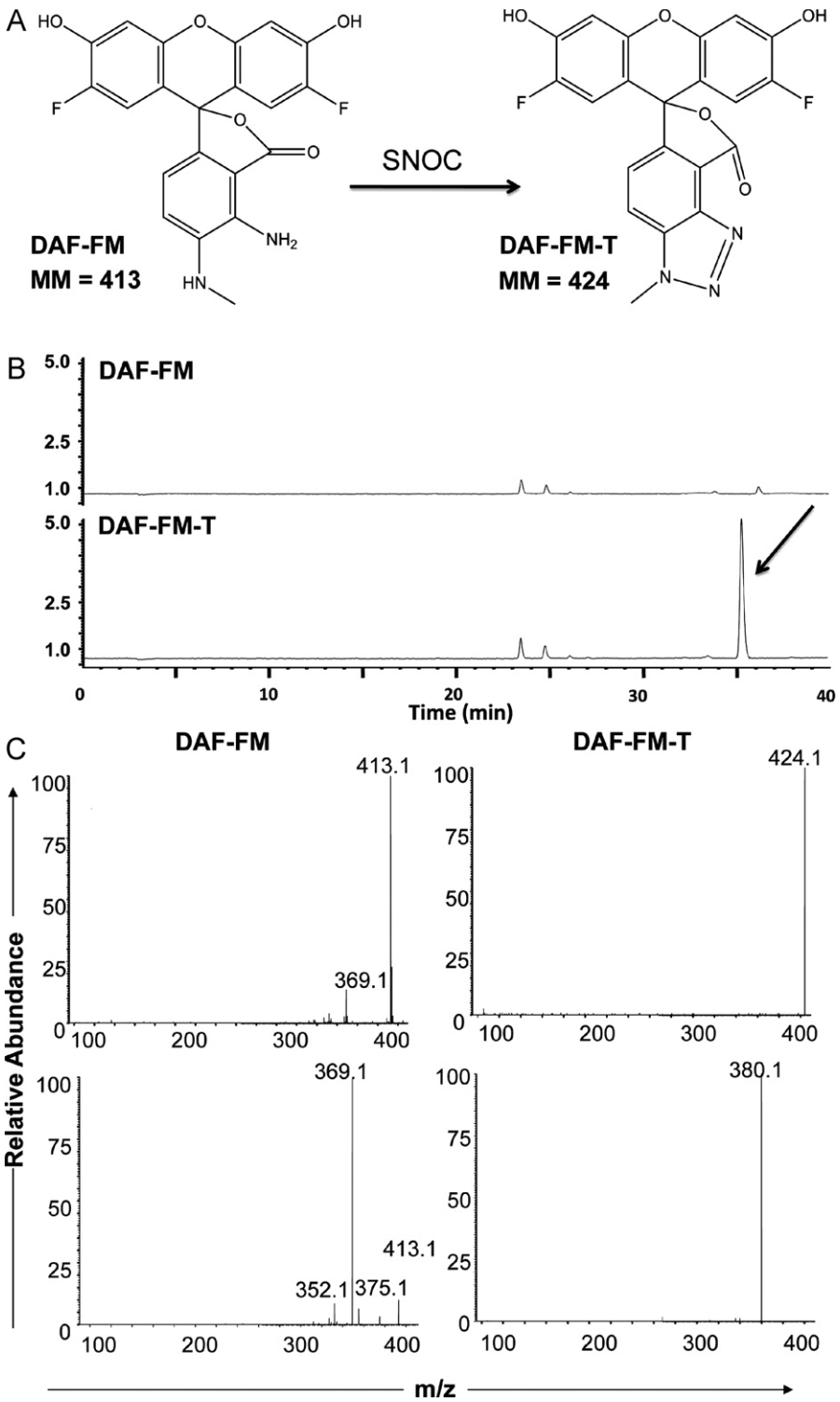

Fig. 6. Analysis of DAF-FM and DAF-FM-T by HPLC and LC-MS/MS. (A) Preparation of DAF-FM-T by reaction of DAF-FM with SNOC. (B) Representative chromatograms of DAF-FM (top) and DAF-FM-T (bottom). The peak corresponding to DAF-FM-T is marked by an arrow. (C) Representative mass spectra of DAF-FM and DAF-FM-T using LC-MS/MS; lower row represents MS/MS data of the main peak.

spectrum projected on the top in Fig. 8C; δ_H 10.69 ppm does not appear in this expansion), which is fewer than 14 peaks predicted by the molecular formula. Similarly, the ^{13}C NMR spectrum (projected on the left side of Fig. 8C; δ_C 30.1 ppm does not appear in this expansion) displays only 15 distinct resonances from a possible 21. Both ^{1}H and ^{13}C NMR spectra therefore indicate some degree of symmetry in the structure of DAF-FM. The critical resonance for elucidating the structure of DAF-FM is the quaternary carbon of the spiro-γ-lactone group at δ_C 80.9 ppm in the ^{13}C NMR spectrum. This chemical shift is consistent with an aliphatic carbon substituted by an electronegative oxygen substituent, but much less so with an aromatic carbon. It is located at the center of the molecule, as shown by four long-range connections (Fig. 8B, due to both $^{3}J_{CH}$ and $^{4}J_{CH}$)

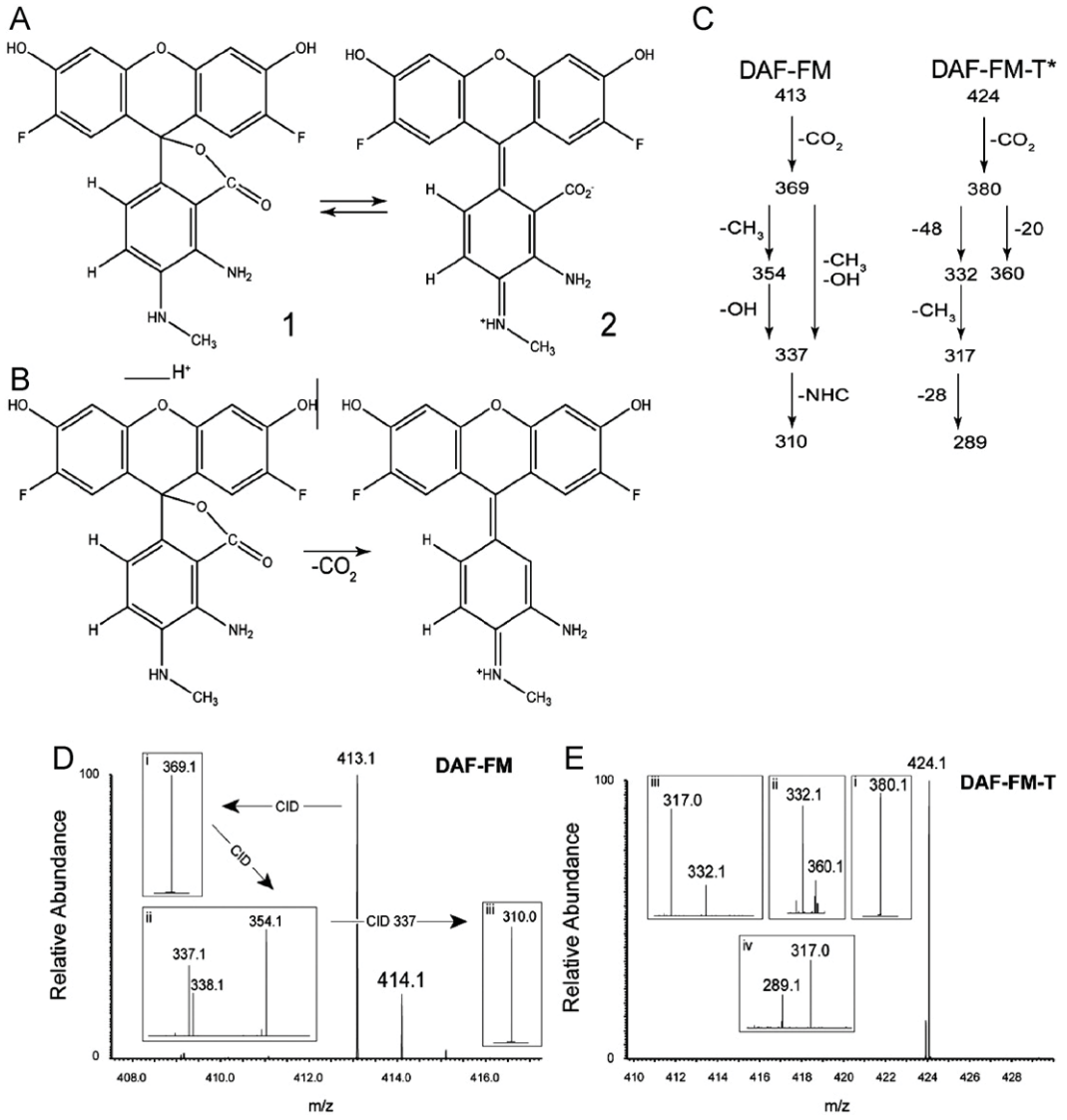

Fig. 7. Structure and fragmentation reactions of DAF-FM and DAF-FM-T. (A) Possible rearrangement of DAF-FM in solution. (B) The main fragmentation reaction of DAF-FM and DAF-FM-T in positive ionization mode is the loss of CO_2. (C) Detailed fragmentation pathway of DAF-FM and DAF-FM-T. (D, E) Fragmentation spectra of (D) DAF-FM and (E) DAF-FM-T.

in the HMBC spectrum of DAF-FM. Fig. 8B shows long-range ^{13}C–^{1}H couplings from δ_C 80.9 ppm to both hydrogens in the two (symmetrical) fluorinated aromatic rings (δ_H 6.83 and δ_H 6.48 ppm) as well as to both hydrogen atoms in the aromatic system bearing the γ-lactone moiety (δ_H 6.65 and δ_H 6.23 ppm).

HPLC and LC-MS/MS analysis of the nitrosation products of DAF-FM in Human RBCs treated with NO donors

A protocol for the detection of DAF-FM-T formation in RBCs after treatment with SNOC or the NO donor spermine/NO (Sper/NO) is provided here as an example for application of this technique to detect DAF-FM-T formation in cells (Fig. 2). As discussed above, the use of analytical separation techniques is crucial to confirm that the fluorescent signals detected by fluorimetry, laser-scanning microscopy, or flow cytometry are indeed due to intracellular nitrosation of DAF-FM (and thus originate from NO) rather than the formation of an adduct that enhances DAF-FM fluorescence in an NO-independent fashion. In addition, it offers the advantage of providing an independent semiquantitative assessment of intracellular NO production.

Preparation of Sper/NO solution

(1) dissolve Sper/NO at a concentration of 50 mM in 0.01 M NaOH, keep on ice, and use the same day.
(2) Dilute Sper/NO to desired final concentration in phosphate buffer (check that buffer strength is sufficient to bring pH to 7.4); the release of NO will begin immediately and all dilutions should be made fresh just before experimental use.

Isolation of Human RBCs

(1) Collect blood (10–12 ml) from the antecubital vein of healthy volunteers and add heparin (5000 U/ml).
(2) Transfer 10 ml of blood to a 20-ml syringe. The bottom of the syringe should be closed with a stopper. Place the syringe into a 50-ml plastic centrifugation tube and close the top with Parafilm.

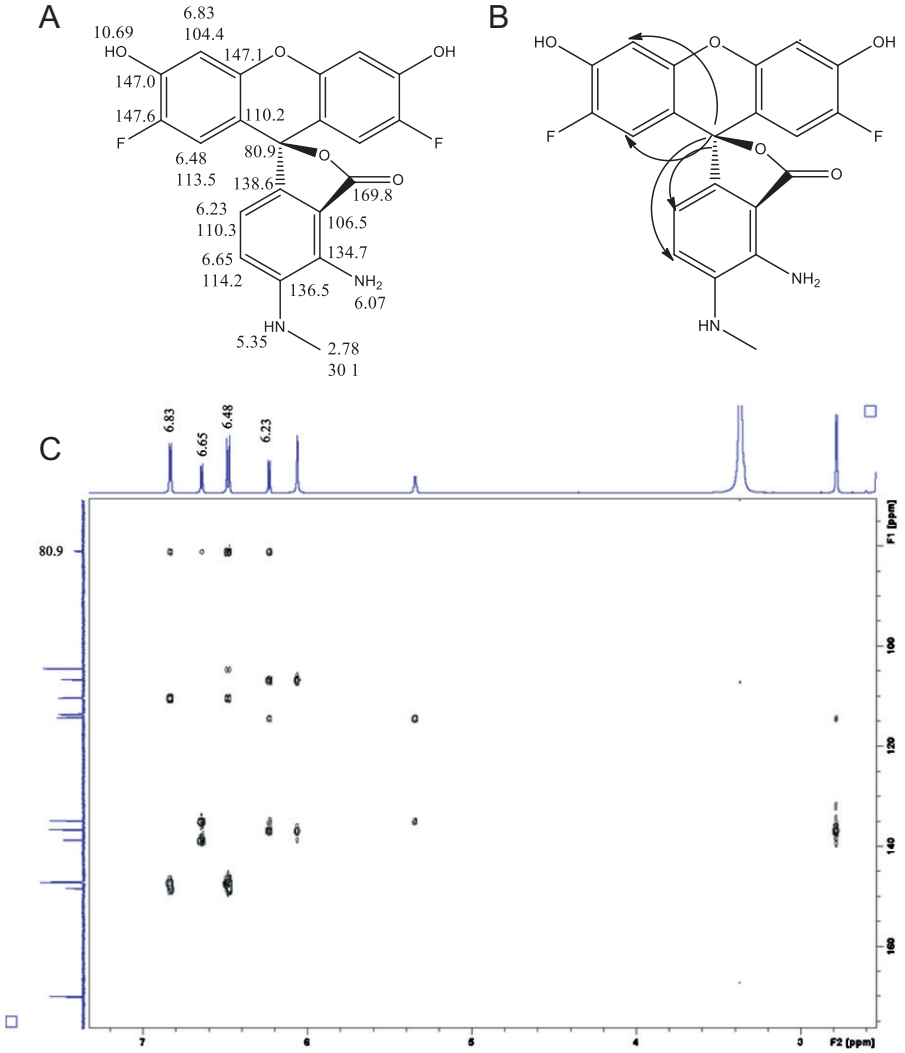

Fig. 8. Structural analysis of DAF-FM by NMR. (A) Structure and complete NMR assignments of DAF-FM. (B) Long-range ^{13}C–^{1}H couplings from δ_C 80.9 ppm to both hydrogens in the two (symmetrical) fluorinated aromatic rings (δ_H 6.83 ppm and δ_H 6.48 ppm) as well as to both hydrogens in the aromatic system, which bears the γ-lactone moiety (δ_H 6.65 ppm and δ_H 6.23 ppm). (C) HMBC spectrum with ^{13}C NMR spectrum superimposed on left side and ^{1}H NMR spectrum on top.

(3) Centrifuge the blood at 800 g for 15 min at RT. The red cell pellet can now be eluted from the bottom of the syringe.
(4) RBC concentrate should be kept on ice and used within 2 h.

Loading RBCs with DAF-FM and HPLC analysis

(1) Dilute RBC pellets 1:500 or 1:1000 in PBS (as indicated) and divide into 500-µl aliquots in amber centrifuge tubes.
(2) Add 1 µl of a 5 mM DAF-FM-DA stock solution (prepare by dissolving 5 µg in 20 µl DMSO, and use immediately); final concentration will be 10 µM DAF-FM. Incubate for 30 min at RT in the dark. Leave one sample untreated to use as matrix control (see Fig. 2).
(3) Wash by centrifugation at 300 g for 10 min at 4 °C and remove the supernatant by aspiration.
(4) Extract DAF-FM and DAF-FM-T by adding 500 µl of HPLC-grade DMSO, and incubate 30 min at RT. Keep the samples at RT from here on to avoid freezing of DMSO.
(5) Transfer the supernatant into amber Eppendorf tubes, and spin down at 13,000 g for 10 min to remove precipitates and debris.
(6) Transfer the supernatants into amber vials for HPLC and LC-MS analysis (please refer to the methods described for analysis of DAF-FM and DAF-FM-T standards).

Preparation of matrix controls

The matrix effects should be tested to document eventual changes in retention time or peak appearance and/or the presence of fluorescent contaminants.

(1) Prepare RBC lysate by diluting RBC pellets in 10 volumes of distilled water. These should be further diluted in PBS to reach a final dilution of 1:500 or 1:1000 for HPLC analysis samples.
(2) DAF-FM-T should be prepared from DAF-FM by reaction with SNOC in PBS as described above.
(3) DAF-FM-T should be diluted in the RBC lysate.

Calculations and expected results

Preliminary considerations

Subsequent loss of fluorescence of the reaction product notwithstanding, the interaction of NO (and derived nitrosated

species) with DAF-FM to form DAF-FM-T is an irreversible reaction. This suggests that increases in DAF-FM-related fluorescence intensity are cumulative in nature rather than indicative of a certain steady-state concentration of NO. Although little is known about the half-life of DAF-FM-T in cells, this compound is relatively stable in vitro. Thus, irrespective of the pitfalls described below—in particular the dependence of DAF-FM-T formation on reactive oxygen species (ROS) production (Fig. 1)—all measurements of NO using this fluorescent dye represent cumulative assessments of NO production during the chosen incubation integral.

Laser-scanning microscopy of DAF-FM-loaded RBCs

Fig. 3 depicts a typical fluorescence image of RBCs loaded with 30 μM DAF-FM-DA. To compare the fluorescence intensity of different specimens, exposure time should always be adjusted on the positive control (e.g., the SNOC-treated cells or the sample with expected maximal intensity) and kept constant during all measurements. The fluorescence intensity of individual cells can be quantified using an image-processing software package such as ImageJ (NIH) and expressed as a ratio vs DAF-FM-loaded but untreated cells. Images can be further processed for publication presentation with Adobe Photoshop CS5 (Adobe Systems GmbH, Munich, Germany) following the international guidelines for preserving image integrity [33,34].

In attempts to identify the localization of the DAF-FM-associated fluorescence within the cell membrane we co-incubated RBCs with DAF-FM-DA and the membrane tracker dye DiD (5 μg DiD/ml cell suspension). Although we found some colocalization of the green (DAF-dependent fluorescence) and the deep red (DiD) fluorescence, probe diffusion seems to limit the ability to localize NO/NO_x source(s) using this method. This may be of lesser concern if cell types other than RBCs are studied. However, both dye loading efficiency and probe distribution across cellular compartments, as well as ROS-dependent probe activation (which may differ between cell compartments), may be important confounding issues [22]. It is conceivable that particularly redox-active cell organelles such as mitochondria even support the formation of nonspecific DAF-related fluorescence by promoting dye coupling with ascorbate, for example. Thus, in our hands the technique has its limitations in terms of identifying the precise site of NO formation within the cell and may make it rather difficult to distinguish whether probe localization or reactivity accounts for a certain pattern of staining observed.

Flow cytometric and fluorimetric analysis of DAF-FM-loaded RBCs

In Fig. 4 typical data from a flow cytometric analysis of RBCs loaded with DAF-FM are presented. Data presented here were analyzed using FlowJo version 7.5.5 (TreeStar). RBCs are gated based on their size (forward light scatter) and granularity (side light scatter, SSC) in a double-logarithmic scatter-dot plot (Fig. 4A). The median fluorescence intensity (MFI) of 30,000 events within the RBC population is determined by analyzing a SSC fluorescence dot plot (Fig. 4B) or the distribution histogram (Fig. 4C). For each experiment unloaded cells served as autofluorescence control (Fig. 4, gray samples), and fluorescence activity was expressed as MFI − MFI of unloaded cells (ΔMFI).

Fig. 5 shows the change in fluorescence intensity upon variation of the concentration of SNOC (Fig. 5A), DAF-FM diacetate (Fig. 5B), or cell number (Fig. 5C). The fluorescence intensity differences obtained by flow cytometric analysis and fluorimetry are compared side by side. In fluorimetric measurements the signal is typically expressed in arbitrary units. Autofluorescence controls serve as a blank and are subtracted from the samples loaded with DAF-FM. The fluorescence activity may be expressed as percentage of maximum (as shown in Fig. 5) or as fold increase compared to samples treated with DAF-FM only.

We found that both intracellular fluorescence activity as assessed by flow cytometry (Fig. 5A, I) and total fluorescence activity as assessed by fluorimetry (Fig. 5A, II) increase with increasing SNOC concentrations in similar fashions until they reach a maximum at ~100 μM. Intracellular fluorescence increased with increasing DAF-FM concentrations in a logarithmic fashion using flow cytometry, reaching saturation around 100–200 μM DAF-FM (Fig. 5B, I), whereas total fluorescence activity linearly increased with increasing DAF-FM concentrations using fluorimetry (Fig. 5B, II). Both intracellular and total DAF-FM fluorescence intensities decreased with increasing RBC numbers (Fig. 5C). Whereas no changes in cell morphology or hemolysis were observed with these treatments at the concentrations used (which could have impeded flow cytometric analysis), a high NO/NO synthase (NOS)-independent background signal was apparent using either of these techniques, even after correction for autofluorescence, which limits the sensitivity as discussed elsewhere [22].

Detection and quantification of DAF-FM-T in RBCs by HPLC and LC-MS/MS

The structural changes associated with the preparation of DAF-FM-T from SNOC (or other NO donors) are depicted in Fig. 6A. Representative chromatograms of DAF-FM (commercial product) and DAF-FM-T (prepared by incubating DAF-FM with an excess of SNOC for 30 min at RT in the dark) standards are shown in Fig. 6B. LC-MS/MS analysis of DAF-FM and DAF-FM-T confirmed peak identities and allowed characterization of their fragmentation patterns. DAF-FM identity was additionally confirmed by ^{1}H NMR and ^{13}C NMR analysis (Fig. 8). The mass spectra of either standard, with pseudomolecular ions ($[M+H]^+$) of DAF-FM (m/z 413.1) and DAF-FM-T (m/z 424.1), are shown in Fig. 6C (top). The main fragmentation reaction for both compounds is the loss of CO_2 (m/z 44; see Fig. 7 for more details). This fragmentation reaction (413.1 → 369.1 for DAF-FM and 424.1 → 380.1 for DAF-FM-T) along with their retention times was used to detect these compounds in RBCs.

To confirm that the NO-donor-dependent fluorescent signals detected by laser-scanning microscopy, fluorimetry, and flow cytometry (Figs. 3, 4, and 5) were indeed due to intracellular nitrosation of DAF-FM to form DAF-FM-T, we analyzed the products of these reactions by HPLC and LC-MS/MS (Fig. 9). As described in detail above, RBCs were pre-loaded with DAF-FM DA and treated with SNOC or Sper/NO. Representative HPLC chromatograms are shown in Fig. 9A. The identity of an unknown peak from a cellular extract can be determined by comparing it to the retention time of the DAF-FM-T standard, and the concentration can be determined by peak integration using ChemStation (Agilent Technologies) software. A concentration-dependent increase in DAF-FM-T formation was observed in RBCs exposed to either 25–100 μM SNOC or 10–500 μM Sper/NO (Fig. 9B). No difference in retention time and/or peak area for DAF-FM-T was apparent between standards diluted in PBS and RBC lysates (to control for matrix effects). If combined with selected-reaction monitoring (i.e., multiple-reaction monitoring of the 413.1 → 369.1 and 424.1 → 380.1 transitions) by LC-MS/MS this allows both quantification and unequivocal identification of DAF-FM and DAF-FM-T in cells.

Statistical analysis

All values are reported as means ± SEM. Comparisons between groups were made using either two-tailed Student's t test or ANOVA followed by Bonferroni post hoc test for multiple comparisons. Differences were deemed significant when $p < 0.05$.

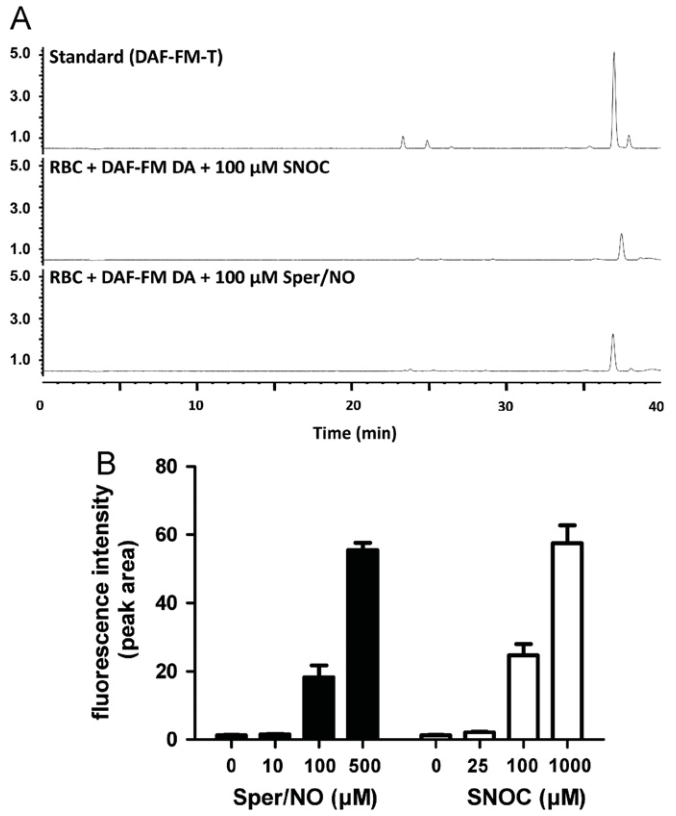

Fig. 9. Formation of DAF-FM-T and associated fluorescence increase within RBCs after addition of NO donors. (A) Representative HPLC chromatograms of DAF-FM-T standard in lysate of unlabeled RBCs (top), DAF-FM diacetate-loaded RBCs treated with SNOC (middle), or DAF-FM diacetate-loaded RBCs treated with Sper/NO (bottom). (B) Increases in DAF-FM-T formation in RBCs after treatment with NO donors as assessed by HPLC. Means ± SEM from three independent blood donors.

Statistical analyses were performed using GraphPad Prism 5.00 (GraphPad) or IBM SPSS 18.0 statistics (IBM).

Caveats

Is DAF-FM a suitable probe for measuring intracellular NO production, or Is this technique still a "triumph of Hope over reality" [35]?

Several authors have discussed the many pitfalls of using fluorescent probes for the determination of free radicals, in particular the limitations of diaminofluoresceins. Although numerous investigators are happily unaware of any such issues, others may be discouraged from experimental use altogether by this. This is unfortunate as few other techniques exist that lend themselves to assessing *intracellular* NO formation by cells. Using these probes can provide additional useful information if the following caveats are carefully considered before DAF-FM (or another diaminofluorescein) is used in biological experiments.

Probe reactivity with NO

The reaction mechanism leading to the formation of DAF-FM-T may involve nitrosative (oxidation of NO, mechanism I) or oxidative (oxidation of the probe, mechanism II) chemistry. This implies that depending on the cellular environment the probe could detect nitrosative reaction products of NO, NO itself, or both. Although testing whether the activity involves NO synthase by applying an NOS inhibitor is straightforward (see below), untangling which species accounts for the fluorescence increase can be challenging.

Presence of Interfering molecules

Oxidants and reactive oxygen species may interfere with the formation of nitrosative species from NO (according to mechanism I) and the formation of the anilinyl radical intermediate (according to mechanism II); either possibility may potentially increase the rate of formation of DAF-FM-T independent of an increase in NO formation from NOS (or another NO source). Vice versa, antioxidants can decrease it, as shown for reduced glutathione [28]. This implies that tissues/cells/conditions characterized by changes in redox-active molecules might be very difficult to compare without parallel determination of the levels of other redox parameters, including glutathione (GSH) or ROS formation.

Non-specific fluorescence products

The specificity of the DAF-FM related signal should be confirmed using NO scavengers. A typical NO scavenger used in the literature is the nitronyl nitroxide CPTIO (2-(4-carboxyphenyl)-4,4,5,5-tetramethylimidazoline-1-oxyl-3-oxide), which produces NO_2 after reaction with NO and can lead to enhanced nitrosation [36]. This may also occur with DAFs, leading to false-negative results by enhancing rather than quenching fluorescence. In our hands $Fe(DETC)_2$—which is normally used as a spin trap in ESR experiments [37]—works reasonably well as an NO scavenger, as NO is incorporated into an adduct rather than released as reactive, higher nitrogen oxide. The formation or presence of fluorescence signals unrelated to NO (adducts with, e.g., ascorbate or dehydroascorbate [27]) can be excluded by applying analytical separation techniques.

Probe accumulation and sensitivity

Effective intracellular dye accumulation may be the main reason nitrosation of DAF-FM is possible in RBCs, as demonstrated here and in vascular tissue before [22]. However, the true sensitivity of DAFs to NO donors in the cellular environment is considerably lower (in the present studies it amounted to ~25 µM Sper/NO) than in simple aqueous systems (reported to be around 5 nM) [11–14]. Probe accumulation and sensitivity should be established in your cellular system of choice, as described for RBCs here (Fig. 5).

Loading efficiency

Similar to other esterase-sensitive dyes [20], the loading efficiency of DAF-FM diacetate depends on its membrane permeability and intracellular esterase activity and thus efficiency of dye trapping. The latter may be affected by the experimental conditions (e.g., treatments) and markedly differ between cell types. Assessment of loading efficiency would require dye extraction after cell sorting, absolute determination of all DAF-FM diacetate derivates (including DAF-FM monoacetate, DAF-FM, and DAF-FM-T), and subsequent normalization to cell volume. This is rather laborious and justified only when the main objective of the study is to compare various cell types. A less accurate but much simpler approach is to use NO donors under saturating conditions, which will fully convert all intracellular DAF-FM into DAF-FM-T, and compare maximal fluorescence intensities. As long as investigators ensure that NO fluxes applied are indeed maximal for all cell types under study (requiring careful titration of the NO donor concentration) such comparison will suffice in most cases.

Photochemical reactions

Photochemical reactions may affect the probe directly by triggering nitrosative/oxidative chemistry within the cells, e.g., by inducing decomposition of preformed *S*-nitrosothiols or by UV photolysis of nitrite/nitrate. Thus, contact with light during sample preparation, incubation, and measurements should be kept to a minimum to avoid such artifacts (unless the purpose of the study is to gain information about such storage forms, of course; potential effects of added substances—to probe for specific NO-storage forms as described for $HgCl_2$ [22]—need to be verified in control experiments, e.g., in the absence of cells).

NO source

The source of NO production (e.g., endothelial NOS in RBCs) can be confirmed by pretreating cells with NOS inhibitors and/or using knockout approaches. In addition to light, thermolysis of preformed NO stores can also give rise to NO and thus increase DAF-FM-related fluorescence intensity; thus, care should be taken to carry out all experiments using reproducible temperature conditions. The diffusibility of both probe and reaction product (DAF-FM and DAF-FM-T) within the intracellular compartments and NO/NO_x, as well as the unknown kinetics of the reactions involved, can make it difficult to use DAFs for intracellular localization of an NO source.

Freezing artifacts

Introducing additional freeze/thaw cycles tends to increase autofluorescence. The reason for this is unclear, but a large (nonspecific) peak at retention time 20 min is observed in the HPLC chromatogram of standards that were kept frozen. Although this will not affect the usefulness of the standards for HPLC analysis, it does affect sensitivity and potentially signal specificity.

Nitrosative chemistry of DAF-FM within RBCs

Because RBCs contain an abundance of both low-molecular-weight antioxidants, such as GSH and ascorbate, and the NO scavenger hemoglobin one wonders how DAF-FM can still detect NO and/or nitrosating species in these cells. Effective intracellular dye accumulation may be the main reason nitrosation of DAF-FM is possible in these and other cells [22]. Indeed, by analyzing the saturation curves shown in Fig. 5, we found that the probe accumulates in RBCs in a concentration- and cell number-dependent manner. However, the sensitivity of intracellular DAF-FM for extracellular added NO is rather low. In fact, HPLC and flow cytometric analyses revealed that the minimal concentration of SNOC required to significantly increase intracellular fluorescence intensity is 25 μM, and saturation of the signal under the conditions applied for flow cytometric analysis is achieved with 100 μM SNOC. At the same time, intracellular dye accumulation might strongly contribute to autofluorescence of diaminofluoresceins, e.g., because of autoxidation [22] and/or the formation of adducts with, e.g., ascorbate or dehydroascorbate [27]. Therefore, by using only fluorimetry, flow cytometry, or microscopy, the fluorescence of these secondary/nonspecific products cannot be distinguished from specific DAF-FM-T fluorescence.

For the study of DAF-FM-T formation in RBCs we characterized the structure of DAF-FM authentic standard by ^1H NMR and ^{13}C NMR spectrometry, as well as the fragmentation patterns of DAF-FM and DAF-FM-T. Mass spectrometric analyses of DAF-2 have been described by others previously [12,38], but to the best of our knowledge this is the first time LC-MS/MS has been used to analyze the fragmentation pattern of DAF-FM and DAF-FM-T and to confirm DAF-FM-T production in cells.

Formation of DAF-FM-T in RBCs can be induced by treatment with low micromolar concentrations of the NO donors SNOC and Sper/NO. Both NO donors are cell permeative: SNOC can be transported into RBCs by the amino acid transporters LAT-1 and LAT-2 [39,40]. However, as a nitrosothiol, SNOC not only releases NO but is also an efficient nitrosating agent. Thus, SNOC could directly nitrosate DAF-FM without the intermediacy of free NO [41]. For this reason we additionally employed the NO donor Sper/NO, which spontaneously releases NO [42]. A concentration of 100 μM Sper/NO, which translates into a constant release of 2.1–3.6 μM NO/min within the first 30 min of decomposition, also increased the formation of DAF-FM-T in RBCs with an efficacy comparable to that of SNOC.

Conclusions

Although diaminofluorescein-based fluorimetry seems to be a relatively user-friendly technique for measuring NO compared to EPR, mass spectrometry, and reductive chemiluminescence detection, in reality it is not that easy to apply. Multiple competing and confounding reactions can provide a formidable challenge to comparing different conditions (such as cell types, healthy vs diseased, etc.), which may be associated with differences in the formation of other radicals/antioxidants or oxidants at the same time. Nevertheless, and in addition to performing standard controls most investigators in this field will be familiar with, the use of analytical separation techniques capable of positively identifying the triazole product permits one to apply such probes with a fair degree of confidence for the detection of NO formation in cellular systems.

Acknowledgments

This work was supported by the Deutsche Forschungsgemeinschaft (DFG 405/5-1 and FOR809 TP7 Me1821/3-1), the Anton Betz Stiftung (26/2010), and the Susanne-Bunnenberg-Stiftung at Düsseldorf Heart Center to M.K. and the Forschungskommission of the Medical Faculty of the Heinrich Heine University of Düsseldorf (to M.C.K.). The authors thank Katharina Lysaja, Sivatharsini Thasian-Sivarajah, and Tristan Römer for indispensable assistance; Peter Heath for his support with NMR analyses; and Professor Victoria Kolb-Bachofen, Professor Dieter Häussinger, and Professor Jeremy Spencer for allowing us to use the FluostarOPTIMA, the FACS Canto II flow cytometer, and the HPLC, respectively.

References

[1] Moncada, S. Nitric oxide in the vasculature: physiology and pathophysiology. *Ann. N. Y. Acad. Sci.* **811:**67–69; 1997.
[2] Hill, B. G.; Dranka, B. P.; Bailey, S. M.; Lancaster Jr J. R.; Darley-Usmar, V. M. What part of NO don't you understand? Some answers to the cardinal questions in nitric oxide biology *J. Biol. Chem.* **285:**19699–19704; 2010.
[3] Thomas, D. D.; Ridnour, L. A.; Isenberg, J. S.; Flores-Santana, W.; Switzer, C. H.; Donzelli, S.; Hussain, P.; Vecoli, C.; Paolocci, N.; Ambs, S.; Colton, C. A.; Harris, C. C.; Roberts, D. D.; Wink, D. A. The chemical biology of nitric oxide: implications in cellular signaling. *Free Radic. Biol. Med.* **45:**18–31; 2008.
[4] Feelisch, M.; Stamler, J. *Methods in Nitric Oxide Research*. Chichester: Wiley; 1996.
[5] Feelisch, M.; Rassaf, T.; Mnaimneh, S.; Singh, N.; Bryan, N. S.; Jourd'heuil, D.; Kelm, M. Concomitant S-, N-, and heme-nitros(yl)ation in biological tissues and fluids: implications for the fate of NO in vivo. *FASEB J* **16:**1775–1785; 2002.
[6] Rassaf, T.; Bryan, N. S.; Maloney, R. E.; Specian, V.; Kelm, M.; Kalyanaraman, B.; Rodriguez, J.; Feelisch, M. NO adducts in mammalian red blood cells: too much or too little? *Nat. Med* **9:**481–482; 2003.
[7] Bryan, N. S.; Rassaf, T.; Rodriguez, J.; Feelisch, M.; Bound, NO in human red blood cells: fact or artifact? *Nitric Oxide* **10:**221–228; 2004.

[8] Giustarini, D.; Milzani, A.; Colombo, R.; le-Donne, I.; Rossi, R. Nitric oxide, S-nitrosothiols and hemoglobin: is methodology the key? *Trends Pharmacol. Sci.* **25:**311–316; 2004.
[9] Yang, B. K.; Vivas, E. X.; Reiter, C. D.; Gladwin, M. Methodologies for the sensitive and specific measurement of S-nitrosothiols, iron-nitrosyls, and nitrite in biological samples. *Free Radic. Res.* **37:**1–10; 2003.
[10] Robinson, J. K.; Bollinger, M. J.; Birks, J. W. Luminol/H_2O_2 chemiluminescence detector for the analysis of nitric oxide in exhaled breath. *Anal. Chem.* **71:**5131–5136; 1999.
[11] Kojima, H.; Sakurai, K.; Kikuchi, K.; Kawahara, S.; Kirino, Y.; Nagoshi, H.; Hirata, Y.; Nagano, T. Development of a fluorescent indicator for nitric oxide based on the fluorescein chromophore. *Chem. Pharm. Bull.* **46:**373–375; 1998.
[12] Kojima, H.; Nakatsubo, N.; Kikuchi, K.; Kawahara, S.; Kirino, Y.; Nagoshi, H.; Hirata, Y.; Nagano, T. Detection and imaging of nitric oxide with novel fluorescent indicators: diaminofluoresceins. *Anal. Chem.* **70:**2446–2453; 1998.
[13] Kojima, H.; Urano, Y.; Kikuchi, K.; Higuchi, T.; Hirata, Y.; Nagano, T. Fluorescent indicators for imaging nitric oxide production. *Angew. Chem. Int. Ed. Engl.* **38:**3209–3212; 1999.
[14] Nagano, T.; Yoshimura, T. Bioimaging of nitric oxide. *Chem. Rev.* **102:**1235–1270; 2002.
[15] Nakatsubo, N.; Kojima, H.; Kikuchi, K.; Nagoshi, H.; Hirata, Y.; Maeda, D.; Imai, Y.; Irimura, T.; Nagano, T. Direct evidence of nitric oxide production from bovine aortic endothelial cells using new fluorescence indicators: diaminofluoresceins. *FEBS Lett* **427:**263–266; 1998.
[16] Feelisch, M.; Kubitzek, D.; Werringloer, J. The oxyhemoglobin assay. In: Feelisch, M., Stamler, J., editors. *Methods in Nitric Oxide Research*. Chichester: Wiley; 1996. p. 455–478.
[17] Berliner, J. L.; Fujii, H. Magnetic resonance imaging of biological specimens by electron paramagnetic resonance of nitroxide spin labels. *Science* **227:**517–519; 1985.
[18] Villamena, F. A.; Zweier, J. L. Detection of reactive oxygen and nitrogen species by EPR spin trapping. *Antioxid. Redox Signaling* **6:**619–629; 2004.
[19] Davies, I. R.; Zhang, X. Nitric oxide selective electrodes. *Methods Enzymol.* **436:**63–95; 2008.
[20] Wardman, P. Fluorescent and luminescent probes for measurement of oxidative and nitrosative species in cells and tissues: progress, pitfalls, and prospects. *Free Radic. Biol. Med* **43:**995–1022; 2007.
[21] Kalyanaraman, B.; Darley-Usmar, V.; Davies, K. J.; Dennery, P. A.; Forman, H. J.; Grisham, M. B.; Mann, G. E.; Moore, K.; Roberts, L. J.; Ischiropoulos, H. Measuring reactive oxygen and nitrogen species with fluorescent probes: challenges and limitations. *Free Radic. Biol. Med.* **52:**1–6; 2012.
[22] Rodriguez, J.; Specian, V.; Maloney, R.; Jourd'heuil, D.; Feelisch, M. Performance of diamino fluorophores for the localization of sources and targets of nitric oxide. *Free Radic. Biol. Med.* **38:**356–368; 2005.
[23] Planchet, E.; Kaiser, W. M. Nitric oxide production in plants: facts and fictions. *Plant Signaling Behav* **1:**46–51; 2006.
[24] Hong, H.; Sun, J.; Cai, W. Multimodality imaging of nitric oxide and nitric oxide synthases. *Free Radic. Biol. Med.* **47:**684–698; 2009.
[25] Tarpey, M. M.; Wink, D. A.; Grisham, M. B. Methods for detection of reactive metabolites of oxygen and nitrogen: in vitro and in vivo considerations. *Am. J. Physiol Regul. Integr. Comp. Physiol* **286:**R431–R444; 2004.
[26] Kim, W. S.; Ye, X.; Rubakhin, S. S.; Sweedler, J. V. Measuring nitric oxide in single neurons by capillary electrophoresis with laser-induced fluorescence: use of ascorbate oxidase in diaminofluorescein measurements. *Anal. Chem.* **78:**1859–1865; 2006.
[27] Zhang, X.; Kim, W. S.; Hatcher, N.; Potgieter, K.; Moroz, L. L.; Gillette, R.; Sweedler, J. V. Interfering with nitric oxide measurements: 4,5-diaminofluorescein reacts with dehydroascorbic acid and ascorbic acid. *J. Biol. Chem.* **277:**48472–48478; 2002.
[28] Jourd'heuil, D. Increased nitric oxide-dependent nitrosylation of 4,5-diaminofluorescein by oxidants: implications for the measurement of intracellular nitric oxide. *Free Radic. Biol. Med* **33:**676–684; 2002.
[29] Hong, H.; Sun, J.; Cai, W. Multimodality imaging of nitric oxide and nitric oxide synthases. *Free Radic. Biol. Med.* **47:**684–698; 2009.
[30] Kröncke, K. D.; Kolb-Bachofen, V. Measurement of nitric oxide-mediated effects on zinc homeostasis and zinc finger transcription factors. *Methods Enzymol* **301:**126–135; 1999.
[31] Feelisch, M. The use of nitric oxide donors in pharmacological studies. *Naunyn Schmiedebergs Arch. Pharmacol* **358:**113–122; 1998.
[32] Cortese-Krott, M. M.; Munchow, M.; Pirev, E.; Hessner, F.; Bozkurt, A.; Uciechowski, P.; Pallua, N.; Kroncke, K. D.; Suschek, C. V. Silver ions induce oxidative stress and intracellular zinc release in human skin fibroblasts. *Free Radic. Biol. Med.* **47:**1570–1577; 2009.
[33] Rossner, M.; Yamada, K. M. What's in a picture? The temptation of image manipulation *J. Cell Biol.* **166:**11–15; 2004.
[34] Cromey, D. W. Avoiding twisted pixels: ethical guidelines for the appropriate use and manipulation of scientific digital images. *Sci. Eng. Ethics* **16:**639–667; 2010.
[35] Tarpey, M. M.; Fridovich, I. Methods of detection of vascular reactive species: nitric oxide, superoxide, hydrogen peroxide, and peroxynitrite. *Circ. Res.* **89:**224–236; 2001.
[36] Lakshmi, V. M.; Zenser, T. V. 2-(4-Carboxyphenyl)-4,4,5,5-tetramethylimidazoline-1-oxyl-3-oxide potentiates nitrosation of a heterocyclic amine carcinogen by nitric oxide. *Life Sci* **80:**644–649; 2007.
[37] Kleschyov, A. L.; Mollnau, H.; Oelze, M.; Meinertz, T.; Huang, Y.; Harrison, D. G.; Munzel, T. Spin trapping of vascular nitric oxide using colloid Fe(II)-diethyldithiocarbamate. *Biochem. Biophys. Res. Commun.* **275:**672–677; 2000.
[38] Ye, X.; Xie, F.; Romanova, E. V.; Rubakhin, S. S.; Sweedler, J. V. Production of nitric oxide within the Aplysia californica nervous system. *ACS Chem. Neurosci* **1:**182–193; 2010.
[39] Zhang, Y.; Hogg, N. The mechanism of transmembrane S-nitrosothiol transport. *Proc. Natl. Acad. Sci. USA* **101:**7891–7896; 2004.
[40] Satoh, S.; Kimura, T.; Toda, M.; Maekawa, M.; Ono, S.; Narita, H.; Miyazaki, H.; Murayama, T.; Nomura, Y. Involvement of L-type-like amino acid transporters in S-nitrosocysteine-stimulated noradrenaline release in the rat hippocampus. *J. Neurochem.* **69:**2197–2205; 1997.
[41] Hogg, N. Biological chemistry and clinical potential of S-nitrosothiols. *Free Radic. Biol. Med.* **28:**1478–1486; 2000.
[42] Maragos, C. M.; Morley, D.; Wink, D. A.; Dunams, T. M.; Saavedra, J. E.; Hoffman, A.; Bove, A. A.; Isaac, L.; Hrabie, J. A.; Keefer, L. K. Complexes of NO with nucleophiles as agents for the controlled biological release of nitric oxide: vasorelaxant effects. *J. Med. Chem.* **34:**3242–3247; 1991.

Arteriosclerosis, Thrombosis, and Vascular Biology

Journal of the American Heart Association

Nitric Oxide Synthase Expression and Functional Response to Nitric Oxide Are Both Important Modulators of Circulating Angiogenic Cell Response to Angiogenic Stimuli

Christian Heiss, Andrea Schanz, Nicolas Amabile, Sarah Jahn, Qiumei Chen, Maelene L. Wong, Tienush Rassaf, Yvonne Heinen, Miriam Cortese-Krott, William Grossman, Yerem Yeghiazarians and Matthew L. Springer

Arterioscler Thromb Vasc Biol 2010, 30:2212-2218: originally published online August 12, 2010
doi: 10.1161/ATVBAHA.110.211581
Arteriosclerosis, Thrombosis, and Vascular Biology is published by the American Heart Association. 7272 Greenville Avenue, Dallas, TX 72514
 Print ISSN: 1079-5642. Online ISSN: 1524-4636

Nitric Oxide Synthase Expression and Functional Response to Nitric Oxide Are Both Important Modulators of Circulating Angiogenic Cell Response to Angiogenic Stimuli

Christian Heiss, Andrea Schanz, Nicolas Amabile, Sarah Jahn, Qiumei Chen, Maelene L. Wong, Tienush Rassaf, Yvonne Heinen, Miriam Cortese-Krott, William Grossman, Yerem Yeghiazarians, Matthew L. Springer

Objective—Circulating angiogenic cells (CACs), also termed endothelial progenitor cells, play an integral role in vascular repair and are functionally impaired in coronary artery disease (CAD). The role of nitric oxide (NO) in CAC function is poorly understood. We hypothesized that CAC migration toward angiogenic signals is modulated by both NO synthase (NOS) expression and functional response to NO.

Methods and Results—Similar to endothelial cells, CAC chemotaxis to vascular endothelial growth factor (VEGF) was blocked by inhibition of NOS, phosphatidylinositol 3-kinase, or guanylyl cyclase or by treatment with an NO scavenger. Addition of an NO donor (*S*-nitroso-*N*-acetylpenicillamine) and the NOS substrate L-arginine increased random cell migration (chemokinesis) and enhanced VEGF-dependent chemotaxis. Healthy CACs expressed endothelial NOS, but endothelial NOS was not detected in CAD patient CACs. Both chemokinesis and chemotaxis to VEGF of patient CACs were decreased compared with healthy CACs but were restored to healthy values by *S*-nitroso-*N*-acetylpenicillamine. In parallel, CAD patients exhibited lower flow-mediated vasodilation and plasma NO source nitrite than young, healthy subjects, indicating endothelial dysfunction with reduced NO bioavailability.

Conclusion—NOS activity is required for CAC chemotaxis. In CAD patients, impairment of NOS expression and NO bioavailability, rather than response to NO, may contribute to dysfunction of CACs and limit their regenerative capacity. **(*Arterioscler Thromb Vasc Biol*. 2010;30:2212-2218.)**

Key Words: cell physiology ■ coronary artery disease ■ endothelium ■ nitric oxide ■ nitric oxide synthase ■ circulating angiogenic cells

NO is an important signaling molecule in vascular biology.[1] Physiologically, many integral functions of the vascular endothelium are modulated by endothelial nitric oxide synthase (eNOS)-derived NO, including the inhibition of platelet and leukocyte adhesion, smooth muscle relaxation, and proliferation. Newer literature shows that NO not only acts in paracrine manner but may also exert systemic effects via reversible formation of more stable storage forms, including nitrite and nitoso-adducts. The disruption of this pathway in endothelial cells is associated with chronic vascular disease.[2] Risk factors appear to selectively damage the vascular endothelium, leading to a dysfunctional, maladaptive endothelial phenotype.[3,4] Studies suggest that eNOS activity and expression as well as circulating NO storage forms in blood are progressively decreased with cardiovascular risk factors including aging, hypertension, hypercholesterolemia, diabetes, and smoking and cigarette smoke exposure.[2,5–7] Over time, chronic endothelial dysfunction leads to intimal hyperplasia and enhanced plaque formation in predisposed areas of the vascular tree. Notably, the functional capacity of the vascular endothelium not only depends on the degree of damage but also on the presence and status of repair systems, including circulating angiogenic cells (CACs).[8]

Vascular repair involves not only local migration and proliferation of mature endothelial cells but also angiogenic cells that circulate in blood and the recruitment of the latter cells to sites of injury. Literature from the last 10 years suggests that circulating proangiogenic blood cells can enhance angiogenesis and the replacement of vascular endothelium.[8–10] These cells were initially termed endothelial progenitor cells because of their phenotypic similarities to mature endothelial cells, including kinase insert domain

Received on: June 8, 2009; final version accepted on: July 26, 2010.

From the Division of Cardiology (C.H., N.A., S.J., M.L.W., W.G., Y.Y., M.L.S.), Cardiovascular Research Institute (Q.C., M.L.S.), Eli and Edythe Broad Center of Regeneration Medicine and Stem Cell Research (Y.Y., M.L.S.), and Department of Cell and Tissue Biology (A.S.), University of California, San Francisco; Division of Cardiology, Heinrich-Heine University, Duesseldorf, Germany (T.R., Y.H., M.C.-K.). Current affiliations: Division of Cardiology, Heinrich-Heine University, Duesseldorf, Germany (C.H.); Department of Cardiology, Centre Marle Lannelongue, Le Plessis Robinson, Paris, France (N.A.); Department of Gynecology and Obstetrics, Heinrich-Heine University, Duesseldorf, Germany (A.S.).

Correspondence to Matthew L. Springer, PhD, Division of Cardiology, Box 0124, University of California, San Francisco, San Francisco, CA 94143-0124. E-mail matt.springer@ucsf.edu

Arterioscler Thromb Vasc Biol **is available at http://atvb.ahajournals.org** **DOI: 10.1161/ATVBAHA.110.211581**

receptor, eNOS, and platelet endothelial cell adhesion molecule (CD31), but also to stem cells (CD34 and CD133) and myeloid cells (CD14 and CD45). Newer literature suggests that these early outgrowth angiogenic cells temporarily aid endothelial repair, rather than developing into mature endothelial cells, in contrast to late outgrowth endothelial colony-forming cells, which can form endothelial tubes and monolayers.[11,12] Therefore, these cells are herein referred to as CACs rather than early endothelial progenitor cells. Clinical and experimental studies show that the reparative and therapeutic potency of CACs is determined by their functional status, which, in turn, are characterized by migratory capacity toward chemotactic signals, such as vascular endothelial growth factor (VEGF).[13,14]

Several studies suggest that cardiovascular disease not only may be caused by endothelial damage but also may cause or be caused by CAC dysfunction. The number or function of these cells is reduced with aging,[6] hypertension, diabetes,[15] smoking,[16] and environmental smoke exposure.[17] CAC dysfunction was shown to limit the therapeutic potency of these cells when transplanted.[13] It is conceivable that the functional capacities of CACs in patients may also be affected by the pathomechanisms that impair endothelial cell dysfunction, including decreased NO production and bioavailability, further facilitating vascular disease progression.[18] The role of NO activity in fundamental functional CAC capacities is not well studied. We hypothesized that CAC migration is modulated by NO and that CAC dysfunction in coronary artery disease (CAD) patients is a result of reduced NO bioavailability in blood or decreased NOS expression.

We first characterized the chemotactic response of CACs and compared the results with human umbilical vein endothelial cells (HUVECs), serving as a standard endothelial cell system. We then studied the effect of the NO donor *S*-nitroso-*N*-acetylpenicillamine (SNAP) on migration of CACs and HUVECs. Finally, we measured eNOS expression and migratory responses in ex vivo–differentiated CACs isolated from CAD patients, who were shown to experience endothelial dysfunction with impaired NO bioavailablity, and compared them with results from young, healthy volunteers.

Methods

Study Subjects

CACs were isolated from 10 young, healthy subjects without cardiovascular risk factors (hypertension, diabetes mellitus, smoking, and hypercholesterolemia, which are associated with impaired number and function of CACs), and with normal endothelial function (as measured by flow-mediated dilation [FMD] of the brachial artery of greater than 6%).[2,6,19] (See Supplemental Table I, available online at http://atvb.ahajournals.org, for characteristics.) We also isolated CACs from 10 patients with angiographically documented CAD as defined by >70% stenosis of at least 1 coronary artery on optimal medical therapy according to current secondary prevention guidelines[20] and endothelial dysfunction with FMD <5%. The characterization of CACs, including mechanistic experiments, was performed in CACs isolated from the healthy subjects. The protocol was approved by the University of California, San Francisco, Committee on Human Research, and volunteers gave written informed consent.

Cell Culture and Characterization of Blood-Derived CACs

CACs were differentiated ex vivo from peripheral blood mononuclear cells as previously described (see supplemental material for more detailed characterization protocols).[11,21] CACs were isolated from mononuclear cells as adherent cells on fibronectin-coated dishes after 7 days. Culture was preceded by 1 day of preplating to remove platelets and shed endothelial cells. eNOS protein was quantitated in cell lysates of CACs at day 7 and VEGF in cell medium of adherent and nonadherent cells using commercially available ELISA kits following the manufacturer's protocol (Quantikine, R&D Systems). Marker expression (CD45, CXCR4, CD31, kinase insert domain receptor, CD11b, CD14, CD3, CD34, CD133) of day 7 cells was determined by flow cytometry.

Pooled HUVECs were purchased from Cambrex (Walkersville, Md), cultured in EBM-2 (supplemented with Singlequots 5% FBS) and used no later than passage 3.

Chemotaxis and Chemokinesis Assay

Cell migration was quantified by a transwell chemotaxis assay using a modified Boyden chamber.[13,22,23] Migration of both CACs and HUVECs was measured as follows: cells (2×10^4) were plated in EBM-2 medium (0.5% BSA, without other supplements, containing 63 mg/L L-arginine) in the upper of 2 chambers divided by a membrane with 8-μm pores (Corning Transwell). We tested the chemotactic properties of the following chemoattractants in only the lower chamber: vascular endothelial growth factor (VEGF, Sigma), stromal cell–derived factor (SDF-1α; Sigma), and pleiotrophin (PTN; Sigma) at 10 to 500 ng/mL; and monocyte chemoattractant protein 1 (Sigma), sphingosine-1-phosphate (Sigma), and interleukin 6 (Sigma) at 10 to 100 ng/mL. The following were added to both the upper and lower chamber: the NOS substrate L-arginine (100 μmol/L), NOS inhibitor N^G-nitro-L-arginine (100 μmol/L), NO scavenger 2-(4-carboxyphenyl)-4,4,5,5-tetramethylimidazoline-1-oxyl-3-oxide (PTIO; 100 μmol/L), guanylyl cyclase inhibitor 1*H*-[1,2,4]oxadiazolo[4,3-a] quinoxalin-1-one (ODQ; 100 μmol/L), PI3K inhibitor wortmannin (WM; 100 nmol/L), and NO donor SNAP (Sigma) at 1 nmol/L to 10 μmol/L. The number of migrated cells was determined on 5 random $\times$100 optical fields per membrane. To distinguish chemokinetic from chemotactic properties of VEGF and SNAP, both substances were added to upper and lower chambers in a checkerboard fashion.

Cell Proliferation and Apoptosis Assays

5-Bromodeoxyuridine incorporation assays were performed in 96-well dishes following the manufacturer's protocol (Cell Proliferation BrdU Assay, Roche). Apoptosis assays were performed with fluorescence-activated cell sorting essentially as described in the manufacturer's protocol (Guava, Hayward, Calif). cGMP levels were measured in 10^5 cells under baseline unstimulated conditions and after incubation with SNAP at 1 μmol/L for 30 minutes using an ELISA kit following the manufacturer's protocol (GE Healthcare).

FMD

Endothelium-dependent dilation of the brachial artery was measured by ultrasound (Sonosite Micromax, Bothell, Wash) in combination with an automated analysis system (Brachial Analyzer, Medical Imaging Applications, Iowa City, Iowa) as described (see supplemental material for details).[17]

Plasma Nitrite Level

The plasma nitrite levels, representing a sensitive readout of NOS activity, were measured as recently described using gas-phase chemiluminescence (see supplemental material for details).[24]

Statistical Analyses

Data are presented as mean±standard error of the mean. Group differences were calculated with repeated measurements ANOVA and consecutive post hoc test. Probability values of less than 0.05 were regarded as significant. Correlations were by the Pearson *r*. All experiments were performed in triplicate.

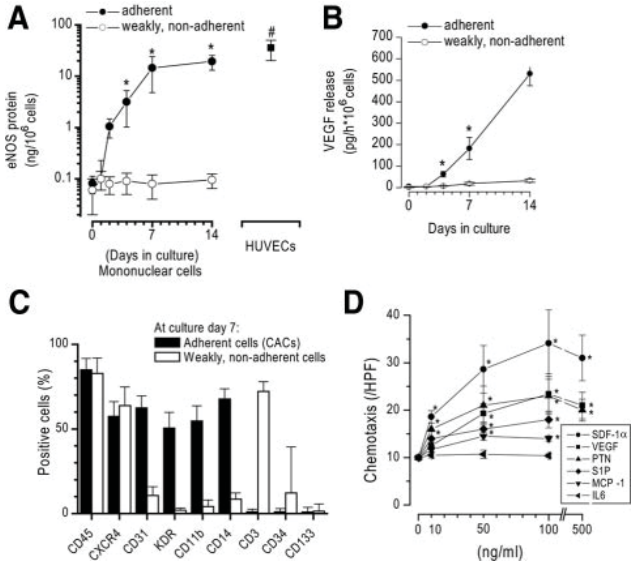

Figure 1. Characterization of CACs. Adherence-selected mononuclear cells progressively expressed eNOS (A); released VEGF (B); and expressed hematopoietic, monocytic, and endothelial markers (C). D, Day 7 CACs exhibited chemotaxis toward VEGF, PTN, SDF-1α-, monocyte chemoattractant protein 1 (MCP-1), and sphingosine-1-phosphate (S1P) but not toward interleukin 6. *$P<0.05$ versus control.

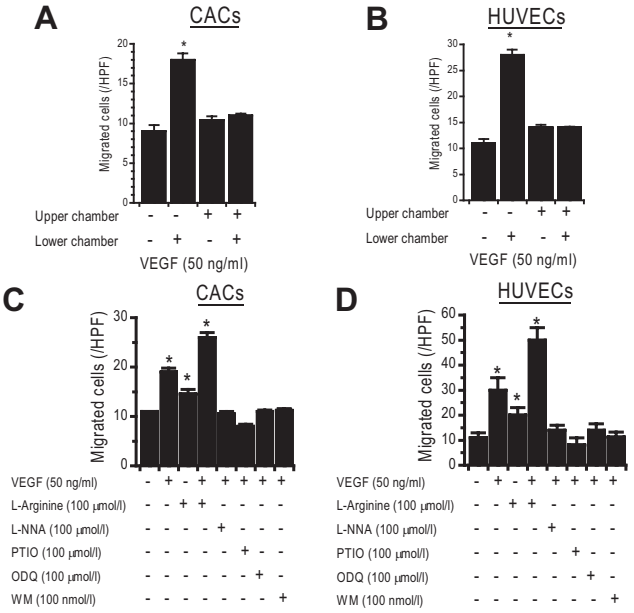

Figure 2. Mechanisms of CAC chemotaxis are similar to those of HUVECs. VEGF is a chemotactic stimulus for CACs (A) and HUVECs (B). Chemotaxis to VEGF was inhibited by L-NNA (NOS inhibitor), PTIO (NO scavenger), ODQ (guanylyl cyclase inhibitor), and WM (PI3K inhibitor) and was increased by L-arginine (NOS substrate). *$P<0.05$ versus control. (C and D, VEGF was added only to the lower chamber; L-NNA, ODQ, PTIO, WM, and L-arginine were added to the upper and lower chambers.) HPF indicates high-power field.

Results

CAC Characterization

During culture, mononuclear cells gave rise to adherent cells progressively expressing eNOS and releasing VEGF (Figure 1). At day 7, the majority of adherent cells expressed markers consistent with the early proangiogenic hematopoietic endothelial progenitor cell type as described in the literature, whereas nonadherent cells, which were not further studied herein, were mainly consistent with lymphocytes.[11,25,26] CACs migrated dose-dependently to a number of chemokines including VEGF, SDF-1α, PTN,[23] sphingosine-1-phosphate, and monocyte chemoattractant protein 1 but not to interleukin 6 at the concentrations tested (Figure 1D). Of the investigated chemokines, SDF-1α exerted the strongest migratory response (SDF-1α>VEGF=PTN>monocyte chemoattractant protein 1=sphingosine-1-phosphate).

Mechanisms of CAC Chemotaxis: Similarity With Endothelial Cells (HUVECs)

Further experiments showed that random cell movement in the presence of VEGF (50 ng/mL) in the upper and lower chambers (that is, no gradient) did not lead to significantly more cells on the lower side of the membrane compared with the negative control lacking VEGF (Figure 2A and 2B). This confirms that VEGF does not merely induce a significant chemokinetic response but stimulates specific chemotactic responses in CACs and HUVECs.[23]

To gain mechanistic insight into chemotaxis of CACs, we performed inhibitor studies to attempt to block the VEGF-induced chemotaxis (Figure 2C and 2D). Chemotaxis toward VEGF at 50 ng/mL was inhibited in the presence of a NOS inhibitor (L-NNA), an NO scavenger (PTIO), a phosphatidylinositol 3-kinase inhibitor (WM), and a guanylyl cyclase inhibitor (ODQ). Nondirectional cell movement, without addition of chemokines, remained unaffected by these inhibitors, suggesting that the observed lack of chemotaxis is due to specific inhibition of the pathways in question and cannot be explained by unspecific cell toxicity or globally disabled cell motility. Furthermore, our experiments show that the mechanisms involved in CAC chemotaxis are similar in HUVECs. Interestingly, L-arginine in the upper and lower chambers (no gradient) not only increased chemotaxis toward the VEGF gradient but enhanced chemokinesis.

NO Donor Induces Chemokinesis and Enhances Chemotaxis

To test how NO itself affects CAC motility and whether CACs follow a gradient of NO, we performed migration assays with the NO donor SNAP (Figure 3). As opposed to VEGF, SNAP induced a strong increase in random cell movement (chemokinesis). However, the number of migrated cells when SNAP (1 μmol/L; measured NO concentration in medium, 2.7 and 0.8 nmol/L at 0 and 3 hours, respectively) was present in both the upper and lower chambers was greater than when SNAP was present only in the lower chamber, suggesting that NO is a stronger inductor of chemokinesis than chemotaxis. Dose-dependent chemokinesis at 0.01 to 50 μmol/L showed a maximum at 1 μmol/L (28±3 cells/high-power field). Directional cell movement toward a VEGF gradient was also present at these SNAP concentrations. The highest absolute number of migrated cells was observed with a VEGF gradient (50 ng/mL) in the presence of SNAP at 1 μmol/L (34±4 cells/high-power field). These findings illustrate that SNAP-mediated chemokinesis acts synergisti-

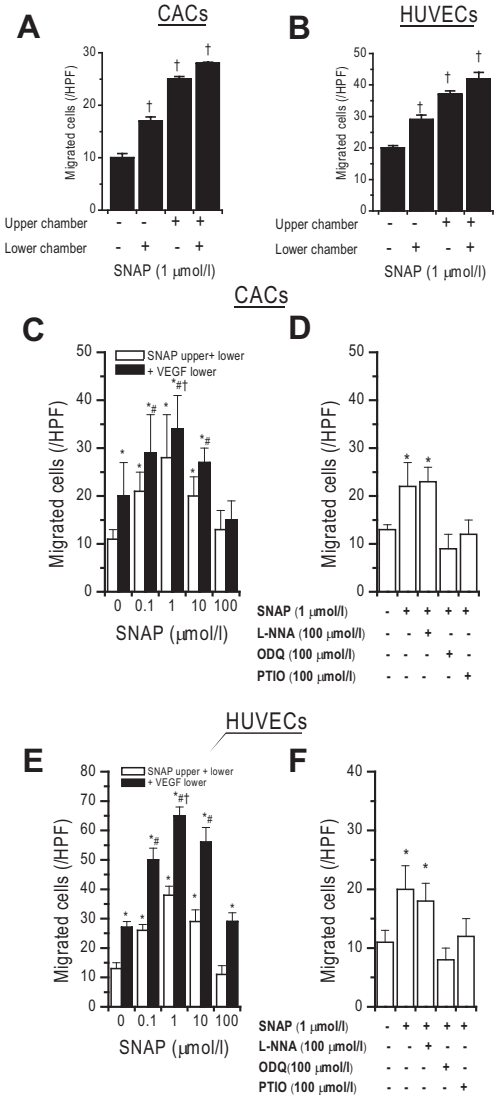

Figure 3. NO donor SNAP caused dose-dependent chemokinesis and enhanced VEGF-mediated chemotaxis. A and B, SNAP stimulated random cell movement (chemokinesis). C and E, Dose-dependent stimulation of chemokinesis and chemotaxis toward VEGF. D and F, Inhibition by ODQ (guanylyl cyclase inhibitor) and PTIO (NO scavenger) but not by NOS inhibitor L-NNA. †$P<0.05$ versus the respective column to the left; *$P<0.05$ versus control; #$P<0.05$ versus the respective white column; †$P<0.05$ versus VEGF alone. HPF indicates high-power field.

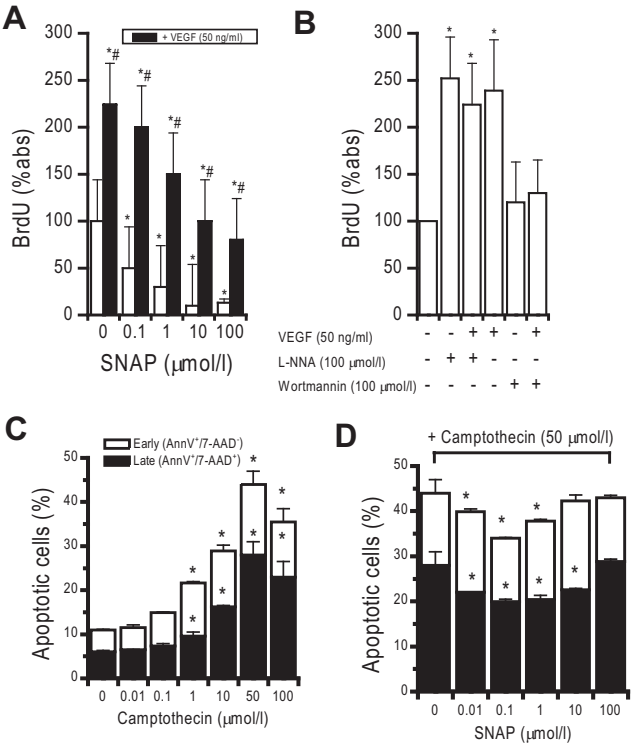

Figure 4. Effect of SNAP on CAC proliferation and apoptosis. A, Proliferation of CACs. B, VEGF-induced proliferation was increased by addition of L-NNA (NOS inhibitor), and inhibited by WM (PI3K inhibitor). C, Dose finding for camptothecin-induced apoptosis (early apoptotic cells: $AnnV^+/7\text{-}AAD^-$ [white columns]; late apoptotic cells: $AnnV^+/7\text{-}AAD^+$ [black columns]). D, SNAP dose-dependently inhibited apoptosis. %abs, percent absorption.

cally with VEGF-induced chemotaxis to enhance the number of net migrated cells, suggesting that exogenous NO facilitated directional cell movement to a chemokine stimulus. Addition of ODQ and PTIO but not L-NNA inhibited the chemokinetic SNAP (1 μmol/L) response, suggesting guanylate cyclase dependence, NO specificity, and NOS independence. This shows that both CACs and HUVECs similarly distribute faster in the presence of NO but are still responsive toward chemotactic stimuli.

In addition to its effects on cell migration, SNAP dose-dependently inhibited both VEGF-induced and spontaneous CAC proliferation (Figure 4). Conversely, inhibition of NOS by L-NNA stimulated proliferation to a degree similar to VEGF, suggesting opposite effects of VEGF and NO with respect to proliferation, as previously shown.[23] VEGF-induced proliferation was inhibited by WM, suggesting dependence of this effect on phosphatidylinositol 3-kinase but not NOS.

SNAP also dose-dependently inhibited camptothecin-induced apoptosis of CACs (Figure 4). Early apoptosis was identified by annexin V binding ($AnnV^+$) along with 7-AAD exclusion ($7\text{-}AAD^-$), showing that the cell membrane was intact. $AnnV^+$, along with 7-AAD uptake (ie, disrupted membrane), identified late apoptosis. Vital cells were identified as being negative for $AnnV^+$ and 7-AAD. Camptothecin dose-dependently induced apoptosis in CACs. Maximal apoptosis of CACs was achieved with >10 μmol/L camptothecin at 3 hours (40% early apoptosis $AnnV^+/7\text{-}AAD$; 20% late apoptosis $AnnV^+/7\text{-}AAD^+$). Coincubation of SNAP at 0.1 to 100 μmol/L led to dose-dependent inhibition of camptothecin-induced apoptosis at 50 μmol/L, with significantly higher numbers of vital cells ($AnnV^-/7\text{-}AAD^-$). Maximal effects were observed at 1 μmol/L SNAP. The degree of apoptosis inhibition was similar to that induced by VEGF (50 ng/mL), which is known to inhibit apoptosis. Similar results were obtained when apoptosis was induced by staurosporin (data not shown).

Impaired CAC Migration and NOS Expression in CAD Patients

To show the clinical relevance of these findings to human cardiovascular disease, we measured CAC migration as a

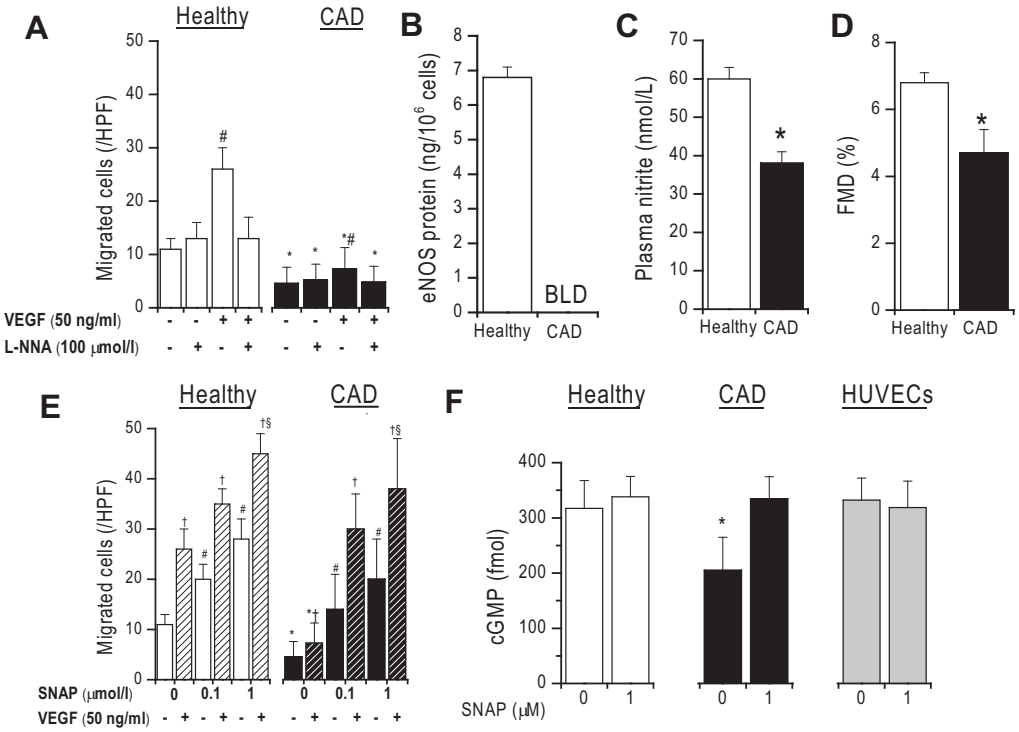

Figure 5. Impaired chemotaxis and eNOS expression in CAD patients. A, L-NNA-inhibitable CAC migration was significantly reduced in CAD patients as compared with healthy controls. B, eNOS protein expression in CAD CACs was below the limit of detection (BLD). C and D, Plasma nitrite (C) and flow-mediated vasodilation (FMD) (D) were impaired in CAD, reflecting endothelial dysfunction. E, CAC random cell movement and chemotaxis (toward 50 ng/mL VEGF; hatched columns) dose-dependently increased in CACs from both groups. F, The respective cGMP levels. *$P<0.05$ versus the respective condition in the healthy group; #$P<-0.05$ versus random cell movement without additives in the same group; †$P<0.05$ versus the respective no-VEGF condition; §$P<0.05$ versus VEGF alone in the same group. HPF indicates high-power field.

readout of therapeutic potency and quantitated eNOS protein in CACs from older CAD patients compared with those from younger, healthy subjects (age, 56±3 versus 30±2 years; $P<0.001$). Supplemental Table I summarizes the clinical baseline characteristics. Flow-mediated vasodilation (FMD; 4.7±0.7 versus 6.8±0.3%, $P<0.001$, Figure 5) and plasma nitrite (38±3 versus 60±3 nmol/L, $P<0.001$) were significantly lower in the patients, demonstrating endothelial dysfunction and impaired systemic NO bioavailability in these patients despite optimal medical therapy including statins.

In vitro assays showed that in CAD both unstimulated random CAC movement and chemotaxis toward VEGF (5±3 and 7±4 cells/high-power field, respectively) were significantly impaired compared with healthy subjects (11±2 and 26±4 cells/high-power field, each $P<0.001$; Figure 5). Importantly, eNOS levels were also significantly reduced (below the detection limit of the assay) in older CAD patients compared with healthy volunteers, offering a feasible explanation for the decreased functional capacity of these patients' CACs. SNAP added to both chambers at 0 to 1 μmol/L led to a similar dose-dependent chemokinetic migratory response in both groups and enhanced chemotaxis to VEGF (healthy n=10, CAD n=5, because of insufficient number of cells from 5 of the patients). In the presence of SNAP at >0.1 μmol/L, the migratory response was not significantly different between healthy and CAD patients. Whereas baseline intracellular cGMP levels were significantly lower in CAD, there was no significant difference between healthy and CAD after incubation with SNAP (1 μmol/L). No significant differences were seen in CD45 (98±2%, 97±1%) and CD31 (26±4%, 34±9%) expression by fluorescence-activated cell sorting, and inducible NOS mRNA was not detected in either kind of cell (data not shown). This suggests that response to exogenous NO was preserved in CAD patients despite a reduction in NOS-dependent response to endogenous NO.

Discussion

Our data show that both endogenous NOS activity and exogenous NO modulate CAC motility. NOS activity is required for chemotactic migration of CACs to angiogenic chemokines, whereas exogenous NO induces chemokinesis, enhancing directional chemotaxis toward VEGF, without directly acting as a chemoattractant itself. Notably, the effects of the NO donor SNAP and NOS on the CACs were qualitatively similar to their effects on HUVECs, despite the presumption that these early proangiogenic CACs do not function as direct endothelial precursors. We show clinical relevance in that CAC migration in CAD patients is limited by decreased endogenous NOS activity because of impaired expression rather than impaired response to exogenous NO.

NOS plays an important regulatory role in vascular biology, and defective endothelial NO synthesis may limit angiogenesis in patients with endothelial dysfunction.[27] An impairment of the endogenous NO signaling in endothelium is coupled with the inability to produce an angiogenic

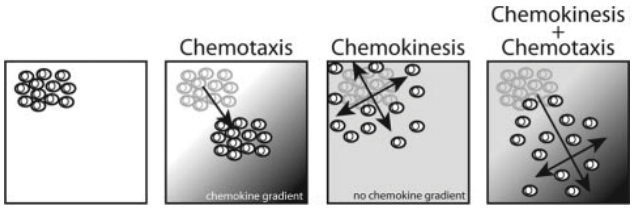

Figure 6. Schematic to illustrate the proposed additive effects of directional (chemotaxis) and nondirectional (chemokinesis) random cell movement.

response to VEGF.[28,29] The effects of NO on CACs, which are important cells for endothelial repair, are not well understood. We describe here how the presence or absence of NO affects CAC motility. Corroborating previous studies,[17,23,30] we demonstrate that CACs NOS-dependently migrate to a number of chemokines. This supports the notion that NOS represents an integral pathway for cell migration. We have recently shown that CACs migrate to a gradient of PTN in a manner that is dependent on NOS, cGMP, NO, and PI3K.[23] Similarly, it was previously shown by others that SDF-1α induces CAC migration in an eNOS-, Akt-, and PI3K -dependent manner.[30] We show here that the migration to VEGF involves the same pathways as migration to PTN and SDF-1α. This is important because a number of risk factors promoting arteriosclerosis and poor tissue regeneration, including smoking, aging, diabetes, hypertension, and hypercholesterolemia, have been shown to also inhibit NO production.[2,17] These factors may mediate part of their vascular pathology by affecting vascular maintenance exerted by lowered NOS activity potentially via oxidative stress not only in endothelial cells but also in CACs, leading to dysfunction of these cells. This is supported by several studies in animal models and human clinical studies. In a recent clinical report, we have shown that passive smoke may decrease CAC migration by blocking NO production.[17] Animal hindlimb ischemia experiments have revealed that angiogenesis is impaired in eNOS$^{-/-}$ mice and that the eNOS substrate L-arginine can enhance angiogenesis in rabbits.[27] Another study suggests that diabetes may impair reendothelialization by impaired CAC function due to decreased eNOS expression.[31] More recently, it was shown in diabetic rats and patients that diabetes may impair CAC functions by uncoupling eNOS.[15] Taken together, our data suggest that dysfunctional CAC migration in CAD patients may be due to lower eNOS expression rather than impaired response to exogenous NO in CACs.

To our knowledge, this is the first report to show the effect of exogenous NO on CAC migratory function. We show that an NO donor induces chemokinesis. It is important to note that this does not impair the CACs' capacity to sense chemoattractant gradients and follow them, but actually significantly also increases the net number of migrated cells at the site of higher chemokine concentration (Figure 6). This is in agreement with previously published results by others showing that HUVECs cGMP-dependently migrate toward a gradient of NO using different NO donors, 1,1-diethyl-2-hydroxy-2-nitroso-hydrazine and 2,2′-(Hydroxynitrosohydrazono)bis-ethanimine, which have a longer half-life than SNAP.[32] To methodically exclude the possibility that SNAP merely increases cell proliferation at the lower side of the membrane, we performed proliferation assays showing that NO in fact decreases proliferation.[33] Corroborating results by others, we show that SNAP also decreased apoptosis.[34] In the context of the present study, we cannot exclude the possibility that NO increases survival of CACs and may thereby explain part of the migration results, potentially contributing to more cells recovered at the lower side of the membrane. Mechanistically, both CACs and HUVECs release NO, and chemotaxis of both cell types is enhanced by NO-related chemokinesis. This suggests that NO may serve as a signal coordinating and potentially stimulating endothelial and proangiogenic cell interactions. NO and chemokines released by proangiogenic CACs that have homed to sites of injury may further attract new cells in a positive feedback loop by facilitating chemotaxis and chemokinesis. Once cells reach each other, higher NO levels may enhance adhesion (Heiss et al, unpublished results, 2007) and inhibit proliferation and apoptosis while facilitating even dispersal via chemokinesis of CACs and endothelial cells. As the observed effects were dose dependent, the effect may likely differ between sites with different NO levels, such as inflammation with expression of high-output inducible NOS (micromolar range) or vascular endothelium (low nanomolar range). Furthermore, these results may have clinical importance in disease states with lowered NO bioavailability, eg, decreased levels of plasma *S*-nitrosothiols or nitrite, which represent physiological NO donors with cardiovascular risk factors.[2,24,35,36]

Our data further support the concept that the NOS/NO pathway is a strong modulator of CAC functions, as it is in endothelial cells. CAC functions are likely to be affected both by factors that impair this pathway of endothelial cells in patients with cardiovascular disease in vivo and by reduced NO bioavailability.[2]

Acknowledgments

We thank Dr Sourabh Kharait for helpful discussion and Dr Matthias Totzeck for technical assistance.

Sources of Funding

This work was supported by awards from the American Heart Association (0525078Y) and Forschungskommission, University Duesseldorf (to C.H.); the Wayne and Gladys Valley Foundation (to W.G.); the National Institutes of Health (HL086917) (to M.L.S. and Y.Y.); the University of California, San Francisco, Academic Senate Committee on Research and the American Heart Association (0535244N) (to M.L.S.); and the Deutsche Forschungsgemeinschaft (RA969/4-1) (to T.R.).

Disclosures

Dr Springer has received research funding from N30 Pharmaceuticals.

References

1. Cooke JP, Losordo DW. Nitric oxide and angiogenesis. *Circulation*. 2002;105:2133–2135.
2. Heiss C, Lauer T, Dejam A, Kleinbongard P, Hamada S, Rassaf T, Matern S, Feelisch M, Kelm M. Plasma nitroso compounds are decreased in patients with endothelial dysfunction. *J Am Coll Cardiol*. 2006;47:573–579.
3. Widlansky ME, Gokce N, Keaney JF Jr, Vita JA. The clinical implications of endothelial dysfunction. *J Am Coll Cardiol*. 2003;42:1149–1160.

4. Libby P, Ridker PM, Maseri A. Inflammation and atherosclerosis. *Circulation*. 2002;105:1135–1143.
5. Heiss C, Kleinbongard P, Dejam A, Perré S, Schroeter H, Sies H, Kelm M. Acute consumption of flavanol-rich cocoa and the reversal of endothelial dysfunction in smokers. *J Am Coll Cardiol*. 2005;46:1276–1283.
6. Heiss C, Keymel S, Niesler U, Ziemann J, Kelm M, Kalka C. Impaired progenitor cell activity in age-related endothelial dysfunction. *J Am Coll Cardiol*. 2005;45:1441–1448.
7. Celermajer DS, Sorensen KE, Bull C, Robinson J, Deanfield JE. Endothelium-dependent dilation in the systemic arteries of asymptomatic subjects relates to coronary risk factors and their interaction. *J Am Coll Cardiol*. 1994;24(6):1468–1474.
8. Dimmeler S, Zeiher AM. Vascular repair by circulating endothelial progenitor cells: the missing link in atherosclerosis? *J Mol Med*. 2004;82:671–677.
9. Hristov M, Weber C. The therapeutic potential of progenitor cells in ischemic heart disease: past, present and future. *Basic Res Cardiol*. 2006;101:1–7.
10. Murasawa S, Asahara T. Endothelial progenitor cells for vasculogenesis. *Physiology*. 2005;20:36–42.
11. Hirschi KK, Ingram DA, Yoder MC. Assessing identity, phenotype, and fate of endothelial progenitor cells. *Arterioscler Thromb Vasc Biol*. 2008;28:1584–1595.
12. Rehman J, Li J, Orschell CM, March KL. Peripheral blood "endothelial progenitor cells" are derived from monocyte/macrophages and secrete angiogenic growth factors. *Circulation*. 2003;107:1164–1169.
13. Britten MB, Abolmaali ND, Assmus B, Lehmann R, Honold J, Schmitt J, Vogl TJ, Martin H, Schachinger V, Dimmeler S, Zeiher AM. Infarct remodeling after intracoronary progenitor cell treatment in patients with acute myocardial infarction (TOPCARE-AMI): mechanistic insights from serial contrast-enhanced magnetic resonance imaging. *Circulation*. 2003;108:2212–2218.
14. Keymel S, Kalka C, Rassaf T, Yeghiazarians Y, Kelm M, Heiss C. Impaired endothelial progenitor cell function predicts age-dependent carotid intimal thickening. *Basic Res Cardiol*. 2008;103:582–586.
15. Thum T, Fraccarollo D, Schultheiss M, Froese S, Galuppo P, Widder JD, Tsikas D, Ertl G, Bauersachs J. Endothelial nitric oxide synthase uncoupling impairs endothelial progenitor cell mobilization and function in diabetes. *Diabetes*. 2007;56:666–674.
16. Michaud SE, Dussault S, Haddad P, Groleau J, Rivard A. Circulating endothelial progenitor cells from healthy smokers exhibit impaired functional activities. *Atherosclerosis*. 2006;187:423–432.
17. Heiss C, Amabile N, Lee AC, Real WM, Schick SF, Lao D, Wong ML, Jahn S, Angeli FS, Minasi P, Springer ML, Hammond SK, Glantz SA, Grossman W, Balmes JR, Yeghiazarians Y. Brief secondhand smoke exposure depresses endothelial progenitor cells activity and endothelial function: sustained vascular injury and blunted nitric oxide production. *J Am Coll Cardiol*. 2008;51:1760–1771.
18. Thum T, Tsikas D, Stein S, Schultheiss M, Eigenthaler M, Anker SD, Poole-Wilson PA, Ertl G, Bauersachs J. Suppression of endothelial progenitor cells in human coronary artery disease by the endogenous nitric oxide synthase inhibitor asymmetric dimethylarginine. *J Am Coll Cardiol*. 2005;46:1693–1701.
19. Vasa M, Fichtlscherer S, Aicher A, Adler K, Urbich C, Martin H, Zeiher AM, Dimmeler S. Number and migratory activity of circulating endothelial progenitor cells inversely correlate with risk factors for coronary artery disease. *Circ Res*. 2001;89:E1–E7.
20. Smith SC Jr, Allen J, Blair SN, Bonow RO, Brass LM, Fonarow GC, Grundy SM, Hiratzka L, Jones D, Krumholz HM, Mosca L, Pasternak RC, Pearson T, Pfeffer MA, Taubert KA. AHA/ACC guidelines for secondary prevention for patients with coronary and other atherosclerotic vascular disease: 2006 update: endorsed by the National Heart, Lung, and Blood Institute. *Circulation*. 2006;113:2363–2372.
21. Hill JM, Zalos G, Halcox JP, Schenke WH, Waclawiw MA, Quyyumi AA, Finkel T. Circulating endothelial progenitor cells, vascular function, and cardiovascular risk. *N Engl J Med*. 2003;348:593–600.
22. Falk W, Goodwin RH Jr, Leonard EJ. A 48-well micro chemotaxis assembly for rapid and accurate measurement of leukocyte migration. *J Immunol Methods*. 1980;33:239–247.
23. Heiss C, Wong ML, Block VI, Lao D, Real WM, Yeghiazarians Y, Lee RJ, Springer ML. Pleiotrophin induces nitric oxide dependent migration of endothelial progenitor cells. *J Cell Physiol*. 2007;215:366–373.
24. Rassaf T, Preik M, Kleinbongard P, Lauer T, Heiss C, Strauer BE, Feelisch M, Kelm M. Evidence for *in vivo* transport of bioactive nitric oxide in human plasma. *J Clin Invest*. 2002;109:1241–1248.
25. Hur J, Yoon CH, Kim HS, Choi JH, Kang HJ, Hwang KK, Oh BH, Lee MM, Park YB. Characterization of two types of endothelial progenitor cells and their different contributions to neovasculogenesis. *Arterioscler Thromb Vasc Biol*. 2004;24:288–293.
26. Kalka C, Masuda H, Takahashi T, Kalka-Moll WM, Silver M, Kearney M, Li T, Isner JM, Asahara T. Transplantation of ex vivo expanded endothelial progenitor cells for therapeutic neovascularization. *Proc Natl Acad Sci U S A*. 2000;97:3422–3427.
27. Murohara T, Asahara T, Silver M, Bauters C, Masuda H, Kalka C, Kearney M, Chen D, Symes JF, Fishman MC, Huang PL, Isner JM. Nitric oxide synthase modulates angiogenesis in response to tissue ischemia. *J Clin Invest*. 1998;101:2567–2578.
28. Morbidelli L, Donnini S, Ziche M. Role of nitric oxide in the modulation of angiogenesis. *Curr Pharm Des*. 2003;9:521–530.
29. Kimura H, Esumi H. Reciprocal regulation between nitric oxide and vascular endothelial growth factor in angiogenesis. *Acta Biochim Pol*. 2003;50:49–59.
30. Zheng H, Fu G, Dai T, Huang H. Migration of endothelial progenitor cells mediated by stromal cell-derived factor-1alpha/CXCR4 via PI3K/Akt/eNOS signal transduction pathway. *J Cardiovasc Pharmacol*. 2007;50:274–280.
31. Ii M, Takenaka H, Asai J, Ibusuki K, Mizukami Y, Maruyama K, Yoon YS, Wecker A, Luedemann C, Eaton E, Silver M, Thorne T, Losordo DW. Endothelial progenitor thrombospondin-1 mediates diabetes-induced delay in reendothelialization following arterial injury. *Circ Res*. 2006;98:697–704.
32. Isenberg JS, Ridnour LA, Thomas DD, Wink DA, Roberts DD, Espey MG. Guanylyl cyclase-dependent chemotaxis of endothelial cells in response to nitric oxide gradients. *Free Radic Biol Med*. 2006;40:1028–1033.
33. Bussolati B, Dunk C, Grohman M, Kontos CD, Mason J, Ahmed A. Vascular endothelial growth factor receptor-1 modulates vascular endothelial growth factor-mediated angiogenesis via nitric oxide. *Am J Pathol*. 2001;159:993–1008.
34. Zheng H, Dai T, Zhou B, Zhu J, Huang H, Wang M, Fu G. SDF-1alpha/CXCR4 decreases endothelial progenitor cells apoptosis under serum deprivation by PI3K/Akt/eNOS pathway. *Atherosclerosis*. 2008;201:36–42.
35. Cannon RO, Schechter AN, Panza JA, Ognibene FP, Pease-Fye ME, Waclawiw MA, Shelhamer JH, Gladwin MT. Effects of inhaled nitric oxide on regional blood flow are consistent with intravascular nitric oxide delivery. *J Clin Invest*. 2001;108:279–287.
36. Lundberg JO, Weitzberg E. NO generation from nitrite and its role in vascular control. *Arterioscler Thromb Vasc Biol*. 2005;25:915–922.

Supplement Material.

Methods

Characterization of blood-derived CACs

Blood was drawn from the cubital vein into vacuum tubes pre-filled with a liquid density gradient medium and MNCs were isolated based on the Ficoll method (Vacutainer CPT, Becton Dickinson, Franklin Lakes, NJ). In order to remove mature endothelial cells from the harvested cell population, the cells were preplated on fibronectin-coated culture plates for 1 day in EBM-2 MV (supplemented with Singlequots, 20% fetal bovine serum, HyClone, Logan, UT). The initially firmly adherent cells were discarded and the non-adherent cells (>95%) were moved to a new dish and cultured for another 6 days, during which time many cells (10% on average) became newly adherent.

To confirm that the *in vitro* adhesion selection of initially weakly or non-adherent MNCs gives rise to pro-angiogenic CACs, we characterized newly adherent cells and non-adherent cells at day 7 by their ability to take up acLDL and bind to UEA lectin, specific surface markers, VEGF, and eNOS expression.[1,2] Adherent CACs on fibronectin-coated glass slides (Nalge NUNC, Naperville, IL) were incubated for 1 h with 2 μg/mL DiI-acLDL (Invitrogen, Carlsbad, CA) in EBM-2 MV, washed twice with PBS and fixed in 2% formaldehyde/PBS. After blocking with 2% goat serum/PBS for 1 h, cells were washed and incubated with 23 μg/mL FITC-conjugated *Ulex europeus* agglutinin-1 (UEA-1, Sigma, St. Louis, MO). The nuclei were stained with 125 ng/mL Hoechst 33258 (Invitrogen). The slides were observed using a Nikon E800 fluorescence microscope and Openlab software (Improvision, Lexington, MA). To further characterize the cells, FACS analysis was performed with the CACs (large mainly spindle shaped, firmly adherent)

and compared to the small weakly or non-adherent cells (non-CACs) in the same cultures. After harvesting weakly or non-adherent cells and rinsing the dish with PBS, adherent cells were detached by repetitive flushing with cold 1 mM EDTA/PBS. CACs and non-adherent cells were pelleted, adjusted to 10^6 cells/mL, and incubated for 20 min with normal human IgG (1 mg/mL, Zymed, San Francisco, CA) to block F_C receptor. Staining was performed for 20 min with 100 μL cell suspension and the following fluorescently labeled antibodies: CD45-PerCP, CD34-PE, CD133-PE (Miltenyi Biotech, Auburn, CA), KDR-APC, CD31-PC5, CXCR4-APC, CD14-PerCP, and CD11b-APC (Pharmingen, San Diego, CA). After washing with FACS buffer, cells were fixed with 1% formaldehyde/PBS and stored at 4°C until flow-cytometry analysis. 10,000 events were counted (FACSCalibur, BD, San Diego, CA). Further characterization was performed by measuring eNOS protein levels in cell lysates before and after 2, 4, 7, and 14 days culture using a commercially available ELISA kit (Quantikine, R&D) following the recommended protocol. Lysates were produced by addition of supplied lysis buffer to frozen cell pellets.

Cell proliferation and apopotosis assays

BrdU incorporation assays were performed following the manufacturer's protocol (Cell Proliferation BrdU Assay, Roche). Cells were detached, resuspended in EBM-2 supplemented with 1% BSA, and plated at 10^4 /well in 96-well cell culture plates (Corning). The cells were preincubated with test mitogens for 48 h. BrdU was added and cells were incubated for another 24 h. BrdU incorporation was determined in an ELISA plate reader by light absorption at 450 nm after incubation with anti-BrdU antibodies conjugated with horseradish peroxidase. Apoptosis assays were performed with FACS

essentially as described in the manufacturer's (Guava, Hayward, CA) protocol. Day 7 CACs were washed 2x with PBSE (phosphate buffered saline, 1 mM EDTA), detached, and resuspended in EBM-2 (without supplements other than 1% BSA). 100 uL of cell suspension containing 40,000 CACs were incubated with the apoptosis inductor camptothecin (0.01-100 µmol/l), SNAP (0.01-100 µmol/l), or VEGF (50 ng/mL) at 37˚C. After 3 h, cells were washed in assay buffer on ice and resuspended in 40 uL assay buffer. 5 uL of AnnexinV-PE/7-amino actinomycin D (7-AAD) staining solution was added to cell suspension and incubated 20 min on ice. After addition of 450 uL assay buffer, cells were run on a flow cytometer (Guava). Analyses were performed automatically (Nexin, Guava). Apoptotic cells were positive for AnnexinV binding ($AnnV^+$). Additionally, $AnnV^+$ cells that excluded 7-AAD ($AnnV^+$ $7\text{-}AAD^-$), indicating an intact cell membrane, were defined as early apoptotic. 7-AAD positivity ($AnnV^+/7\text{-}AAD^+$) indicated disrupted cell membrane integrity and late apoptosis.

Additional information for chemotaxis

In preparation for the migration experiments, bottom chambers were blocked with 10% BSA/PBS for 10 min and rinsed with PBS 3 times, as our preliminary experiments have shown that VEGF binds to the plastic and the concentration in the solution drops precipitously if the wells are not blocked. Preliminary recovery experiments were performed by measuring VEGF in the upper and lower chamber after adding VEGF to the lower chamber. These experiments confirmed that there was significantly higher VEGF concentration in the lower chamber for up to 12 h.

Both CACs and HUVECs were detached non-enzymatically by flushing with cold EDTA-containing dissociation buffers (Invitrogen) to avoid digestion of receptors by

trypsin. After detachment, cells were resuspended in EBM-2 (without supplements, 1% BSA) and $2x10^4$ plated in the upper of two chambers divided by a membrane with 8 μm pores (Corning Transwell). The bottom of the membrane was coated with vitronectin, fibronectin, and gelatin (Sigma). Chemoattractants specific to the experiment were added to the lower chamber only. The following were added to both the upper and lower chamber: NOS substrate L-arginine (100 μmol/l), NOS inhibitor L-NNA (100 μmol/l), NO scavenger PTIO (2-(4-Carboxyphenyl)-4,4,5,5-tetramethylimidazoline-1-oxyl-3-oxide, 100 μmol/l), guanylyl cyclase inhibitor ODQ (1H-[1,2,4]Oxadiazolo[4,3-a]quinoxalin-1-one, 100 μmol/l), and the PI3 Kinase inhibitor Wortmannin (100 nmol/l). We tested the chemotactic properties of vascular endothelial growth factor (VEGF, Sigma) and stromal cell-derived factor (SDF-1α; Sigma), and pleiotrophin (PTN, Sigma) at 10-500 ng/mL, monocyte chemoattractant protein-1 (MCP-1, Sigma), sphingosine-1-phosphate (S1P, Sigma), and interleukin-6 (IL6, Sigma) at 10-100 ng/ml, and S-nitroso-N-acetylpenicillamine (SNAP, Sigma) at 1 nmol/l-10 μmol/l. To test the chemokinetic properties of SNAP inducing random cell movement, SNAP was added to the upper and lower chambers. Each experimental condition was performed in triplicate and the number of migrated cells was determined on 5 random 100x optical fields (0.998 mm^2) per membrane.

Flow-mediated dilation (FMD)

Endothelium-dependent dilation of the brachial artery (BA) was measured by ultrasound (Sonosite Micromax, Bothell, WA) in combination with an automated analysis system (Brachial Analyzer, Medical Imaging Applications, Iowa City, IA). Baseline data for diameter and blood-flow velocity of the BA were quantified after 10 min of supine rest in

a 21°C room. A forearm blood-pressure cuff was placed distal to the antecubital fossa and inflated to 250 mmHg for 5 min. Diameter was measured immediately after cuff deflation, at 20, 40, 60, and 80 sec. FMD was expressed as: ($diameter_{max}$-$diameter_{baseline}$)/$diameter_{baseline}$.

Plasma nitrite level

The plasma nitrite levels, representing a sensitive read-out of NOS activity, were measured by chemiluminecence. In brief, venous blood supplemented with heparin (10 IU/mL), and EDTA (2 mmol/L) was centrifuged for 10 minutes at 800 *g* and 4°C immediately after sample drawing. The separated plasma samples were stored on ice. Nitrite was measured using a mixture of iodine/iodide in glacial acetic acid and subsequent detection of the liberated NO by its gas-phase chemiluminescence reaction with ozone. Concentrations of nitrite were determined by the difference in peak areas of untreated aliquots and those subjected to preincubation with 0.5% sulfanilamide/HCl.

RNA expression analyses

RNA was isolated by using an RNAeasy mini kit (Qiagen) following the manufacturer's instructions. The RNA (0.5 or 1 μg) was then reverse transcribed in a MyCycler personal thermal cycler (Bio-Rad Laboratories GmbH, Munich, Germany) using a QuantiTect Reverse Transcription Kit (Qiagen) following the manufacturer's instructions. DNA (5 ng) or control RNA was used as a template for real-time PCR performed in triplicate using TaqMan universal PCR master mix in a ABI PRISM 7900 system (Applied Biosystems, Foster City, CA). The following primers and probes were purchased from Applied Biosystems: nitric oxide synthase 3, endothelilal (Hs00167166_m1), nitric oxide-synthase 2, inducible (Hs01075527_m1), and 18s rRNA, which was chosen as a

housekeeping gene. As a positive control HUVECs were activated by incubation with TNFα 500 U/mL, INFγ 500 U/mL, and IL-1β 500 U/mL over 24 h.

Results

CAC characterization. To confirm that the *in vitro* adhesion selection of initially weakly or non-adherent MNCs gave rise to pro-angiogenic CACs, we characterized large, firmly adherent, mainly spindle shaped or round flat cells as well as small non-adherent cells by their ability to take up acLDL and bind to UEA lectin, and by expression of specific surface markers, the angiogenic growth factor VEGF, and eNOS.[1] During culture of MNCs from healthy subjects, one population of cells firmly adhered to fibronectin and progressively increased eNOS protein content up to 19.3±6.1 ng/10^6 cells plateauing after 7 days. Expression of eNOS by the non-adherent cells was very low, below the detection limit of the ELISA assays (Figure 1a). The eNOS protein content in the CACs was significantly lower than that measured in HUVECS (33.5 ng/10^6 cells, p=0.03). We have previously shown by experiments with the NO-sensitive fluorescent dye DAF-2DA that CACs isolated under our conditions express a functional NOS.[1] Furthermore, adherent cells progressively secreted increasing amounts of VEGF (Figure 1b). The majority of firmly adherent cells also expressed both endothelial (KDR, CD31) and monocyte markers (CD11b, CD14) (Figure 1c). The majority of non-adherent cells expressed CD3, consistent with an identity of lymphocytes. Both populations expressed the hematopoietic marker CD45 and CXCR4. 92±8% of the firmly adherent cells took up acLDL and stained positive with UEA lectin, whereas none of the non-adherent cells took up acLDL (data not shown). Neither one of the populations differentiated into endothelial cells as defined by formation of tube-like structures or contact-inhibited monolayers (data not

shown). Taken together, the adherent cell population that was studied in the present paper and is herein referred to as CACs is consistent with the early pro-angiogenic hematopoietic EPC type, whereas non-adherent cells which were not further studied herein were mainly consistent with lymphocytes.[3-5]

SNAP also dose-dependently inhibited camptothecin-induced apoptosis of CACs (Figure 2). Early apoptosis was identified by annexinV-binding ($AnnV^+$) along with 7-AADexclusion ($7\text{-}AAD^-$) showing that the cell membrane was intact. AnnexinV binding along with 7-AAD uptake (i.e. disrupted membrane) identified late apoptosis. Vital cells were identified as being negative for annexin V-binding and 7-AAD. Camptothecin dose-dependently induced apoptosis in CACs. Maximal apoptosis of CACs was achieved with >10 μmol/l camptothecin at 3 h (40% early apoptosis $AnnV^+/7\text{-}AAD$ 20% late apoptosis $AnnV^+/7\text{-}AAD^+$). Coincubation of SNAP at 0.1-100 μmol/l led to dose-dependent inhibition of camptothecin-induced apoptosis at 50 μmol/l with significantly higher numbers of vital cells ($AnnV^-/7\text{-}AAD^-$). Maximal effects were observed at 1 μmol/l SNAP. The degree of apoptosis inhibition was similar to that induced by VEGF (50 ng/ml), which is known to inhibit apoptosis. Similar results were obtained when apoptosis was induced by staurosporin (data not shown).

Supplement Table I Characteristics of study population

	Healthy	**CAD**	***p***
N (m/f)	10 (7/3)	10 (7/3)	
Age (yr)	30±1	56±3	*<0.001*
BMI (kg/m^2)	24.3±1.1	27.8±1.8	*0.098*
Diabetes mellitus (%)	0	40	
Hypertension (%)	0	80	
Hyperlipidemia (%)	0	100	
Prior smoking (%)	0	50	
ACE inhibitor/angiotensin receptor blocker (%)	0	90	
Aspirin (%)	0	100	
Beta blocker (%)	0	80	
Statin (%)	0	100	
Heart rate (/min)	63±3	59±2	*0.206*
Systolic blood pressure (mmHg)	100±3	128±5	*0.002*
Diastolic blood pressure (mmHg)	58±2	80±3	*<0.001*
Total cholesterol (mg/dL)	179±7	145±7	*0.005*
LDL cholesterol (mg/dL)	121±9	75±5	*<0.001*
HDL cholesterol (mg/dL)	51±5	50±4	*0.821*
Triglycerides (mg/dL)	77±9	102±15	*0.188*
Fasting glucose (mg/dL)	73±3	94±4	*0.001*
Flow-mediated dilation (%)	6.8±0.3	4.7±0.7	*0.007*
Plasma nitrite (nmol/L)	60±3	38±3	*<0.001*

Data given as mean±SEM

References

(1) Heiss C, Wong ML, Block VI, Lao D, Real WM, Yeghiazarians Y, Lee RJ, Springer ML. Pleiotrophin induces nitric oxide dependent migration of endothelial progenitor cells. *J Cell Physiol.* 2007;215:366-373.

(2) Asahara T, Murohara T, Sullivan A, Silver M, van der ZR, Li T, Witzenbichler B, Schatteman G, Isner JM. Isolation of putative progenitor endothelial cells for angiogenesis. *Science.* 1997;275:964-967.

(3) Hur J, Yoon CH, Kim HS, Choi JH, Kang HJ, Hwang KK, Oh BH, Lee MM, Park YB. Characterization of two types of endothelial progenitor cells and their different contributions to neovasculogenesis. *Arterioscler Thromb Vasc Biol.* 2004;24:288-293.

(4) Kalka C, Masuda H, Takahashi T, Kalka-Moll WM, Silver M, Kearney M, Li T, Isner JM, Asahara T. Transplantation of ex vivo expanded endothelial progenitor cells for therapeutic neovascularization. *Proc Natl Acad Sci U S A.* 2000;97:3422-3427.

(5) Hirschi KK, Ingram DA, Yoder MC. Assessing identity, phenotype, and fate of endothelial progenitor cells. *Arterioscler Thromb Vasc Biol.* 2008;28:1584-1595.

Free Radical Research, June 2011; 45(6): 653–661

informa
healthcare

Nitric oxide influences red blood cell velocity independently of changes in the vascular tone

PATRICK HORN[1*], MIRIAM M. CORTESE-KROTT[1*], STEFANIE KEYMEL[1], INTAN KUMARA[1], SANDRA BURGHOFF[2], JÜRGEN SCHRADER[2], MALTE KELM[1] & PETRA KLEINBONGARD[1,3]

[1]*Division of Cardiology, Pneumology and Angiology, Medical Faculty of the Heinrich Heine University of Duesseldorf, Germany,* [2]*Institute of Cardiovascular Physiology, Medical Faculty of the Heinrich-Heine-University of Duesseldorf, Germany, and* [3]*Institute of Pathophysiology, University of Essen Medical School, Essen, Germany*

(Received date: 10 January 2011; Accepted date: 18 Mar 2011)

Abstract

Nitric oxide (NO) plays a key role in regulation of vascular tone and blood flow. In the microcirculation blood flow is strongly dependent on red blood cells (RBC) deformability. *In vitro* NO increases RBC deformability. This study hypothesized that NO increases RBC velocity *in vivo* not only by regulating vascular tone, but also by modifying RBC deformability. The effects of NO on RBC velocity were analysed by intra-vital microscopy in the microcirculation of the chorioallantoic membrane (CAM) of the avian embryo at day 7 post-fertilization, when all vessels lack smooth muscle cells and vascular tone is not affected by NO. It was found that inhibition of enzymatic NO synthesis and NO scavenging decreased intracellular NO levels and avian RBC deformability *in vitro*. Injection of a NO synthase-inhibitor or a NO scavenger into the microcirculation of the CAM decreased capillary RBC velocity and deformation, while the diameter of the vessels remained constant. The results indicate that scavenging of NO and inhibition of NO synthesis decrease RBC velocity not only by regulating vascular tone but also by decreasing RBC deformability.

Keywords: *Intra-vital microscopy, microcirculation, chorioallantoic membrane, NO, erythrocyte deformability.*

Introduction

Capillary blood flow supplies organs with oxygen and nutrients and is regulated by both vascular tone changes [1] and rheological properties of blood cells [2]. In the capillaries, RBC must deform to enter and transit vessels narrower than their own diameter. Therefore, RBC velocity and capillary blood flow strongly depend on RBC deformability [3–6], defined as the ability of RBC to deform under a given force.

Nitric oxide (NO) plays a key role in blood flow control [7,8]. In the cardiovascular system NO is continuously produced in endothelial cells from L-arginine in a reaction catalysed by the type III isoform of NO synthase (NOS3, EC 1.14.13.39), commonly defined as endothelial NOS (eNOS) [9]. Endothelium-derived NO relaxes the smooth muscle cells in the vascular wall and controls vascular resistance. In the vascular lumen, NO can be scavenged by oxyhaemoglobin, the most abundant protein expressed in RBC. In addition, RBC are known to accumulate and transport NO metabolites, like nitrite [10,11] and under hypoxic conditions induce aortic ring relaxation [12,13]. Moreover, RBC express an active NOS [14,15] and under normoxic conditions release NO metabolites *in vitro* in a NOS-dependent fashion [15].

A role of NO in the control of RBC deformability has been proposed. NO donors affect RBC deformability as measured *in vitro* [16–21] and *ex vivo* [20]. Treatment of freshly isolated human RBC with a

[*]These authors contributed equally to this work.

Correspondence: Professor Malte Kelm, MD, Duesseldorf University Hospital, Division of Cardiology, Pneumology and Angiology, Moorenstrasse 5, 40225 Duesseldorf, Germany. Tel: +49 211 811 8801. Fax: +49 211 81 18812. Email: malte.kelm@med.uni-duesseldorf.de

ISSN 1071-5762 print/ISSN 1029-2470 online
DOI: 10.3109/10715762.2011.574288

NOS inhibitor decreased RBC deformability as measured *in vitro* [17,22]. It is not known whether NO-dependent changes of RBC deformability affect RBC velocity and blood flow in the microcirculation. *In vivo*, application of NOS inhibitors reduced RBC velocity and blood flow in the microcirculation of skeletal muscle [23] or the liver [24] and affected vascular tone [23,24]. In these models it was not possible to distinguish whether the NOS inhibitors decreased RBC velocity not only by inducing vasoconstriction, but also by decreasing RBC deformability.

Here we tested whether scavenging of NO or NOS inhibition decrease RBC velocity *in vivo* also by decreasing RBC deformability. We have taken advantage of using the microcirculation of the avian chorioallantoic membrane (CAM), which is an extra-embryonic vessel system arising from differentiated mesodermal endothelial cells. This model has previously been applied to study angiogenesis [25] and vasoreactivity in response to epoxyeicosatrienoic acids [26]. RBC velocity and deformation of single RBC passing through the capillaries of the CAM were quantified by intra-vital microscopy using a high-speed camera. The experiments were performed on day 7 post-fertilization, when all vessels lack smooth muscle cells [25,27]. Thus, in this model vascular diameter cannot be modified by NO, as shown previously [26]. This allowed us to focus on the effect of NO on RBC velocity and cell deformation *in vivo*, independently of changes on vascular tone.

Methods

Materials

Glutaraldehyde was purchased from Merck (Darmstadt, Germany), phosphate buffered saline (PBS) from Serag Wiessner (Naila, Germany), Parafilm®M from Brand (Wertheim, Germany), haemoglobin and L-arginine from Sigma-Aldrich (Deisenhofen, Germany) and L-N^5-(iminoethyl)ornithine (LNIO) from Alexis Biochemicals (Enzo Lifescience GmbH, Lörach, Germany). 4–amino–5-methylamino-2, 7- difluorofluorescein (DAF-FM) diacetate was from Invitrogen (Darmstadt, Germany). S-nitrosocysteine (SNOC) was synthesized as described [28].

Experimental design

We analysed and compared the effects of NO scavenger and NOS inhibitors on RBC deformability and NO levels *in vitro*, as well as on RBC velocity and cell deformation *in vivo* in the microcirculation of the CAM of the avian embryo.

In vitro experiments

Avian blood samples. Blood samples were collected from the brachial vein of adult chicken, anti-coagulated with heparin and stored for max 2 h at 4°C. Probes were kindly provided by Professor Dr Schaub (Zoology/Parasitology Group, Ruhr-University of Bochum, Germany). All animal procedures were authorized by the Landesamt für Natur, Umwelt und Verbraucherschutz Nordrhein-Westfalen, Recklinghausen, Germany.

Intracellular staining with DAF-FM and flow cytometry

The effects of NOS inhibitors on intracellular NO levels in avian RBC were assessed by staining RBC with DAF-FM diacetate, which in the presence of NO and O_2 is converted to a highly fluorescence triazole derivate by an unstable nitrosating species mainly derived from oxidation of NO [29,30]. The best staining conditions (cell and dye concentrations, temperature, incubation time and pH) as well as the effects of NO donors and intracellular NO scavenging were carefully optimized by using human RBC. Moreover, the reactivity of DAF-FM for anion superoxide and hydrogen peroxide has been also tested (not shown).

Avian blood was diluted 1:500 (4×10^5 cells/µl) in PBS, divided in aliquots and treated for 30 min at 37°C with the NOS inhibitor L-NIO (3 mM) or with L-arginine (3 mM). As a positive control RBC were treated with the NO donor and nitrosating species SNOC (25 µM) [31]. Intracellular NO was s cavenged by incubation of RBC for 30 min at 37°C with 250 µM of iron diethyldithiocarbamate ($Fe(DETC)_2$) prepared as previously described [28]. Cells were stained for 30 min at 37°C with 10 µM DAF-FM diacetate, washed in cold PBS and measured within 15 min in a flow cytometer (FACS CANTO II) within the FITC channel (ex 488 nm, em 530 ± 30 nm). Number of counted cells: 30 000, $n = 3$. Median fluorescence intensity (MFI) was determined in the fluorescence distribution plot by using the FlowJo V7.5.5 (TreeStar, Ashland, OR) software package. For each experiment unstained cells served as autofluorescence control. Reliability of fluorescence acquisition was assured adjusting fluorescence acquisition voltage with fluorescent latex beads (Rainbow beads, BD Bioscience, Heidelberg, Germany).

Measurement of avian RBC deformability by ektacytometry

Blood samples were treated with glutaraldehyde (0.01%) to increase the stiffness of RBC, with the NO scavenger oxyhaemoglobin (0.1 mM), with the NOS inhibitor L-NIO (0.1 mM), with the NOS substrate L-arginine (3 mM) or with PBS as a control for 30 min at 37°C. These concentrations chosen have previously been shown to affect the filterability of human RBC *in vitro* [22]. Avian RBC deformability was determined at various fluid shear stresses by laser

diffraction analysis using an ektacytometer (laser-assisted optical rotational cell analyser (LORCA), RR Mechatronics, Hoorn, Netherlands). This system has been described elsewhere [32]. Briefly, an elongation index (EI) was calculated on the basis of the geometry of the ellipitical diffraction pattern: EI = (L - W)/(L + W), where L and W are the length and width of the diffraction pattern, respectively. EI values were calculated for shear rates between 0.5–15 Pa. An increased EI at a given shear stress indicates greater cell deformation and hence greater RBC deformability. All measurements were carried out at 37°C.

In vivo experiments

Preparation of the avian chorioallantoic membrane. Fertile eggs (Deindl, Rietberg, Germany) were incubated for 7 days at 37°C and 55% relative humidity in a custom-built glass bowl. The eggs were rotated twice per day until day 5. At this time point 2 ml of egg white were drawn using a syringe with a diameter of 0.9 mm, the upper half of the eggshell was removed and a 1.0 × 1.5 cm window was opened above the CAM. This 'window' was covered with Parafilm®M to prevent the drying of the egg and the incubation was continued without rotation until day 7.

Measurement of rheological parameters by intra-vital microscopy

The microcirculation of the CAM was analysed by using an intra-vital microscope (DML Leica, Wetzlar, Germany) equipped with a 10-fold (10 ×) magnification ocular. The focal plane was set as shown in Figure 1. To analyse rheological parameters of RBC before and after intervention, images obtained by differential interference microscopy (DIC) were recorded at a rate of 50 fields/s with a long working distance 50 × objective by using a charge-coupled device camera (AVT B-C71, Horn, Germany), obtaining videos showing single RBC passing through the microcirculation of the CAM (Figure 1). Videos were taken before intervention as well as 10 and 60 min after intervention and analysed by using Cap-Image 1.1 (Dr. Zeintl GmbH, Heidelberg, Germany).

Vessel diameters and RBC velocity were measured in the pre-capillary and capillary over a period of 2 min. Diameter of pre-capillary, capillary and the large arteries upstream were measured before and after intervention by using the appropriate software tool. RBC velocity was analysed according to the line-shift-diagram method, a semi-automatic computer analysis method, following the manufacturer's instruction. Briefly, a line is drawn along the main axis of the vessel. Each RBC that passed the measurement line causes a shift in grey level pattern, measured in μm, over time, measured in seconds (s). The velocity (μm/s) of all RBC passing through the vessel during 2 mins was averaged.

RBC length (L) and width (W) were measured during the entrance of the RBC from pre-capillary into a following capillary (Figure 1) before and after intervention. The passage of a single RBC from the pre-capillary to capillary was tracked by direct visualization. L and W were measured at two defined measurement points in the pre-capillary and capillary. Entering a capillary the process of RBC deformation led to an increase in L and a decrease in W. Values obtained from the analysis of 30 RBC per time-point per intervention per egg were averaged (the total number of cells analysed per treatment was 90 RBC). RBC deformation was assessed by the deformation index (DI) [33], defined as in (1):

$$DI = L/W \tag{1}$$

A decrease in *DI* indicates a decrease in RBC deformation.

RBC flow rate (Q_{RBC}) along the pre-capillary–capillary flow was estimated using the following equation:

$$\text{RBC flow rate} = \tfrac{1}{4}\,\pi\, Dc^2\, V_{RBC} \tag{2}$$

where *Dc* is the interior diameter of the pre-capillary or capillary and V_{RBC} is the RBC velocity measured in the pre-capillary or capillary.

Shear rate was calculated from RBC velocity and capillary diameter according to the Poiseuille parabolic intra-arterial velocity distribution:

$$\text{Shear rate} = 8\, Vi/Di \tag{3}$$

where *Vi* is the velocity and *D* is the vessel diameter at point *i*.

Heart rate was assessed by directly observing the heart contraction and counting the number of beats over a period of 60 s before intervention, as well as 5 and 10 min after intervention. Data are expressed as beats per minute (bpm). During all experimental procedures eggs were placed in a custom-made glass bowl perfused with water at 37°C.

Intervention procedure

Experiments were performed on day 7 of embryonic development. All compounds were injected into a conduit artery of the CAM using a smoothed borosilicate glass capillary with an exterior diameter of 0.5 mm. Glutaraldehyde (0.01%) was injected to assess the effect of changes in the RBC deformability on RBC velocity. To influence vascular NO bioavailability we applied the NO scavenger oxyhaemoglobin (0.1 mM). To modify endogenous NO synthesis the NO synthase inhibitor LNIO (0.1 mM) or the NOS substrate L-arginine (3 mM) were injected.

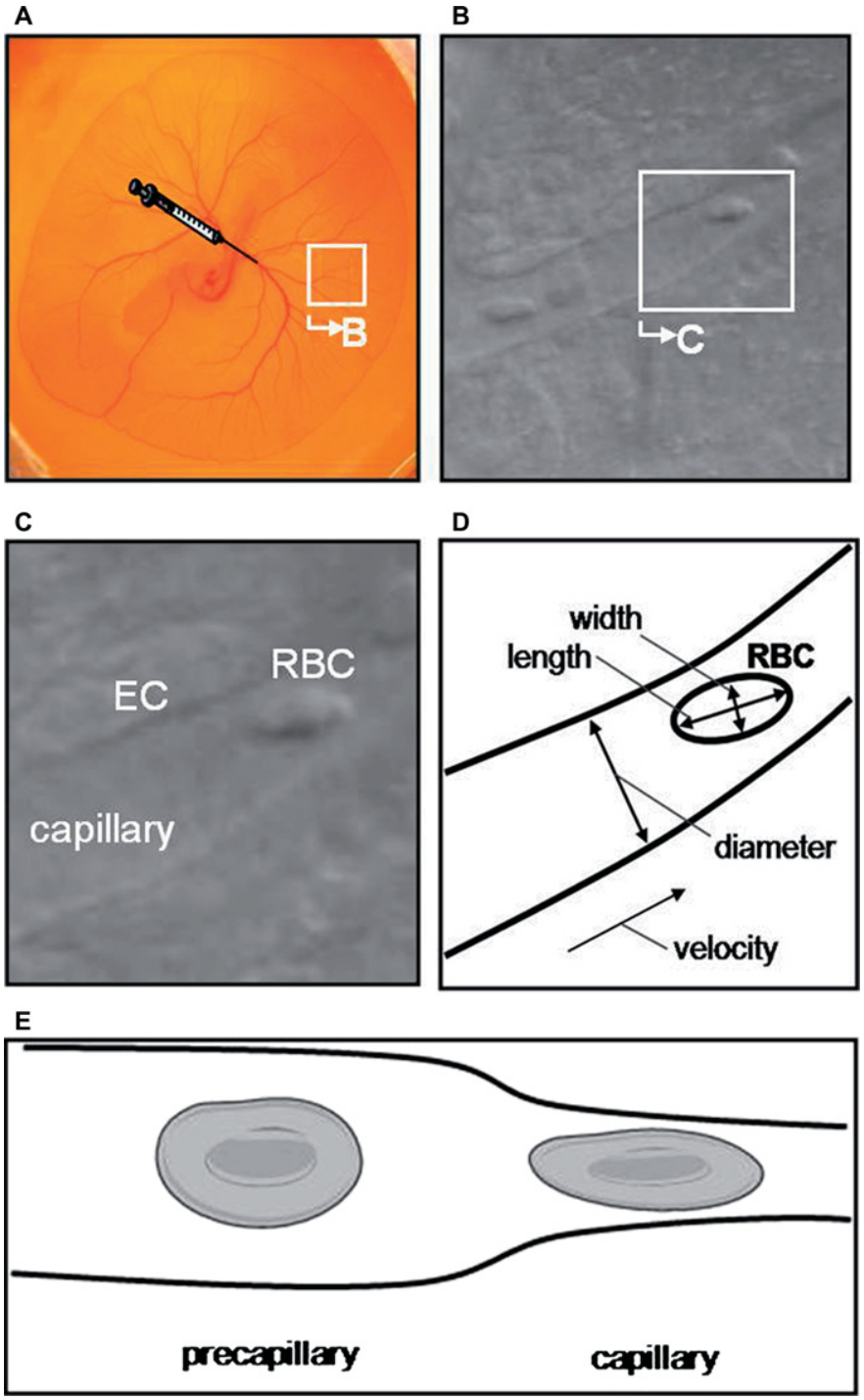

Figure 1. The avian chorioallantoic membrane model: a functional microcirculatory system. Representative picture of a chicken embryo at day 7 of embryonic development showing the chorioallantoic membrane and the site of injection (A), the microvascular bed (B) with a magnified (C) and a schematic (D) illustration of the measured parameters using an intra-vital microscope with a 10 × ocular and 50 × objective at long working distance. Schematic illustration of RBC deformation (increase in cell length and a decrease in cell width) within the capillary (E). EC = endothelial cell.

Application of PBS served as control. Final concentrations have been calculated considering a total blood volume of 750 µl at day 7 of embryonic development. All compounds were injected as a 10 µl bolus over 10 s and at a temperature of 37°C to exclude influence of volume changes or temperature on blood flow. Each treatment was repeated in five different eggs (total number of eggs: 30).

Statistical analysis

Data are reported as mean ± SEM. Paired *t*-test was used to assess significant differences in the mean values for data from the same egg before and after intervention. Mann-Whitney rank sum test and analysis of variance with Bonferroni correction for multiple *t*-tests were used to compare different eggs. *p*-values < 0.05 were considered as statistically significant.

Results

NOS inhibition and NO scavenging decreased deformability and intracellular NO levels of avian RBC in vitro

Addition of L-NIO (0.1 mM) as well as treatment with the extracellular NO scavenger oxyhaemoglobin (0.1 mM) significantly decreased RBC deformability as compared to treatment with PBS (Figure 2A), while treatment with the NOS substrate L-arginine (3 mM) did not affect RBC deformability. As a positive control, avian RBC were treated with glutaraldehyde (0.01%), which has been previously applied to cross-link RBC membrane proteins and thus decrease their deformability [34,35]. Treatment with glutaraldehyde decreased RBC deformability as compared to PBS-treated control ($p < 0.05$).

The effects of L-NIO and L-arginine on the intracellular NO levels of avian RBC were assessed by staining with DAF-FM and flow cytometry. Avian RBC stained with DAF-FM diacetate were strongly fluorescent, as compared to the unlabelled control. Addition of the NOS inhibitor L-NIO (0.1 mM) decreased intracellular fluorescence activity (Figure 2B), while treatment with the NOS substrate L-arginine (3 mM) did not affect intracellular DAF-FM fluorescence. To control for reactivity and specificity of intracellular DAF-FM for NO we added SNOC (25 μM) or the cell-permeable NO scavenger $Fe(DETC)_2$ (250 μM). We found that SNOC increases intracellular DAF-FM fluorescence activity (Figure 2B), while $Fe(DETC)_2$ decreased it. Thus, intracellular DAF-FM fluorescence in the RBC depends on NO levels.

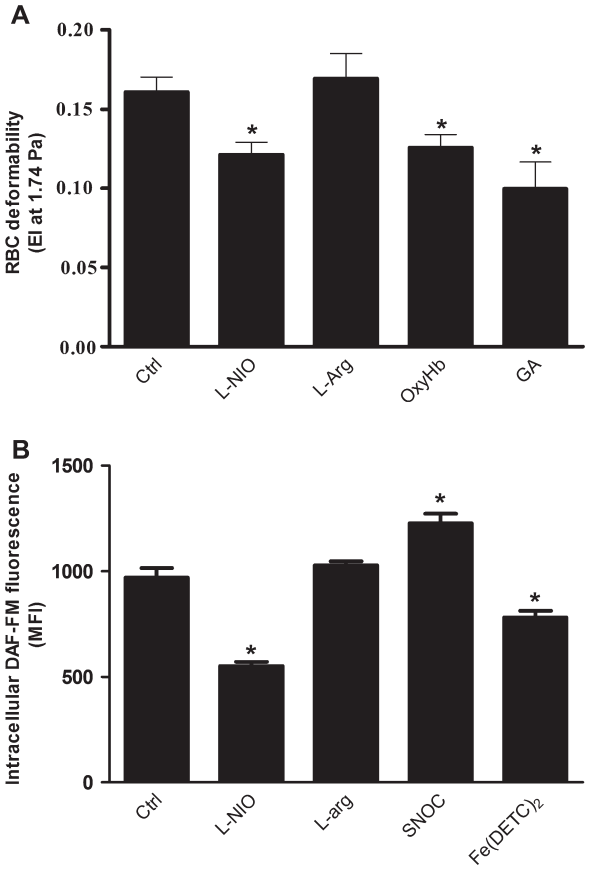

Figure 2. NOS inhibition and NO scavenging decrease deformability and intracellular NO levels of avian RBC *in vitro*. (A) RBC were treated with L-NIO (0.01 mM), oxyhaemoglobin (OxyHb; 0.01 mM), L-arginine (L-Arg; 3 mM) and glutaraldehyde (GA; 0.01%) or left untreated (Ctrl). RBC deformability was assessed by ektacytometry (*indicates significant difference as compared to Ctrl). (B) RBC were treated with L-NIO (3 mM) or with L-Arginine (L-Arg; 3 mM) or left untreated (Ctrl). As control, RBC were treated with SNOC (25 μM) or with the NO scavenger $Fe(DETC)_2$ (250 μM). Cells were washed, stained with 10 μM DAF-FM and analysed by flow cytometry. Median fluorescence intensity (MFI) within the RBC gate was calculated by analysing the fluorescence distribution plot of the green channel (Ex 488 Em 530 ± 30 nm). Data represent the difference between MFI of stained cells minus the autofluorescence. *indicates significant difference as compared to Ctrl ($p < 0.05$).

NOS inhibition and NO scavenging decreased RBC velocity and cell deformation in the microcirculation of the CAM

We aimed to determine whether the NOS inhibition and NO scavenging-mediated decrease in RBC deformability affect RBC velocity and deformation in the microcirculation of the CAM independently of changes in vascular tone. We found that the microcirculation of the CAM was suitable for the reliable and precise measurements of rheological parameters, e.g. vessel diameter, RBC velocity and cell deformation, by direct visualization of single cells (Figure 1). The basal rheological parameters are described in Table I.

Injection of oxyhaemoglobin to scavenge extracellular NO decreased RBC velocity and deformation index (DI) both in the pre-capillary and capillary as compared to basal values before injection ($p < 0.05$; Figure 3). The NOS inhibitor L-NIO decreased RBC velocity and DI in the capillary ($p < 0.05$). Injection of L-arginine did not influence RBC velocity or DI. Injection of glutaraldehyde decreased RBC velocity and DI both in pre-capillaries ($p < 0.05$) and in capillaries ($p < 0.05$) as compared to basal levels measured before intervention (Figure 3). Injection of PBS did not exert any effect on RBC velocity or DI as

Table I. Basal rheological parameters.

Rheological parameters	pre-capillary	capillary	*p*-value
Eggs (*n*)	30	30	
Vessel Diameter (μm)	13.5 ± 0.3	6.2 ± 0.2	<0.05
No. of measured RBC (*n*)	900	900	
Mean RBC length (μm)	14.8 ± 0.1	16.1 ± 0.2	<0.05
Mean RBC width (μm)	7.5 ± 0.2	5.8 ± 0.2	<0.05
DI	2.02 ± 0.03	2.94 ± 0.04	<0.05
RBC velocity (μm/s)	100 ± 15	304 ± 20	<0.05
Shear rate (s^{-1})	57 ± 3	340 ± 24	<0.05
RBC flow rate ($\mu m^3/s$)	12 500 ± 400	11 500 ± 700	n.s.
Heart rate (bpm)	216 ± 12		
Diameter of artery upstream (μm)	342 ± 8		

Values are means ± SE. RBC length increased up to 11% and RBC width decreased about 25% when RBC enter from pre-capillary into the capillary. RBC length-to-width ratio increased in capillaries up to 28% under basal conditions. RBC velocity in the artery upstream was measured with 720 ± 30 μm/s. The RBC flow rate did not change on passing from pre-capillary to capillary.

compared to basal conditions (Figure 3). The observed effects were stable over the duration of the experiments (60 min). Other physiological parameters such as diameter of pre-capillary, capillary and the arteries upstream, as well as heart rate did not change after any treatment (Table II—supplemental material).

To investigate the relationship between RBC velocity and RBC deformation, we calculated the shear rate, i.e. the force deforming the RBC in the microcirculation, from RBC velocity and vessel diameter (Figure 3C). We formed a linear relationship ($R^2 = 0.87$, $p < 0.01$) between shear rate and DI, suggesting that in our model RBC deformation is a function of shear rate.

Discussion

Our findings demonstrate that NOS inhibition and NO scavenging decrease RBC deformability *in vitro* and RBC velocity and deformation in the microcirculation of the CAM independently of changes in vascular tone.

The microcirculation of the CAM offers many advantages as a model for measuring NO-dependent changes on rheological parameters and blood flow. Study of rheological parameters by intra-vital microscopy in this model does not require application of anaesthetic and single circulating cells can be directly observed and measured. Moreover, until day 12 post-fertilization the vessels of the CAM lack smooth muscle cells [27]. Therefore, NO does not influence vascular diameter via regulation of smooth muscle cell relaxation, as previously shown by using NO donors [26]. Thus, we measured rheological parameters independently from changes in vascular diameter.

Although avian RBC are nucleated and elliptical, they present many similarities with mammalian non-nucleated RBC. Like human [14,22] and mouse RBC [36], avian RBC produce NOS-derived NO metabolites, as shown here by staining with DAF-FM. Avian and mammalian RBC present similar membrane protein composition. Despite a lower deformability of nucleated avian RBC, the deformation process of nucleated and non nucleated RBC is qualitatively similar [27]. We here show that NOS inhibition by adding L-NIO and NO scavenging by treatment with oxyhaemoglobin significantly decreased RBC deformability *in vitro* as compared to treatment with PBS. Similar effects of NOS inhibition or NO scavenging on RBC deformability have previously been measured in non-nucleated mammalian RBC *in vitro* [17,22]. Thus, it has been proposed that NOS-derived NO in RBC plays a central role in maintaining deformability [17,21,22]. We have also found that treatment with the NOS substrate L-arginine (3 mM) did not affect avian RBC deformability as shown for human RBC elsewhere [17]. In contrast, we have observed previously that L-arginine increased filterability of human RBC [22]. While ektacytometry measures deformability, RBC filterability is influenced by both RBC deformability as well as aggregability [37]. Thus, in our previous setting L-arginine might have affected aggregability of RBC. As expected, increasing RBC stiffness by treatment with glutaraldehyde, which is known to cross-link RBC membrane proteins in mammals [34] and avians [35], decreased deformability of the cells *in vitro*. The mechanisms involved in NO-mediated modulation of RBC deformability are not well understood. NO may affect RBC deformability depending on guanylate cyclase activity and cyclic guanosine monophosphate concentrations [17,38], on $Ca2^+$-dependent K^+ channels [39], on K^+ transporters [17] or on cyclic adenosine monophosphate concentrations [40].

In the microcirculation of the CAM, we found that the NO-dependent changes in RBC deformability measured *in vitro* are reflected by changes in capillary blood flow *in vivo*. Inhibition of enzymatic NO synthesis by L-NIO not only reduced RBC deformability *in vitro*, but also decreased RBC velocity and cell deformation *in vivo*, while the diameters of pre-capillary, capillary and the arteries upstream remained

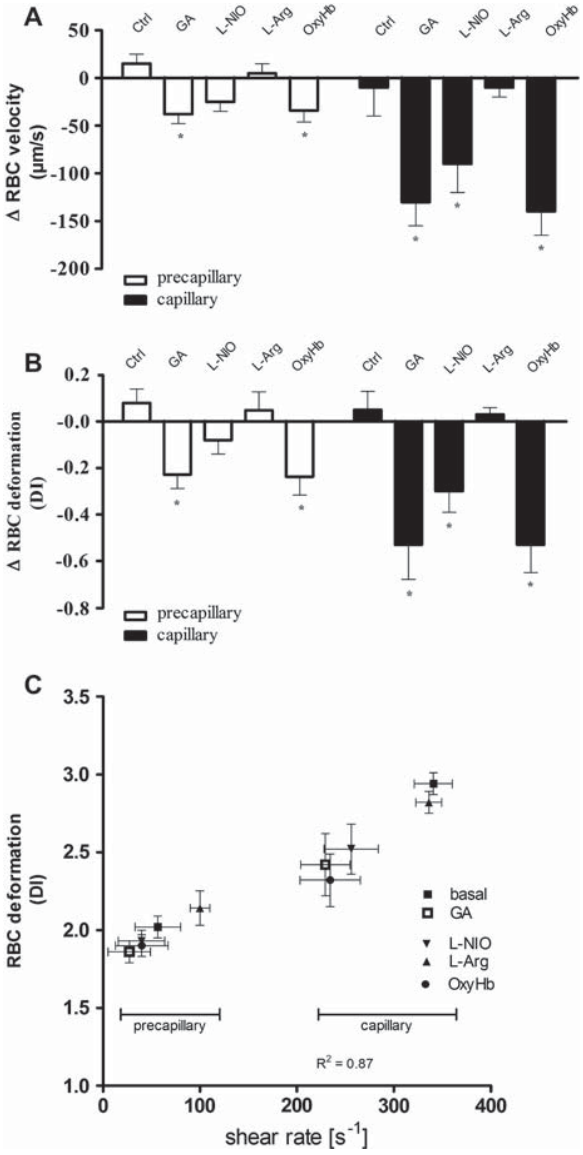

Figure 3. NOS inhibition and NO scavenging decrease RBC velocity and RBC deformation *in vivo*. A bolus volume (10 µl) of oxyhaemoglobin (OxyHb; 0.1 mM), LNIO (0.01 mM), Larginine (L-Arg; 3 mM), glutaraldehyde (GA; 0.01%) or PBS were injected into a conduit artery of the CAM. (A) RBC velocity and (B) RBC deformation index (DI) were measured off-line at a defined point of the pre-capillary and at a defined point of the capillary by using CapImage® software and were compared to basal values before intervention. *indicates significant differences ($p < 0.05$). (C) Shear rate and RBC DI significantly correlate in pre-capillary and capillary ($R^2 = 0.87$, $p < 0.01$).

constant. Injection of oxyhaemoglobin produced a more pronounced decrease in RBC velocity and deformation, as compared to L-NIO. While L-NIO inhibits enzymatic NO synthesis within the cells, oxyhaemoglobin is not cell permeable and scavenges NO present in the interstitium and in the vessel lumen, affecting the circulating NO pool [41]. For technical reasons (difficulties in blood drawing and small blood volume), it was not possible to assess NO metabolites in embryonic blood cells or rheological parameters of embryonic avian RBC *ex vivo*. Injection of L-arginine did not affect RBC velocity and cell deformation *in vivo*, as expected considering the lack of effect of L-arginine on RBC deformability *in vitro*.

RBC velocity depends on vessel diameter, pulse pressure or changes in rheological parameters, i.e. RBC deformability, RBC aggregation, RBC adhesion, hematocrit or blood viscosity [42]. Many of these parameters might be affected by NO. Changes of vascular diameter due to NO-mediated vasodilation can be excluded as smooth muscle cells are absent [25–27]. In fact, we did not measure any changes of the vessel diameter of pre-capillary, capillary or large arteries upstream after treatment with L-NIO or oxyhaemoglobin. However, minor changes in the internal diameter of the vessel lumen due to changes of the glycocalyx [43] cannot be excluded. Heart rate and the diameter of the arteria upstream did not change, which indicate that in our model pressure gradients or other haemodynamic parameters also did not change. The effects of blood dilution on hematocrit due to injection of the compounds were the same for all treatments as same volumina were injected. Effects of L-NIO or oxyhaemoglobin on RBC adhesion or aggregation *in vivo* cannot be fully excluded. However, we did not observe any formation of RBC aggregates *in vivo*. Taken together, our data indicate that the decrease in RBC velocity *in vivo* after injection of L-NIO and oxyhaemoglobin was strongly dependent on reduced RBC deformability.

The correlation between decreased RBC deformability and RBC velocity *in vivo* within the microcirculation has previously been demonstrated by others who injected glutaraldeyde-treated RBC in the microcirculation of rodents [3–6]. In our model, injection of glutaraldehyde also decreased RBC velocity and deformation. We cannot exclude that some of the effects of glutaraldeyde were due to cross-linking of vessel or plasma proteins. However, we did not observe any changes in heart rate or vessel diameter after glutaraldehyde injection.

To explain the correlation between RBC deformability and RBC velocity *in vivo*, it has been proposed that a decrease in RBC deformability causes RBC plugging into the capillary, followed by a more heterogeneous distribution of hematocrit and an increase of blood viscosity [5,44]. As a consequence of these, regional flow resistance increases and RBC velocity within the capillaries decreases.

Conclusions

To summarize, our data indicate that endogenous NO directly affects RBC velocity and cell deformation *in vivo* not only by regulating vascular diameters as previously shown [23,24], but also by affecting RBC deformability. These data point to new aspects of

NO-mediated regulation of blood flow, which are independent of changes of the vascular tone.

Acknowledgements

We wish to thank Professor Dr G. Schaub (Zoology und Parasitology Ruhr-University of Bochum) for providing the blood of adult chickens and Professor Klaus-D. Kröncke and Dr Thomas Jax for helpful discussions and for critically revising the manuscript.

Declaration of interest

All authors of this manuscript disclose any financial and personal relationships with other people or organizations that could have influenced this work. This work was supported by the Deutsche Forschungsgemeinschaft, Sonderforschungsbereich 612 (to M. Kelm) and Ke405/5-1 (to M. Kelm).

References

[1] Mellander S. Functional aspects of myogenic vascular control. J Hypertens Suppl 1989;7:S21–S30.
[2] Pries AR, Secomb TW. Rheology of the micorcirculation. Clin Hemorheol Microcirc 2003;29:143–148.
[3] Cabrales P. Effects of erythrocyte flexibility on microvascular perfusion and oxygenation during acute anemia. Am J Physiol Heart Circ Physiol 2007;293:1206–1215.
[4] Driessen GK, Haes CWt, Heidtmann H, Kamp D, Schmid-Schonbein H. Effect of reduced red cell "deformability" on flow velocity in capillaries of rat mesentery. Pflugers Archiv. Eur J Physiol 1980;388:75–78.
[5] Lipowsky HH, Cram LE, Justice W, Eppihimer MJ. Effect of erythrocyte deformability on *in vivo* red cell transit time and hematocrit and their correlation with in vitro filterability. Microvasc Res 1993;46:43–64.
[6] Simchon S, Jan KM, Chien S. Influence of reduced red cell deformability on regional blood flow. Am J Physiol 1987;253: H898–H903.
[7] Ignarro LJ, Cirino G, Casini A, Napoli C. Nitric oxide as a signaling molecule in the vascular system: an overview. J Cardiovasc Pharmacol 1999;34:879–886.
[8] Moncada S. Nitric oxide in the vasculature: physiology and pathophysiology. Ann N Y Acad Sci 1997;811:60–69.
[9] Moncada S, Palmer RMJ, Higgs EA. Nitric oxide, biology pathophysiology and pharmacology. Pharmacol Rev 1991;43: 109–142.
[10] Gladwin MT, Shelhamer JH, Schechter AN, Pease-Fye ME, Waclawiw MA, Panza JA, Ognibene FP, Cannon RO, III. Role of circulating nitrite and S-nitrosohemoglobin in the regulation of regional blood flow in humans. Proc Natl Acad Sci USA 2000;97:11482–11487.
[11] Stamler JS, Jia L, Eu JP, McMahon TJ, Demchenko IT, Bonaventura J, Gernert K, Piantadosi CA. Blood flow regulation by S-nitrosohemoglobin in the physiological oxygen gradient. Science 1997;276:2034–2037.
[12] Cosby K, Partovi KS, Crawford JH, Patel RP, Reiter CD, Martyr S, Yang BK, Waclawiw MA, Zalos G, Xu X, Huang KT, Shields H, Kim-Shapiro DB, Schechter AN, Cannon RO, III, Gladwin MT. Nitrite reduction to nitric oxide by deoxyhemoglobin vasodilates the human circulation. Nat Med 2003;9:1498–1505.
[13] Webb A, Bond R, McLean P, Uppal R, Benjamin N, Ahluwalia A. Reduction of nitrite to nitric oxide during ischemia protects against myocardial ischemia-reperfusion damage. Proc Natl Acad Sci USA 2004;101:13683–13688.
[14] Chen LY, Mehta JL. Evidence for the presence of L-arginine-nitric oxide pathway in human red blood cells: relevance in the effects of red blood cells on platelet function. J Cardiovasc Pharmacol 1998;32:57–61.
[15] Kleinbongard P, Dejam A, Lauer T, Jax T, Kerber S, Gharini P, Balzer J, Zotz RB, Scharf RE, Willers R, Schechter AN, Feelisch M, Kelm M. Plasma nitrite concentrations reflect the degree of endothelial dysfunction in humans. Free Radic Biol Med 2006;40:295–302.
[16] Bor-Kucukatay M, Meiselman HJ, Baskurt OK. Modulation of density-fractionated RBC deformabilityby nitric oxide. Clin Hemorheol Microcirc 2005;33:363–367.
[17] Bor-Kucukatay M, Wenby RB, Meiselman HJ, Baskurt OK. Effects of nitric oxide on red blood cell deformability. Am J Physiol Heart Circ Physiol 2003;284:H1577–H1584.
[18] Kuwai T, Hayashi J. Nitric oxide pathway activation and impaired red blood cell deformability with hypercholesterolemia. J Atheroscler Thromb 2006;13:286–294.
[19] Mesquita R, Picarra B, Saldanha C, Martins e Silva J. Nitric oxide effects on human erythrocytes structural and functional properties - An *in vitro* study. Clin Hemorheol Microcirc 2002;27:137–147.
[20] Starzyk D, Korbut R, Gryglewski RJ. Effects of nitric oxide and prostacyclin on deformability and aggregability of red blood cells of rats *ex vivo* and *in vitro*. J Physiol Pharmacol 1999;50:629–637.
[21] Uyuklu M, Meiselman HJ, Baskurt OK. Role of hemoglobin oxygenation in the modulation of red blood cell mechanical properties by nitric oxide. Nitric Oxide 2009;21:20–26.
[22] Kleinbongard P, Schulz R, Rassaf T, Lauer T, Dejam A, Jax TW, Kumara I, Gharini P, Kabanova S, Özüyaman B, Schnürch H-G, Gödecke A, Weber A-A, Robenek MJ, Robenek H, Bloch W, Rösen P, Kelm M. Red blood cells express a functional endothelial nitric oxide synthase. Blood 2006;107: 2943–2951.
[23] Persson MG, Gustafsson LE, Wiklund NP, Hedqvist P, Moncada S. Endogenous nitric oxide as a modulator of rabbit skeletal muscle microcirculation *in vivo*. Br J Pharmacol 1990;100:463–466.
[24] Bauer C, Walcher F, Kalweit U, Larsen R, Marzi I. Role of nitric oxide in the regulation of the hepatic microcirculation *in vivo*. J Hepatol 1997;27:1089–1095.
[25] Ribatti D, Nico B, Vacca A, Roncali L, Burri PH, Djonov V. Chorioallantoic membrane capillary bed: a useful target for studying angiogenesis and anti-angiogenesis *in vivo*. Anat Rec 2001;264:317–324.
[26] Dunn LK, Gruenloh SK, Dunn BE, Reddy DS, Falck JR, Jacobs ER, Medhora M. Chick chorioallantoic membrane as an *in vivo* model to study vasoreactivity: characterization of development-dependent hyperemia induced by epoxyeicosatrienoic acids (EETs). Anat Rec A Discov Mol Cell Evol Biol 2005;285:771–780.
[27] Gaehtgens P, Schmidt F, Will G. Comparative rheology of nucleated and non-nucleated red blood cells. I. Microrheology of avian erythrocytes during capillary flow. Pflugers Arch 1981;390:278–282.
[28] Kroncke KD, Kolb-Bachofen V. Measurement of nitric oxide-mediated effects on zinc homeostasis and zinc finger transcription factors. Methods Enzymol 1999;301: 126–135.
[29] Nagano T, Yoshimura T. Bioimaging of nitric oxide. Chem Rev 2002;102:1235–1270.
[30] Nakatsubo N, Kojima H, Kikuchi K, Nagoshi H, Hirata Y, Maeda D, Imai Y, Irimura T, Nagano T. Direct evidence of nitric oxide production from bovine aortic endothelial cells

using new fluorescence indicators: diaminofluoresceins. FEBS Lett 1998;427:263–266.
[31] Hogg N. Biological chemistry and clinical potential of S-nitrosothiols. Free Radic Biol Med 2000;28:1478–1486.
[32] Baskurt OK, Hardeman MR, Uyuklu M, Ulker P, Cengiz M, Nemeth N, Shin S, Alexy T, Meiselman HJ. Comparison of three commercially available ektacytometers with different shearing geometries. Biorheology 2009;46:251–264.
[33] Jeong JH, Sugii Y, Minamiyama M, Okamoto K. Measurement of RBC deformation and velocity in capillaries *in vivo*. Microvasc Res 2006;71:212–217.
[34] Arevalo F, Bellelli A, Brancaccio A, Ippoliti R, Lendaro E, Brunori M. Biochemical and rheodynamic properties of red blood cells crosslinked with glutaraldehyde. Biotechnol Appl Biochem 1992;16:195–200.
[35] Horisberger M. Adhesion of human and chicken red blood cells to polystyrene: influence of electrolyte and polyethylene glycol concentration. Physiol Chem Phys 1980;12: 195–204.
[36] Mihov D, Vogel J, Gassmann M, Bogdanova A. Erythropoietin activates nitric oxide synthase in murine erythrocytes. Am J Physiol Cell Physiol 2009;297:C378–C388.
[37] Chien S. Filterability and other methods of approaching red cell deformability. Determinants of blood viscosity and red cell deformability. Scand J Clin Lab Invest Suppl 1981;156:7–12.

This paper was first published online on Early Online on 19 April 2011.

Supplementary material available online

Table 2. Supplemental Material.

[38] Petrov V, Lijnen P. Regulation of human erythrocyte Na^+/H^+exchange by soluble and particulate guanylate cyclase. Am J Physiol Cell Physiol 1996;271:C1556–C1564.
[39] Shields M, La Celle P, Waugh RE, Scholz M, Peters M, Passow H. Effects of intracellular $Ca2^+$ and proteolytic digestion of the membrane skeleton on the mechanical properties of the red blood cell membrane. Biochim Biophys Acta 1987; 905:181–194.
[40] Oonishi T, Sakashita K, Uyesaka N. Regulation of red blood cell filterability by $Ca2^+$ influx and cAMP-mediated signaling pathways. Am J Physiol 1997;273:C1828–C1834.
[41] Rassaf T, Feelisch M, Kelm M. Circulating NO pool: assessment of nitrite and nitroso species in blood and tissues. Free Radic Biol Med 2004;36:413–422.
[42] Mchedlishvili G. Disturbed blood flow structuring as critical factor of hemorheological disorders in microcirculation. Clin Hemorheol Microcirc 1998;19:315–325.
[43] Henry CB, Kleinstein E, Shum W, Defouw DO. Glycoconjugate expression in the chick embryonic chorioallantoic membrane: comparisons of the chorionic ectoderm and allantoic endoderm. Anat Rec 1995;241:411–416.
[44] Driessen GK, Fischer TM, Haest CW, Inhoffen W, Schmid-Schonbein H. Flow behaviour of rigid red blood cells in the microcirculation. Int J Microcirc Clin Exp 1984;3: 197–210.